Dredged Material Fate Study at the Portland Disposal Site 1998–2000

Disposal Area Monitoring System DAMOS

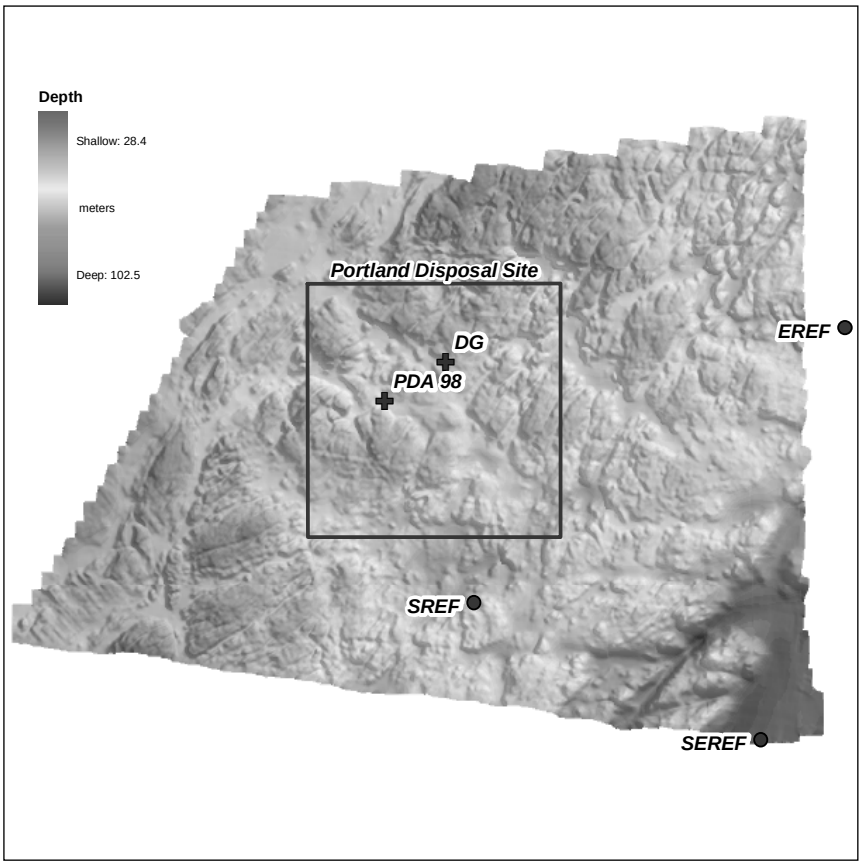

D A M O S

DISPOSAL AREA MONITORING SYSTEM

Contribution 153
August 2004

US Army Corps of Engineers ®
New England District

REPORT DOCUMENTATION PAGE

form approved
OMB No. 0704-0188

1. AGENCY USE ONLY (LEAVE BLANK)	2. REPORT DATE	3. REPORT TYPE AND DATES COVERED
	August 2004	FINAL REPORT

4. TITLE AND SUBTITLE
Dredged Material Fate Study at the Portland Disposal Site1998–2000

5. FUNDING NUMBERS

6. AUTHOR(S)
Science Applications International Corporation

7. PERFORMING ORGANIZATION NAME(S) AND ADDRESS(ES)
Science Applications International Corporation
221 Third Street
Newport, RI 02840

8. PERFORMING ORGANIZATION REPORT NUMBER
SAIC No. 552

9. SPONSORING/MONITORING AGENCY NAME(S) AND ADDRESS(ES)
US Army Corps of Engineers-New England District
696Virginia Rd
Concord, MA 01742-2751

10. SPONSORING/MONITORING AGENCY REPORT NUMBER
Contribution No. 153

11. SUPPLEMENTARY NOTES
Available from DAMOS Program Manager, Regulatory Division
USACE-NAE, 696 Virginia Rd, Concord, MA 01742-2751

12a. DISTRIBUTION/AVAILABILITY STATEMENT
Approved for public release; distribution unlimited

12b. DISTRIBUTION CODE

13. ABSTRACT

Building upon the results of the 1995-1997 capping demonstration project at the Portland Disposal Site (PDS), a comprehensive field data measurement effort and follow-on modeling program was performed at PDS study the behavior of the dredged material placed at the disposal site during the 1998-1999 dredging season. Results derived from the Short Term Fate (STFATE) and Multiple Dump Fate (MDFATE) models developed by the US Army Corps of Engineers, Waterways Experiment Station (WES) were compared to survey data collected over PDS to evaluate the capability of the models to forecast the extent and behavior of the sediment plume associated with a single disposal event (STFATE), as well as predict the location and extent of the disposal mound resulting from multiple barge placements (MDFATE). SAIC conducted a variety of field surveys over a two year period (1998-2000) to address the following two broad objectives: 1) obtain information on the physical characteristics of the dredged material and on the characteristics of the water column and seafloor at PDS for use as input to the numerical models, and 2) obtain information on the actual settling of dredged material out of the water column and the actual distribution of dredged material on the seafloor at PDS for use in evaluating the accuracy of the model predictions.

The STFATE model results depicted the expected plume migration pattern associated with the placement of a barge-load of "average" Portland Harbor dredged material subjected to hydrodynamic forces that were documented over PDS. Using a representative flood and ebb cycle from the current record, the STFATE model results depicted the expected plume migration pattern associated with the placement of a barge-load of typical Portland Harbor dredged material. Seafloor topography would often impact the morphology of the sediment plume, as steep ridges in the path of a moving plume served as containment features at depth. The MDFATE model results depicted the predicted seafloor deposit resulting from the 197 individual disposal events associated with all of PDS placement activity between the 1998 and 2000 multibeam surveys. The disposal mound morphology depicted by the MDFATE model was very closely correlated with the positions of the disposal events. The MDFATE results showed the largest accumulations of material over the shallower bedrock outcrop south of the PDA 98 buoy, where the highest numbers of large scow releases were recorded. In contrast, the depth difference results showed little or no accumulation over these exposed bedrock areas. In the time between the completion of disposal operations and the final multibeam survey, it is likely that a large percentage of the material had settled into the fault and crevice features within the areas of exposed bedrock or was advected out of these areas by natural processes and re-deposited into deeper depositional areas adjacent to the PDA 98 buoy location.

14. SUBJECT TERMS Portland Disposal Site, Dredged Material

15. NUMBER OF TEXT PAGES: 144

16. PRICE CODE

17. SECURITY CLASSIFICATION OF REPORT	18. SECURITY CLASSIFICATION OF THIS PAGE	19. SECURITY CLASSIFICATION OF ABSTRACT	20. LIMITATION OF ABSTRACT
Unclassified			

DREDGED MATERIAL FATE STUDY AT THE PORTLAND DISPOSAL SITE 1998–2000

CONTRIBUTION #153

August 2004

Report No.
SAIC-552

Submitted to:

Regulatory Division
New England District
U.S. Army Corps of Engineers
696 Virginia Road
Concord, MA 01742-2751

Submitted by:
Science Applications International Corporation
Admiral's Gate
221 Third Street
Newport, RI 02840
(401) 847-4210

US Army Corps of Engineers®
New England District

TABLE OF CONTENTS

Page

LIST OF TABLES

LIST OF TABLES (continued)

Page

LIST OF FIGURES

LIST OF FIGURES (continued)

Page

LIST OF FIGURES (continued)

Page

LIST OF FIGURES (continued)

Page

LIST OF FIGURES (continued)

Page

LIST OF FIGURES (continued)

Page

EXECUTIVE SUMMARY

Under the Disposal Area Monitoring System (DAMOS), sponsored by the New England District (NAE) of the U.S. Army Corps of Engineers (USACE), Science Applications International Corporation (SAIC) conducted a comprehensive field data measurement effort and follow-on modeling program to study the behavior of the dredged material placed at the Portland Disposal Site (PDS) during the 1998-1999 dredging season. Building upon the results of the 1995-1997 capping demonstration project at PDS, this follow-on study was intended to monitor the large-scale 1998-1999 Portland Harbor dredging project and to evaluate how well the Short Term Fate (STFATE) and Multiple Dump Fate (MDFATE) models forecasted the results of dredged material disposal operations at PDS. Both of these models were developed by the USACE Waterways Experiment Station (WES) and are widely used within the dredged material management field to predict the behavior of dredged material during different phases of overboard placement operations. The STFATE model is used to predict the extent and behavior of the sediment plume associated with a single disposal event, while the MDFATE model is used to predict the location and extent of the disposal mound resulting from multiple barge placements.

Dredged material generated from many of the dredging projects in New England is deposited at ten regional open water dredged material disposal sites. The DAMOS Program utilizes a flexible, tiered management approach centered on comprehensive environmental monitoring to oversee the placement of sediments at these open water disposal sites. These disposal sites are regularly monitored to ensure that the environmental impacts associated with dredged material placement are minor and temporary. PDS is located approximately 13.16 km east of Dyer Point, Cape Elizabeth, Maine and encompasses a 3.42 km^2 area of rocky and irregular seafloor, with water depths that range from 42 to 74 m. The regulated and monitored placement of dredged material has been occurring at this site since 1977. However, documented use of this area for dredged material placement dates back to 1946, when material was disposed over a 17.7 km^2 irregularly-shaped area of seafloor surrounding the current PDS boundaries. During the 1998-1999 and 1999-2000 Portland Harbor dredging projects, a total of 488,900 m^3 of material was deposited within PDS.

SAIC conducted a variety of field surveys over a two year period (1998-2000) to address the following two broad objectives: 1) obtain information on the physical characteristics of the dredged material and on the characteristics of the water column and seafloor at PDS for use as input to the numerical models, and 2) obtain information on the actual settling of dredged material out of the water column and the actual distribution of dredged material on the seafloor at PDS for use in evaluating the accuracy of the model predictions.

To address the first objective, SAIC conducted multibeam bathymetric and side-scan sonar surveys at PDS, obtained gravity cores and surface grab samples to characterize the sediments in the dredging areas and at the disposal site, and performed studies of water column currents, density and meteorology at PDS. To address the second objective, sediment traps were deployed in and around PDS to measure water column transport and settling of dredged material, and both multibeam bathymetric and REMOTS® sediment-profile imaging surveys were conducted to evaluate the morphology and delineate the footprint of the dredged material deposit on the seafloor. In addition, a special investigation was undertaken to determine whether there were any unique microscopic characteristics (e.g., mineralogy or microfossil composition) that might serve to distinguish the Portland Harbor dredged material from naturally-occurring surface sediments on the seafloor at PDS. The existence of one or more unique "tracers" would be of potential use in determining the origin of material captured in the sediment traps at various locations in and around the disposal site.

The seafloor in the PDS region is characterized by numerous steep, bedrock ridges and a prominent northwest-southeast trending trough. The high-resolution, full-bottom coverage multibeam and side-scan sonar surveys conducted prior to the 1998-1999 Portland Harbor dredging project provided better insight into the complexity of the PDS seafloor relative to previous single-beam surveys. These data also highlighted numerous natural basin features that could potentially serve as containment cells for future dredging projects. The multibeam data were used to provide the background bathymetry for both the MDFATE and STFATE model runs. More than a year after the completion of the 1998-1999 dredging project, a second high-resolution multibeam survey and a REMOTS® sediment-profile imaging survey were conducted over PDS. Based on the combined REMOTS® and multibeam depth difference results, it appeared that most of the deposited dredged material had settled in the deeper depositional areas, though a relatively thin surface layer of recent dredged material existed over the surrounding bedrock areas.

The sediment sampling and subsequent geotechnical analyses that were conducted on the Portland Harbor and PDS sediments produced the Portland Harbor sediment characterization data needed for input into the STFATE and MDFATE models. Samples were also analyzed for the presence of unique tracers that could be used to differentiate between the Portland Harbor sediments and those that existed within PDS prior to the disposal operations. These results showed that the Portland Harbor sediments were comprised of mostly clay and silt, with primarily marsh and shallow water foraminifera, while the PDS sediments were primarily comprised of mostly fine sand with shelf foraminifera. However, there was considerable variability in the number of individuals and taxa among different samples from the same area, and there was also evidence of estuarine taxa at the PDS sample locations (likely due to historic disposal activities) and continental shelf taxa in the Portland Harbor samples (likely due to cross-shelf transport processes).

During Phase 3 of the Portland Harbor dredging project, sediment traps were deployed around the perimeter of PDS in an attempt to capture sediment settling through the water column. Due primarily to disturbance from fishing activity, only three of the ten traps were recovered with any analyzable material present. Despite the limitations noted above in the use of microfossils, comparisons of the occurrence of freshwater, estuarine and continental shelf microfossils provided supporting evidence used to evaluate the likely sources of material collected in sediment traps. A combination of qualitative comparisons of the volume of material in the traps, trap location and local hydrodynamic processes, and the microfossil evidence were used to draw conclusions about the source of material in the sediment traps. Based on that evidence, it was concluded that the traps likely contained material that had settled out of the dredged material disposal plumes, as well as sediments resuspended from the surrounding substrate by storms such as the March 1999 storm event that occurred shortly after trap deployment.

Deployment of an acoustic Doppler current profiler (ADCP) for 31 days provided information on hydrodynamics in the vicinity of PDS. The data indicated moderate tidal current velocities at depth, with conditions in the near-surface portion of the water column affected by wind waves (near-surface maximum velocity during the deployment period of 50 $cm \cdot s^{-1}$), which is expected given the open fetch in this region. In general, the water column currents displayed a strong northwest-southeast trend, likely related to tidal oscillations within Casco Bay. Filtering of the high-frequency data revealed residual currents related to the counterclockwise gyre driving circulation in the Gulf of Maine. Besides documenting current flow over PDS, the ADCP data were also used as inputs to multiple STFATE and MDFATE model runs.

The STFATE model results depicted the expected plume migration pattern associated with the placement of a barge-load of “average” Portland Harbor dredged material subjected to hydrodynamic forces documented over PDS. Using a representative flood and ebb cycle from the current record, the STFATE model results depicted the expected plume migration pattern associated with the placement of a barge-load of typical Portland Harbor dredged material. Entrained material would migrate northwest from its point of origin with the water mass movement driven by a flood tide. Conversely, an ebb tide would transport the sediment plume to the southeast. Based on the model results, the sediment plume would increase in size as time progressed with a corresponding decrease in the peak suspended sediment concentrations. Seafloor topography would often impact the morphology of the sediment plume, as steep ridges in the path of a moving plume served as containment features at depth.

In addition, the STFATE model was run utilizing averaged currents acquired over PDS to evaluate a worse case scenario for sediment transport. These results showed the sediment plume migrating in a southwest direction away from the PDA 98 buoy in response to the counterclockwise gyre in Gulf of Maine. Once again, the sediment plume increased in size as time progressed with a corresponding decrease in the peak suspended sediment concentrations. The modeled plume migration path was consistent with the sediment trap results that indicated the presence of recent Portland Harbor dredged material along the southern PDS boundary. The relatively sparse sediment trap results show the cumulative effects from all of the disposal events that occurred within PDS while the traps were deployed, while the STFATE results show the expected plume associated with a single, representative disposal event at the PDA 98 buoy position.

The MDFATE model results depicted the predicted seafloor deposit resulting from the 197 individual disposal events associated with all of PDS placement activity between the 1998 and 2000 multibeam surveys. The disposal mound morphology depicted by the MDFATE model was very closely correlated with the positions of the disposal events. The MDFATE results showed the largest accumulations of material over the shallower bedrock outcrop south of the PDA 98 buoy, where the highest numbers of large scow releases were recorded. In contrast, the depth difference results showed little or no accumulation over these exposed bedrock areas. In the time between the completion of disposal operations and the final multibeam survey, it is likely that a large percentage of the material had settled into the fault and crevice features within the areas of exposed bedrock or was advected out of these areas by natural processes and re-deposited into deeper depositional areas adjacent to the PDA 98 buoy location.

1.0 INTRODUCTION

1.1 Background

Among the disposal alternatives that exist for sediments dredged from navigation channels and vessel berthing areas in the New England region, a significant volume of material is placed on the seafloor at ten regional open water dredged material disposal sites (Figure 1-1). The Disposal Area Monitoring System (DAMOS), sponsored by the U.S. Army Corps of Engineers (USACE), New England District (NAE), investigates and works to minimize any adverse physical, biological, or chemical impacts associated with dredging or dredged material disposal. The ten open water disposal sites along the coast of New England are regularly monitored to ensure that the environmental impacts associated with dredged material placement are minor and temporary.

Under DAMOS, Science Applications International Corporation (SAIC), in association with Applied Science Associates (ASA) of Narragansett, RI, conducted a comprehensive field data measurement effort and follow-on modeling program to study the behavior and fate of dredged material placed at the Portland Disposal Site (PDS) during the 1998-99 disposal season. Building upon the results of a capping demonstration project conducted at PDS from 1995 to 1997 (Morris et al. 1998), the overall objective of this follow-on study effort was to evaluate the ability of numerical models to predict the behavior and fate of dredged material placed at PDS. The two models examined, called Short Term Fate (STFATE) and Multiple Dump Fate (MDFATE), were developed by the USACE Waterways Experiment Station (WES) and are widely used within the dredged material management field to predict the behavior of dredged material during different phases of overboard placement operations. The STFATE model is used to predict the extent and behavior in the water column of the sediment plume associated with a single disposal event, while the MDFATE model is used to predict the location and extent of the disposal mound created on the seafloor as a result of multiple barge placements.

As described in more detail in later sections, SAIC conducted a variety of field surveys over a two year period (1998-2000) to address the following two broad objectives: 1) obtain information on the physical characteristics of the dredged material and on the characteristics of the water column and seafloor at PDS for use as input to the numerical models, and 2) obtain information on the actual settling of dredged material out of the water column and the actual distribution of dredged material on the seafloor at PDS for use in evaluating the accuracy of the model predictions.

To address the first objective, SAIC conducted multibeam bathymetric and side-scan sonar surveys at PDS, obtained gravity cores and surface grab samples to characterize the sediments in the dredging areas and at PDS, and performed studies of water column currents, density and meteorology at PDS. To address the second objective, sediment traps were

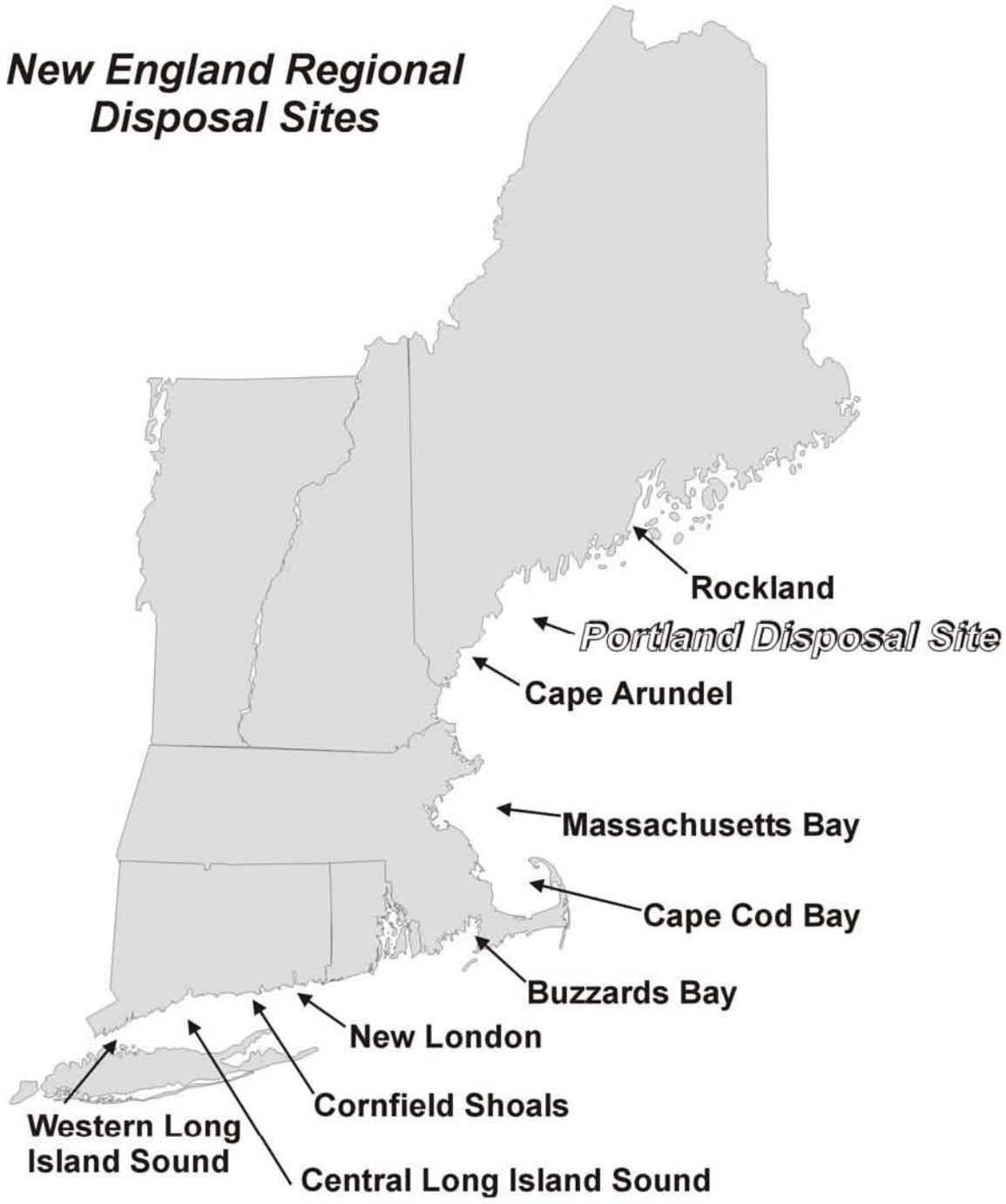

Figure 1-1. Geographic locations of the ten regional dredged material disposal sites located in New England waters and monitored under the DAMOS Program

deployed in and around PDS to measure water column transport and settling of dredged material, and both multibeam bathymetric and sediment-profile imaging surveys were conducted to evaluate the morphology and delineate the footprint of the dredged material deposit on the seafloor.

As part of the sediment trap study, a special investigation was undertaken to determine whether there were any unique microscopic characteristics (e.g., mineralogy or microfossil composition) that might serve to distinguish the dredged material from Portland Harbor from the naturally-occurring surface sediments on the seafloor at PDS. The existence of one or more unique "tracers" would be of potential use in determining the origin of material captured in the sediment traps at various locations in and around the disposal site. This information would in turn be used to evaluate the transport through the water column of the sediment plume resulting from dredged material disposal.

Each of the various surveys and studies conducted by SAIC produced a considerable volume of data and results that are, individually, of significant interest. In this synthesis report, an attempt has been made to summarize the results of each study for the purpose of addressing the central objective: to evaluate the predictive capabilities of the two numerical dredged material fate models at PDS. Wherever possible, individual study results not of direct relevance to this overarching objective are presented in greater detail in an appendix.

The remainder of this section provides background information on the Portland Disposal Site, an overview of the dredging, disposal and monitoring activities that took place from 1998 to 2000, and concludes with a listing of the major objectives and predictions of the PDS dredged material fate study.

1.2 Portland Disposal Site (PDS)

To provide the infrastructure capable of supporting marine commerce in Portland Harbor and elsewhere, dredging of channels and berthing areas is required. Sediments dredged from Portland Harbor and the many smaller ports and channels in the Casco Bay region that are found to be suitable for open-water disposal are usually transported by scow and placed at PDS. The center of PDS is located 13.16 km east of Dyer Point, Cape Elizabeth, Maine (Figure 1-2) and encompasses a 3.42 km² area centered at 43° 34.105´ N, 70° 01.969´ W (NAD 83). The seafloor topography at PDS is rocky and irregular, with water depths that range from 42 to 74 m. The regulated and monitored placement of dredged material has been occurring at this site since 1977. However, documented use of this area for dredged material placement dates back to 1946, when material was disposed over a 17.7 km² irregularly-shaped area of seafloor surrounding the current PDS boundaries (EPA 1996; Figure 1-2).

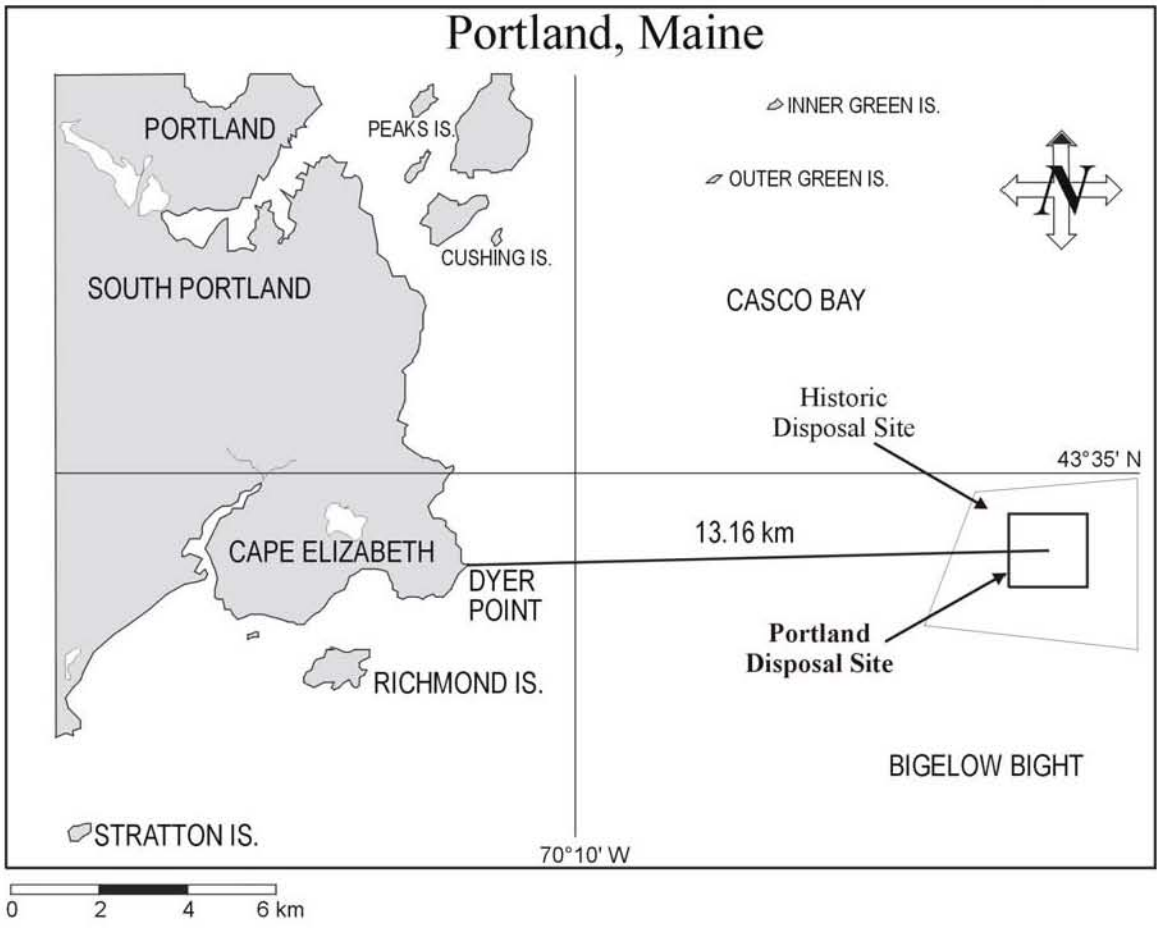

Figure 1-2. Location of the Portland Disposal Site, relative to the Maine shoreline and Casco Bay

The areas of seafloor that exist among the numerous bedrock outcrops and ridges at PDS represent natural containment basins that can be targeted to minimize the lateral spread of dredged material on the bottom. In particular, the steep walls of these containment features tend to shelter the fine-grained dredged material deposits from the effects of long period ocean waves. Surface wave heights of over 3 m associated with the passage of coastal and ocean storms are common at PDS due to the unlimited fetch to the south and southeast (McDowell and Pace 1998). At this disposal site, it is hypothesized that wave-induced, strong oscillatory bottom currents associated with the passage of storms act to move (advect) fine-grained sediments from exposed areas of seafloor into the lower-energy containment areas among the bedrock outcrops, resulting in depositional layers of ambient sediment over the dredged material (McDowell and Pace 1998).

The disposal site typically receives an average annual volume of 99,000 m^3 of sediment deposited at the US Coast Guard, Class-A, Special Purposes buoy, labeled "DG", located in the northern region of the site (Morris 1996). The sediment disposed in close proximity to the DG buoy coalesces into a single, large seafloor deposit composed of multiple layers from many different projects. Dredged material emanating from exceptionally large projects is usually directed to other locations within the disposal site. Such locations are often marked with a secondary buoy to guide the disposal barges and create a discrete seafloor deposit that can be monitored independent of any other mounds at the site.

1.3 Project Timeline

1.3.1 1998-99 Dredging and Disposal Overview

Throughout the 1998-99 dredged material fate study at PDS, the sampling and monitoring efforts in the dredging areas within Portland Harbor and at PDS needed to be closely coordinated with the dredging schedule. A baseline multibeam bathymetric survey was performed at PDS in September 1998 in preparation for the placement of a large volume of dredged material from Portland Harbor and the vicinity (anticipated volume was on the order of 500,000 m^3 of material; actual total volume from 1998-2000 disposal operations was 448,900 m^3). From this detailed multibeam bathymetry, a project-specific disposal point was selected on the seafloor within the PDS boundary. In November 1998, a DAMOS disposal buoy, labeled "PDA 98", was placed at the coordinates 43° 34.147´ N, 70° 02.209´ W (NAD 83) within a naturally occurring basin feature on the PDS seafloor approximately 650 m southwest of the DG buoy (Figure 1-3).

Dredging operations in Portland Harbor began in mid-November 1998. The sequence of dredging, which we display in three phases, was developed in response to concerns of the local lobster fishermen in an attempt to minimize potential adverse impacts on lobster populations within the harbor. Although all sediments to be removed from the federal

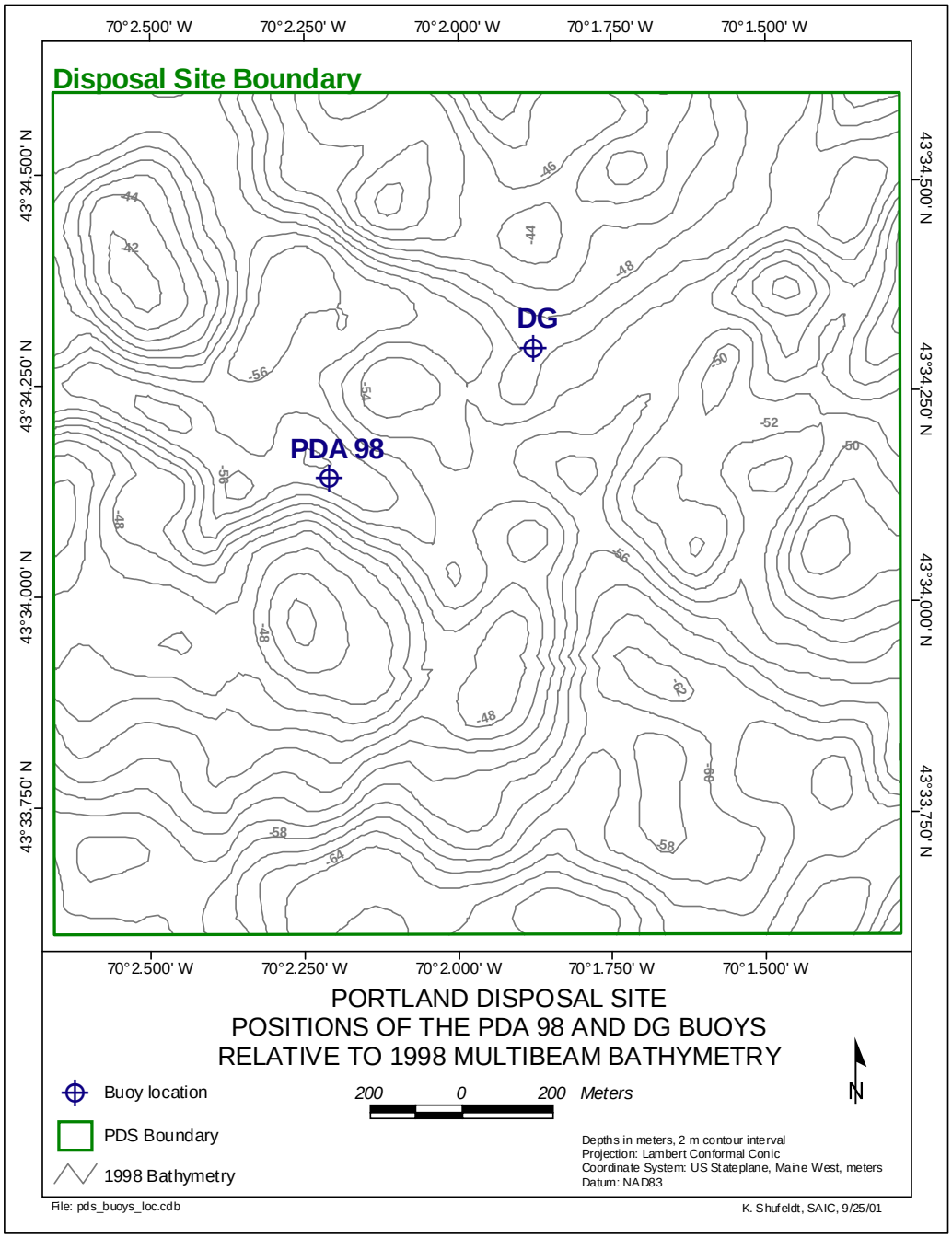

Figure 1-3. Position of the PDA 98 and US Coast Guard "DG" Buoy relative to the Portland Disposal Site boundary and major bathymetric features (contours show depth in meters).

channel had been classified as suitable for unconfined open-water disposal, it was recommended that the interior portions of Portland Harbor (consisting of silts and clay) be dredged and disposed first and eventually covered by the coarser grained sediments present near the harbor entrance. The first phase of dredging resulted in the removal of an estimated barge volume of 291,500 m³ of dredged material from inner Portland Harbor locations between 17 November and 16 December 1998. The material was transported to PDS in 4,588 m^3 (6,000 yd³) split-hull disposal barges and deposited at the PDA 98 buoy (Figure 1-4). The DAMOS disposal logs showing the volumes of sediment associated with specific dredging projects are presented in Appendix A.

The second phase of dredging (mid-December 1998 through early March 1999) consisted of smaller dredging operations removing sediment from individual berthing areas and marinas within Portland Harbor. Dredging of the federal channel was discontinued during this time period to allow inshore lobstermen to complete a catch and release program. Material dredged during this phase of the project was loaded into smaller, pocket-type disposal barges with a capacity of 380 m³ to 900 m³ (500 to 1,200 yd³) and deposited at the PDA 98 buoy. These smaller dredging projects (Dimillo's Marina, Mobil Oil, and Southport Marine) contributed an additional 5,700 m³ of dredged material at PDS (Figure 1-4; Appendix A).

The third and final phase of the project focused on the outer Harbor area and occurred through the spring of 1999. An estimated barge volume of 155,800 m³ was removed from the federal channel, transported to PDS in 3,050 m³ (4,000 yd³) split-hull barges, and deposited at the DG buoy. An additional 18,500 m³ of material produced by dredging projects at the Sprague Energy and Mobil Oil docking facilities was deposited at the PDA 98 buoy during this third phase (Appendix A), using a 1,160 m³ (1,500 yd³) pocket-type disposal barge.

During the 1999-2000 dredging season, an additional 18,300 m³ of material dredged from the Yacht Haven, Inc. and Mobil Oil Co. facilities was deposited within PDS at the DG buoy (Figure 1-4). Because this material was placed within PDS prior to the final multibeam survey that was used to develop the actual disposal mound morphology, it was also taken into account in some of the modeling runs.

1.3.2 1998-2000 Data Acquisition and Monitoring Overview

Data acquisition and monitoring operations took place before, during, and after the 1998-1999 Portland Harbor dredging project (Figure 1-4). To provide realistic input parameters and thereby improve the accuracy of the STFATE and MDFATE models, a series of field surveys was conducted from September 1998 through April 1999. The field effort included multibeam bathymetry and side-scan sonar surveys to characterize bottom topography and seafloor features in and around PDS, gravity coring and grab sampling to

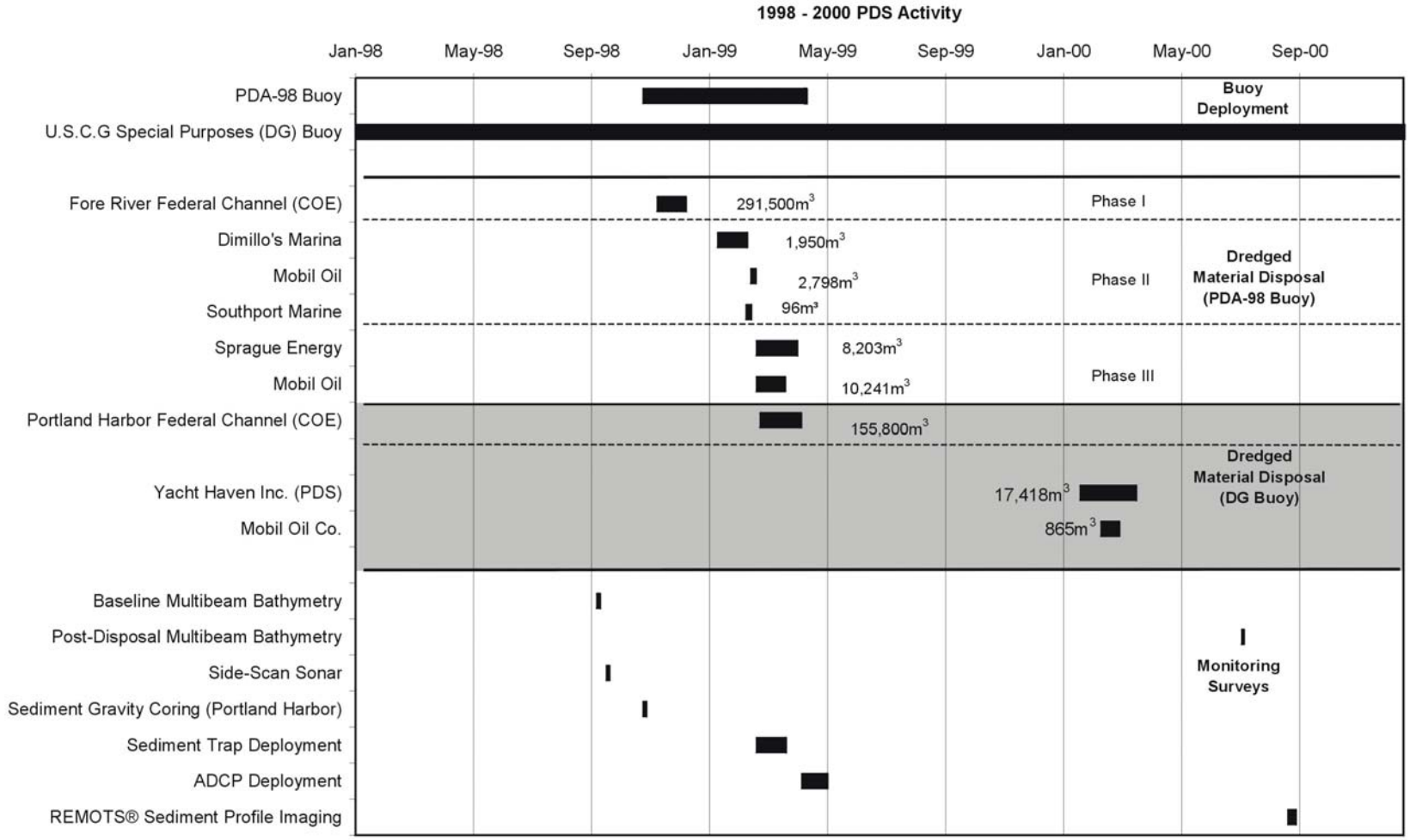

Figure 1-4. Timeline of dredged material disposal and environmental monitoring efforts at the Portland Disposal Site from 1998 through September 2000

characterize sediments at both the dredging area and the disposal site, measurements of current speed and direction throughout the water column at PDS using an Acoustic Doppler Current Profiler (ADCP), and characterization of water column density structure using a Conductivity-Temperature-Depth (CTD) instrument (Figure 1-4). The measurement data were used to develop project-specific inputs to the STFATE and MDFATE models and to improve the general understanding of water column dynamics at PDS.

During dredged material placement operations in March 1999, sediment traps were positioned within and around PDS in an attempt to measure the potential transport and settling of the disposed material onto the bottom at various locations. As part of the sediment trap study, selected pre-dredging core and grab samples from Portland Harbor and PDS, as well as the material captured within the sediment traps, were analyzed to determine the presence of potential mineralogical and microfossil tracers. The results of the sediment trap survey were, in turn, used to evaluate the output from the STFATE model with respect to dredged material transport and deposition. More than a year after the completion of the dredging and disposal operations, a sediment-profile imaging survey and a second multibeam bathymetric survey were conducted during summer 2000 to generate accurate depictions of the disposal mound footprint and morphology, which were subsequently used to evaluate the output from the MDFATE model. The various data acquisition and monitoring techniques are described in full detail in Section 2.0.

1.4 Objectives and Predictions

The comprehensive dredged material fate study described in this synthesis report was designed to address the following objectives:

1) Use the bathymetric, water column, and sediment composition data acquired at Portland Harbor and PDS from 1998 through 2000 to provide project-specific input to the STFATE and MDFATE models;

2) Use the STFATE model results to estimate the extent and duration of the sediment plume generated by a single disposal event at PDS based on a number of different variables (e.g., dredged material composition, barge volume, current patterns, etc.); and

3) Use the MDFATE model results to estimate the size and extent of the dredged material deposit resulting from multiple placement events.

The dredged material fate study conducted at PDS was designed to test the following predictions:

- The sediment plume generated by a disposal event at the PDA 98 buoy would tend to spread beyond the disposal site boundaries before dissipating to background turbidity levels (based on the water column current patterns and the water depths within PDS, as well as the composition of the dredged material); and

- The actual disposal mound morphology as depicted by the before- and after-placement multibeam survey data would be comparable to the mound morphology predicted by the MDFATE model.

2.0 METHODS

The dredged material fate study conducted at PDS required a multi-disciplinary approach, with several field data collection and computer-based modeling elements. The field efforts employed a variety of sampling equipment and instrumentation, the specific uses of which are described in detail below.

Survey vessel support over the two-year period was provided by the M/V *Beavertail*, operated by P&M Marine Services in Jamestown, RI; the University of New Hampshire's R/V *Gulf Challenger* from Portsmouth, NH; the F/V *Susan Caitlyn* from Portland Harbor, ME; and SAIC's R/V *Ocean Explorer*. These vessels were used to conduct different survey elements based on duration of the field effort, technical discipline, and their availability (Table 2-1). Over a two-year period, SAIC performed precision multibeam bathymetry and side-scan sonar surveys, sediment-profile imaging, sediment grab sampling and coring operations, as well as the deployment and recovery of a disposal buoy. In addition, current profilers and sediment traps were deployed and recovered at PDS. Because the surveys were conducted under several separate mobilizations, the specifics regarding the positioning and navigation systems used for each survey are described below in the individual sections.

In general, the field operations supported one of two main objectives: 1) to provide the detailed site- and time-specific data required for input to the STFATE and MDFATE models; and 2) to provide the "ground-truth" monitoring data needed to evaluate the results of the STFATE and MDFATE models. With the exception of the final multibeam survey, the sediment-profile imaging survey, and the sediment trap deployment, all other data acquisition efforts were geared primarily toward the development of accurate modeling parameters. The initial multibeam survey data, which provided the baseline seafloor bathymetry for the modeling runs and was also used to generate the depth difference results, was the only data set that was used to fulfill both main objectives.

2.1 Sediment Coring

The sediment collection activities in Portland Harbor were conducted prior to dredging operations to characterize the geotechnical properties (i.e., grain size distribution, bulk density, specific gravity, and Atterberg Limits) of the ambient, pre-dredged sediments. A series of 20 stations were originally established for the collection of sediment cores and surface sediment grab samples in Portland Harbor. Sampling stations were specifically placed in areas identified for dredging in the NAE dredging plan to achieve the 11 m (35 ft) controlling depth (Figure 2-1; Table 2-2). One station (Station 12) was omitted from the sampling plan due to concerns related to an underwater cable crossing in the interior portions of Portland Harbor; therefore, Figure 2-1 depicts the locations of a total of 17 coring and 19 grab stations occupied as part of the sediment characterization effort.

Table 2-1. Summary of Field Operations over the Portland Disposal Site 1998-2000

Work Site	Operation	Date	Vessel
PDS	Multibeam Survey	9/14/98	M/V Beavertail
PDS	Side Scan Sonar Survey	9/24/98	M/V Beavertail
PDS	Buoy Deployment	11/02/98	R/V Gulf Challenger
Portland Harbor	Sediment Collection	11/03/98	R/V Gulf Challenger
Portland Harbor	Sediment Collection	3/03/99, 3/11/99, 3/18/99	M/V Beavertail
PDS	ADCP Deployment and Sediment Trap Deployment	3/18/99	M/V Beavertail
PDS	ADCP Recovery and Sediment Trap Recovery	4/19/99, 4/20/99	M/V Beavertail
PDS	Sediment Trap Recovery	5/27/99	F/V Susan Caitlyn
PDS	Multibeam Survey	6/01/00	R/V Ocean Explorer
PDS	Sediment-Profile Imaging Survey	9/21/00, 9/22/00	M/V Beavertail

Table 2-2. Portland Harbor Coring Locations November 1998 and March 1999

Station	Location	Latitude	Longitude
		NAD 83	
PH3	Harbor Entrance	43° 39.600´ N	70° 14.114´ W
PH4	Harbor Entrance	43° 39.622´ N	70° 14.376´ W
PH5	Portland Harbor	43° 39.218´ N	70° 14.637´ W
PH6	Portland Harbor	43° 38.743´ N	70° 15.319´ W
PH7	Portland Harbor	43° 38.956´ N	70° 15.096´ W
PH8	Portland Harbor	43° 38.947´ N	70° 15.274´ W
PH9	Portland Harbor	43° 30.219´ N	70° 14.925´ W
PH10	Portland Harbor	43° 39.057´ N	70° 14.925´ W
PH11	Portland Harbor	43° 30.113´ N	70° 14.808´ W
PH13	Fore River	43° 38.487´ N	70° 17.015´ W
PH14	Fore River	43° 38.322´ N	70° 16.649´ W
PH15	Fore River	43° 38.408´ N	70° 16.526´ W
PH16	Fore River	43° 38.515´ N	70° 16.351´ W
PH17	Fore River	43° 38.504´ N	70° 16.113´ W
PH18	Fore River	43° 38.559´ N	70° 15.953´ W
PH20	Fore River	43° 38.604´ N	70° 15.710´ W

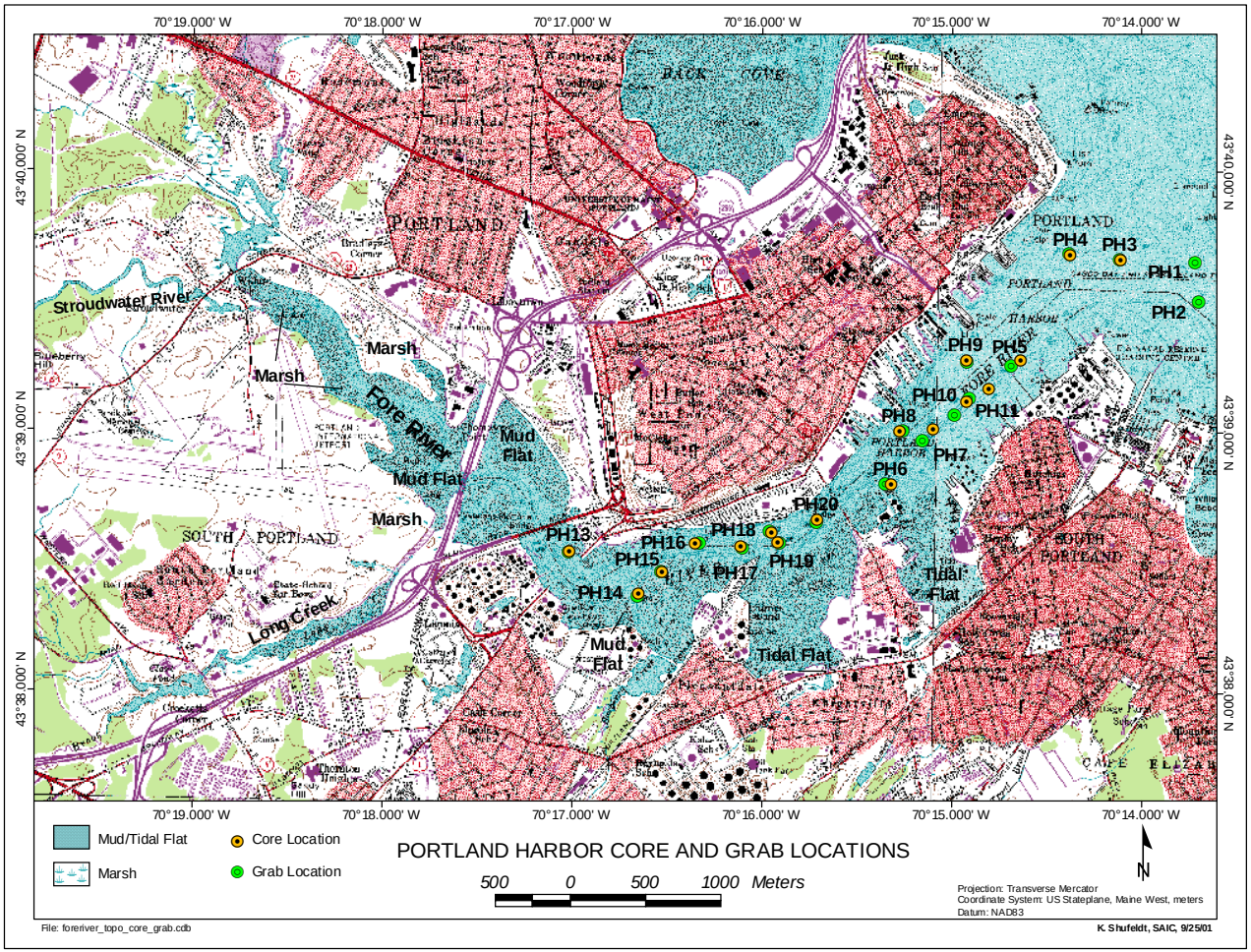

Figure 2-1. USGS topographic quad map showing the location of the Portland Harbor sediment cores and grab samples. This aerial view also illustrates the freshwater sources, marshes, and tidal mudflats in close proximity to the dredging area

The sediment coring operation was divided into two field efforts to facilitate the survey and dredging project logistics. During the 3 November 1998 field effort, a single gravity core sample was obtained at each of seven stations located in the upstream portion of the project area (Figure 2-1; Table 2-2). On 3 March 1999, a single core sample was obtained at each of an additional nine stations located in outer portions of the project area (Figure 2-1; Table 2-2). Although repeated attempts were made, no acceptable cores could be collected from Stations PH-1 and PH-2 near the harbor entrance due to the presence of a thick layer of sand. Firm glacial clay likewise prevented the collection of a deep cross-sectional sample at Station PH-19, where only a short clay plug was retained.

2.1.1 Positioning and Navigation

A Trimble 4000 DSi Global Positioning System (GPS) receiver interfaced with a Magnavox MX50R differential beacon receiver provided precise navigation data during the sediment sampling operations. The U.S. Coast Guard differential beacon broadcasting from Brunswick, ME (316 kHz), was used for generating the real-time differential corrections because of its proximity to the survey area. During sampling operations, the Trimble DGPS system output real-time navigation data (latitude and longitude) in the North American Datum of 1983 (NAD 83) at a rate of once per second to an accuracy of ±3 m.

The DGPS positioning data were ported to SAIC's Portable Integrated Navigation and Survey System (PINSS). This system utilizes a Toshiba DX3200 series computer to provide real-time navigation, data logging, and helm display. PINSS maintains a project database for the storage of target sampling locations as well as recording actual position and time for individual samples.

2.1.2 Sediment Core Collection

Sediment cores were collected with a gravity coring device to obtain cross-sections of the Portland Harbor sediment to the depth of dredging, including the allowable over-depth when possible. The coring device consisted of a weighted driver section attached to a 1.5 m (5 ft) steel core barrel (9.5 cm I.D.). A chemically inert, clear Lexane® liner (8.9 cm I.D.) was fitted within the core barrel, with stainless steel core cutter and catcher assemblies secured to the end (Figure 2-2). The core was suspended in the water column by the research vessel via a single steel cable attached to a deck winch. Once on station, the gravity corer was allowed to free-fall approximately 6 to 8 meters before impacting the bottom. The corer was then retrieved using the winch and placed on the deck of the research vessel.

Upon retrieval of the coring device, the internal liner containing the sediment sample was removed from the core barrel. The cores were inspected to ensure that there was a sufficient quantity of material for the intended analyses. The core was then capped with a foam plug and plastic core cap to prevent loss of sediment, labeled with a unique identifier,

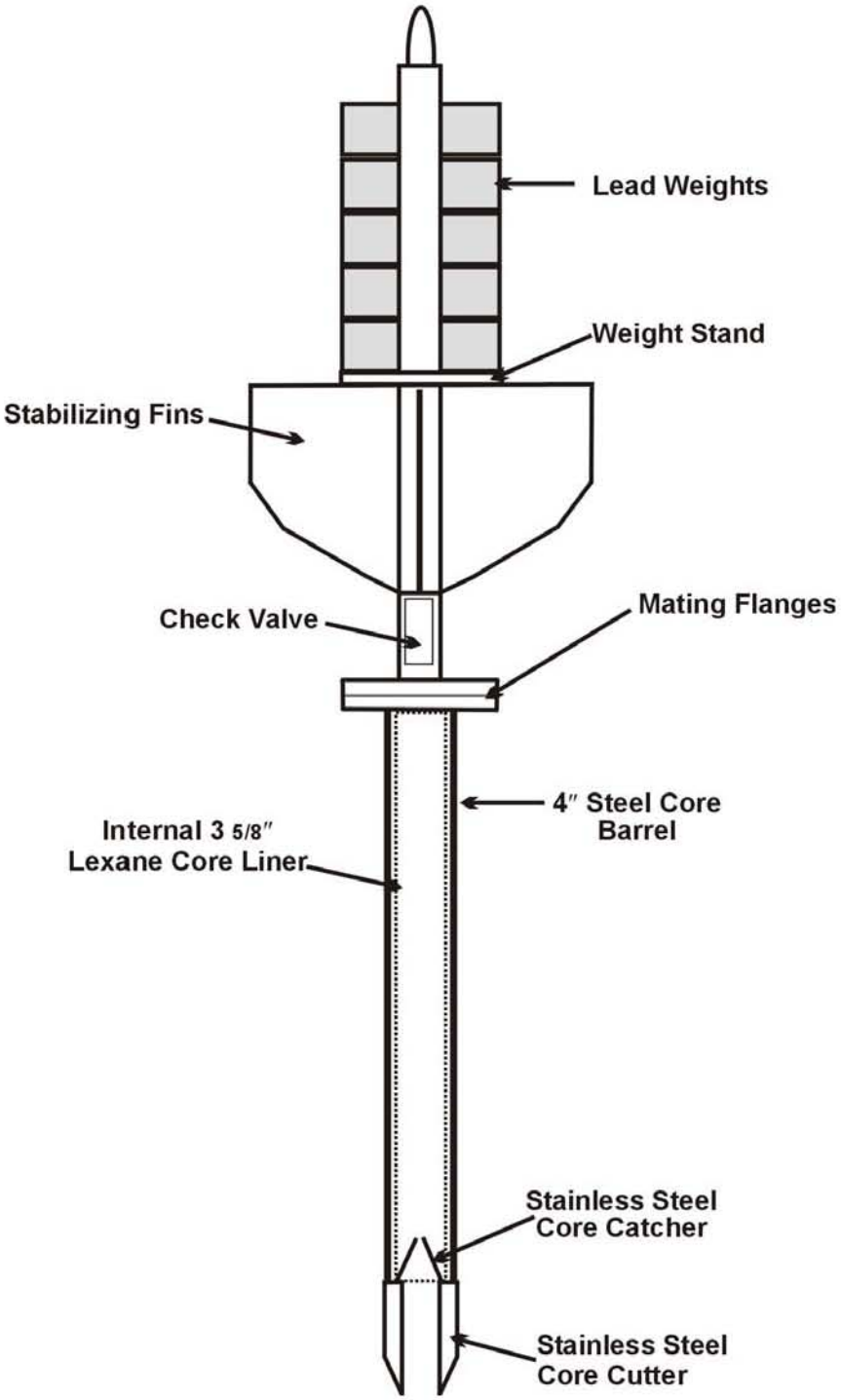

Figure 2-2. Schematic diagram of the gravity coring device utilized as part of the Portland Harbor and Fore River sediment characterization effort

measured, and stored at 4°C with minimal exposure to sunlight. At the conclusion of this field operation, all cores were transported to the University of Rhode Island Graduate School of Oceanography (GSO) core facility and refrigerated at 4°C until analyzed.

2.1.3 Sediment Core Processing

Four of the nine cores collected during the 3 March 1999 survey (PH-4, PH-6, PH-7, and PH-9) were processed (split, described, photographed, and sub-sampled) at the GSO Rock and Core Laboratory on 10 June 2000. These four cores were selected because they were considered to be representative of the types sediment removed from the outer Portland Harbor and deposited at PDS during the third phase of the maintenance project. It was anticipated that the fine-grained fraction of this material would comprise the sediment plume formed by disposal operations during the third phase of the project which would potentially be captured by a series of sediment traps (see Section 2.7) deployed around PDS during that period.

The liner for each core was split using a specialized core splitting device. During this process, care was taken to cut only the core liner and not the enclosed sediment. The scored liner was then transferred to a laboratory bench where the thin layers of the grooved core Lexane® tube were cut using a pre-cleaned utility knife. Finally, thin piano wire was pulled through to split the sediment axially into two halves. This process eventually yielded two core halves maintained in a natural, undisturbed condition. After splitting, one half-section of each core was placed in a specially designed cradle labeled with a centimeter scale to determine sampling depth and to provide a linear reference for core sampling and descriptions using standard logging procedures. The standard core logging procedures consisted of recording visual descriptions of each sedimentary layer in a standardized spreadsheet using Munsell™ color charts and codes. Sediment grain size was visually assessed using the Wentworth grade scale (Wentworth 1922).

The definition of lithologic boundaries and criteria of subfacies types were noted. The depth or depth intervals of various features within each core were recorded to the nearest centimeter. Macroscopic information included color patterns, mottling, sedimentary structures, the nature of contacts and boundaries (sharp-gradational), and the character of laminations, rhythms, layers, and transitions. Special features, such as occurrences of fossils, wood, organics, etc., were noted in the spreadsheet.

The second core half was mounted in an identical cradle device and photographed with a digital camera. The camera was mounted on a specialized copy stand equipped with a daylight-balanced light source. A series of photographs were taken at a 1 m distance from the core, each encompassing a 50 cm interval along the core. The focal distance was kept constant so that individual photographs were properly scaled, allowing the digital images to be merged to form a continuous representation of the core. The descriptions and

photographs were later combined using commercial software to produce the annotated cores presented in the appendix. Upon completion of photography, the core halves were sealed with plastic wrap to prevent excess drying and stored at the core facility until chemical data were received.

The remaining 12 cores (PH-03, PH-05, PH-08, PH-10, PH-11, PH-13 through PH-18, and PH-20), obtained during both the November 1998 and March 1999 surveys, were split and visually described in the manner described above. Each core was archived and stored at the core facility so that additional sampling for geochemical data such as specific gravity, grain size or x-ray diffraction could be performed, if necessary. Photographs and detailed descriptions of these cores are also presented in Appendix B.

2.1.4 Sediment Core Analyses

Three horizons from each of Cores PH-4, PH-6, PH-7, and PH-9 were sampled and subsequently analyzed for sediment grain size, bulk density, specific gravity, water content, and Atterberg Limits, using the standard methods described below. Applied Marine Science, Inc. of League City, TX, performed the geotechnical analyses for this study.

Grain Size

Grain size analyses were conducted using a modified American Society for Testing and Materials (ASTM) Method D422-63 (sieve and hydrometer). The samples from each core were sieved into size fractions greater than 62.5 µm (sand and gravel), and less than or equal to 62.5 µm (silt and clay). The gravel and sand fractions were subdivided further by mechanically dry sieving through a graded series of screens. The silt and clay fractions were subdivided using a partial hydrometer technique. Data on grain size were then used to determine percent composition of gravel, sand, silt, and clay for reporting in this document.

Wet Bulk Density

Wet bulk density analysis determines the weight of a known volume of wet sediment. Bulk density analysis is useful to track changes in porosity and thus compaction state of a sediment sample. ASTM Method D2937, which covers the determination of in-place density of a soil by the drive-cylinder method, was utilized. Similar to USACE Method EM 1110-2-1906, this testing method involves obtaining a relatively undisturbed soil/sediment sub-sample by driving a thin-walled cylinder of a known volume into a section of the core to obtain test material. The sub-sample is then weighed to provide a mass per unit volume ($g \cdot cm^{-3}$). Assuming no void space due to air, the wet mass of sediment is divided by the volume and yields the bulk density of the sediment.

Specific Gravity

Specific gravity is a measurement that determines the density of minerals within a sediment sample. Two minerals may be the same size, but their weight may be quite different. The specific gravity of a mineral determines how heavy it is by measuring its weight relative to water. Specific gravity values are based on the mass of a sediment sample, relative to an equal volume of water.

The determination of specific gravity utilized ASTM Method D854, which determines the specific gravity of soil solids that pass the 4.75-mm (No. 4) sieve by means of a water pycnometer. Specific gravity is the ratio of the mass of a unit volume of a material at a known temperature to the mass in air of gas-free distilled water with the same volume and at a known temperature. Thus, the results of the specific gravity analyses are reported as a ratio and are unitless.

Water content

The determination of water (seawater) content utilized ASTM Method D2216. This test method covers the laboratory determination of the water (moisture) content by mass of soil, rock, and similar materials where the reduction in mass by drying is due to complete loss of water. The water content is defined as the ratio of the mass of water in a given sediment sample to the mass of the solid particles. The results of these tests are expressed as a percentage and can often range from 50% for very cohesive and dry material to 250% for unconsolidated, wet sediments.

Atterberg Limits

Plastic sediment is a soil that has a range of water content over which it exhibits plasticity and which will retain its shape on drying. The liquid limit and plastic limit of soils (along with the shrinkage limit) are often collectively referred to as the Atterberg limits. These limits distinguish the boundaries of the several consistency states of soils or sediments (solid, semisolid, plastic, and liquid) and are primarily based on water content. The liquid limit defines the water content boundaries between plastic and viscous fluid states and is expressed as a water content percentage. The plastic limit is also a measure of the water content percentage of a soil, but defines the boundary between the plastic and brittle (semisolid) states of a soil at the arbitrarily defined boundary. The plasticity index defines the complete range of the plastic state. Numerically, the plasticity index is the difference between the liquid limit and the plastic limit.

The Atterberg limits test method is used as an integral part of several engineering classification systems to characterize the fine-fraction of soils. This test method (ASTM-D4318) is a standardized wet multi-point procedure for determining the liquid limit (LL),

plastic limit (PL), and plasticity index (PI) of soils and sediments. Fine-grained, marine sediments (silts and clays) are tested to determine the liquid and plastic limits and produce comparable numbers for use in sediment identification, classification, as well as correlation to bearing and shear strength.

2.2 Sediment Grab Sampling

In conjunction with the gravity coring conducted on 3 November 1998, a single sediment grab sample was collected at each of the 19 stations located in Portland Harbor (Figure 2-1, Table 2-3). Each surface grab sample was physically described upon retrieval in an effort to characterize the general composition of sediment throughout the harbor, with findings recorded in standardized data sheets. Each grab sample was then sub-sampled to provide sufficient quantity of material for geotechnical and sediment tracer analyses. In addition, a baseline sediment grab sample was collected within PDS (sample PDS-Buoy2) at the location of the PDA 98 disposal buoy prior to the deposition of Portland Harbor material (Table 2-3).

Sediment sampling was performed using a Young-modified, Van Veen grab with a surface area of 0.1 m^2. The grab sampler was constructed entirely of stainless steel, and the bucket and doors were Kynar® coated to provide a chemically inert sampling device. The grab sampler was deployed at each coring station to aid in characterizing the surface sediments and supplement the information provided by the cores. The sub-sample retained for sediment tracer analyses was preserved in a stained and buffered seawater/formalin solution to prevent the oxidation of the calcareous shells, or tests, of the microorganisms. These sub-samples were then stored at the SAIC Environmental Testing Center in Narragansett, RI, as archived samples for possible further analysis. The second sub-sample from each grab was placed in a sealed plastic bag and stored in preparation for supplemental geotechnical analysis. The material retained from Stations PH-13 and PH-17 was eventually used for both geotechnical and sediment tracer analysis in order to characterize the surficial sediments of the interior portion of Portland Harbor.

2.3 Sediment Tracer Analyses

Sediment tracers were first introduced to the DAMOS Program in support of the 1995-1997 Portland Disposal Site Capping Demonstration Program (Morris et al. 1998). A sediment tracer is a unique identifier that allows a layer of sediment placed at a disposal site to be linked back to the source area. Sediment tracers can be based on chemistry, grain size, mineralogy, organic load, microorganisms, or a host of other sediment characteristics. After evaluating several options, the most effective sediment tracer examined as part of the PDS capping demonstration project was determined to be microfossil content. The use of this type of tracer required detailed microscopic examination and characterization of the project sediments.

Table 2-3. Portland Harbor and PDS Grab Sampling Locations
November 1998

Station	Location	Latitude	Longitude
		NAD 83	
PH1	Harbor Entrance	43° 39.591´ N	70° 13.723´ W
PH2	Harbor Entrance	43° 39.444´ N	70° 13.700´ W
PH3	Harbor Entrance	43° 39.603´ N	70° 14.117´ W
PH4	Harbor Entrance	43° 39.626´ N	70° 14.382´ W
PH5	Portland Harbor	43° 39.195´ N	70° 14.692´ W
PH6	Portland Harbor	43° 38.742´ N	70° 15.351´ W
PH7	Portland Harbor	43° 38.908´ N	70° 15.159´ W
PH8	Portland Harbor	43° 38.944´ N	70° 15.261´ W
PH9	Portland Harbor	43° 39.211´ N	70° 14.923´ W
PH10	Portland Harbor	43° 39.009´ N	70° 14.985´ W
PH11	Portland Harbor	43° 39.073´ N	70° 14.911´ W
PH13	Fore River	43° 38.480´ N	70° 17.020´ W
PH14	Fore River	43° 38.314´ N	70° 16.659´ W
PH15	Fore River	43° 38.408´ N	70° 16.534´ W
PH16	Fore River	43° 38.515´ N	70° 16.332´ W
PH17	Fore River	43° 38.498´ N	70° 16.103´ W
PH18	Fore River	43° 38.564´ N	70° 15.961´ W
PH19	Fore River	43° 38.515´ N	70° 15.913´ W
PH20	Fore River	43° 38.596´ N	70° 15.719´ W
PDS Buoy2	PDS	43° 34.069´ N	70° 02.074´ W

During the 1995-1997 capping project, foraminifera (unicellular organisms that produce minute shells) assemblages were found to be significantly different between dredged material layers which originated from the Royal River and the underlying ambient sediment in cores collected previously at PDS (Morris et al. 1998). Furthermore, the strong zonation within the Royal River estuary yielded sufficient differences in the species of foraminifera and other microscopic, unicellular organisms (e.g., thecamoebians) to allow identification of individual layers within the disposal mound (UDM/CDM). Consequently, the sediment tracer analysis was found to be a useful tool, and in the case of the 1995-1997 PDS Capping Demonstration Project, was proven to be a strong indicator of change in the origin of the sediment within a multi-layered deposit.

Prior to performing the same detailed sediment tracer analyses on cores and grab samples collected in association with the 1998-1999 Portland Harbor dredging project, a literature search was conducted to investigate differences in the estuarine sediments of Portland Harbor and the marine sediments of the Gulf of Maine. Detailed information on mineralogical content or biota specific to the surface sediments to be dredged from the Fore River and Portland Harbor was not found from an extensive search. However, significant differences in water depths, salinity, and distance from terrestrial sources that exist between the harbor and PDS were expected to result in different sediment compositions and therefore to yield unique tracers.

In general, microorganism populations differ between freshwater, brackish, and saltwater habitats, allowing for potential unique identification of sediments corresponding to the origin of the microorganism. Based on the success of the 1995-1997 project, foraminifera and thecamoebians were once again selected for examination as potential useful sediment tracers in the present study. The classification of these microfossils is based primarily on characteristics of the shell. Wall composition and structure, chamber shape and arrangement, the shape and position of any apertures, surface ornamentation, and other morphologic features of the shell are all used to define taxonomic groups.

In the present study, each sample was initially sieved to separate the sediment into "coarse" and "fine" fractions. The coarse fraction consisted of the material retained on a 500 µm (0.5 mm) screen, while the fine fraction consisted of the material that had passed through the 500 µm screen but was retained on a 63 µm screen. The coarse fraction was examined to determine its primary and secondary components and to evaluate if any of these components represented a unique tracer. However, it is the fine sediment fraction (sediment grain diameters ranging in size from 63 to 500 µm) that typically contains the microfossils and other potential microbiological tracers. This fraction was examined to identify and enumerate microfossils, different types of minerals (e.g., mica or quartz), and various biological constituents (e.g., insect parts, plant fragments, diatoms, ostracods, shell fragments) that might serve as tracers and ultimately yield insight into the potential transport and settlement of plume sediments at PDS.

A total of nine sediment samples were examined microscopically to determine their mineralogical and microbiological components. This included the sediment core samples collected on 3 March 1999 at stations PH-4 and PH-7 in Portland Harbor (samples PH-4 and PH-7; Figure 2-1), one grab sample collected at station PH-17 in Portland Harbor in November 1998 (sample PH-17AG; Figure 2-1), one grab sample collected at the PDA-98 buoy location in November 1998 (sample PDS-Buoy2), and one grab sample collected in March 1999 at the deployment location of Sediment Trap 3 (sample PDS-3G). The remaining four samples were analyzed from the sediment traps following their retrieval: sample PDS-ST3 (upper 0-2.5 cm interval), sample PDS-ST3 (2.5 to 5.0 cm interval), sample PDS-ST8 and sample PDS-ST10. The laboratory methods used to determine mineralogy and microfossil content are described in the following section.

The coarse sediment fraction (retained on the 0.5 mm, or 500 µm, screen) was first examined to identify relatively large-scale components and then dried and weighed. The fine sediment fraction was retained on a stainless steel U.S. Standard Sieve No. 230 having mesh openings of 63 µm, while the silt-clay fraction (<63 µm) was allowed to flow through the sieve and was discarded. The fine fraction samples as defined herein therefore represent the very fine to medium sand component of the sediment. These were examined through a microscope to determine type and number of microfossils, as well as mineralogical composition. For this study, the term microfossil includes only foraminifera and thecamoebians, some of which may have been living meiofauna at the time of collection. However, most of the identified microfossils were likely the shells, or tests of previously living organisms that had been preserved with the accumulation of sediment since the last dredging operation.

To prepare the samples for analysis, the fine fraction material retained on the 63 µm sieve was soaked in a distilled water and Calgon solution to separate the sediment particles from the microfossils. The water/sediment mixture was then washed under a gentle stream of distilled water, and any silt-clay sized sediment passing through the sieve was discarded. The sediment remaining on the sieve was a concentration of sand-sized material that included foraminifera and any other microfossils present in the sample. This material was rinsed onto filter paper and placed within a funnel, allowing the sample to drain and then air dry. When dry, the grains typically did not adhere to one another. If they did, the soaking/sieving procedure was repeated. When satisfactorily clean, each dried sample was stored in a labeled vial until ready for microscopic examination. This procedure was performed at the laboratory facilities of Normandeau Associates, Inc. (NAI) in Bedford, NH.

For the preliminary sediment tracer analyses, selected samples were analyzed under a binocular microscope (magnification 40 to 100×). Using a metal spatula, a small amount of material randomly taken from each sample was placed on a brass micropaleontological picking tray having a grid of rectangular subdivisions, all of equal size. The surface of the tray was a dull black (to minimize reflection), and the grid lines were white. Microfossils

(foraminifera and thecamoebians) were picked until 30-100 specimens of foraminifera were collected, or 5-10 full trays of material had been analyzed. The microfossils were mounted on cardboard slides with aluminum holders and glass cover slides.

Individual foraminifera specimens encountered while examining samples across the picking tray were picked and mounted for permanent reference. A recessed area in an 18-ply cardboard slide provided a black background that was coated with water-soluble glue (Tragacanth). Any foraminifera specimens encountered on the picking tray were captured using the wetted tip of an artist's brush (size 000, sable hair). This procedure involved simply dipping the tip of the brush in water, touching it to the specimen to be picked, and then transferring the specimen to the glued slide. The glue, being water soluble, then dried and secured the specimen to the slide. Adding water will release the glue, so that specimens can be turned and viewed from different perspectives. Finally, after completion of picking each sample, a metal clip was used to hold a glass cover slide over the cardboard micropaleontology slide to protect specimens for prolonged storage at the SAIC Newport office.

During the examination of the sediment samples for microfossils, observations of minerals and other potential sediment tracers (e.g., microorganisms such as diatoms and ostracods) were also recorded. The relative abundance of each parameter was noted and described. For displaying and interpreting data, the microfossils were grouped into five categories based on a combination of factors: the identified informal group (foraminifera or thecamoebian), the ecological zonation (freshwater, mudflat, marsh, or continental shelf), and shell composition (agglutinated [silica] or calcareous) for foraminifera only.

To determine the abundance of freshwater thecamoebians, marsh foraminifera, mudflat foraminifera, shelf agglutinated foraminifera, and shelf calcareous foraminifera, the number of individuals per category were recorded. Because the microfossil data were part of a preliminary feasibility study to determine the utility of this tracer technique for the 1998-1999 Portland Harbor dredging project, expert micropaleontologic analysis was not conducted to verify the initial taxonomic identifications.

2.4 Multibeam Bathymetric Surveys

In recent years, the limitations of precision single-beam bathymetry have been noted in studies performed over PDS. The topography of PDS consists of steep ridges and deep depressions which promote the development of significant, slope-related survey artifacts when comparing two sequential, single-beam bathymetric surveys (Morris et al. 1998). As a result, the use of swath bathymetry (multibeam) capable of providing complete coverage of the seafloor was recommended in an attempt to reduce the occurrence and significance of survey artifacts in depth difference comparisons.

Two high-resolution multibeam bathymetric surveys were completed over PDS in support of the dredged material fate study. The baseline survey for this study was performed in September 1998 and covered a large area of seafloor surrounding PDS. This was the first master bathymetric survey completed with the use of DGPS in the horizontal control datum of NAD 83. It provided the high-resolution bathymetry of the PDS seafloor that was an important component for the subsequent dredged material disposal modeling efforts. The second survey was performed in July 2000 and covered a much smaller area over PDS. This data set was used in conjunction with the baseline survey to determine the actual morphology of the dredged material deposit at PDS resulting from the disposal operations associated with dredging projects conducted between the two surveys. Detailed explanations pertaining to multibeam bathymetry and the configuration of the survey system employed at PDS during the September 1998 and July 2000 surveys are presented in Appendices C and D.

2.4.1 Survey Areas

In September 1998, SAIC conducted a DGPS master bathymetric survey over the historic 17.7 km^2 disposal area with a high-resolution multibeam survey system. The current 3.42 km^2 disposal site lies within this larger dredged material disposal site established by the War Department in 1946 (Figure 2-3; Table 2-4; EPA 1996). The master bathymetric survey was performed over this much larger area to characterize the seafloor surrounding the current disposal site boundary and to develop insight regarding the dynamics influencing the behavior of sediments deposited at PDS.

The 1998 survey covered the trapezium-shaped area and consisted of 32 lanes along an azimuth of 97°, which corresponds to the southern boundary of the area. Lane spacing was controlled to provide a minimum of 150% swath coverage of the seafloor. Due to the irregular configuration of the survey area, survey lane lengths ranged from approximately 6,000 meters in the southern portion of the survey to less than 400 meters along the northern boundary. The M/V *Beavertail* was used as the survey platform for the September 1998 data collection effort.

The July 2000 multibeam survey was performed over the current PDS disposal site boundary aboard the R/V *Ocean Explorer*. A 2100 × 2100 m (4.41 km^2) area centered at 43° 34.125´ N, 70° 01.958´ W was established to document any changes in seafloor topography relative to the September 1998 survey (Figure 2-3). To maximize the swath coverage of the seafloor, the survey consisted of a square-shaped area with 34 primary lanes spaced at 70 m intervals and oriented along an azimuth of 81°. Due to their orientation, lane lengths ranged from 2,100 to 250 meters. Three cross lanes were run perpendicular to the main survey lanes (an azimuth of 172°), with distances ranging from 2,124 to 845 meters. In addition, multiple shorter lanes were occupied over the PDS survey area to resolve data gaps or areas of insufficient coverage.

Table 2-4. Boundaries for the 1998 and 2000 Multibeam Surveys

Survey	Corner	Latitude	Longitude
2000	NW	43° 34.692´ N	70° 01.179´ W
	SW	43° 33.558´ N	70° 01.179´ W
	SE	43° 33.558´ N	70° 02.739´ W
	NE	43° 34.692´ N	70° 02.738´ W
1998	NW	43° 35.205´ N	69° 59.969´ W
	SW	43° 32.855´ N	69° 59.969´ W
	SE	43° 33.255´ N	70° 04.169´ W
	NE	43° 34.905´ N	70° 02.819´ W

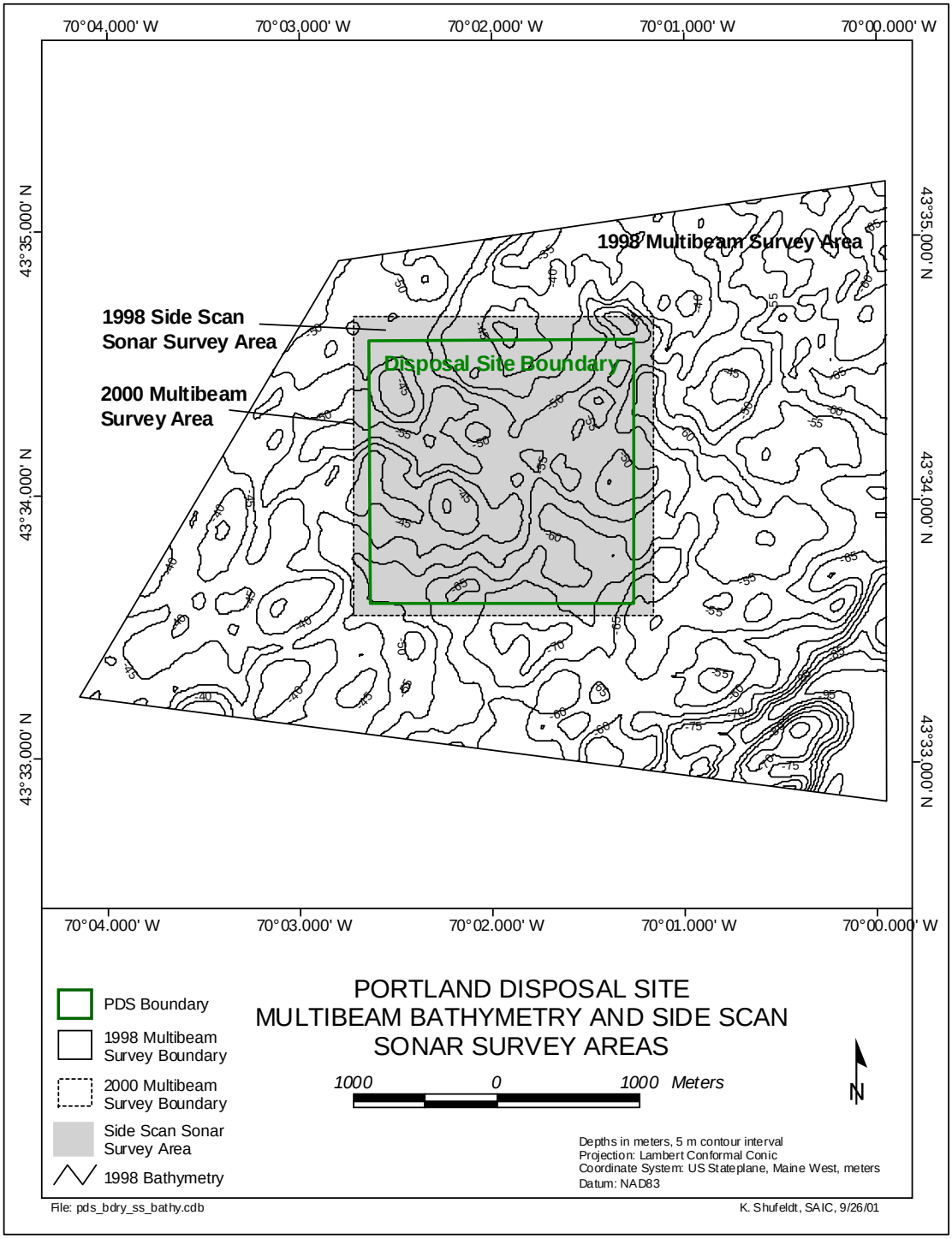

Figure 2-3. Survey boundaries established over the Portland Disposal Site as part of the 1998 and 2000 data collection efforts

2.4.2 Bathymetric Data Collection and Processing

In addition to differences in the size of the survey areas occupied, there were slight variations in the methods employed for the 1998 and 2000 multibeam bathymetric surveys performed over PDS. Summaries of the techniques are presented below, while the details pertaining to the collection and processing of the data acquired over PDS are presented in Appendix C.

2.4.2.1 Survey System

Swath bathymetry data were collected using the Reson Model 8101 SeaBat Multibeam Echo Sounder System interfaced to a Reson SeaBat 6042 Multibeam Data Collection System. The RESON 8101 utilizes 101 individual narrow beam (1.5°) transducers capable of yielding a total swath coverage of 150° (75° per side). The actual width of coverage is adjustable through range scale settings with a maximum equivalent to 7.4 times the water depth to a maximum 300 m slant range. The SeaBat 6042 Multibeam Data Collection System combines both hardware and software into a stand-alone system that provides real-time corrected displays of multibeam bathymetry data.

The primary positioning control consisted of differentially corrected GPS data from an on-board receiver ported to a central data acquisition and survey system. Differential correctors emanating from USCG differential beacon broadcasting from Brunswick, ME, (316 kHz) were used to improve geodetic positions to a tolerance of ±3 m. The GPS receivers were configured to navigate using a minimum of four satellites at an elevation angle no lower than 8°. Horizontal dilution of precision (HDOP) and age of the differential correctors were monitored automatically by the survey system so that the resulting hydrographic positioning control met predetermined specifications.

The data acquisition and survey system consisted of several subsystems (Integrated Navigation Subsystem [INS]; System control display console; Multibeam display; Multibeam sonar subsystem; and Helmsman display console) connected by a high-speed local area network (LAN). Data were time tagged and transferred between the major subsystems in real-time to facilitate the collection of all external data including DGPS position, vessel heading and information, as well as depth data. The helmsman display console was located in the pilothouse and consisted of a terminal node and a graphics monitor. The helmsman display provided the pilothouse with data on ship position as well as position relative to the survey lane and cross-track error. The helmsman display was controlled using a standard computer keyboard and pointing device, giving the helmsman the ability to change many display parameters such as display scale and center and display orientation.

2.4.2.2 Multibeam Data Corrections and Processing

A variety of corrections are typically applied to the multibeam data to ensure accurate representation of the bathymetry. Application of corrections to the PDS survey data is described in detail in Appendix C, and includes corrections for vessel position (heading, heave, pitch, and roll factors), water column structure (which affects the speed of the sound pulse transmitted from the transducer to the substrate and back), and tide stage (assessed via data from the NOAA data buoy in Portland Harbor, with corrections made for tide stage and height at the project area).

The multibeam depth data were collected by the RESON 8101/6042 system in the Generic Sensor Format (GSF) that allows flags to be set as an indication of the validity of each ping or beam within the bathymetric data. A real-time coverage monitor was used during data collection to ensure adequate coverage of multibeam data that met or exceeded International Hydrographic Organization (IHO) standards. Multibeam backscatter imagery data, similar to side-scan sonar, were collected in eXtended Triton Format (XTF). These data were collected by the RESON 6042 and stored to the hard drive. The imagery data are useful for bottom-type classification and can be mosaiced into a 1 × 1 m grid using the Triton Elics ISIS processing software.

Once the depth data were fully processed and reviewed, the data sets were gridded into 1 × 1 m, 5 × 5 m, and 20 × 20 m cells. Each cell contained a single depth value derived from averaging all of soundings that fell within that cell. When large differences were detected between soundings within the same cell, the edited multibeam files were re-examined and re-edited as needed. The resulting gridded data sets were used to evaluate coverage and quality, and to facilitate comparison between bathymetric data sets. Additional details of the comprehensive data processing methods are provided in Appendix C.

2.5 Side-Scan Sonar Survey

2.5.1 Side-Scan Sonar Data Acquisition

Side-scan sonar systems provide an acoustic representation of the seafloor topography, bottom targets, and generalized sediment characteristics by detecting the back-scattered signals emitted from a towed transducer housed in a “towfish.” The transducers emit and receive sound waves at specific frequencies typically ranging from 100 to 500 kHz. The transducer’s transmittal angles can be adjusted so that a specific swath of area is covered, such as 75 or 100 m range scale on both sides of the towfish.

Side-scan sonar data provide information on general seafloor characteristics and the size and position of distinct objects on the seafloor. Dense objects (e.g., rocks, man-made features, and firm sediment) reflect strong signals and appear as dark areas on the side-scan

records. Conversely, areas characterized by soft features (e.g., silt or muddy sediments), which absorb sonar energy, appear as lighter areas in the side-scan records.

As part of the dredged material fate study at PDS, a side-scan sonar survey was performed over a 4.41 km² area, centered at 43° 34.125´ N, 70° 01.958´ W (Figure 2-3). Sonar data were collected with an EdgeTech DF1000 side-scan sonar towfish, transmitting at a frequency of 100 kHz. The acoustic data were used to help identify depositional areas on the PDS seafloor and to investigate areas likely to be subjected to sediment advection.

Side-scan sonar operations were conducted aboard the M/V *Beavertail* on 20 and 28 September 1998. A 2100 × 2100 m survey area was established over PDS with 21 lanes spaced 100 m apart, oriented in an east-west direction, to ensure complete coverage of the disposal site. The towfish altitude was controlled to insure 120-150 percent bottom coverage over PDS. The digital data were transmitted from the towfish to the DCU and were then ported to an EdgeTech 260-TH topside paper recorder to produce real-time imagery of collected side-scan sonar data. Data were also recorded digitally onto 8 mm DAT tapes for archival and post-processing routines.

A significant amount of lobster fishing gear located within the survey area hindered data collection efforts. On 20 September, SAIC personnel began survey operations, collecting data over nine survey lanes before the towfish snagged a buoyed lobster pot recovery line. The side-scan sonar tow cable was damaged and returned to the manufacturer for repair. On 28 September, the repaired data cable was put back into operation, and the remaining side-scan survey lanes were completed.

Navigation for the side-scan sonar survey activity was accomplished with the use of a Trimble 7400 DSI Global Positioning System (GPS) receiver interfaced with a Leica MX41R differential beacon receiver. Differential corrections to the satellite data were provided by the USCG beacon broadcasting from Brunswick, ME (316 kHz) to improve the positioning data to an accuracy of ±3 m.

The DGPS positioning data were ported to SAIC's Portable Integrated Navigation Survey System (PINSS). The position of the towfish was calculated in real-time by PINSS, based on cable scope (layback) and speed of the survey vessel. This information was embedded within the digital side-scan sonar data to allow for the geo-referencing of each acoustic return. After the survey the side-scan records were replayed through the topside recorder to remove water column artifacts and distortion, providing a better hard copy representation of the PDS seafloor through side-scan sonar.

2.5.2 Side-Scan Sonar Data Processing

Using Triton-Elics ISIS software, the sonar data were played back digitally and the return signal from the water column was removed to produce better quality imaging for

mosaic purposes. The "water column" is depicted on the side-scan records as a white gap down the center of each record. This gap corresponds with the time it takes for the acoustic signal to travel from the towfish to the seafloor below and return. As the towfish gains altitude above the seafloor, the amount of time it takes for the signals to reach the seafloor increases, thus increasing the white gap on the side-scan data record.

Each survey lane was saved as a separate filename to ease processing procedures. Individual survey lines were played back in ISIS and converted to a format for use in the Delph Map mosaicing program. Upon playback of the side-scan records adjustments were made to the time-varying-gain (TVG) of the return signal. The TVG adjustments allow the user to alter the gain tracking of the record as needed based upon the elapsed time between the send and receive signals.

As each lane was completed in ISIS, it was imported into Delph Map to check for processing accuracy during the file conversion from one program to the other. Upon processing completion of all of the odd numbered survey lanes, a mosaic was generated in Delph Map to check if any coverage gaps were present between survey lanes. After the mosaic was completed, it was saved and exported out of Delph Map as a geo-referenced Tiff file. This Tiff image was then imported into a geographic information system (GIS) capable of being compared with various existing and future data sets from the corresponding area.

2.6 Acoustic Doppler Current Profiling

The behavior of water column currents over a dredged material disposal site plays a major role in the development and dissipation of a sediment plume. Therefore, accurate modeling of a disposal event and resulting sediment plume requires current velocity data from several levels above the seafloor. Near bottom current, wave, and turbidity data were collected from PDS in the winter and spring of 1996, as part of the capping demonstration project. However, this data set only examined activity at the bottom boundary layer and did not provide the necessary information for the water column. To supplement the near-bottom current data, two acoustic Doppler current profilers (ADCPs) were placed near PDS in the winter of 1999 to interrogate the water column for a full 28-day tidal cycle.

Two up-looking RD Instruments (RDI) 300 kHz ADCPs were secured within trawl resistant bottom mounts and placed on the seafloor by the M/V *Beavertail* on 18 March 1999. The first ADCP (ADCP 1) was deployed at 43° 33.154´ N, 70° 01.268´ W in a naturally occurring valley feature on the seafloor south of PDS (Figure 2-4). Residing at a depth of 70 m, the ADCP unit was configured to average water column current data into discrete 1 m intervals ("bins") and provide information for as many as 65 individual depth intervals. The second unit (ADCP 2) was deployed at 43° 35.026´ N, 70° 01.489´ W on an exposed bedrock pinnacle detected north of the disposal site boundary (Figure 2-4). This instrument was placed at a depth of approximately 40 m and configured to average current

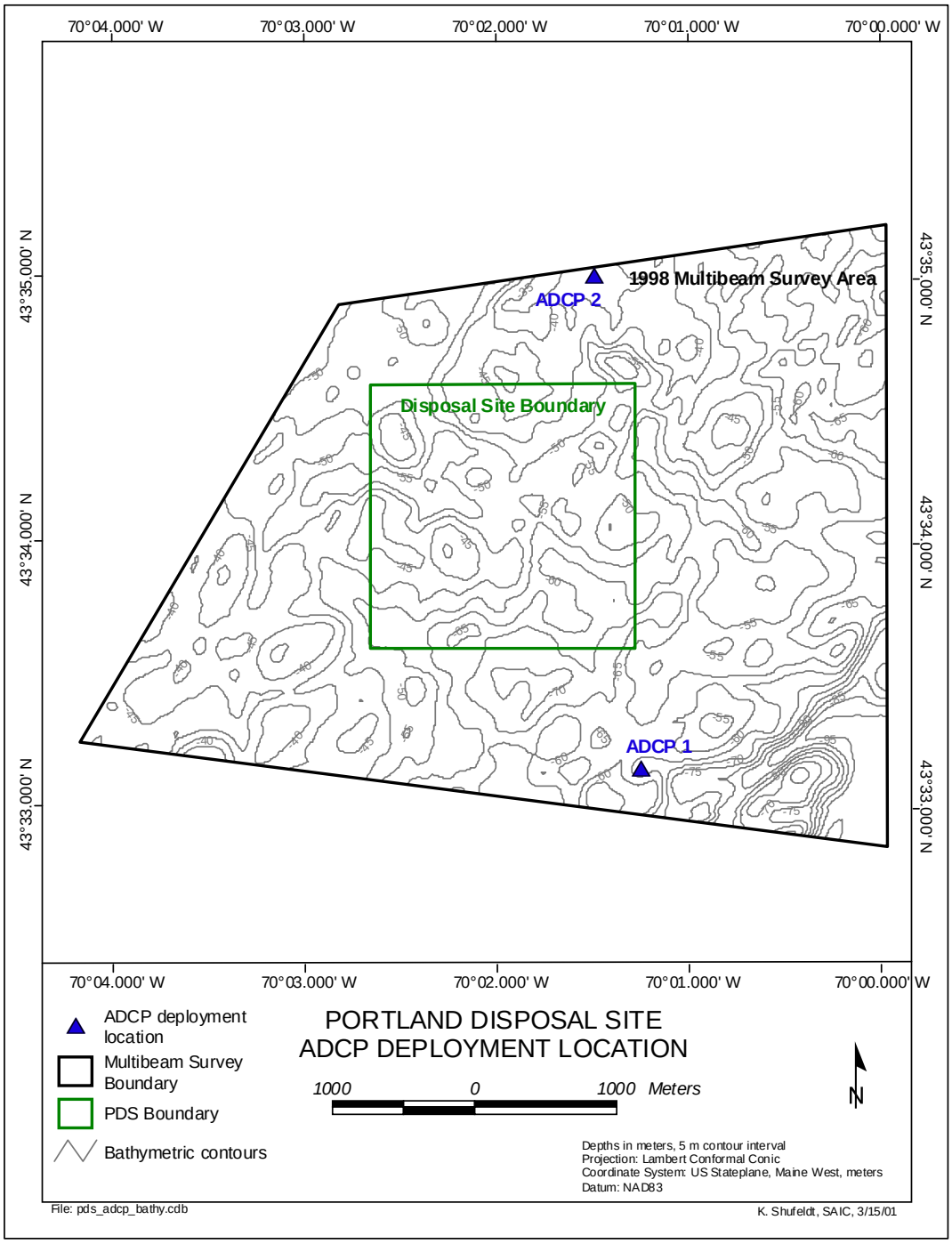

Figure 2-4. ADCP deployment locations relative to large-scale bathymetric features and the current Portland Disposal Site boundary

data into 0.5 m bins, providing speed and direction data for 38 levels within the water column.

A Trimble 7400 DSi GPS Receiver interfaced with a Leica MX-41R differential beacon receiver was utilized for vessel positioning information during the instrument deployment operation. The differential beacon receiver decoded satellite correction information broadcast from the USCG station in Brunswick, ME (316 kHz) to improve navigational accuracy to ±3 m. SAIC's PINSS was used to provide a helmsman display and store positional fixes upon deployment. An Odom DF 3200 fathometer interfaced to a narrow beam (3°) 208 kHz transducer was also utilized to verify the depth and bottom topography at each deployment site.

Recovery operations commenced aboard the M/V *Beavertail* on 19 April 1999. ADCP 1 was recovered from its original deployment site as planned with a full data record. ADCP 2 did not surface as expected on 19 April, and was recovered with a team of SCUBA divers on 20 April. The divers found the trawl resistant bottom mount upside-down on the pinnacle originally targeted during the 18 March deployment operations. The initial data analysis indicated the data record was invalid, as the unit was tripped during initial placement and rested in an improper orientation for the 31-day period. The data obtained from both instruments were sent to SAIC's offices in Raleigh, NC for processing and analysis. Only the data from ADCP1 were processed and later used to drive the STFATE and MDFATE modeling routines.

2.7 Sediment Traps

Sediment traps are unique oceanographic devices designed to capture and hold suspended particulate matter as it slowly settles through the water column to the seafloor. The purpose of the sediment trap deployments at PDS was to attempt to capture and quantify the amount of dredged material from the Portland Harbor project entrained within the water column and transported beyond the disposal buoy location. Based on the volume and type of material collected by the sediment traps, some inferences can be made concerning the impacts of the dredged material sediment plumes.

2.7.1 Sediment Trap Configuration and Deployment

The sediment traps utilized as part of the PDS dredged material fate study were Government Furnished Equipment (GFE) originally developed for an Environmental Protection Agency waste disposal site monitoring program. The sediment traps consisted of a thick walled polyvinylchloride (PVC) pipe 100 cm high and 30 cm in diameter (Figure 2-5). A polyethylene funnel was attached to the inside of the PVC pipe to channel sediments into a bottom collection tube 7.6 cm in diameter. An acrylic core liner was fitted inside the collection tube to contain the sample, maintain stratification, and facilitate easy withdrawal from the sediment trap.

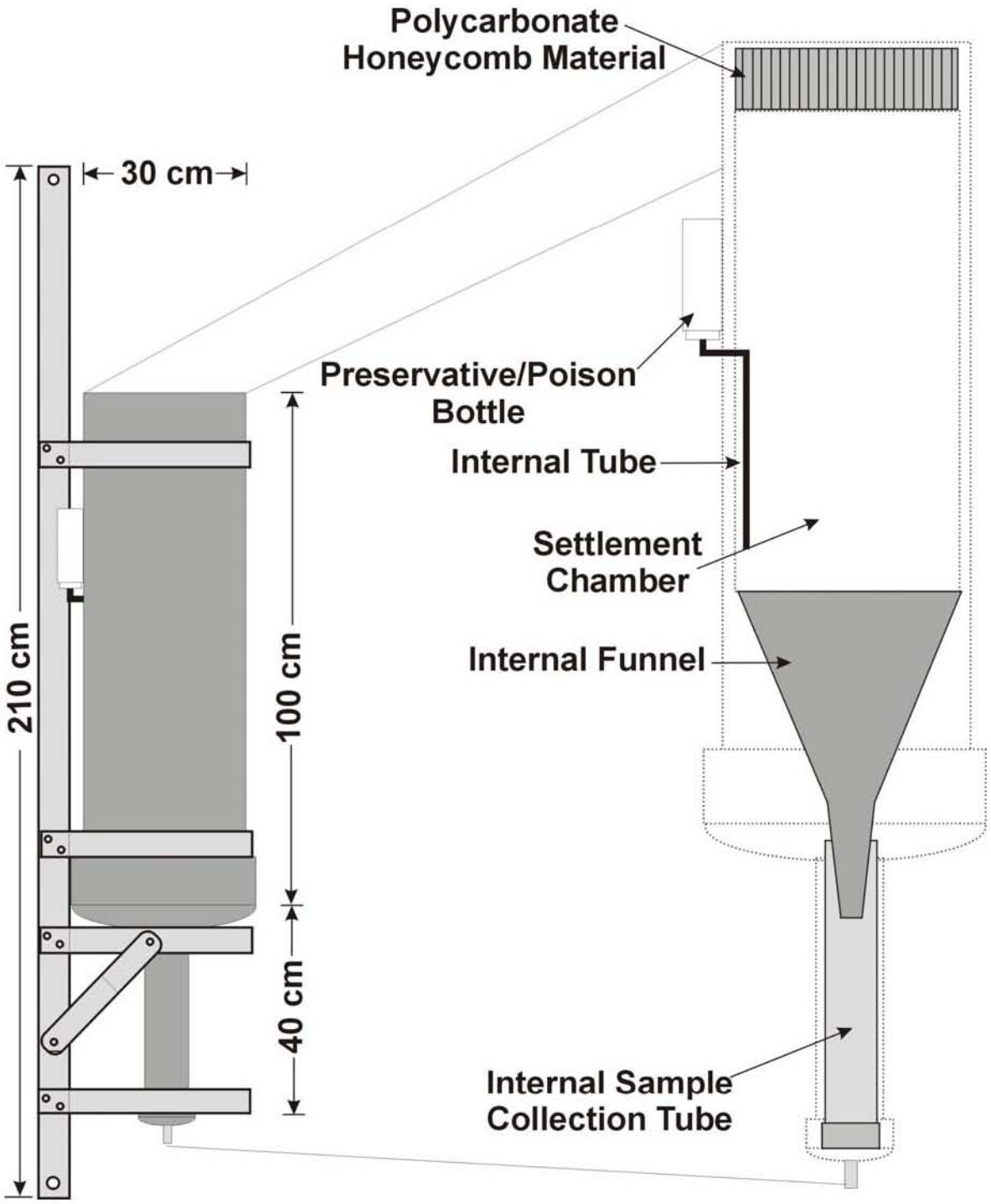

Figure 2-5. Schematic diagram of the government-furnished sediment traps that were deployed around the perimeter of the Portland Disposal Site

The inside of the sediment trap was constructed to prevent sample material from being stirred up by the effects of currents passing over the trap opening. At the top of the trap, a sheet of polycarbonate honeycomb material was used to shed the current vortices and prevent the removal of material within the housing. The internal funnel system served as a one-way port, directing suspended sediments to the bottom of the cylinder where the plastic liner retained the sediment. These features ensured that any material falling inside the trap remained captured.

A buffered seawater/formalin solution was added to each sediment trap to prevent disturbance of the stratigraphy within the sample tubes by microorganisms, to stain/preserve living tissue, and to prevent the oxidation of the calcareous tests of microfossils. The preservative/poison solution was contained in a plastic bottle mounted on the side of the sediment trap (Figure 2-5). The bottles were half full of the liquid to allow increasing water pressure at depth to expel the solution into the main chamber through a small tube and port on the side of the sediment trap.

The sediment trap was mounted to a stainless steel spine 210 cm high that allowed for the attachment of subsurface flotation as well as an anchoring system (Figure 2-5). The configuration utilized included a 350 lb weight directly under each sediment trap with a ground line leading to 110 lb of chain attached to a surface line and flotation system (Figure 2-6). To keep the sediment trap vertical in the water column, subsurface flotation consisted of a Benthos® 17-inch glass float and two 14-inch trawl floats. The surface markers were configured similar to offshore lobster gear buoys. A polypropylene float with a high-flyer and a radar reflector was attached to a down-line, which was secured to the 110 lb chain on the seafloor. The down-line was sized to accommodate tidal variation and expected wave activity at each selected site. The placement of each sediment trap mooring was performed in a manner that avoided entanglement in lobster fishing equipment on site.

Each sediment trap and plastic liner was thoroughly scrubbed with a non-reactive, biodegradable detergent and sealed with plastic to prevent surface dirt from entering the trap prior to deployment. Eight sediment traps were placed at strategic locations at PDS, based on the results of first-order STFATE modeling and the anticipated trajectory of the sediment plume (Figure 2-7; Table 2-5). Two sediment traps were also deployed at the SEREF reference area, which was expected to be free from the effects of the sediment plume. The sediment trap deployment operations were conducted on the M/V *Beavertail* on 18 March 1999 along with the ADCP deployments. A grab sample was collected in close proximity to each sediment trap deployment location to characterize the surface sediments existing on the bottom.

As part of the study design, the traps were paired to facilitate recovery of five traps 30 days after deployment and the remainder after 60 days. The project plan was to evaluate the fine-grained particles captured by the first five traps as they settled out of the water

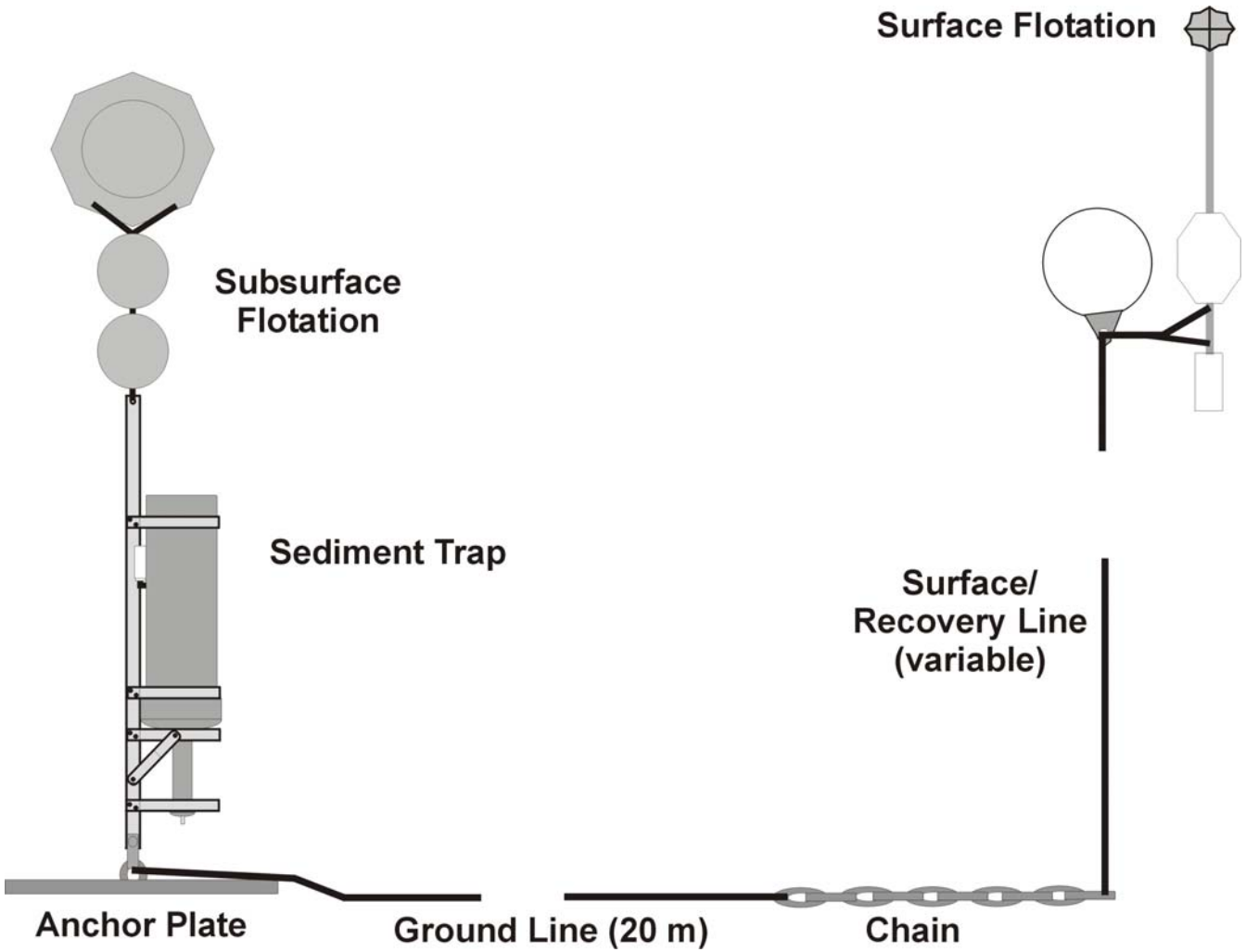

Figure 2-6. Diagram of the mooring system employed to secure the sediment traps to the seafloor around the Portland Disposal Site

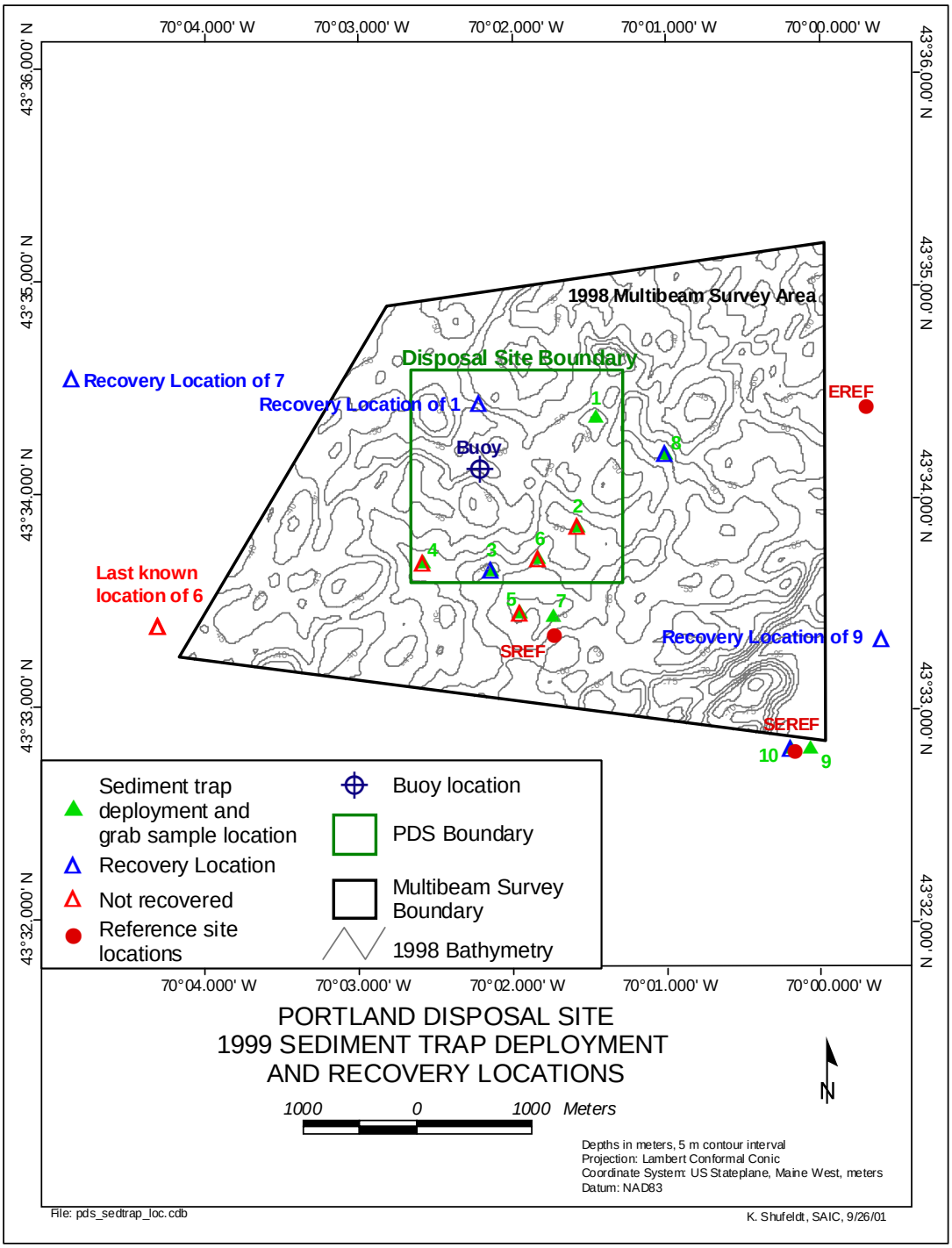

Figure 2-7. Deployment and recovery locations for the ten sediment traps that were deployed around the Portland Disposal Site

Table 2-5. Sediment Trap Deployment Locations at Portland Disposal Site and the PDS Reference Areas

Station	Location	Latitude	Longitude
		NAD 83	
ST 1	PDS	43° 34.386´ N	70° 01.458´ W
ST 2	PDS	43° 33.870´ N	70° 01.578´ W
ST 3	PDS	43° 33.666´ N	70° 02.136´ W
ST 4	PDS	43° 33.702´ N	70° 02.580´ W
ST 5	SREF	43° 33.462´ N	70° 01.956´ W
ST 6	PDS	43° 33.720´ N	70° 01.830´ W
ST 7	SREF	43° 33.450´ N	70° 01.734´ W
ST 8	PDS	43° 34.212´ N	70° 01.008´ W
ST 9	SE REF	43° 32.826´ N	70° 00.066´ W
ST 10	SE REF	43° 32.826´ N	70° 00.192´ W

column during disposal of Portland Harbor sediments. The second set would remain on site after the completion of dredging and disposal activity to identify and evaluate the significance of sediment resuspension and advection into the small depositional areas between the exposed bedrock outcrops.

On April 19, 1999 Sediment Traps 1, 3, 7, 8 and 10 were recovered (Figure 2-7). Sediment Trap 7 was recovered to the west of the site and had apparently been dragged off station. The steel frame bracing the sediment trap was severely bent and mangled from dragging across the rugged seafloor at PDS and West Cod Ledge. Sediment Trap 1 was also retrieved off station, and although the trap itself and the captured material appeared in good condition, the data were viewed with caution. The other traps were recovered where originally placed and appeared to be in good condition with valid samples. Thirty days later, a second effort was initiated to recover Sediment Traps 2, 4, 5, 6, and 9. However, no surface buoys were visible on or near the deployment locations and alternate recovery methods were unsuccessful. Sediment Trap 9 was eventually recovered in the nets of a shrimp-fishing vessel, approximately 50 days after deployment.

2.7.2 Sediment Trap Data Processing and Analysis

Upon recovery, the five sediment trap samples were extracted from the bottom of the device and retained within the plastic liner. The thickness of the sediment samples within each liner ranged from several millimeters to several centimeters thick. All samples recovered from the sediment traps were preserved further with a second addition of a buffered and stained seawater/formalin solution, then capped and stored for microfossil and geotechnical analyses. Only the material from Sediment Traps 3, 8, and 10 was determined to be valid and subjected to further analysis.

On 10 June 2000, the sediment was photographed and analyzed by SAIC. Sub-samples were extracted from the material retained in each sediment trap, however, the volume of sediment retained in the sample tube dictated the analysis performed. Material from Sediment Trap 3 was subjected to full analysis consisting of grain size, bulk density, and microfossil analyses. Sediment Trap 8 material was divided among bulk density, and microfossil analyses, while the scarcity of sediment in Sediment Trap 10 provided sufficient material for microfossil analysis only. All of the geotechnical and microfossil analyses were performed in accordance with the methods described in Sections 2.2 and 2.3 above.

2.8 Sediment-Profile Imaging Survey

Remote Ecological Monitoring of the Seafloor (REMOTS®) sediment-profile imaging is a useful tool to detect the distribution of dredged material layers, to map benthic disturbance gradients, to evaluate benthic habitat quality, and to monitor ecosystem recovery after disturbance abatement. This is a reconnaissance survey technique used for rapid

collection, interpretation, and mapping of data pertaining to physical and biological seafloor characteristics. Within the PDS dredged material fate study, REMOTS® sediment-profile images were used to examine the distribution and thickness of the Portland Harbor sediment deposit developed in close proximity to the PDA 98 buoy (43° 34.147´ N, 70° 02.210´ W). A total of 28 REMOTS® stations established on an eight-arm star-shaped station grid were occupied in September 2000 (Figure 2-8; Table 2-6). Stations were oriented to allow the collection of photographs in likely areas of dredged material accumulation. Three replicate images were obtained at each of the PDA 98 stations to calculate the average thickness of any surface layers of dredged material found to be present.

2.8.1 Survey Vessel Navigation and Positioning

A Trimble 7400 DSi GPS Receiver interfaced with a Leica MX-41R differential beacon receiver was utilized for positioning information. The differential beacon receiver decoded satellite correction information broadcast from the USCG station in Brunswick, ME (316 kHz) to improve navigational accuracy to ±3 m. The DGPS data were ported to Coastal Oceanographic's HYPACK® navigation and survey software for position logging and helm display. The target stations for REMOTS® sediment-profile imaging were determined before the commencement of survey operations and stored in a project database. Throughout the survey, individual stations were selected and displayed in order to position the survey vessel at the correct geographic location for sampling. The position of each replicate sample was logged with a time stamp in Universal Time Coordinate (UTC) and a text identifier to facilitate Quality Control (QC) and rapid input into a Geographic Information System (GIS) database.

2.8.2 REMOTS® Data Acquisition and Processing

REMOTS® sediment-profile imaging is a benthic sampling technique in which a specialized camera is used to obtain undisturbed, vertical cross-section photographs (*in situ* profiles) of the upper 15 to 20 cm of the seafloor. The REMOTS® hardware consists of a wedge-shaped optical prism having a standard 35 mm camera mounted horizontally above in a watertight housing (Figure 2-9). The prism resembles an inverted periscope, with a clear Plexiglas window measuring 15 cm wide and 20 cm high and an internal mirror mounted at a 45° angle to reflect the image in the window up to the camera. To equalize pressure and minimize refraction, the prism is filled with distilled water, and light is provided by an internal strobe. The prism is supported inside a stainless steel external frame, and the entire assembly is lowered to the seafloor using a standard winch mounted aboard the survey vessel. Upon contact with the bottom, the prism descends slowly into the seafloor, cutting a vertical cross-section profile of the upper 15 to 20 cm of sediment, and a photograph is taken of the sediment in contact with the window. The resulting 35 mm slides (images) showing relatively undisturbed sediment-profiles are then analyzed for a standard suite of measured parameters (Rhoads and Germano 1982; 1986).

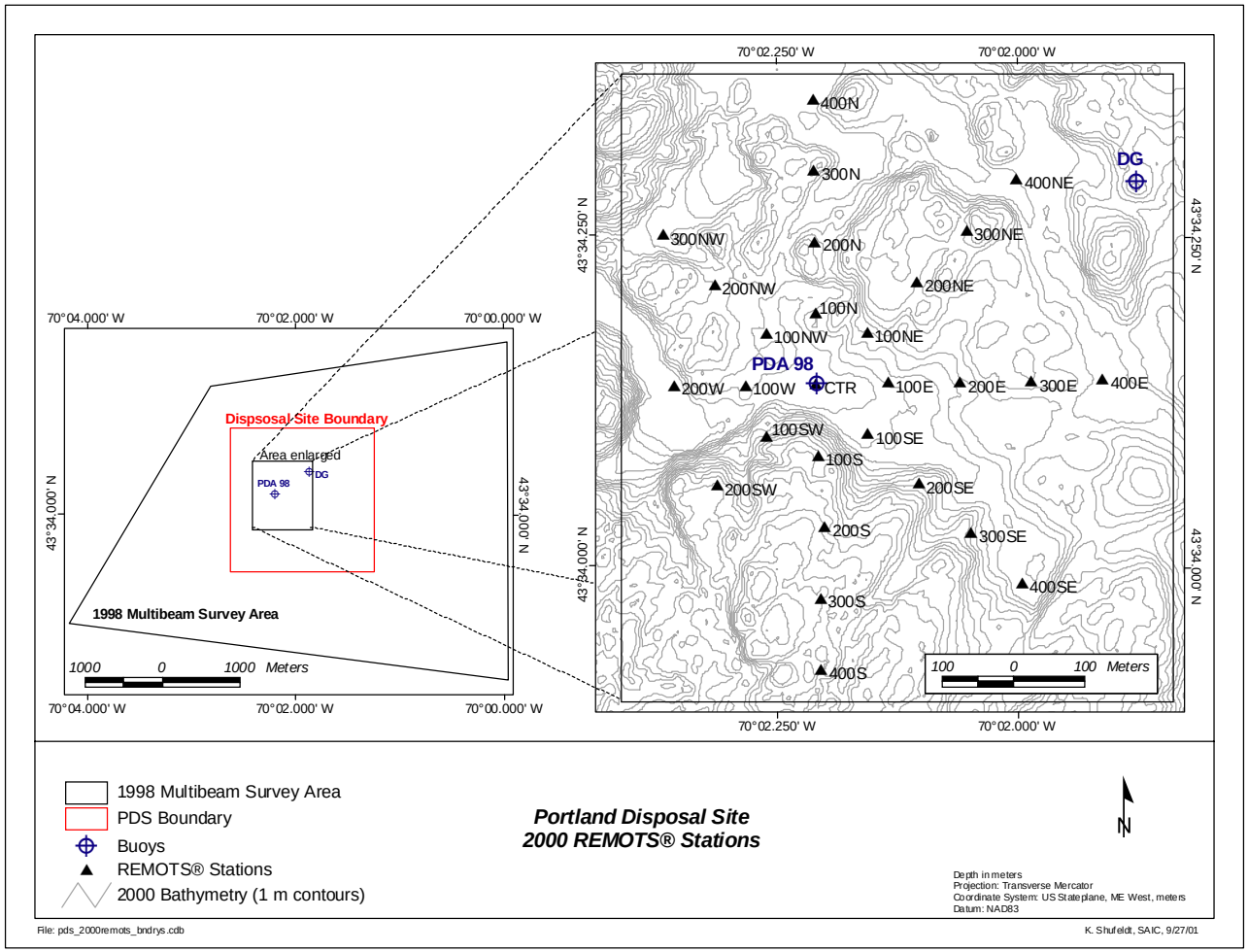

Figure 2-8. Distribution of REMOTS® sediment-profile imaging stations established around the PDA 98 disposal buoy position

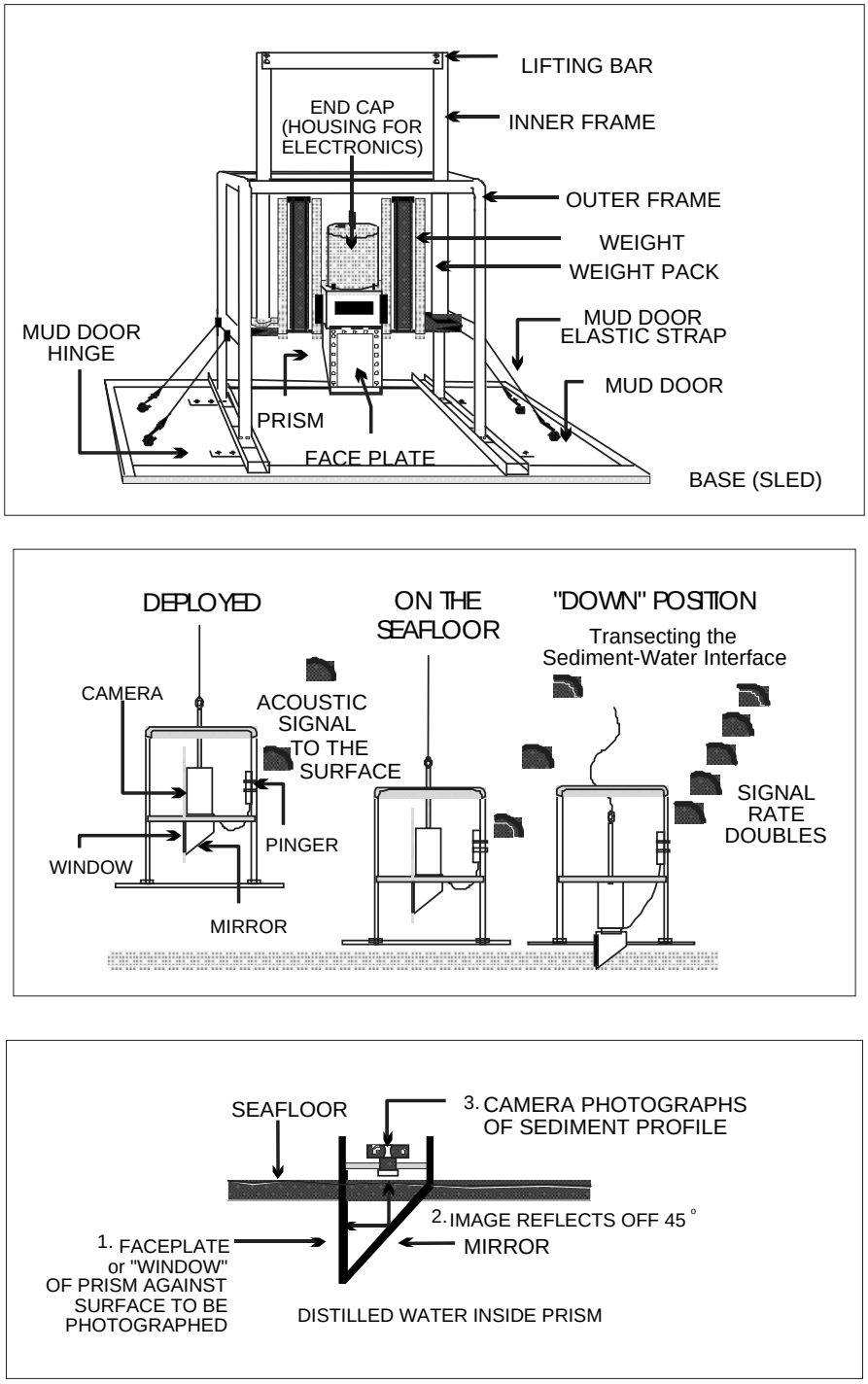

Figure 2-9. Schematic diagram of Benthos, Inc. Model 3731 REMOTS® sediment-profile camera and sequence of operation on deployment

Table 2-6. REMOTS® Sediment-Profile Imaging Stations over the PDA 98 Mound, September 2000

Area	Station	Latitude	Longitude
		NAD 83	
PDA 98 43° 34.147´ N 70° 02.210´ W	CTR	43° 34.147´ N	70° 02.210´ W
	100N	43° 34.201´ N	70° 02.210´ W
	200N	43° 34.255´ N	70° 02.211´ W
	300N	43° 34.309´ N	70° 02.212´ W
	400N	43° 34.363´ N	70° 02.213´ W
	100NE	43° 34.186´ N	70° 02.157´ W
	200NE	43° 34.224´ N	70° 02.105´ W
	300NE	43° 34.263´ N	70° 02.053´ W
	400NE	43° 34.302´ N	70° 02.001´ W
	100E	43° 34.148´ N	70° 02.135´ W
	200E	43° 34.148´ N	70° 02.060´ W
	300E	43° 34.149´ N	70° 01.986´ W
	400E	43° 34.150´ N	70° 01.912´ W
	100SE	43° 34.109´ N	70° 02.156´ W
	200SE	43° 34.072´ N	70° 02.103´ W
	300SE	43° 34.034´ N	70° 02.049´ W
	400SE	43° 33.996´ N	70° 01.996´ W
	100S	43° 34.093´ N	70° 02.208´ W
	200S	43° 34.039´ N	70° 02.201´ W
	300S	43° 33.985´ N	70° 02.206´ W
	400S	43° 33.931´ N	70° 02.205´ W
	200SW	43° 34.070´ N	70° 02.313´ W
	100SW	43° 34.108´ N	70° 02.261´ W
	200W	43° 34.146´ N	70° 02.358´ W
	100W	43° 34.146´ N	70° 02.283´ W
	300NW	43° 34.260´ N	70° 02.369´ W
	200NW	43° 34.222´ N	70° 02.315´ W
	100NW	43° 34.185´ N	70° 02.262´ W

Computer-aided analysis of each REMOTS® sediment-profile image yielded a suite of measurements. Standard measured parameters include sediment grain size major mode (expressed in phi units), camera prism penetration depth (an indirect measure of sediment bearing capacity/density), depth of the apparent redox potential discontinuity (RPD), infaunal successional stage, and Organism-Sediment Index (OSI; a summary parameter reflecting the overall benthic habitat quality). For the purposes of this report, only the physical parameters of the REMOTS® analysis are reported.

2.9 Computer-based Modeling of Dredged Material Fate

2.9.1 Overview of the Dredged Material Fate Models

As previously described, computer-based modeling played a significant role in the dredged material fate study performed at PDS. The following section provides a brief overview of both the STFATE and MDFATE models, primarily focusing on a general description of the input parameters required to run these models and also the expected output from these models. More extensive descriptions of these models are provided in Clausner et al. (2001) and references therein. Because these models are complex and also sensitive to relatively minor variations in many of the input parameters, a thorough understanding of each of the required input parameters is necessary before these models can be used reliably. Some of these issues will be addressed further in Sections 3.0 and 4.0.

2.9.1.1 Short Term Fate (STFATE) Model

The Short Term Fate (STFATE) model simulates the behavior of dredged material during a single placement event and provides an estimate of the extent and duration of the sediment plume associated with that event. Use of the model is most often driven by permitting regulations that require an estimate of the size of the mixing zone that may be required for an open-water dredged material disposal operation. The mixing zone is the small area in the immediate vicinity of a discrete placement event, where the local water quality standards may not be met following the disposal operation. The size of a mixing zone depends on a number of factors including the contaminant or dredged material concentrations in the discharge, concentrations in the receiving water, the applicable water quality standards, potentially affected biological resources, discharge density and flow rate, receiving water flow rate and turbulence, and the geometry of the discharge vessel, pipeline, or outlet structure and the receiving water boundaries. Since the maximum allowable mixing zone specified by regulatory agencies is usually on the order of hundreds of meters, the evaluation of mixing-zone sizes must necessarily be based on calculation of near-field dilution and dispersion processes.

Input data required for the STFATE model are grouped into the following general areas:

(1) Disposal site configuration – including disposal site boundaries, seafloor topography, defined mixing zone.
(2) Ambient water column conditions – including current velocity, density stratification, and water depths over the defined area.
(3) Dredged material characterization – including grain size distribution, specific gravity, cohesiveness, settling velocity, void ratio, and clumping factor.
(4) Description of the disposal operations – disposal point, barge dimensions, draft, and volume.
(5) Model Coefficients – specify entrainment, settling, drag, dissipation of the plume, density gradient differences.

The STFATE output consists of sediment particle and contaminant concentration in the water column in the hours following release from the barge or hopper.

2.9.1.2 Multiple Dump Fate (MDFATE) Model

The Multiple Dump Fate (MDFATE) model predicts the geometry (height, side slope and footprint) of dredged material mounds created by multiple placements of dredged material from hopper dredges or dump scows over time periods of weeks to months. The model is most commonly used as a planning tool for determining an effective material placement scheme for an open water disposal operation. During MDFATE execution, the disposal operation is divided into separate week-long episodes over which long-term fate processes are simulated using a modified version of the LTFATE (Long Term Fate) model. Long-term processes include self-weight consolidation, sediment transport by waves and currents, and mound avalanching. Within each week-long episode, a modified version of the STFATE model is used to simulate the short-term fate processes that impact each individual placement event. Short-term processes are those which influence disposed material up to the point at which all momentum imparted to the material upon its release from the barge at the water's surface is expended through convection, diffusion, and bottom friction.

Input data required to run the MDFATE model can be grouped into the following general areas:

(1) Dredged material characterization – including grain size distribution, specific gravity, cohesiveness.
(2) Ambient water column conditions – including current velocity (tidal and residual), wave spectra, density stratification, and water depths over the disposal site.
(3) Description of the disposal operations – dredged material placement pattern, barge dimensions, volume disposed and duration of disposal operations.

The primary MDFATE model output consists of a bathymetric grid that defines the size and extent of the dredged material deposit on the seafloor.

2.9.2 Application of the Models in the PDS Study

A first-order STFATE model run was performed in the fall of 1998 based on data obtained from a variety of sources. The results of this run were used to determine the locations for sediment trap placement during an active disposal period of the 1998-99 Portland Harbor dredging project. After refining many of the model input parameters based on site-specific data acquired for PDS and the dredged material source areas in Portland Harbor, SAIC contracted ASA to perform additional STFATE and MDFATE modeling to hindcast the behavior of the dredged material releases (both individually and collectively) at PDS. The validity of the results for these later model runs were then evaluated based upon the results of monitoring data acquired during and after the 1998-1999 dredging project. As with most modeling programs, the validity of the model input parameters have a significant impact on the reliability of the modeling results.

2.9.2.1 First-order STFATE Modeling

The first-order STFATE model parameters were derived from various sources (Table 2-7). As many parameters as possible were derived from data sets that were collected at PDS. For example, the most recent multibeam data were used for the seafloor topography, and CTD data obtained during the 1996 field efforts were used to develop a density profile of the water column. However, several physical characteristics of the sediments were not obtained directly from any PDS surveys and were instead interpolated from similar sediments collected as part of past DAMOS monitoring events at other regional disposal sites.

Both the STFATE and MDFATE models require that the total volume of solids in the dredged material be separated into sand, silt, clay, and clumps fractions. These fractions are calculated using average wet bulk density, water content, and sand, silt and clay fraction values from user defined information pertaining to the project sediment at the dredging site. The required characteristics to describe the primarily silt-clay sediments in Portland Harbor were compiled from previous DAMOS coring data sets obtained from similar seafloor areas at the Central Long Island Sound Disposal Site (CLDS) and the New London Disposal Site (NLDS).

Values for the water column current speed and direction were obtained for Bigelow Bight based upon a previous USGS data set. Conductivity, Temperature, and Depth (CTD) probe casts collected at PDS during the winter of 1996 were used to generate a water density profile (McDowell and Pace 1998). The site engineers for Great Lakes Dredge and Dock

Table 2-7. Model Parameter Data Used in PDS STFATE Model Runs

Input Parameter	Data Source	Values Used
Bathymetry	Sept. 1998 Multibeam	10m X 10m grid
Buoy Location	User Determined	43^{o} 34.147' N, 070^{o} 02.209' W
Disposal Site Boundary	DAMOS Site Management Plans, SAIC Report #365	
Run-Time Intervals	User Determined	1, 2, 3, and 4 hours
Water Column Depth Intervals	User Determined	10ft (3m), 30ft (10m), 90ft (30m), 150ft (50m), 300ft (100m)
Water Density Profile	Oceangraphic Measurents at the Portland Disposal Site during Spring 1996, McDowell and Pace 1998, DAMOS Contribution 121	1.0235 $g \cdot cm^{-3}$ at the Surface, 1.0242 at bottom
Water Column Current Speed	USGS Data set	0.595 $ft \cdot s^{-1}$ @ 16.5ft, 0.367 $ft \cdot s^{-1}$ @ 89.1ft
Water Column Current Direction	USGS Data set	163 @ 16.5ft, 218 @ 89.1ft
Moisture Content	Dredged material measurements from cores collected from disposal mounds in Long Island Sound and the NY Mud Dump Site	129%
Specific Gravity of Dredged Material		2.6 $g \cdot cm^{-3}$
Percent Solids		90%
Volumetric Concentration	Calculated by STFATE	
Settling Velocity	Calculated by STFATE	
Void Ratio for Deposition	Calculated by STFATE	
Critical Shear Stress	Calculated by STFATE	
Contaminant Parameters	Default	
Site Bottom Roughness Height	Default	0.005 ft
Barge Volume and Type	User Determined	3,530 m^3 (7000 yd^3) Split Hull
Barge Dimensions	User Determined	64 ft X 280 ft, 15.4ft draft loaded, 4ft draft unloaded
Barge Velocity	User Determined	Stationary

Values for grain size, bulk density, and liquid limit were varied for each of the model runs.

(GLDD) Company and NAE determined a 5,350 m^3 (7,000 yd^3) split-hull barge would be used for the project and therefore served as the basis of the modeling runs.

A total of five models runs were developed to represent the extent of the plume migration in the water column after a disposal event. The first model run was developed with parameters that would best mimic the anticipated conditions associated with the disposal of the Portland Harbor material. A background total suspended solids (TSS) concentration value of 1.5 $mg \cdot l^{-1}$ was used for PDS, based upon the data obtained as part of the 1996 physical oceanographic program. Any concentration of entrained sediment above the 1.5 $mg \cdot l^{-1}$ would constitute the leading edge of the detectable plume. The results of this first-order model run were used to strategically place the sediment traps around PDS during one of the active disposal periods for this project. The four remaining model runs were sensitivity analyses using minimum and maximum values for sediment bulk density and liquid limit to determine the variation in plume morphology and migration.

2.9.2.2 Second-order STFATE Modeling

The second-order STFATE modeling effort was based upon the updated input parameters that were developed from the extensive data that were acquired in the area before and during the 1998-1999 dredging project. Though some of the model parameters were still based on general information, many of the critical parameters were developed based on the detailed project sediment data acquired in Portland Harbor and the water column data acquired in and around PDS. In addition, multiple disposal barge sizes and configurations were used to determine the effects of barge volume and dimensions on the initial plume (Table 2-8a).

The sediment core data extracted from a sub-set of the Portland Harbor cores were used to compute the solids fraction of the dredged material as follows:

Unit weight - the weight of 1 ft^3 of dredged material derived by converting the wet bulk density from the sediment cores in units of $g \cdot cm^{-3}$ to English units of $lb \cdot ft^{-3}$.

Unit weight = 1.47 $g \cdot cm^{-3} \times$ 62.4 $lb \cdot ft^{-3}$
= 91.73 lb.

Dry weight of solids - the weight of solids in 1 unit weight of dredged material

Dry weight of solids = 91.73 / (1 + avg. water content from sediment cores)
= 91.73 / 2.09
= 43.89 lb.

Table 2-8a. Disposal Barge Parameters for Second-order STFATE Simulation

Volume		Barge Length		Barge Beam		Barge Draft	
(m^3)	(yd^3)	(m)	(ft)	(m)	(ft)	(m)	(ft)
3,050	4,000	68	224	7	23	6	20
4,600	6,000	84	277	20	64	7	23
5,500	7,200	84	277	20	64	7	23

Table 2-8b. Non-Clumped Dredged Material Volume Fractions for Second-order STFATE Simulation

Sediment Size	Amount Present (%)	Size Fraction	Solids Fraction	Fraction not in Clumps	Volume Fraction
Sand	7.4	0.074	0.27	0.4	0.007992
Silt	34.4	0.344	0.27	0.4	0.037152
Clay	58.2	0.582	0.27	0.4	0.062856

Volume of solids - the volume of solids in unit volume
Volume of solids = dry wt of solids / (unit wt of water x specific gravity)
= 43.89 / (62.4 × 2.64)
= 0.27 ft^3

Solids Fraction of dredged material = 0.27

For mechanically dredged sediment, an assumption was made that 60% of the solids were in large coherent blocks, or clumps (Table 2-8b). The clumps were comprised of sand, silt and clay particles in proportion to the average amount of each size found in the sediment cores. The volume fractions for sand, silt, and clay not contained in clumps were calculated by multiplying the size fraction times the solids fraction of the bulk material times the fraction not contained in clumps.

Water column current values were calculated from the data record obtained from ADCP1 placed south-southeast of PDS. For these two data model runs, projected current values were based upon either average current speed and direction information or current vector-averaged velocity. The use of average speed and direction provided an elevated current value or "worst case scenario" for particle movement in the water column. Vector-averaged current velocity examined net transport over time and yielded smaller current values, and therefore tended to moderate the transport of the sediment plume over time.

2.9.2.3 MDFATE Modeling

The MDFATE model was used in this study to simulate the deposition of dredged material from 166 individual barge releases at PDS. The output from the MDFATE model is a depth difference grid that displays the extent and thickness of the deposited material from all of the recent disposal operations. This output was then compared to the depth difference comparisons calculated between the September 1998 and July 2000 multibeam bathymetric surveys over PDS.

During the five-month period from November 11, 1998 to April 13, 1999, 166 barge loads of material dredged from Portland Harbor were deposited at PDS. The PDA 98 buoy, located where the water depth was approximately 58 meters, was designated as the disposal point, however, a significant number of the disposal logs reported a disposal position in close proximity to the DG buoy approximately 500 m to the northeast (Figure 1-3). The individual releases varied in size from 100 m^3 (125 yd^3) to 5,000 m^3 (6,500 yd^3) and totaled 465,880 m^3 (609,312 yd^3) of dredged material. The same dredged material characteristics used for the STFATE simulations were used for the MDFATE model simulations (Table 2-9).

The volume fractions calculated for the STFATE model runs were used to define the sediment characteristics of the dredged material for the MDFATE simulation (Table 2-8b).

Table 2-9. Summary of MDFATE Model Input Parameters

Total Barge Volume	465,880 m^3	609,312 yd^3
Barge solids Volume	125,800 m^3	164,514 yd^3
Barge Liquids Volume	340,100 m^3	444,798 yd^3
Near Bottom Current Speed (constant)	13.1 cm/s	0.43 ft/s
Current Direction (true)	240°	240°
Wave Height	1.2 m	4 ft
Wave Period	7 seconds	7 seconds
Wave Direction (true)	240°	240°

The clay volume fraction was specified to be cohesive in the model simulation while the other size fractions, including the clumps, were specified as non-cohesive. Additional model inputs are summarized in Table 2-10.

The volume deposited on the seafloor by the MDFATE model is sensitive to the dredged material characteristics specified, and particularly sensitive to the void ratio and cohesiveness of the material. While the void ratio of the dredged material can be calculated from the sediment core data, the void ratio used for the seafloor deposit of each size fraction is estimated using typical values for recently deposited dredged material. The void ratio can have widely different values, particularly for silt- and clay-sized particles that are capable of taking on a large volume of entrained water. Table 2-10 shows the values used for void ratios in the MDFATE input where the dredged material is characterized.

Similar to the STFATE modeling effort, the MDFATE model was run a second time, based on the vector averaged current velocities, to determine the role of water column currents on the morphology of the disposal mound. Furthermore, because the additional 18,300 m^3 (23,934 yd^3) of material deposited at the DG buoy during the 1999-2000 disposal season was evident in the 2000 multibeam survey, the 33 disposal events from 1999-2000 were also included in the second run. These small modifications in modeling approach increased the validity of the comparisons between the model results and the results derived from the depth difference calculations between the 1998 and 2000 multibeam surveys. Table 2-11 summarizes the input parameters that were altered for the second MDFATE model run; all other input parameters were the same as those used in the previous MDFATE simulation.

Table 2-10. Portland Harbor Dredged Material Characterization

	Type 1	Type 2	Type 3	Type 4
Solid Type	SAND	SILT	CLAY	CLUMPS
Specific Gravity	2.64	2.64	2.64	2.64
Volume Fraction	0.00799	0.03715	0.06286	0.162
Median Grain Size (mm)	0.13	0.0395	0.003	350
Deposit Void Ratio	0.7	5	9	0.6
Critical Shear Stress	0.2	0.1	0.02	99
Cohesive	No	No	Yes	N/A
Strip in Descent	No	No	No	No
Density of Water (g/cm³)	1.0253			
Density of the water portion in the dredged material (g/cm³)	0.98-1.05			

Table 2-11. Summary of Refined MDFATE Model Input

Total Barge Volume	482,400 m³	630,923 yd³
Barge Solids Volume	130,250 m³	170,349 yd³
Barge Liquids Volume	352,150 m³	460,574 yd³
Near Bottom Current Speed (constant)	7 cm/s	0.23 ft/s
Current Direction (true)	236.7°	236.7°
Wave Height	1.2 m	4 ft
Wave Period	7 seconds	7 seconds
Wave Direction (true)	236.7°	236.7°

3.0 RESULTS

3.1 Pre-disposal Sediment Collection

The coring and grab sampling surveys conducted in November 1998 and March 1999 were undertaken mainly to characterize the sediments to be dredged from Portland Harbor and the Fore River (for input to the STFATE and MDFATE models), as well as to determine the feasibility of using sediment tracers to differentiate between the Portland Harbor sediments and those that already existed within PDS. This distinction was important as part of the evaluation to determine the likely source(s) of the material present within the sediment traps.

3.1.1 Portland Harbor Cores

The 17 cores collected within the Portland Harbor dredging area provided a cross section of the material that was to be removed from the Fore River (Figure 2-1). The sampled dredging area included both intertidal and subtidal estuarine zones. A general description of the lithologies recovered in the cores is provided below; detailed core and grab sample descriptions are provided in Appendix B.

Cores PH-13, PH-14, PH-15, and PH-16 were obtained at stations located in the upper reaches of the Fore River, adjacent to a network of tidal mudflats (Figure 2-1). The sediment in these cores consisted primarily of silt-clay (<0.063 mm in diameter) and a minor fine sand (0.250 mm < 0.125 mm in diameter) fraction. Cores PH-5, PH-9, PH-11, PH-10, PH-7, PH-8, PH-6, PH-20, PH-19, PH-18, PH-17 were taken from the subtidal region of Portland Harbor and were composed primarily of soft clay mixed with silt (< 0.063 mm in diameter). Most of these cores displayed dense, glacially-derived clay as the main component, suggesting little accumulation of estuarine sediments in the immediate area since the last dredging operation.

Cores PH-3 and PH-4 were obtained towards the mouth of the harbor, near the outer limits of the subtidal, estuarine zone, and likely contained some material emanating from the discharge of the Presumpscot River. The sediment in these cores was described as a dark greenish gray to black, moist, silty clay (29-47 cm) over drier, firmer clay with varying sand content.

The lithologic unit most commonly recovered in the cores was a subtidal to tidal deposit, consisting of a dark greenish gray to black organic-rich clay to silty clay. On closer inspection, this unit varied from a highly detritus-rich unit in a clay matrix, to a siltier, more consolidated and homogenous unit with finely disseminated organic debris. Some samples contained sporadic and discrete sand layers. The second most common lithology detected at the bottom of several cores (PH-3, PH-4, PH-9, PH-11, PH-10, PH-7, PH-8, PH-6, PH-20, PH-19, PH-18, PH-17) was described as a distinctive homogeneous greenish-gray clay that

was characterized as stiff and well consolidated. Another lithology that had distinct characteristics was the firm, blue-gray clay at the bottom of Core PH-5.

Several lithologic units were recovered from each of the two estuarine zones within the Fore River. The upper reaches of the river are in the transition area between freshwater and brackish environments. The material recovered from the upper reaches of the Fore River consisted primarily of silt-clay, characteristic of a subtidal to intertidal mudflat deposit. Grabs and cores obtained from the middle reaches of the river likewise were predominately silt-clay. Due to the presence of a high percentage of sand, no gravity cores could be obtained in the outer region (mouth of Portland Harbor), although two surface grab samples (PH-01 and PH-02) were collected. This area contained sand flat deposits and flood/tidal channel deposits. Flood/tidal channel deposits contained discrete units of organic debris, shell-rich layers, and a significant sand/gravel component.

Overall, the core samples of bottom sediments from the Fore River and Portland Harbor sites averaged 34% silt, 58% clay, and 7% sand. The predominance of fine-grained sediment was observed in all of the cores as a silt-clay surface layer ranging in thickness from 11 to 55 cm. An underlying layer of glacially deposited fine clay was also observed in most of the cores. This unit was probably the "blue clay" Pleistocene Presumpscot Formation, which underlies the mud and sand flat deposits (Belknap et al. 1989).

Due to the dredging schedule and project logistics, cores PH-4, PH-6, PH-7, and PH-9 were selected as being most representative of the material to be placed at PDS during the winter of 1999. Each of the four cores were split, described in detail, and sub-sampled to a level equivalent to the projected depth of excavation around each core location. The geotechnical analyses performed on multiple horizons within each core included water content, sediment grain size distribution, Atterberg limits, wet/dry bulk density, and specific gravity (Tables 3-1 and 3-2). Figures 3-1 through 3-4 present the split cross-section view of each of these cores.

All four of the cores were from areas described as subtidal, and all of the cores had predominantly fine-grained (i.e., silt-clay) sediments (Figures 3-1 through 3-4). Mean sediment grain diameters for the four cores were in the range of fine sand to clay (between 0.088 to <0.005 mm), and on average the sediment in the four cores consisted predominantly of clay at 58.2%, followed by silt at 34.4%, and sands at 7.4%. These mean values were later used to develop the input data for the STFATE and MDFATE modeling efforts. The use of the Unified Soil Classification System (USCS) for physical characterization was used for the purpose of consistency with USACE engineering evaluations (ASTM D2487). The highest concentration of sand was found toward the outer harbor, present in the top interval of core PH-4.

Table 3-1. Grain Size Distributions for the 1998 Portland Harbor Cores and PDS Grab Samples

Type	Sample ID	Depth Interval (cm)	Complete Grain Size Distribution				Sand Components		
			Gravel >4.76 mm (%)	Sand 0.074 to 4.76 mm (%)	Silt 0.005 to 0.074 mm (%)	Clay <0.005 mm (%)	Coarse 2.0 to 4.76 mm (%)	Medium 0.42 to 2.0 mm (%)	Fine/Very Fine 0.074 to 0.42 mm (%)
Portland Harbor Core	PH-4	0-12	0.0	12.9	33.1	54.0	0.0	1.3	11.6
	PH-4	23-33	0.0	5.4	30.6	64.0	0.1	0.1	5.2
	PH-4	42-52	0.0	6.0	37.0	57.0	0.0	0.1	5.9
	PH-6	0-10	0.0	8.4	30.6	61.0	0.1	0.2	8.1
	PH-6	36-43	0.0	7.1	42.5	50.4	0.0	0.1	7.0
	PH-6	50-60	0.0	8.0	28.1	64.0	0.7	0.5	6.8
	PH-7	0-10	0.0	5.4	31.6	63.0	0.0	0.1	5.3
	PH-7	25-35	0.0	3.3	28.7	68.0	0.1	0.3	2.9
	PH-7	45-55	0.0	9.4	38.6	52.0	0.0	0.2	9.2
	PH-9	1-15	0.0	2.8	31.2	66.0	0.1	0.1	2.6
	PH-9	25-35	0.0	6.7	32.7	60.5	0.0	0.3	6.4
	PH-9	48-58	0.0	6.3	41.7	52.0	0.0	0.2	6.1
Portland Harbor Grab	PH-13		0.0	14.6	31.9	53.5	0.0	0.2	14.4
	PH-17		0.0	7.9	43.1	49.0	0.2	0.2	7.5
PH Average (Cores and Grabs)			**0.0**	**7.4**	**34.4**	**58.2**	**0.1**	**0.3**	**7.1**
Buoy Grab	PDS-BUOY 2G		2.2	69.1	14.7	14.0	2.3	19.9	46.9
Sediment Trap	ST-3	0-5	0.0	1.1	19.8	79.0	0.0	0.0	1.1
	ST-8	0-2	NA	NA	NA	NA	NA	NA	NA

Table 3-2. Geotechnical Results for the 1998 Portland Harbor Cores and PDS Grab Samples

Type	Sample ID	Core Depth Interval (cm)	Water Content (%)	Atterberg Limits		
				Liquid Limit (%)	Plastic Limit (%)	Plasticity Index
Portland Harbor Core	PH-4	0-12	117	106	38	68
		23-33	128	105	39	66
		42-52	116	96	35	61
	PH-6	0-10	116	93	36	57
		36-43	NA	NA	NA	NA
		50-60	111	103	39	64
	PH-7	0-10	135	112	39	73
		23-35	136	107	39	68
		45-55	91	83	35	48
	PH-9	1-15	132	113	45	68
		25-35	111	102	38	64
		48-58	89	78	35	43
Portland Harbor Grab	PH-13		125	77	33	44
	PH-17		102	73	32	41
PH Average (Cores and Grabs)			**116.1**	**96.0**	**37.2**	**58.8**
Buoy Grab	PDS-Buoy 2		NA	NA	NA	NA
Sediment Traps	ST-3		NA	NA	NA	NA
	ST-8		NA	NA	NA	NA

Type	Sample ID	Core Depth Interval (cm)	Specific Gravity (20º)	Wet Bulk Density (g/cm^3)	Dry Bulk Density (g/cm^3)	Water Content (%)
Portland Harbor Core	PH-4	7-9	2.62	1.36	0.54	152
		25-27	2.63	1.36	0.57	140
		47-49	2.66	1.48	0.73	103
	PH-6	7-9	2.63	1.52	0.82	85
		36.5-38.5	2.67	1.56	0.89	76
		53.5-55.5	2.59	1.39	0.63	120
	PH-7	5-7	2.65	1.37	0.61	125
		29-31	2.64	1.36	0.58	135
		45-55	2.66	1.63	0.96	69
	PH-9	10-12	2.61	1.41	0.63	125
		25-35	2.61	1.44	0.65	120
		55-57	2.67	1.56	0.89	76
Portland Harbor Grab	PH-13		2.62	1.53	0.77	99
	PH-17		2.64	1.56	0.77	102
PH Average (Cores and Grabs)			**2.6**	**1.5**	**0.7**	**109.1**
Buoy Grab	PDS-Buoy 2		2.65	2.00	1.56	28
Sediment Trap	ST-3	0-5	2.63	1.30	0.43	204
	ST-8	0-2	2.64	1.29	0.42	204

NOTE: Water Content is uncorrected for salt content.

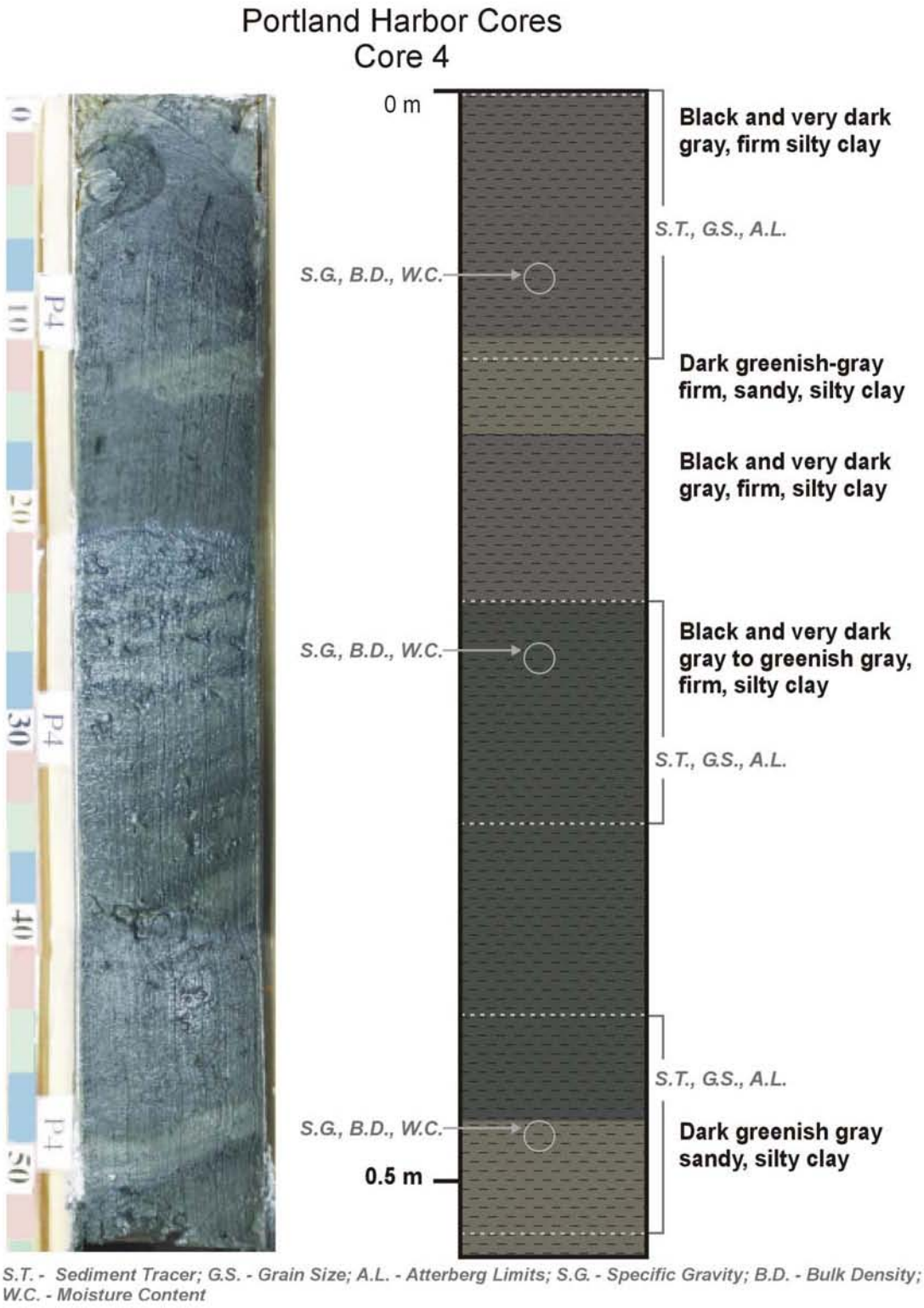

Figure 3-1. Cross-sectional view and lithology of Portland Harbor Core PH4

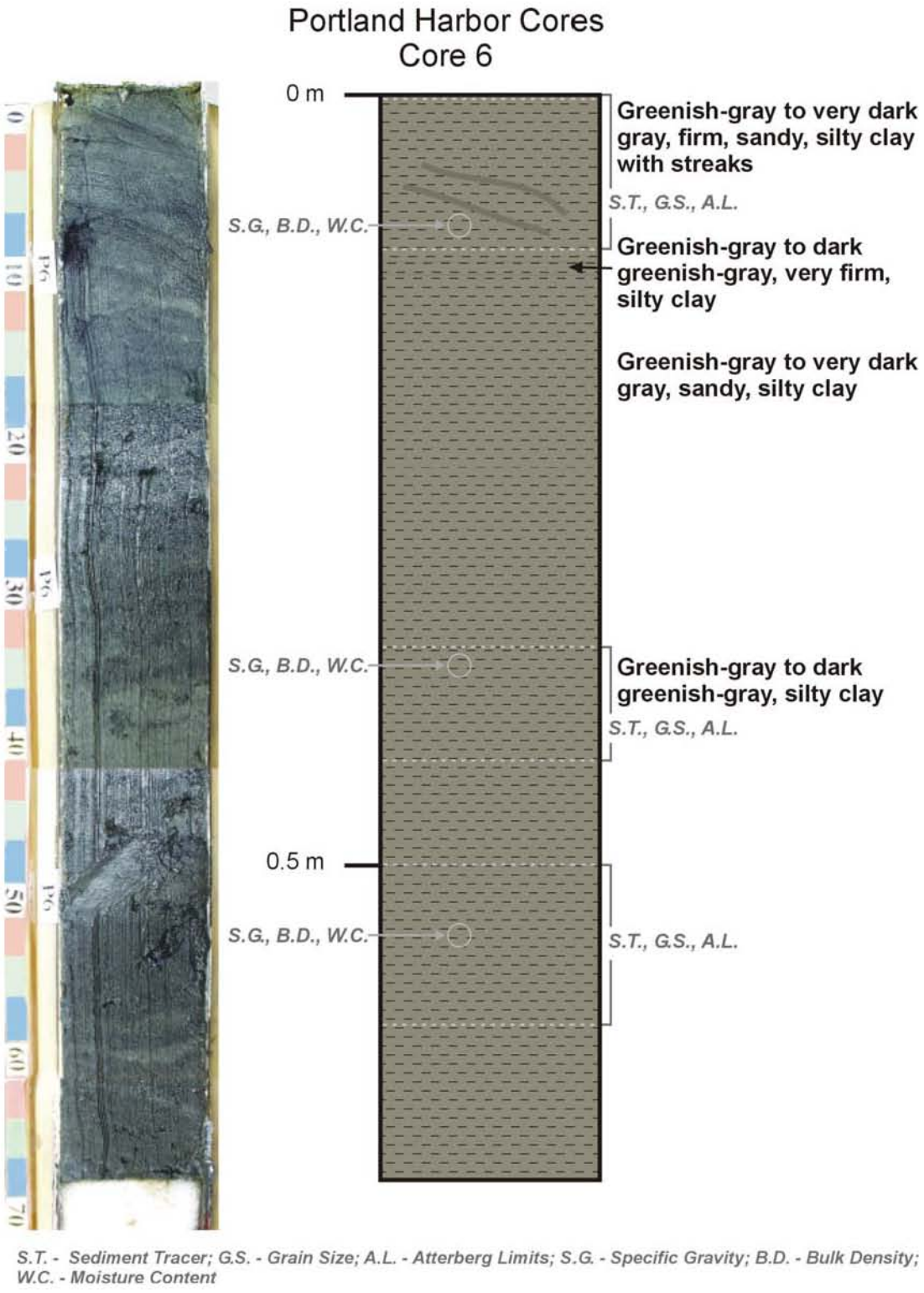

Figure 3-2. Cross-sectional view and lithology of Portland Harbor Core PH6

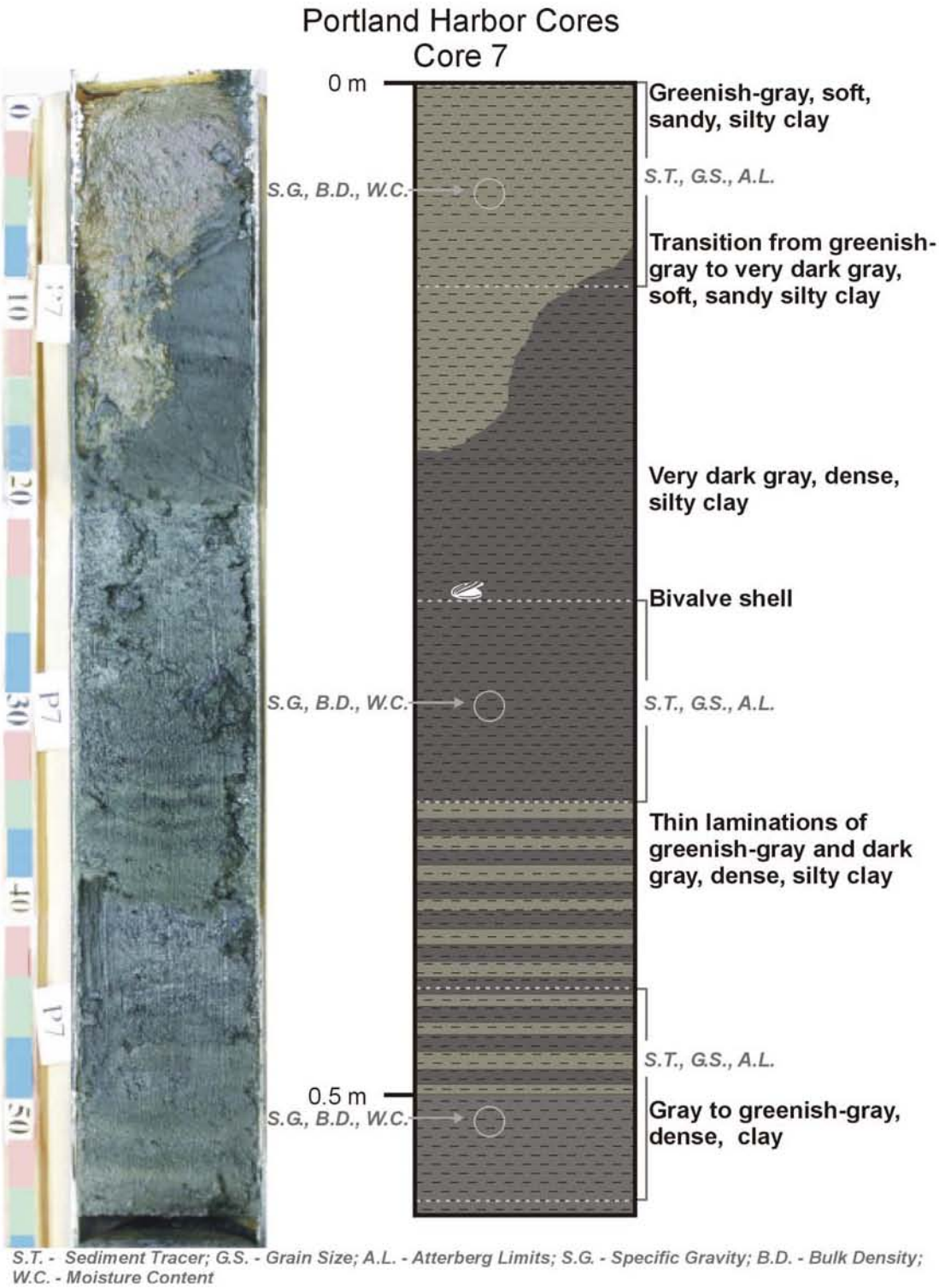

Figure 3-3. Cross-sectional view and lithology of Portland Harbor Core PH7

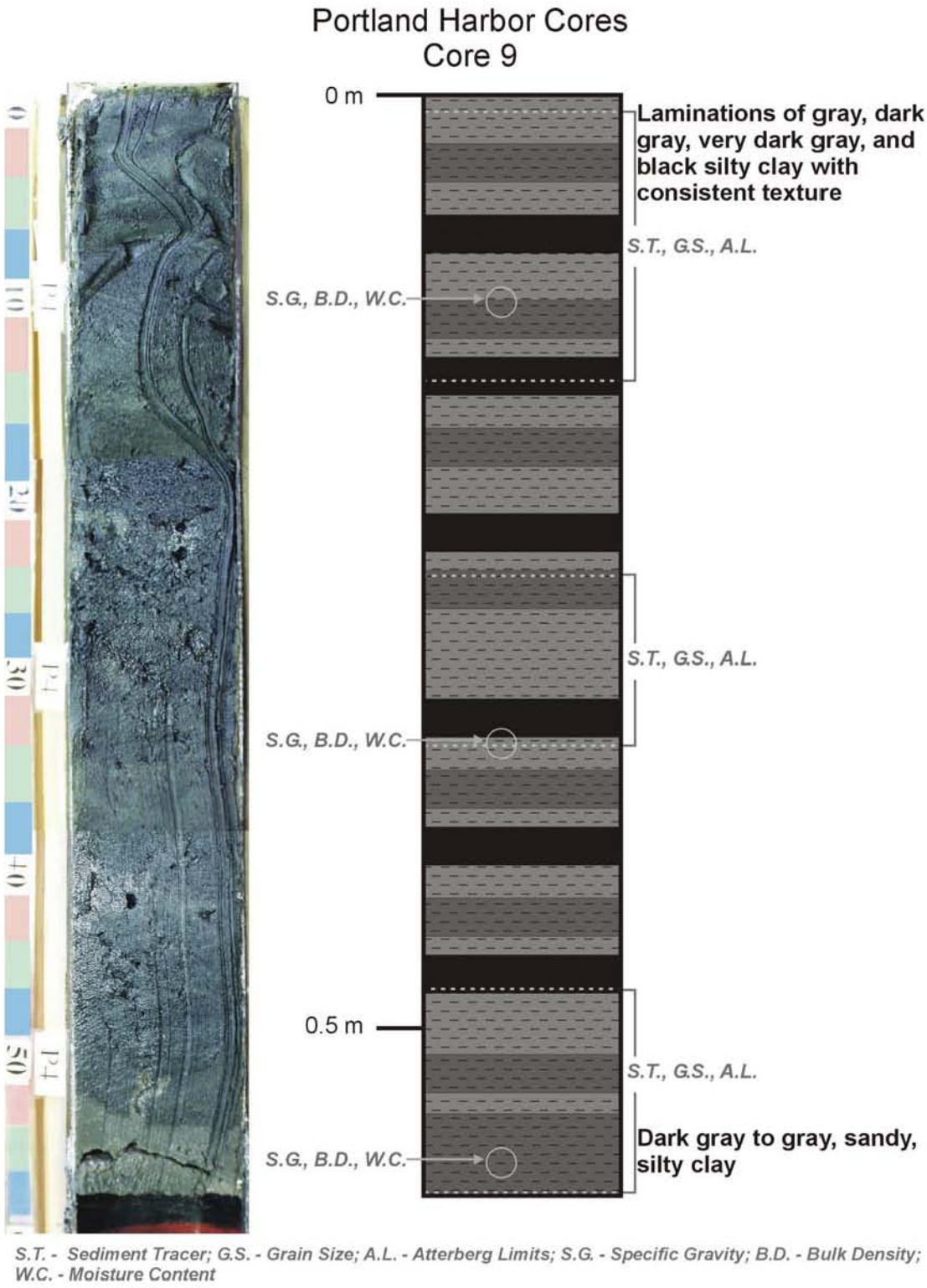

Figure 3-4. Cross-sectional view and lithology of Portland Harbor Core PH9

Due to the relationship between water content and liquid limit, the surface sediments in the four cores were considered likely to be non-cohesive. The basement material generally demonstrated lower liquid limit and water content values, suggesting this material would be more cohesive and likely to form small clumps when removed from the seafloor by a clamshell bucket and transferred into a disposal barge.

3.1.2 Portland Harbor Grab Samples

Sediment grab samples were collected at 19 stations in Portland Harbor and the interior of the Fore River as part of the November 1998 field effort (Figure 2-1). Upon retrieval, the sediment in each grab was described in terms of estimated grain size, color, and texture (Table 3-3). Sub-samples were then removed from each grab for grain size analysis. In general, there was good agreement between the grab samples and the top sections of the cores (upper 10 to 12 cm intervals) in showing that the surface sediments in Portland Harbor were predominantly silt-clay with a minor sand component (Table 3-1).

The most commonly recovered lithologic unit from grabs PH-3, PH-4, PH-5, PH-6, PH-7, PH-8, PH-10, PH-11, PH-14, PH-15, PH-16, PH-17, and PH-18 was a subtidal deposit, which consisted of a dark gray to dark olive gray to black silty clay that was very moist (Table 3-3). Surface sediments in the outer channel had more sand present, as grab sample PH-2 contained silty fine sand and grab sample PH-1 contained silty coarse sand with gravel. In addition, grab PH-9 had silty clay with a few rocks, grabs PH-13 and PH-19 had silty clay with very fine to fine sand, and grab PH-20 had sandy, silty clay (Table 3-3).

Grab samples PH-13 and PH-17 were analyzed further to provide detailed information on the Fore River sediments. Clays dominated both samples, comprising 53.5% of the sediment in grab PH-13 and 49% in grab PH-17 (Table 3-1). Silt was the second dominant grain size fraction, at 31% in grab PH-13 and 43% for PH-17. The sand in the samples was predominately fine to very fine and comprised 14.4% of the sediment in grab PH-13 and 7.5% in PH-17. Both grab samples had similar values for specific gravity (2.6), wet bulk density (1.5) and dry bulk density (0.7), and these values were also similar to those obtained in the cores (Table 3-2). The results provided by these analyses were incorporated in the overall averages used to characterize the Portland Harbor dredged material as part of the computer modeling effort.

3.1.3 Portland Disposal Site Grab Samples

In addition to the sampling in Portland Harbor in November 1998, a grab sample was also collected within PDS in the vicinity of the PDA 98 buoy. Grain size analysis of sample PDS-Buoy2 indicated that the sediment at the PDA 98 buoy location before disposal of Portland Harbor dredged material consisted of 69% medium and fine sand, 28% silts and clays, and 2.2% coarse-grained material (likely shell hash; Table 3-1). Although the specific gravity values were comparable to the Portland Harbor data (Table 3-2), the higher sand

Table 3-3. Descriptions of Grab Samples Collected from Portland Harbor and the PDA Buoy, November 1998

Location	Grab Sample	Date	Est. Grain Size	Color	Texture	Other
Outer Harbor	PH-1	11/3/1998	Silty coarse sand w/ gravel	dark olive gray	coarse- to medium-grained	shell fragments
	PH-2	11/3/1998	silty mud-fine sand	dark gray	medium-grained	normal shell fragments, plant
	PH-3	11/3/1998	Silty clay	black dark olive gray	fine-grained, moist to wet	
	PH-4	11/3/1998	Silty clay	olive gray surface, black	fine-grained, moist to wet	clam
	PH-5	11/3/1998	Silty clay	black	moist to wet	sulfide industrial
	PH-6	11/3/1998	Silty clay	dark gray	very wet	
	PH-7	11/3/1998	Silty clay	dark gray	firm to moist	
	PH-8	11/3/1998	Silty clay	dark olive gray	moist to wet	
	PH-9	11/3/1998	Silty clay w/ a few blk rocks	dark olive gray black/olive gray	moist to wet	
	PH-10	11/3/1998	Silty clay	olive gray surface, black	fine-grained, moist to wet	slightly sulfidic
	PH-11	11/3/1998	Silty clay	olive gray to dark gray	fine-grained, moist to wet	hydrocarbon
Inner Harbor	PH-13*	11/3/1998	Silty clay w/ v.fine sand	black and dark olive gray	very wet	plant stem
	PH-14	11/3/1998	Silty clay	black and dark olive gray	very wet	slightly sulfidic
	PH-15	11/3/1998	Silty clay	black and dark olive gray mixed	very wet	slightly sulfidic
	PH-16	11/3/1998	Silty clay	dark gray and dark olive gray	firm to moist	
	PH-17*	11/3/1998	Silty clay	olive gray to dark gray	fine-grained, very wet	
	PH-18	11/3/1998	Silty clay	olive gray surface, dark gray	very wet	
	PH-19	11/3/1998	Silty clay w/ fine sand	dark olive gray	medium-grained, moist to wet	
	PH-20	11/3/1998	Sandy, silty clay	black to dark gray	moist to wet	
PDS	PDA Buoy*	11/2/1998	Sandy, silty clay	dark olive gray to gray	fine-grained, moist to wet	

* Samples Analyzed

content within the ambient sediments or relic deposited dredged material present near the buoy made the material more dense and compact. As a result, wet and dry bulk density values were higher than those found in the harbor sediments, while the water content was significantly lower (Table 3-2).

Additional grab samples were collected at PDS during the sediment trap deployment effort. One sample was obtained within 50 m of each sediment trap location, described in detail, preserved, and archived in the event future analyses were required (Table 3-4). No geotechnical analyses have been performed, but the grab sample collected from the PDS-ST3 deployment location was analyzed for microfossil content (see section 3.3 below).

3.2 Sediment Traps

Sediment Traps 1, 3, 7, 8 and 10 were recovered from PDS in April 1999 after the third phase of the Portland Harbor dredging project was completed. Only Sediment Traps 3, 8, and 10 were considered to have sufficient volumes of material for further analysis. The material from Sediment Trap 3 (sample PDS-ST3) was analyzed for grain size distribution and bulk density (Tables 3-1 and 3-2). The material from Sediment Trap 8 (sample PDS-ST8) was analyzed for bulk density only, while the scarcity of material recovered in Sediment Trap 10 (sample PDS-ST10) prevented any geotechnical analysis.

Material described as brown silty clay was recovered in each of the three sediment traps. The brown silty clay in PDS-ST3 was 5.8 cm thick and was relatively firm, with a few arrow worms on the surface (Chaetognath *Sagitta* sp.), and no overlying water (Table 3-5 and Figure 3-5). The material in PDS-ST8 was 1.9 cm thick and also contained arrow worms, along with a tree leaf, on the surface and no overlying water (Table 3-5). The material in PDS-ST10 was approximately 2 cm thick and consisted of wet, brown silty clay; it also had arrow worms and a plant fragment on the surface (Table 3-5).

The sediment from PDS-ST3 consisted predominantly of clay (79%), followed by silt (19.8%) and a very small percentage of fine to very fine sand (1.1%; Table 3-1). The specific gravity and bulk density values for samples PDS-ST3 and PDS-ST8 were similar (Table 3-2). The testing performed on the sediment trap samples yielded specific gravity results similar to the values derived from both the Portland Harbor cores and grab samples and the PDS grab sample. Water content of the sediment trap samples (204%) was significantly higher than the Portland Harbor sediments, indicative of the recent water column origin and an abundance of interstitial space between the sediment grains. Wet ($1.3\ g \cdot cm^{-3}$) and dry ($0.43\ g \cdot cm^{-3}$) bulk density values were lower for the sediment trap material compared to the Portland Harbor sediments, again reflecting both the greater abundance of interstitial spaces and the higher clay content.

Table 3-4. Description of Grab Samples Collected from the Sediment Trap Deployment Locations, March 1999

Sample ID	Date	Est. Grain Size	Color (surface/subsurface)		Texture	Odor	Other
PDS-ST-1G	3/18/1999	Silty clay with gravel	olive gray	dk olive gray	firm to moist	normal marine	tubes, worms
PDS-ST-2G	3/18/1999	Sandy silt	dk olive gray	dk gray brown	coarse- to medium-grained	normal marine	shell frag.
PDS-ST-3G	3/18/1999	Sandy silt	olive gray brown	olive gray brown	coarse- to medium-grained	normal marine	worms, plant debris
PDS-ST-4G	3/18/1999	Sandy, silty clay	olive gray brown	dk olive gray brown	coarse- to medium-grained	normal marine	few tubes, worms
PDS-ST-5G	3/18/1999	Silty clay	olive gray brown	dk olive gray	firm to moist	normal marine	tubes, worms
PDS-ST-6G	3/18/1999	Sandy, silty gravel	olive gray	olive gray brown	fine grain with rocks, moist	normal marine	tubes, worms, clam shells
PDS-ST-7G	3/18/1999	Silty clay	olive gray	dk olive gray	firm to moist	normal marine	worm, sea cucumber
PDS-ST-8G	3/18/1999	Sandy silt	olive gray	olive gray	coarse- to medium-grained	normal marine	tubes, worms, shells
PDS-ST-9G	3/18/1999	Silty clay	olive gray	olive gray	fine-grained, moist to wet	normal marine	tubes, worms
PDS-ST-10G	3/18/1999	Silty clay	olive gray	olive gray	fine-grained, moist to wet	normal marine	tubes, worms, plant debris

Table 3-5. Descriptions of Sediment Trap Samples Collected from the Portland Disposal Site, April 1999

Sediment Trap	Total Thickness (cm)	Interval		Description	Sample Type	Sample Depth (cm)		Number of Days Deployed	Approx. Water Depth (m)
PDS-ST-3	4.5-5.8	0	5	firm brown (4/3) silty clay with "normal" marine odor, with a few worms on surface, no overlying water	Sed Tracer Sed Tracer Grain Size B.D., S.G., W.C.	0 2.5 0 0	2.5 5 5 5	33	65
PDS-ST-8	1.9	0	1.9	brown (4/3) silty clay with small worms and leaf on surface, no overlying water	Sed Tracer B.D., S.G., W.C.	0 0	2 2	33	60-65
PDS-ST-10	2	0	2	brown (4/3) silty clay with small worms and leaf on surface, very wet, overlying water was decanted off	Sed Tracer	0	2	33	95-100

* B.D. Bulk Density; S.G. Specific Gravity; W.C. Water Content

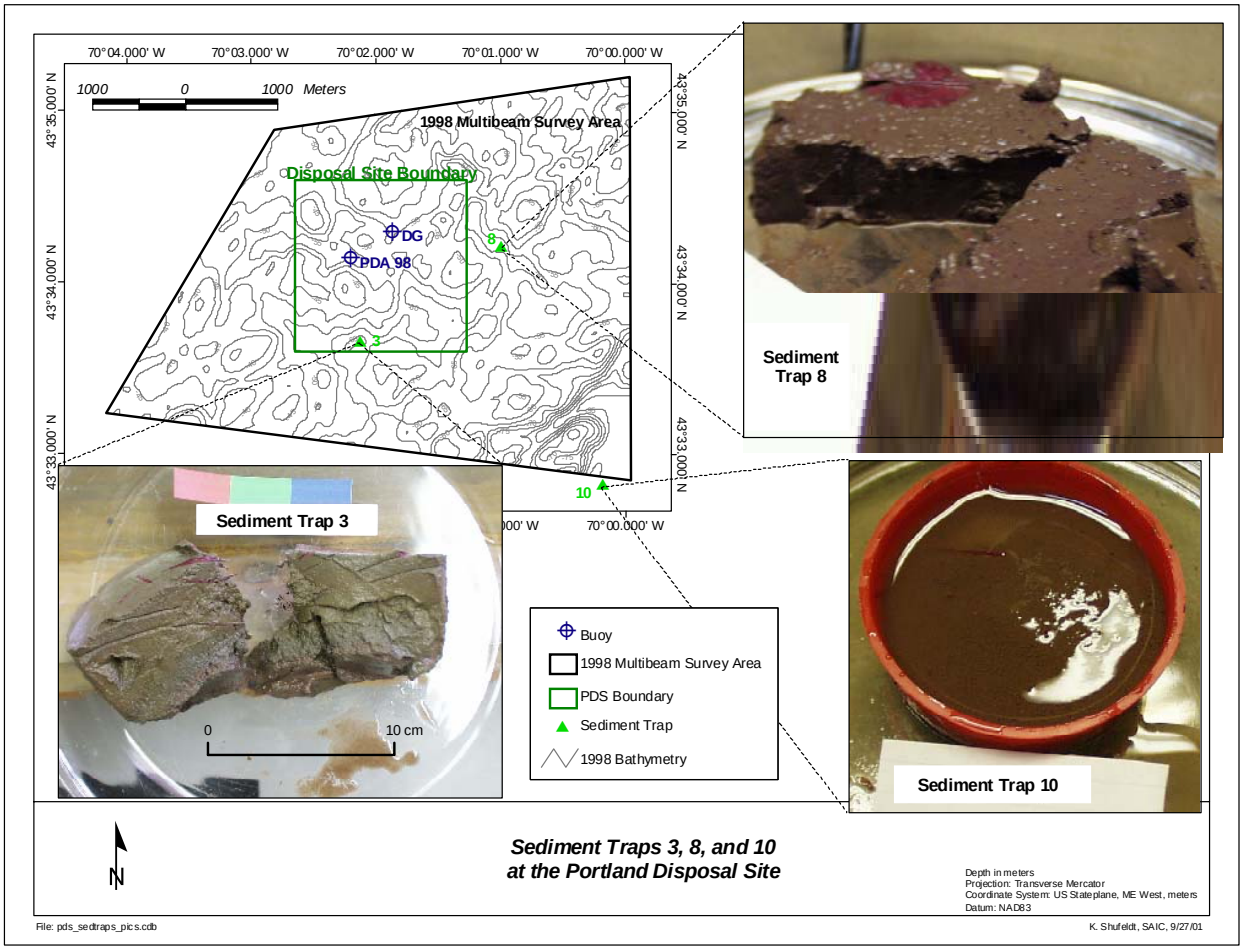

Figure 3-5. View of material retained within Sediment Traps 3, 8, and 10. Material is predominantly brown, moist, firm, silty clay with arrow worms (Chaetognath *Sagitta* sp.) and plant fragments stained red by Rose Bengal preservative

3.3 Sediment Tracer Analyses

As previously described, the nine samples used for the sediment tracer analysis included two of the cores from Portland Harbor (samples PH-4 and PH-7), one of the grab samples from Portland Harbor (sample PH-17AG), a baseline grab sample collected from the PDA-98 disposal buoy at the PDS (sample PDA-Buoy2), a grab sample from the deployment location of Sediment Trap 3 (sample PDS-3G), and four samples of the sediment collected within the sediment traps (samples PDS-ST3 0-2.5 cm, PDS-ST3 2.5-5.0 cm, PDS-ST8 and PDS-ST10). Both the coarse and fine fractions of the sediments were examined for the presence of a suitable sediment tracer. Given the improbability of any of the coarse fraction material (>500 mm) being incorporated into a sediment plume and transported away from the disposal point, any tracer found to be present in this fraction would likely be useful only to distinguish dredged material layers already deposited on the seafloor.

3.3.1 Coarse Fraction Analyses

In all of the samples, the most common components of the coarse sediment fraction were plant fragments, sand, and gravel. The analyses of the coarse fraction failed to find any unique larger-sized material present in any of the samples that might serve to distinguish between the harbor and disposal site sediments. As a result, the coarse fraction data were not considered useful in the identification of any sediment tracers.

3.3.2 Fine Fraction Mineralogy

The descriptions of the mineralogical composition of the fine fraction included analyses of grain size, relative abundance of quartz, mica and fibrous minerals, and relative abundance of several microbiological components (e.g., insect parts, plant fragments, diatoms, ostracods, fecal pellets, and shell fragments; Table 3-6).

In the core and grab samples from Portland Harbor, quartz and plant fragments were most abundant, and micas were common (Table 3-6). The grab samples of ambient surface sediments at the disposal site were different from the harbor samples, with both quartz and planktonic diatoms being abundant, but micas and plant fragments being rare (Table 3-6). None of the constituents that were abundant or common in the harbor and ambient PDS sediments were found to be abundant in the sediment traps (Table 3-6). Insect parts were found in only one harbor sample, and benthic diatoms, though rare, were found exclusively in the harbor sediment samples. Fecal pellets from benthic infauna populations were rare to absent in nearly all samples, while gastropods, bryozoans, and textured and smooth ostracods were absent in all of the samples (Table 3-6).

The heavy quartz grains that were observed to be relatively abundant in the harbor and PDS sediment samples were less apparent within the sediment trap samples after the conclusion of disposal operations. Very fine quartz grains were rare in sediment trap

Table 3-6. Mineralogical Composition of Sediment Obtained from Portland Harbor Cores, PDS Grab Samples, and Sediment Traps

Sample ID	Depth interval (cm)	Location	Grain size	Quartz	Micas	Fibrous minerals	Insect parts	Plant fragments	Benthic Diatoms	Planktonic Diatoms	Textured Ostracods	Smooth Ostracods	Pellets	Shell fragments	Gastropod	Bryozoan
PH-4	0-12 (core)	Portland Harbor	F	x	x	x	x	XX	x				x			
PH-7	0-10 (core)	Portland Harbor	F	XX	x	x		XX	x				x	x		
PH-17AG	0-10 (grab)	Portland Harbor	F	XX	x	x		XX	x							
PDS-3G	0-10 (grab)	PDS (ST-3 location)	M	XX	x	x		x		XX			x			
PDS-Buoy2	0-10 (grab)	PDS (PDA 98 Buoy)	C	XX	x			x		x						
PDS-ST3	0-2.5	Sediment Trap	VF	x	x	x		x		x			x			
PDS-ST3	2.5-5.0	Sediment Trap	VF	x	x	x		x		x			x			
PDS-ST8	0-1.9	Sediment Trap	VF	x	x	x		x		x			x			
PDS-ST10	0-2	Sediment Trap	VF	x	x	x		x		x			x			

KEY	XX-abundant	C-coarse
	X-common	M-medium
	x-rare	F-fine
	absent	VF - very fine

samples PDS-ST8 and PDS-ST10, while the surface layer of sediment within Sediment Trap 3 (sample PDS-ST3 0-2.5 cm interval) showed a higher quartz concentration. Because quartz was abundant both in the harbor sediments and the ambient surface sediments at PDS, it is difficult to ascertain whether the apparent enrichment at the surface of PDS-ST3 was due to differential settling of dredged material entrained within the water column or resuspension from the surrounding seafloor. For this reason, quartz does not represent a useful tracer.

Because micas were relatively abundant in the harbor samples but rare on the ambient seafloor, they represent a better potential tracer of the dredged material than quartz. However, both the mica and quartz particles examined as part of the fine fraction in this study were larger and heavier than the finest-grained sediment fractions (i.e., silt and clay) likely to comprise a disposal plume. Because both the quartz and mica particles are likely to settle out of the water column faster than the finer sediment comprising the plume, the relative absence of these components from the sediment traps does not necessarily indicate a lack of effect from dredged material disposal.

Based on their relative abundance in the harbor samples, plant fragments and benthic diatoms also represented potential unique tracers of the dredged material. However, because benthic diatoms were relatively rare in the harbor samples and may not stay intact during dredging and subsequent transport, their absence from the sediment traps does not unequivocally indicate an absence of harbor dredged material. Plant fragments presumably might be transported through the water column in a manner consistent with the disposal plume; therefore, the absence of this tracer in the sediment traps is considered an indication of the lack of a dredged material influence.

3.3.3 Fine Fraction Microfossil Composition

Microfossil species composition and abundance generally reflect differences in salinity and sediment-types in the intertidal, subtidal, and open water zones. As described in greater detail in the following sections, distinct populations were detected in the brackish and marine reaches of Portland Harbor versus the open water, inner continental shelf environment of the disposal site.

3.3.3.1 Portland Harbor Sediment

A total of 14 different species of benthic foraminifera were recovered from the Portland Harbor sediment samples collected on 3 November 1998 (grab sample PH-17AG) and 3 March 1999 (core samples PH-4 and PH-7; Table 3-7). Of these species, five have a worldwide distribution (*Miliammina fusca*, *Ammotium salsum*, *Trochammina inflata*, *T. macrescens*, and *Tiphotrocha comprimata*), while four more (*Arenoparella mexicana*, *Haplophragmoides manilaensis*, *Eggerella advena*, *Textularia earlandi*) are considered common constituents in the estuarine environment. The common species are found in

Table 3-7. Abundance of the Various Species of Foraminifera Detected within the Portland Harbor, PDS Grab Samples, and Sediment Traps

Foaminifera Coastal Zonation			Salt Marsh Agglutinated Taxa							Shelf Agglutinated Taxa											Mudflat Calcareous			Shelf Calcareous									Planktonic Species				Freshwater
Location	Sample ID	Depth interval (cm)	M. fusca	A. salsum	T. inflata	T. comprimata	T. macrescens	A. mexicana	H. manilaensis	Haplophragmoides sp.	Eggerella advena	T. earlandi	Crib. weddellensis	Crib. jeffreysii	Rheophax scorpiurus	Alveolophragmium advena	Goesella flintii	Gaudryina arenaria	Recurvoides turbinatus	Trochammina squamata	A. beccarii	P. orbiculare	E. excavatum	Ammonia sp.	Elphidium sp.	Buccella frigida	Cassidulina sp.	Cibicides lobatulus	Trifarina angulosa	Trifarina baggi	Nonionella atlantisae	Fissurina sp.	Angulogerina angulosa	Globobulimina sp.	Globocassidulina subglossa	Total foram	thecamoebian
Harbor	PH-4	0-12 (core)			1	7	9				16	2		1						6		1	57													100	0
Harbor	PH-7	0-10 (core)	2	1	1	1	6				2	1								5		4	20			5										48	0
Harbor	PH-17AG	0-10 (grab)	11	1	4	5	17	1	1		6	2																								48	4
PDS	PDS-3G	0-10 (grab)		1						1	7	2		12	40				3	4																70	0
PDS	PDS-Buoy2	0-10 (grab)		1	3	2					5	1		2	14					3		2	9			4					2					48	0
Sediment Trap	PDS-ST3	0-2.5			3		1				9				2	2		1		22	1		16		2	3			1	2	3	1				69	4
Sediment Trap	PDS-ST3	2.5-5.0									3	2				1	2			16		7	3		2	5	2	3		1		1	1			49	0
Sediment Trap	PDS-ST8	0-1.9			1					1	2					3	1		1				8		3	8		2	2	1	2					35	0
Sediment Trap	PDS-ST10	0-2									1	1		2				1		1	1				3	1	2	4	2	2	1					22	0

estuaries along the Atlantic seaboard of North America and have been used as ecological markers within 125,000-year-old sediments as part of studies performed in Massachusetts Bay (Murray 1991).

The microfossil assemblages found in the Portland Harbor core and grab samples consisted primarily of marsh agglutinated and mudflat calcareous foraminifera (Table 3-7 and Figure 3-6). A small number of thecamoebians, indicative of fresh water input, was noted in grab sample PH-17AG collected from the Fore River channel (Table 3-7 and Figure 3-6). Mudflat calcareous species were absent from grab sample PH-17AG, but relatively abundant in samples PH-4 and PH-7. A few shelf agglutinated taxa were found in all three of the samples, and 5 individuals of the shelf calcareous species *Bucella frigida* were observed in sample PH-7 only (Table 3-7 and Figure 3-6). These microfossils were probably transported into the harbor and river via tidal exchange with Casco Bay.

Elphidium excavatum, Ammonia beccarii and *Protelphidium orbiculare* are common, cosmopolitan and very shallow marine calcareous species. These calcareous species typically occur in the lower part of the intertidal zone. All calcareous forms (*Quinqueloculina* sp., *A. beccarii, P. orbiculare* and *E. excavatum*) occur in the lower (higher salinity) areas of the marsh environment, and are most common on the mudflats below the marsh. In Portland Harbor, there were relatively large numbers of the mudflat calcareous species *E. excavatum* and a few individuals of *P. orbiculare* in the core sediments (samples PH-4 and PH-7), but no mudflat calcareous species in the grab sample (PH-17AG) from the Fore River (Table 3-7).

Salt marsh agglutinated forms such as *A. salsum* are most common in the low marsh and on the mudflats, together with the calcareous species listed above. *A. salsum* occurred in the core samples analyzed from PH-7 and the Fore River grab sample (Table 3-7). *M. fusc*a is most common in lower to middle marsh, and may occur on mudflats as well. *M. fusc*a occurred in one of the core samples and was fairly abundant in the Fore River grab sample. *T. macrescens, T. inflata,* and *T. comprimata* are common middle marsh species, with *T. comprimata* usually associated with marsh vegetation (e.g., *Spartina* sp.). *T. inflata* is dominant in salt pannes without vegetation, where salinity can be very high due to evaporation. *T. macrescens, T. inflata,* and *T. comprimata* were found in both the harbor core and the Fore River grab samples (Table 3-7). *A. mexicana* most commonly occurs in the middle to lower marsh, especially in close proximity to creeks. Only one individual of *A. mexicana* was found in the Fore River grab sample.

Salt marsh agglutinated taxa such as *H. manilaensis* are common in the upper regions of the middle marsh to high marsh, especially where there is lowered salinity due to fresh water input. In the highest portion of this type of marsh environment (low salinities), both *H. manilaensis* and *T. macrescens* are typically found in nearly equal distributions. In marsh regions that are brackish, but without large sources of fresh water input, the meiofauna is

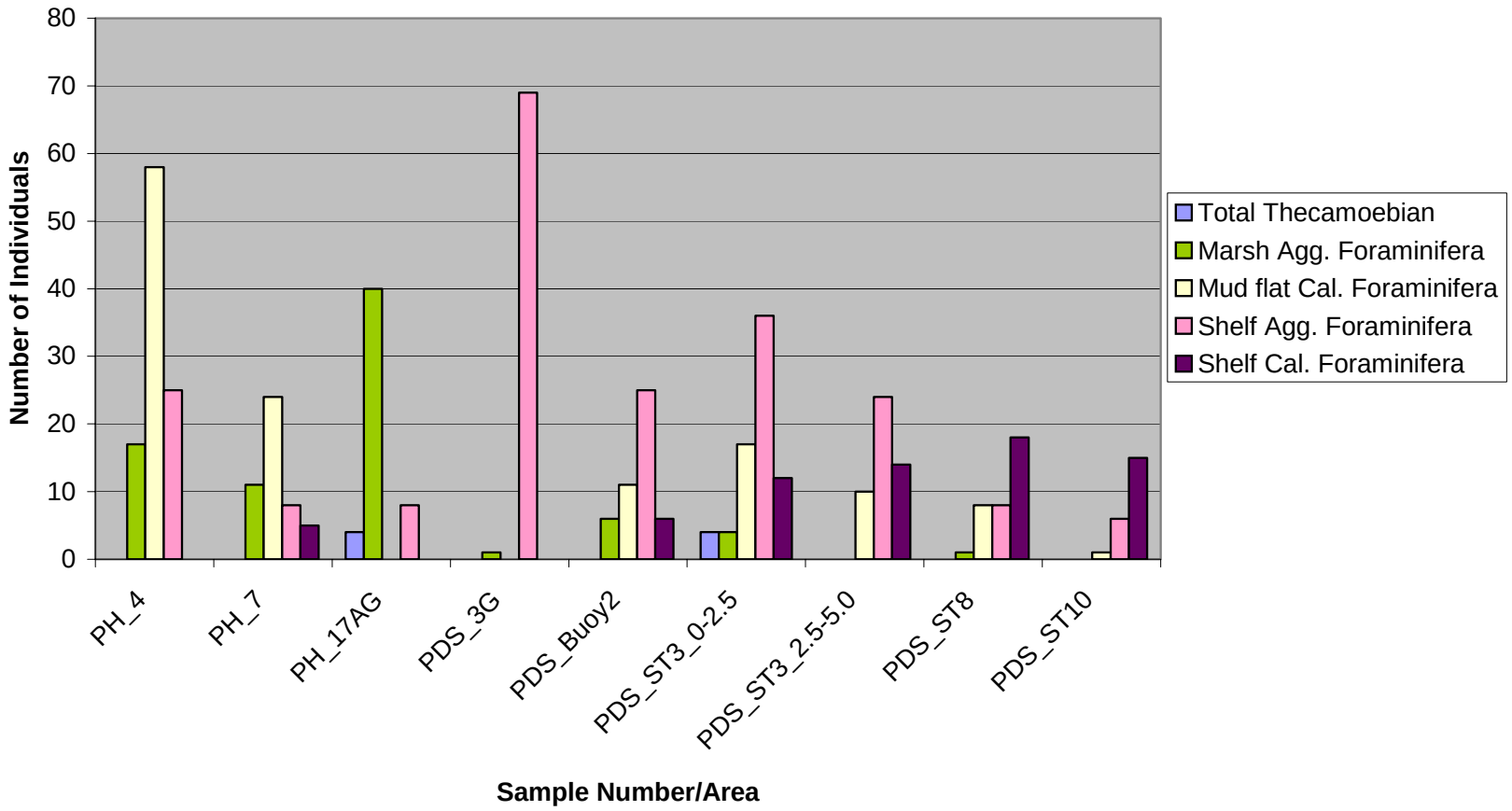

Figure 3-6. Histogram of microfossil assemblage types found in selected Portland Harbor sediment cores and grab samples, Portland Disposal Site grab samples, and Portland Disposal Site sediment traps

typically dominated by *T. macrescens* (>90%). The grab sample from the Fore River (sample PH-17AG) reflects the latter description, as 17 individuals of *T. macrescens* were detected, while only one individual of *H. manilaensis* was found.

3.3.3.2 PDS Grab Samples

Of the two grab samples processed for microfossil content (PDS-Buoy2 and PDS-3G), both showed shelf agglutinated foraminifera in abundance, with relatively small numbers of shelf calcareous foraminifera also present in PDS-Buoy2 (Figure 3-6 and Table 3-7). In addition, marsh agglutinated species were represented in both samples, but mudflat calcareous foraminifera were only detected in grab sample PDS-Buoy2 taken in close proximity to the PDA 98 buoy. No evidence of freshwater thecamoebian species were detected in either of the PDS grab samples.

The shelf agglutinated species *Rheophax scorpiurus* dominated both grab samples, followed by *Cribrostomoides jeffreysii* and *E. advena*. A small number of *B. frigida* and *Nonionella atlantisae* (calcareous species) appeared in the sediments acquired in close proximity to the PDA 98 buoy location (Table 3-7).

Two species of mudflat calcareous foraminifera (*E. excavatum*, and *P. orbiculare*), as well as the marsh agglutinated species *A. salsum*, *T. inflata*, and *T. comprimata*, were detected in the surface sediments at the PDA 98 buoy (sample PDS-Buoy2) in November 1998 (Table 3-7). The presence of these estuarine species around the disposal buoy prior to deposition of the sediment dredged from Portland Harbor is most likely linked to a layer of the historic dredged material or far-field transport of dredged material from the DG buoy deposit.

3.3.3.3 PDS Sediment Traps

Overall, the material captured by the PDS sediment traps was dominated by shelf foraminifera (Figure 3-6 and Table 3-7). For example, an abundance of the shelf agglutinated species *T. squamata* was detected throughout sample PDS-ST3, along with a significant number of *E. advena* (Table 3-7). The density of *E. advena* was lower in sample PDS-ST8, and *T. squamata* was totally absent. Only one individual of each species was present in the PDS-ST10 material. No distinct trends were noted in the distribution or density of calcareous shelf species. *B. frigida* was the most abundant of this type of meiofauna, but still fairly scarce overall. Small numbers of *Elphidium* sp., *Cibicides lobatulus*, and *Trifarina angulosa* also were detected in each sediment trap. However, no representatives from these species were noted in either the harbor samples or the sediment grabs collected from PDS, suggesting a source other than the areas sampled.

Substantial numbers of the mudflat calcareous species *E. excavatum* and *P. orbiculare* were found in the sediment trap samples PDS-ST3 and PDS-ST8, and salt marsh foraminifera and thecamoebians were detected in equal numbers in the top 2.5 cm of sample PDS-ST3 (Figure 3-6; Table 3-7). Estuarine species (salt marsh or mudflat) were largely absent from sediment trap sample PDS-ST10, except for one individual of the mudflat species *A. beccarii*. The presence of salt marsh agglutinated foraminfera, mudflat calcareous formaninfera, and thecamoebians in the traps at PDS-ST3 and 8 may be attributable to transport and deposition of sediment plumes associated with disposal of Portland Harbor dredged material at the PDA 98 buoy. However, individuals of several mudflat calcareous species and salt marsh agglutinated species also were found in the surface sediments at the PDA 98 buoy location. Therefore, the sediment trap results may also reflect some resuspension and lateral transport of dredged material already on the bottom, instead of or in addition to direct settlement out of a disposal plume.

3.4 Multibeam Bathymetry

3.4.1 September 1998 Survey

The September 1998 multibeam survey covered a 17.7 km² area of seafloor surrounding the current PDS boundary. The spatial coverage and resolution of the 1998 data set provided for better insight (relative to previous single-beam surveys) into the complexity of the seafloor within the region. This new master bathymetric survey served as the basis for the computer-based modeling of dredged material placement within PDS, and also aided in identifying probable depositional areas in the region.

This portion of Bigelow Bight demonstrated a significant amount of vertical relief, as water depths ranged from 28.5 m over a bedrock outcrop in the southwest quadrant of the survey to 102.5 m in close proximity to the SE-REF reference area (Figure 3-7). The color, shaded-relief plot presented in Figure 3-8 depicts some of the larger northeast-southwest trending faults in the exposed bedrock, as well as smaller fractures running perpendicular to the faulting. The bedrock within the confines of PDS is likely part of the Cape Elizabeth formation (gray schist), which makes up the majority of the seafloor (West Cod Ledge) and terrestrial (Calendar Islands) features within the region (Caldwell 1998). This type of faulting is common in southeastern Maine, and actually has been noted in similar bathymetric surveys performed over the Cape Arundel Disposal Site. Soft sediment tends to accumulate within these faults, as well as in the troughs, natural depressions, and basins that exist among the bedrock outcrops.

Most past dredged material disposal operations at PDS have targeted the deeper, depositional areas on the seafloor in order to develop discrete, stable disposal mounds (Figure 3-9). The various bedrock ridges surrounding these depositional areas provide protection from bottom currents and thereby enhance containment of fine-grained dredged

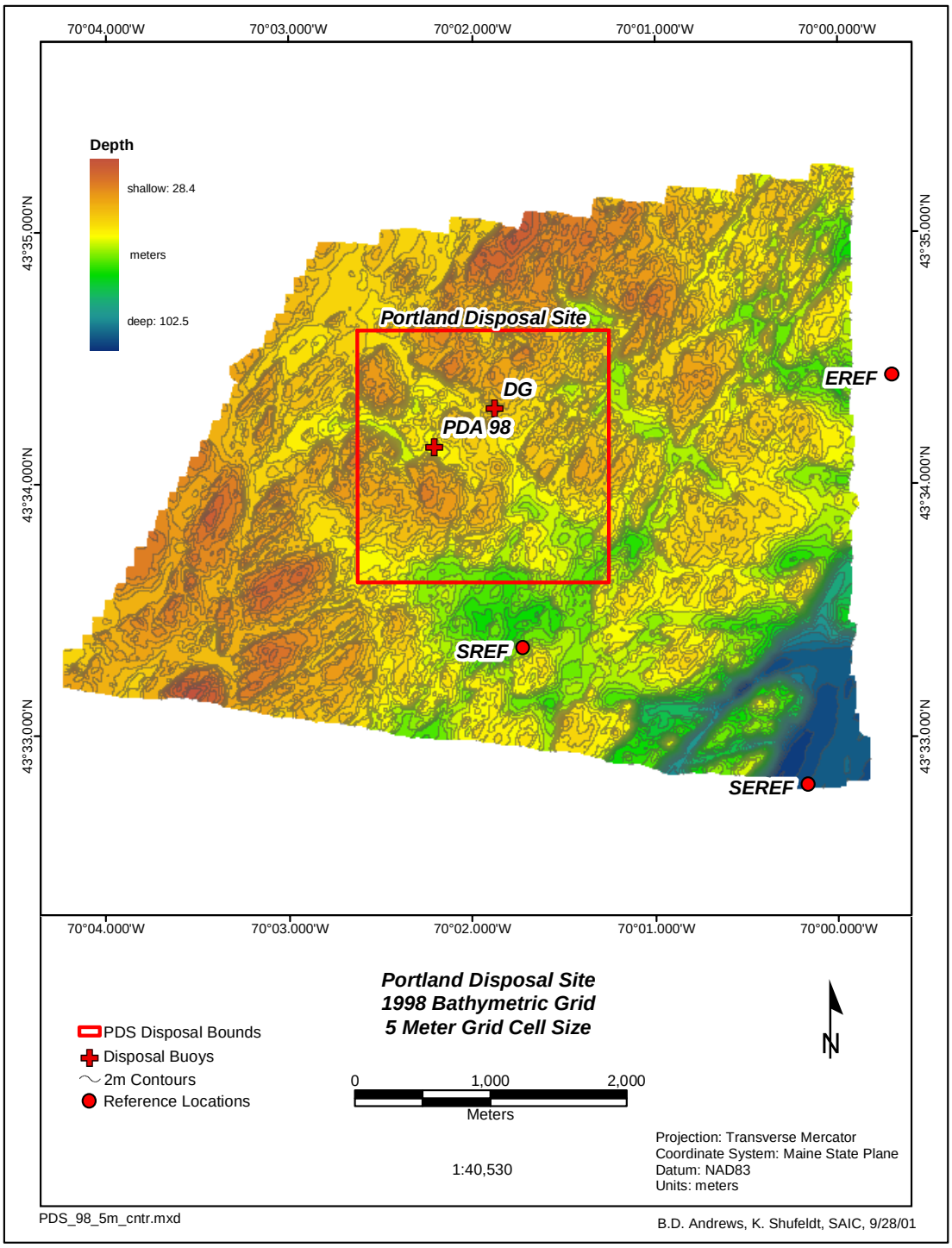

Figure 3-7. Color-filled contour view of the 1998 Portland Disposal Site multibeam survey showing the location of the PDS reference sites

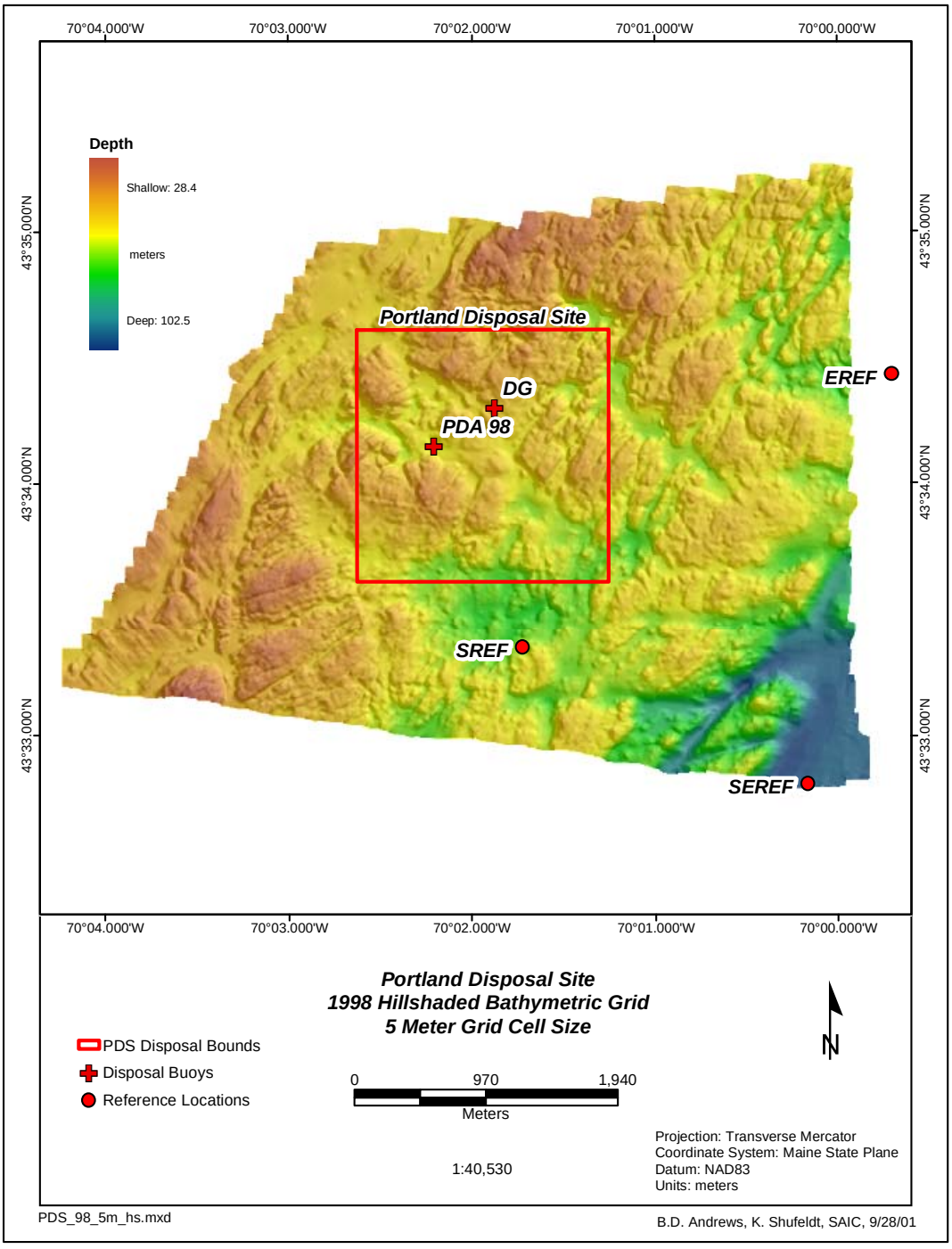

Figure 3-8. Hill-shaded surface view of the 1998 Portland Disposal Site multibeam survey showing the larger northeast-southwest trending faults in the exposed bedrock, as well as smaller fractures running perpendicular to the faulting

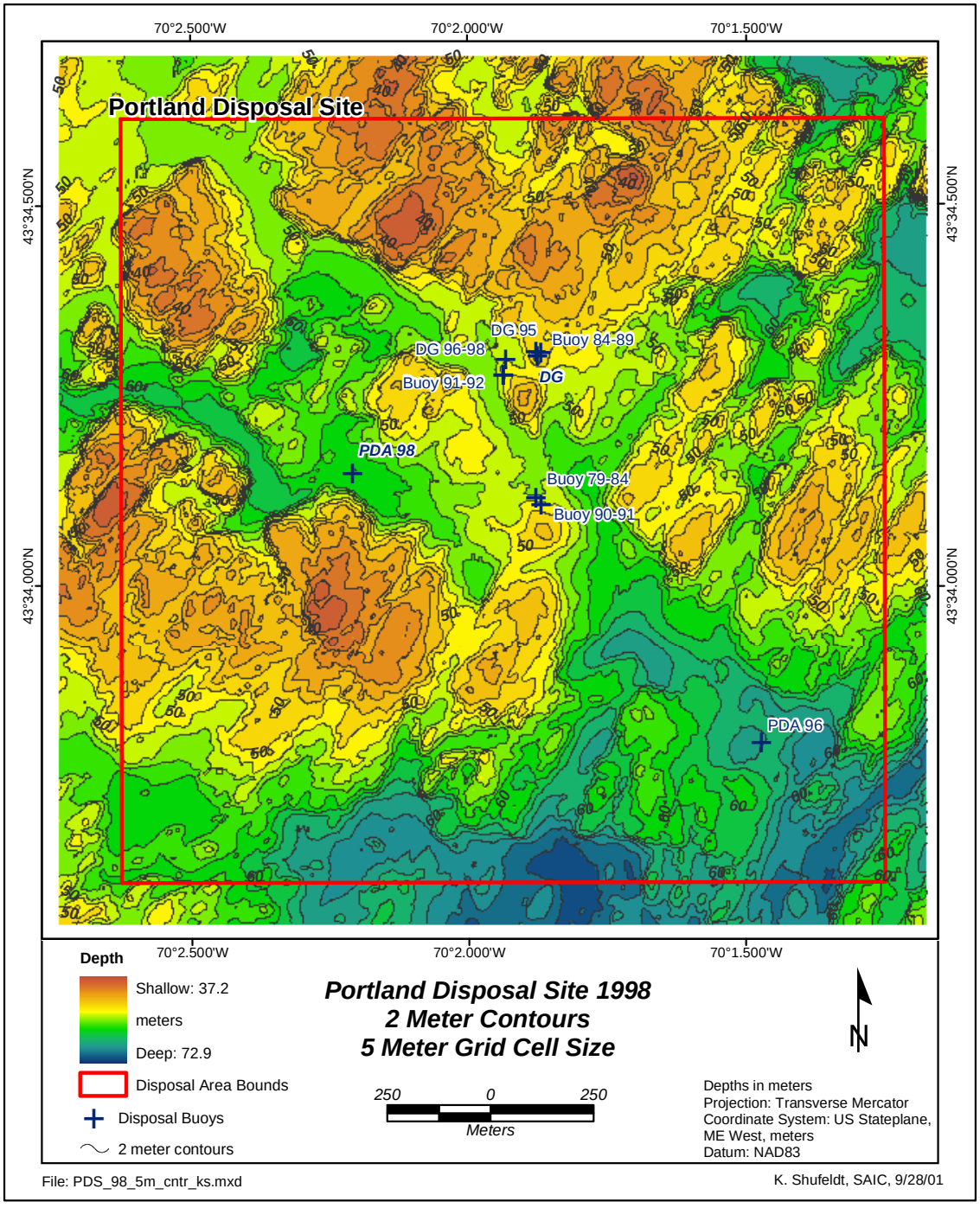

Figure 3-9. Color-filled contour view of the 1998 multibeam survey limited to the boundaries of the Portland Disposal Site and depicting the location of many of the past PDS disposal points

material deposits. In addition, the rock walls of the natural seafloor features are physical barriers that prevent the lateral spread of non-cohesive sediment on the seafloor. The northwest-southeast trending trough that runs through the center of the disposal site has received the bulk of material that has been deposited since 1979. Two gently sloping bathymetric features corresponding to the positions of the DG buoy are easily identified within the trough (Figure 3-10). These dredged material disposal mounds stand in stark contrast to the strong profiles of the surrounding bedrock.

3.4.2 July 2000 Survey

The post-disposal multibeam survey was conducted in July 2000, more than a year after completion of the Portland Harbor dredging project. In addition to the 471,400 m^3 of sediment that was dredged from Portland Harbor and deposited at the PDS during the 1998-1999 season, an additional 18,300 m^3 was deposited during the 1999-2000 dredging season. Though most of the material was placed at the PDA 98 buoy, some material was also deposited around the DG buoy. The post-disposal multibeam survey was performed in July 2000 to examine the changes in seafloor topography related to the placement of dredged material during the 1998-1999 and 1999-2000 disposal seasons.

The 2100 × 2100 m multibeam bathymetric survey provided resolution that was comparable to the September 1998 survey and therefore was useful in depth difference comparisons. The swath bathymetry once again highlighted numerous steep, bedrock ridges and a northwest-southeast trending trough within this complex topographic area (Figures 3-11 and 3-12). A minimum depth of 37 m was detected at the apex of a fairly pronounced bedrock outcrop located approximately 125 m south of the northern disposal site boundary. A maximum depth of 73 m was detected outside the confines of PDS, in a natural basin along the southern margin of the survey area.

3.4.3 1998-2000 Depth Difference Comparisons

Over the two year period between the 1998 and 2000 multibeam surveys, approximately 315,600 m^3 of material was deposited around the PDA 98 buoy and 174,100 m^3 of material was deposited near the DG buoy. First-order depth difference comparisons between the September 1998 and July 2000 multibeam surveys clearly showed the accumulation of dredged material in close proximity to the PDA 98 and the DG buoy locations (Figure 3-13). Closer examination of the area subjected to dredged material disposal activity indicated a thickness 0.25 m to approximately 2 m of recently placed sediment on the seafloor (Figure 3-14). The acoustically detectable dredged material deposit around the PDA 98 buoy was approximately 650 × 200 m, while the sediment deposit around the DG buoy was approximately 250 × 100 m. Both of these sediment deposits tended to follow the confines of the local bathymetry, with most sediment accumulating within the northwest/southeast trending trough (Figure 3-14). The steep bedrock ridge that runs along

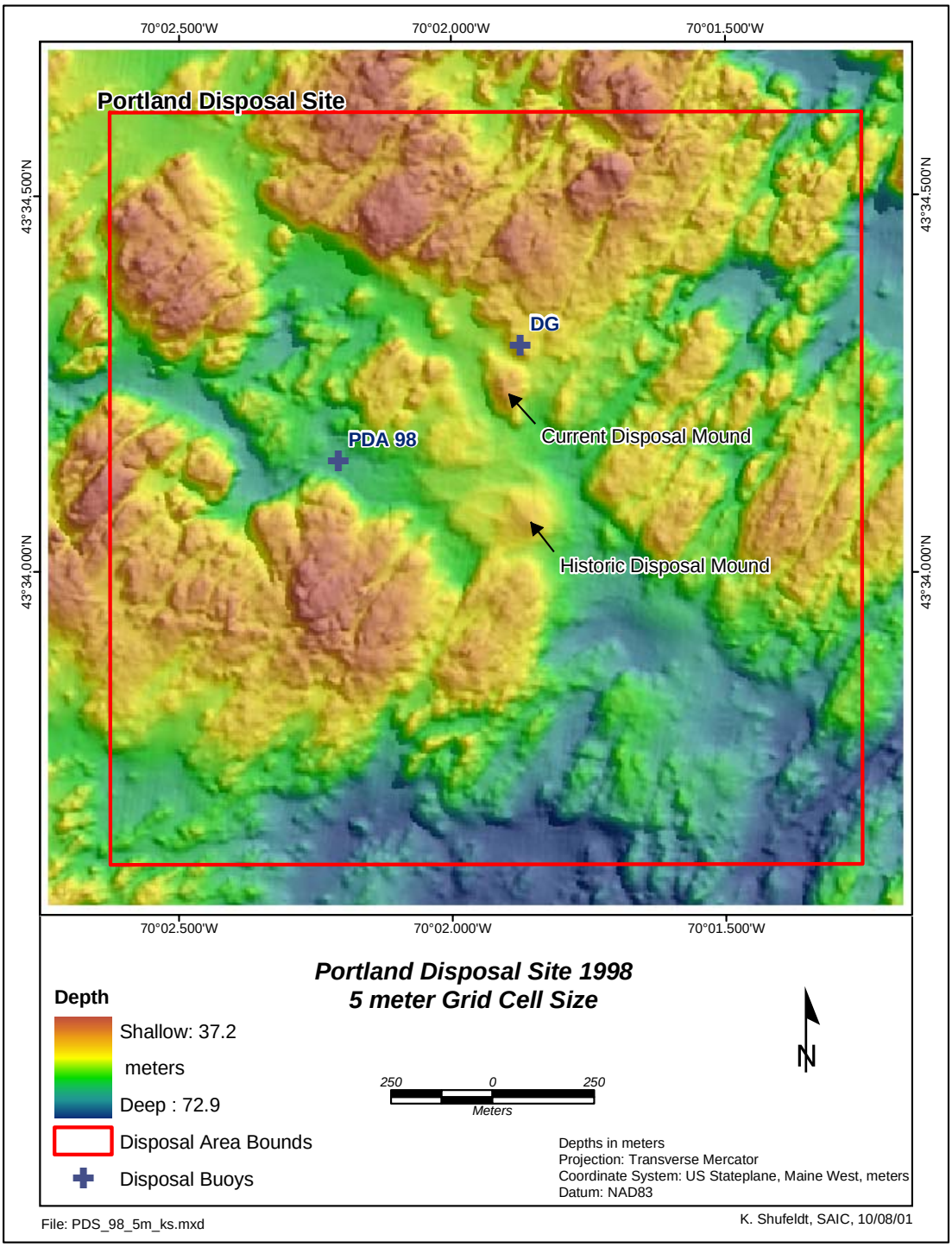

Figure 3-10. Hill-shaded surface view of the 1998 multibeam survey limited to the boundaries of the Portland Disposal Site and depicting the location of recent and historic disposal mounds

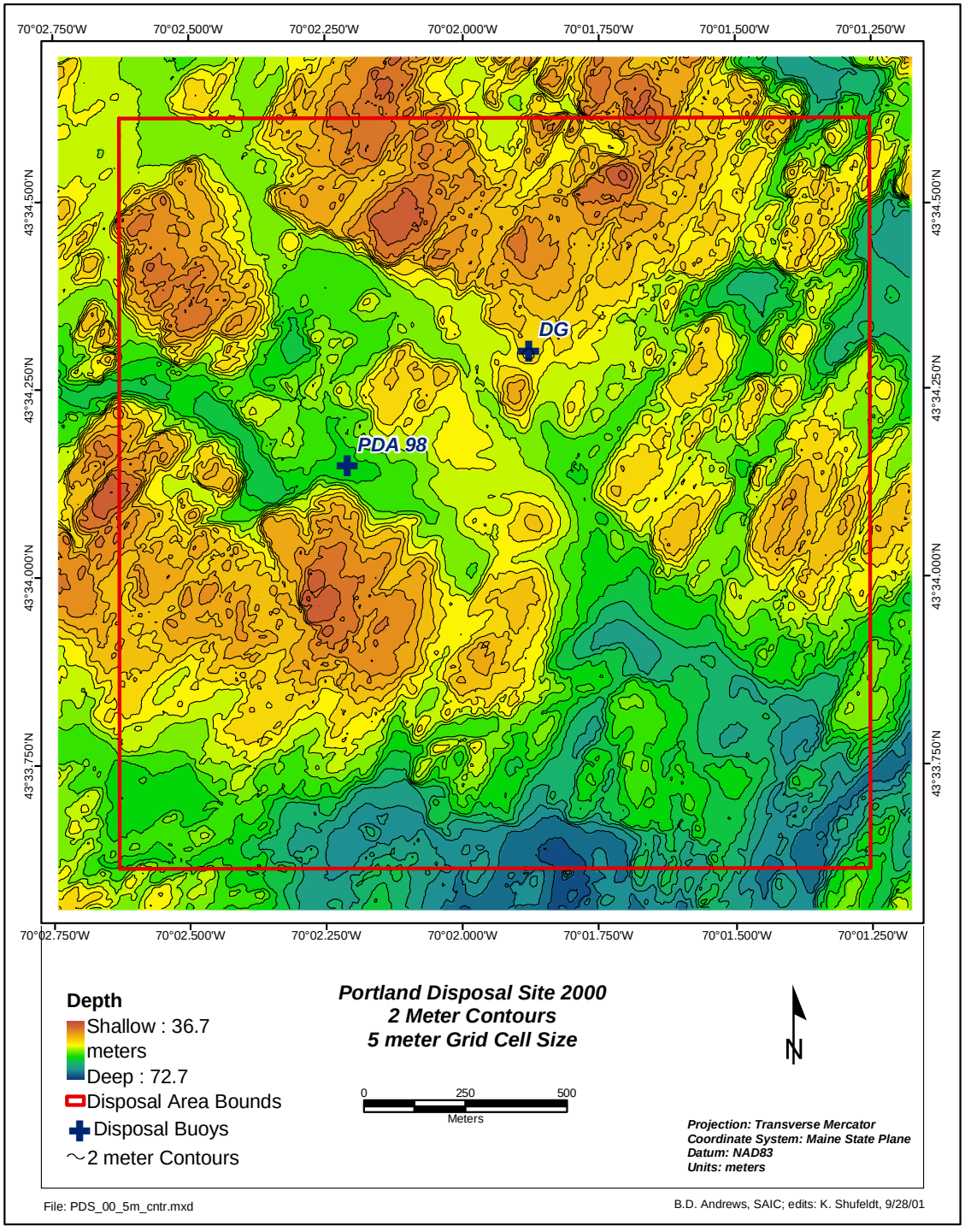

Figure 3-11. Color-filled contour view of the 2000 Portland Disposal Site multibeam survey showing the location of the PDA 98 and DG disposal buoys

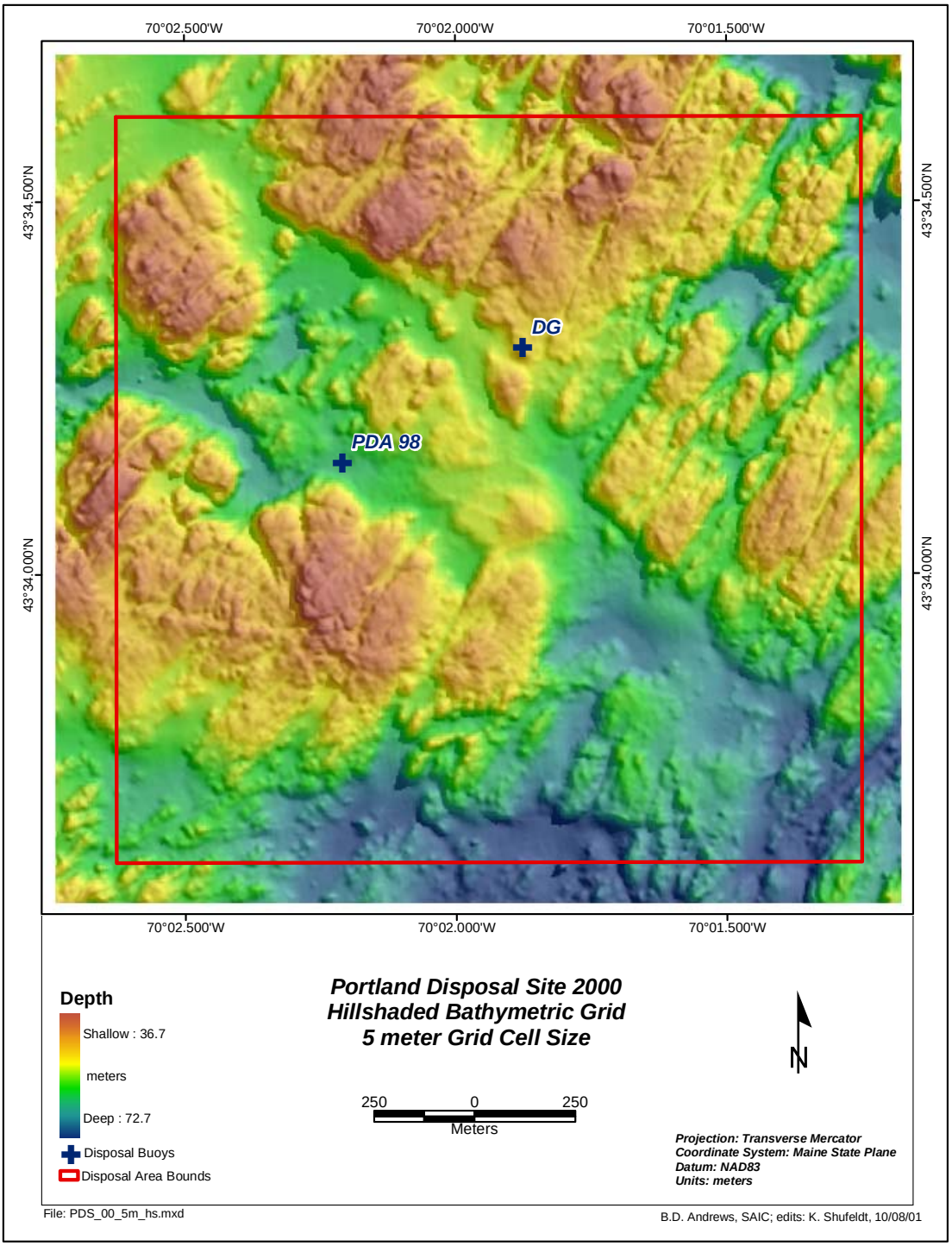

Figure 3-12. Hill-shaded surface view of the 2000 Portland Disposal Site multibeam survey depicting similar features as the 1998 multibeam survey (Figure 3-10)

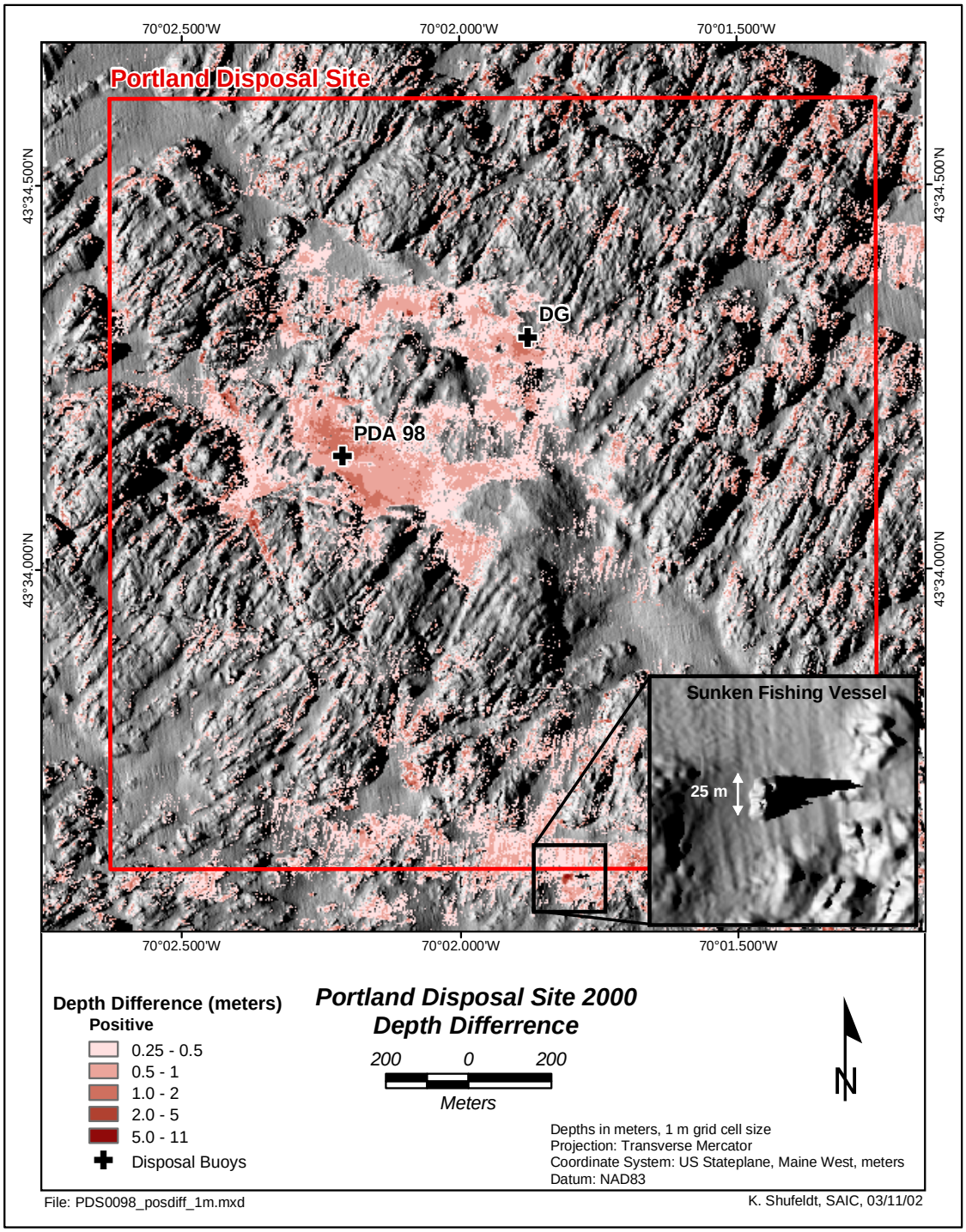

Figure 3-13. Depth difference results between the 1998 and 2000 PDS multibeam surveys showing both accumulation of sediment adjacent to the PDA 98 and DG buoy positions, as well as various survey artifacts

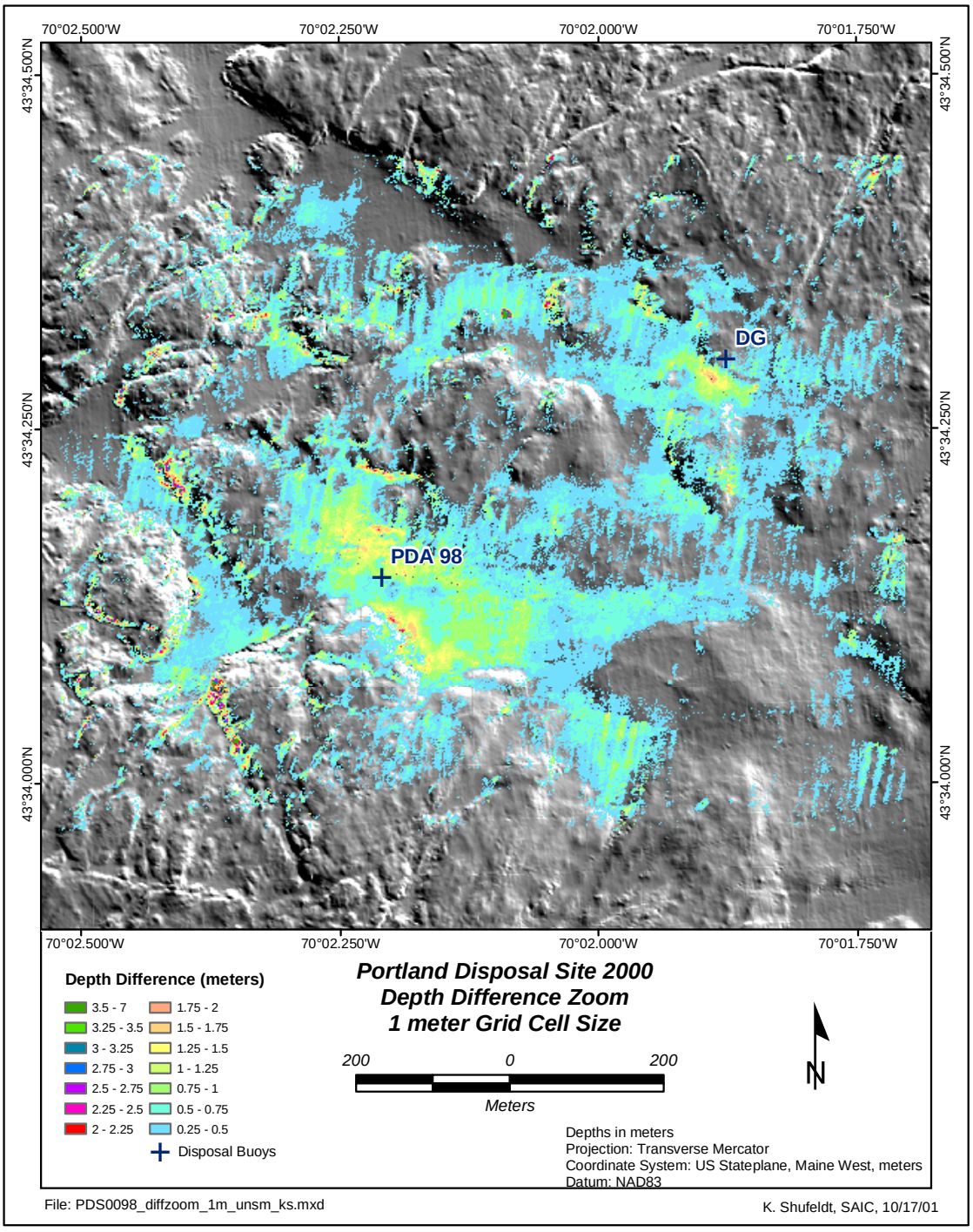

Figure 3-14. Zoomed in view of the depth difference results between the 1998 and 2000 PDS multibeam surveys highlighting the location of the disposal buoys

the southwest side of this deep trough limited the large-scale spread of sediment beyond this wall. Additional dredged material deposits were also apparent in several of the smaller, nearby basin or tough features adjacent to the PDA 98 and DG Mounds (Figure 3-14). Although the depth difference plot displays multiple independent deposits, the spatial distribution of dredged material suggests an apron of sediment less than the 0.25 m threshold of the depth difference comparisons likely connects these thicker accumulations.

Numerous disposal events were reported over the exposed bedrock feature to the south of the PDA 98 buoy (Figure 3-15); the depth difference results show minor accumulation of material in this area (Figure 3-14). The depth difference results also show smaller areas of accumulation to the northwest and southeast of this exposed bedrock feature, though no disposal events were recorded there (Figure 3-15). In addition, it is likely that dredged material settling over this exposed bedrock feature accumulated in small crevices between the bedrock outcrops and was eventually advected to nearby deeper areas.

In addition, a 4 m depth difference was detected in a small basin along the southern boundary of the disposal site. This small feature corresponds to the reported position of a fishing vessel scuttled over PDS as part of an artificial reef program being conducted by the National Marine Fisheries Service (NMFS) for their vessel buy-back program (Figure 3-14).

In addition to the widespread depth difference areas around the PDA 98 and DG buoys, there were also several small areas of large positive depth differences scattered throughout the disposal site. A review of the detailed bathymetry showed that all of these steep depth differences were associated with seafloor areas of strong vertical relief. In these areas, grid cell averaging or a slight misalignment in any of the multibeam sensors may cause some slight distortion of the true seafloor surface. Therefore, the depth difference results in these areas are identified as slope-induced artifacts in Figure 3-14. To gain a better perspective on the dredged material deposit, the view was decreased to a 0.99 km^2 area in the immediate vicinity of the PDA 98 and DG buoys (Figure 3-15).

3.5 Side-Scan Sonar

Side-scan sonar data were used to remotely characterize the entire PDS seafloor during the September 1998 field efforts, prior to the deposition of Portland Harbor dredged material. The side-scan sonar imagery mosaic illustrated bedrock outcrops, large boulders, and sediment-laden valleys on the seafloor (Figure 3-16). The side-scan data confirmed the assumptions made regarding the composition of the seafloor based on the high-resolution, multibeam bathymetry. The side-scan mosaic showed many light areas, representing weak acoustic returns (low reflectance) that are characteristic of softer, lower density sediments such as silts and clays. The darker areas indicate strong acoustic returns (high reflectance) from harder substrates, likely exposed bedrock. Several small holes in the side-scan coverage (white) are the result of avoiding dense aggregations of lobster gear within those immediate areas.

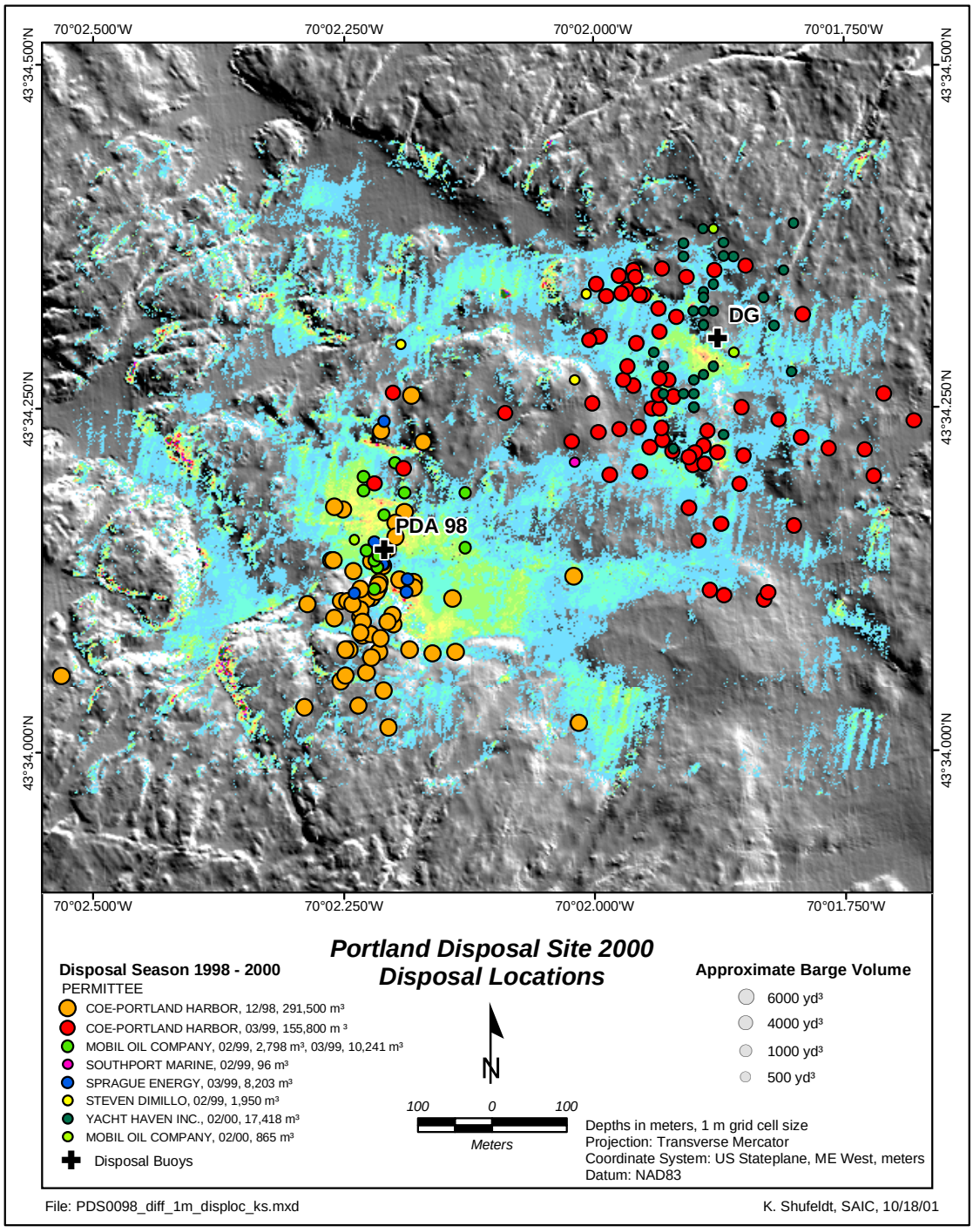

Figure 3-15. Multibeam depth difference results along with plot of barge disposal locations over the Portland Disposal Site between November 1998 and April 2000 as documented by DAMOS disposal logs

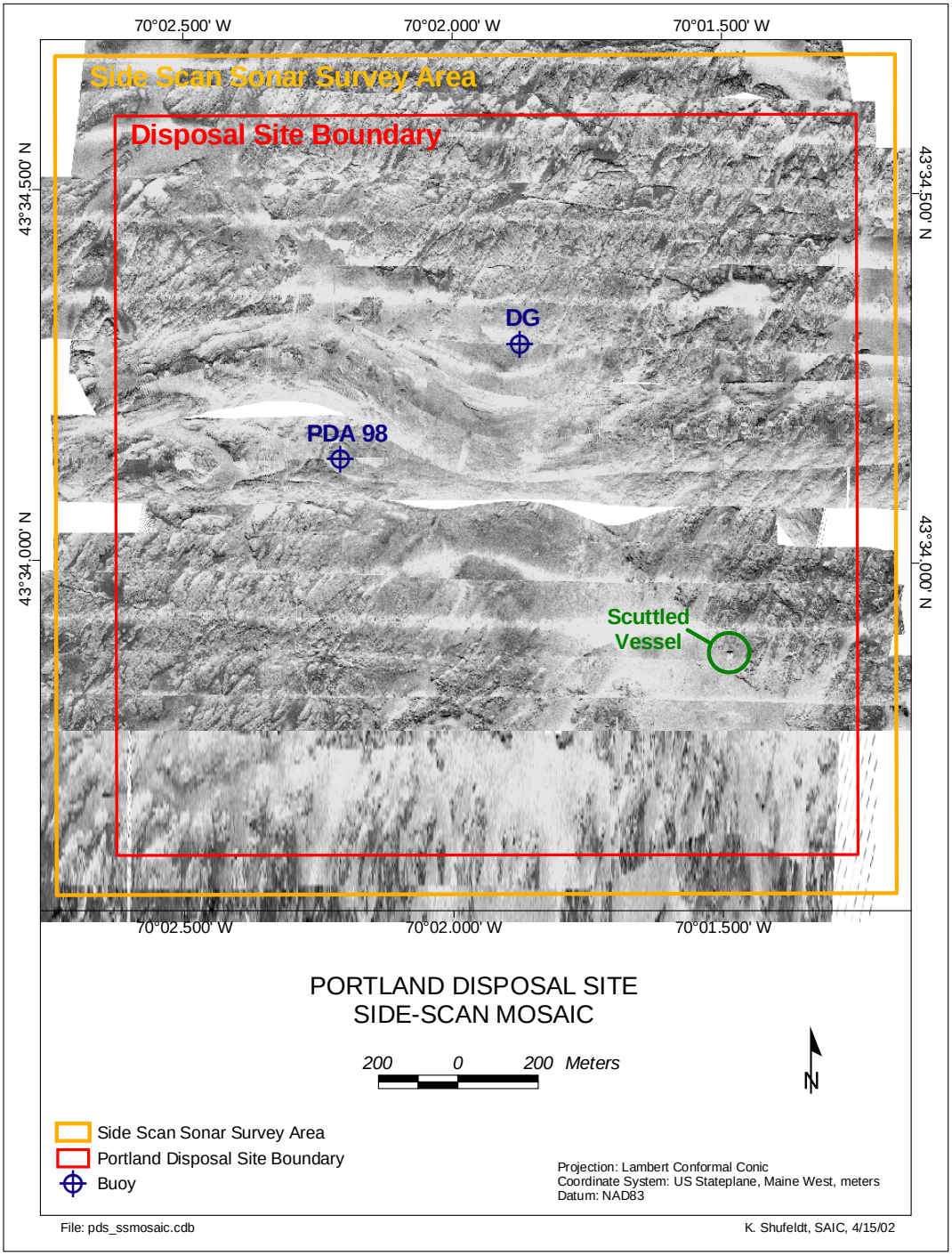

Figure 3-16. Side-scan sonar mosaic of the seafloor at the PDS based on the survey conducted in September 1998

Overall, the 1998 side-scan sonar data set suggested that there has not been any major change in seafloor characteristics within the PDS resulting from past dredged material deposition. The side-scan mosaic depicted a mostly rocky seafloor, with an area of sediment accumulation within a northwest-southeast trending trough that essentially bisected the survey area. Soft sediments deposited at PDS either through dredged material disposal or natural sedimentation processes tend to collect within the valley features or faults through advection. Based on that, dredged material disposal operations at PDS are targeted to those areas to minimize resuspension and large-scale movement of dredged material deposits. Most of the dredged material is deposited at the US Coast Guard DG buoy positioned just north of the central, valley area. The steep ridges of the adjacent bedrock outcrops form a natural containment feature and buffer the deposited sediments from wave energy produced by the unlimited open water fetch that exists to the east and south of the PDS.

In addition to characterizing the seafloor, the side-scan survey also highlighted a large target on the seafloor that was likely a man-made object, measuring approximately 15.5 m in length with a computed height of 4.25 m above the seafloor. Preliminary investigations suggested this target was another commercial fishing vessel scuttled as part of the NMFS artificial reef program (Figure 3-17). This vessel was detected at 43° 33.900´ N, 70° 01.493´ W, in close proximity to the historic Royal River disposal mound in the southeast quadrant of the disposal site. This vessel was scuttled prior to the 1998 multibeam bathymetry and side-scan sonar surveys, and therefore was detected in the side-scan sonar record but not in the bathymetric depth difference comparison between the 2000 and 1998 multibeam surveys. A second vessel, scuttled after the 1998 surveys but prior to the 2000 multibeam survey, was detected in the depth difference comparison (Figure 3-14).

3.6 Water Column Currents

Although two ADCP instruments were originally deployed at the PDS during March and April 1999, valid current measurements were obtained over a 31-day period only from ADCP 1, located at a depth of approximately 70 m in an area south of PDS (Figure 2-4). This instrument provided measurements of water column current velocities in discrete 1 m intervals (“bins”) between approximately 6 m below the water surface and 68 m below the water surface. The main purpose of the ADCP deployment was to obtain data on water column currents at PDS for input to the STFATE and MDFATE dredged material disposal models. Appendix E provides a more detailed evaluation of the ADCP data, including an in-depth assessment of long-term meteorology and the effects of strong wind and wave events on currents at the PDS.

A time series of the high-frequency current velocity components is shown in Figures 3-18 (north-south component) and 3-19 (east-west component). Close examination of this data indicated that water column currents displayed a strong northwest-southeast trend, likely related to tidal oscillations within Casco Bay. A tidal harmonic analysis of this dataset

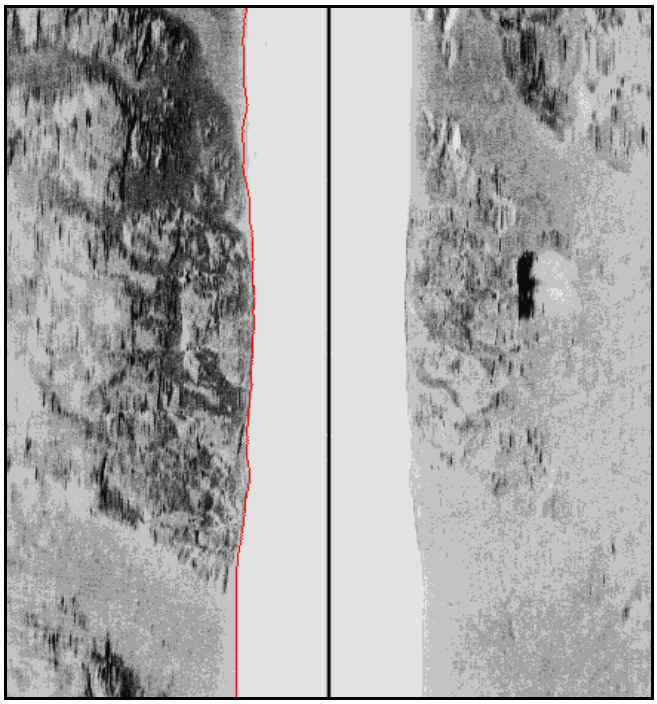

A

B

Figure 3-17. Uncorrected (A) and corrected (B) side-scan sonar returns showing a scuttled fishing vessel on the seafloor within the PDS boundary

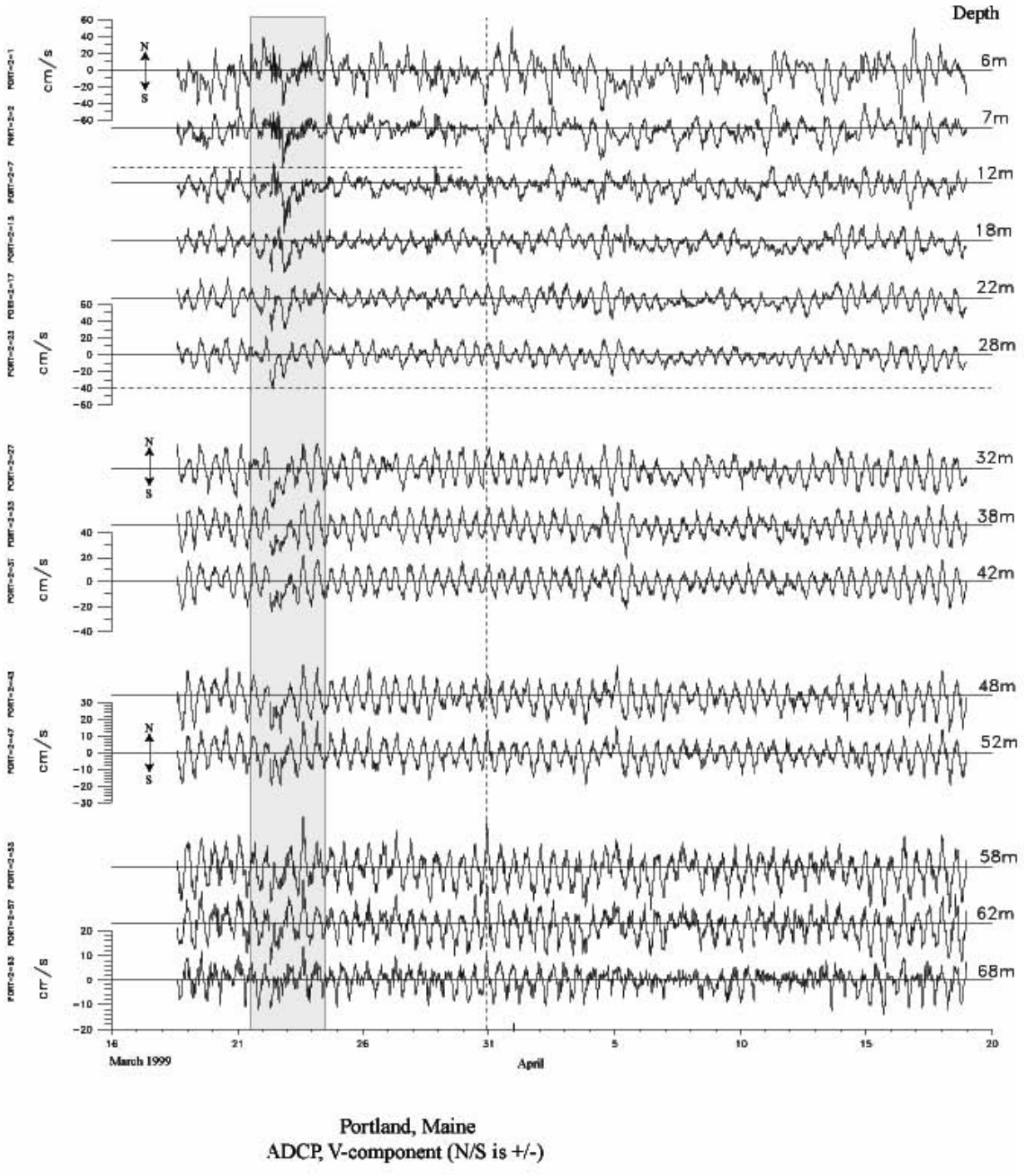

Figure 3-18. Graphical display of high-frequency water column currents (north-south component) collected in close proximity to PDS. The yellow shaded area denotes the timing of a storm event. Note the change in scale on the vertical axis at different depths

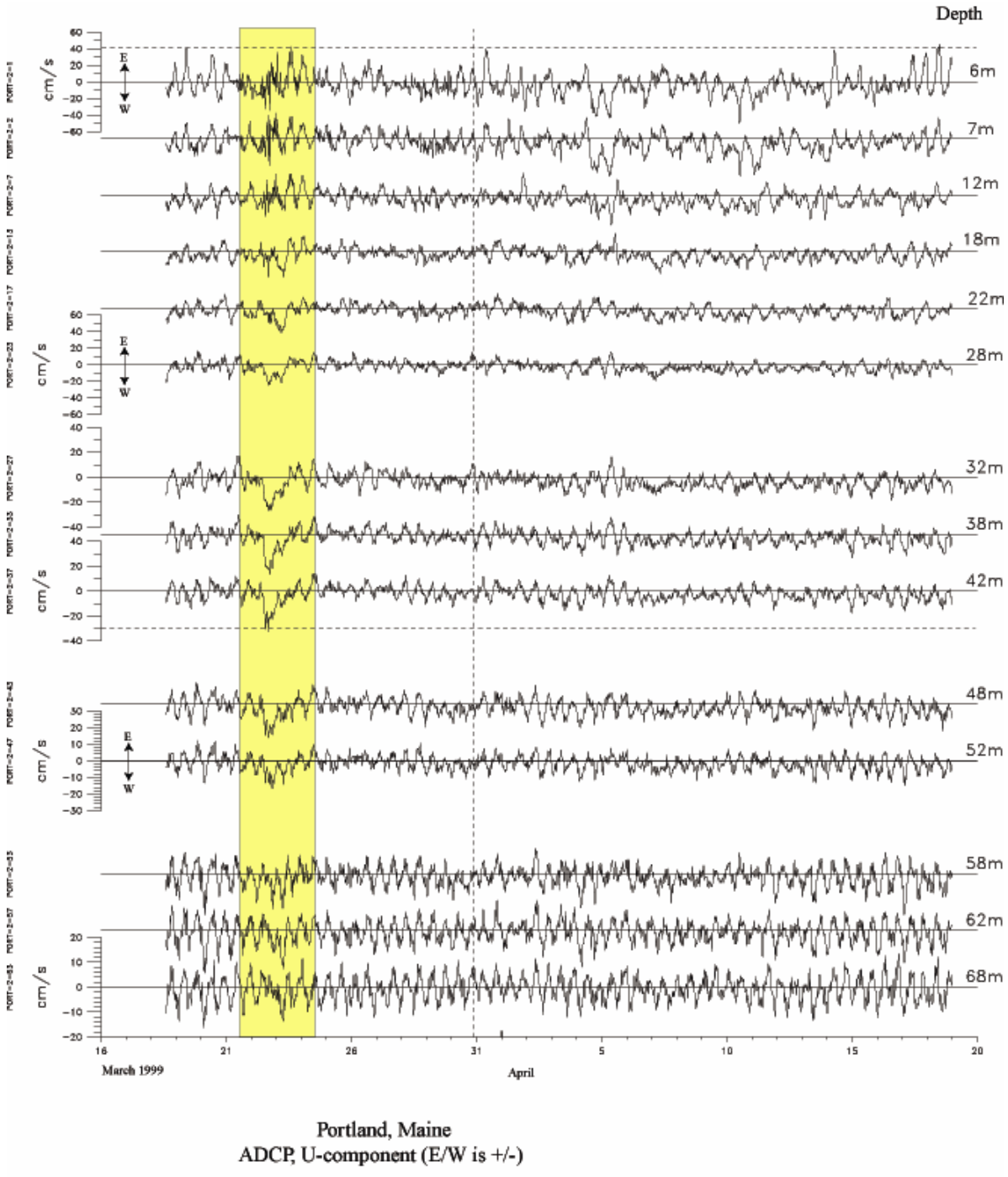

Figure 3-19. Graphical display of high-frequency water column currents (east-west component) collected in close proximity to PDS. The yellow shaded area denotes the timing of a storm event. Note the change in scale on the vertical axis at different depths

showed the lunar semi-diurnal (M_2) tide to be the most significant constituent (Appendix E). The next most significant constituent was the solar semi-diurnal (S_2), at approximately $1/10^{th}$ the magnitude of the M_2.

A winter storm event was documented four days into the ADCP deployment period and was evident in the data record. Winds from the east and southeast (the direction of unlimited fetch) reached a maximum of 18 $m \cdot s^{-1}$ (35 knots), generating surface waves with a height of 5.5 m as recorded by NOAA National Data Buoy Center (NDBC) Buoy 44007 (located in the Gulf of Maine about 10 km south of the PDS). The shaded area in Figures 3-18 and 3-19 indicate the time interval of this strong wind/wave event. Near the surface (i.e., roughly between the 6 and 18 m depth intervals), there did not appear to be a substantial response in either the north-south or east-west current velocity components in conjunction with the increased surface wind stress during the March wind/wave event, although tidal current cycles (timing of transition between flood and ebb tide) may have been distorted (Figures 3-18 and 3-19). Orbital velocities due to waves may have contributed to the slightly "noisier" near-surface current measurements during the high wave event. Compared to the currents measured at each depth during the remainder of the study, the strong wind event appeared to affect current flow at mid depth (water depths ranging from 27-37 m). A pronounced southerly bias was detected in the north-south component measured on 22 March, while an identifiable current maxima (35 $cm \cdot s^{-1}$) was measured in the east-west component. Closer to the bottom, tides remained the primary current signal.

Five depth horizons (7 m, 22 m, 37 m, 52 m, and 68 m) were selected within the water column for focused physical oceanographic analysis and use in subsequent modeling efforts. As anticipated, the high frequency currents were strongest near the surface (7 m) with mean speeds approaching 15 $cm \cdot s^{-1}$. The magnitude of the current decreased with depth, as current speeds averaged 5 $cm \cdot s^{-1}$ near bottom (68 m; Appendix E). The maximum observed speed for the deployment was detected at the surface and was slightly above 50 $cm \cdot s^{-1}$, which correlated with a spring ebb tide and a strong wind emanating from the northwest. The resulting increase in southeasterly current flow detected at the surface was short-lived and was attenuated at depth.

Orientation of both the M_2 and S_2 tidal ellipses from the 31-day data set was predominantly northwest–southeast throughout the water column, rotating to west-northwest–east-southeast at the near bottom (Figure 3-20). However, distinct south and west bias in flow was discernable in the high frequency current data, especially in water depths of 52 m and shallower. Rose histograms of the direction data for the five depth horizons of interest demonstrate these trends more clearly, as well as indicating a westerly trend in the low-frequency mean flow direction (Figure 3-21). The southwesterly trend detected in the ADCP record was likely the product of the cyclonic (counterclockwise) gyre that drives circulation within the Gulf of Maine (Bigelow 1927).

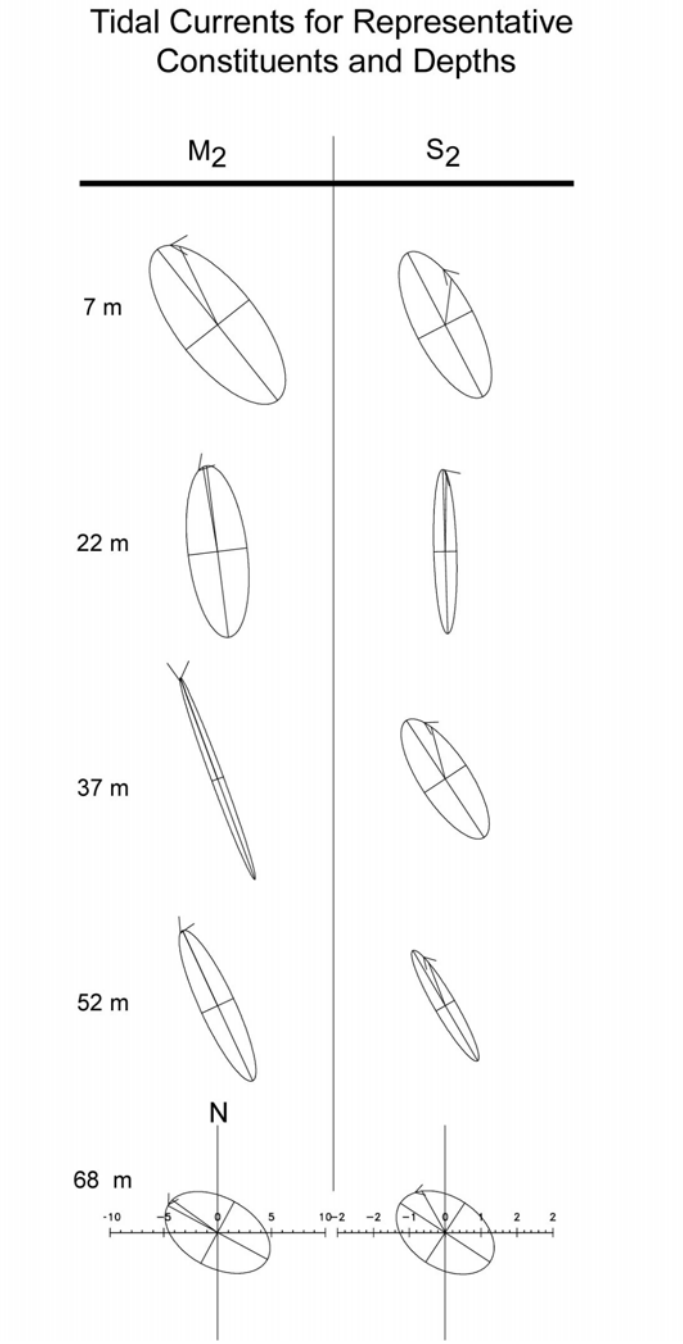

Figure 3-20. Tidal ellipses for the M_2 (lunar) and S_2 (solar) tidal constituents for the five depth horizons of interest based upon the current profiler record. The x and y axes are proportional; current speeds are indicated in $cm \cdot s^{-1}$. The ellipses demonstrate that both the M_2 and S_2 tidal currents rotate in a counterclockwise (cyclonic) direction over PDS.

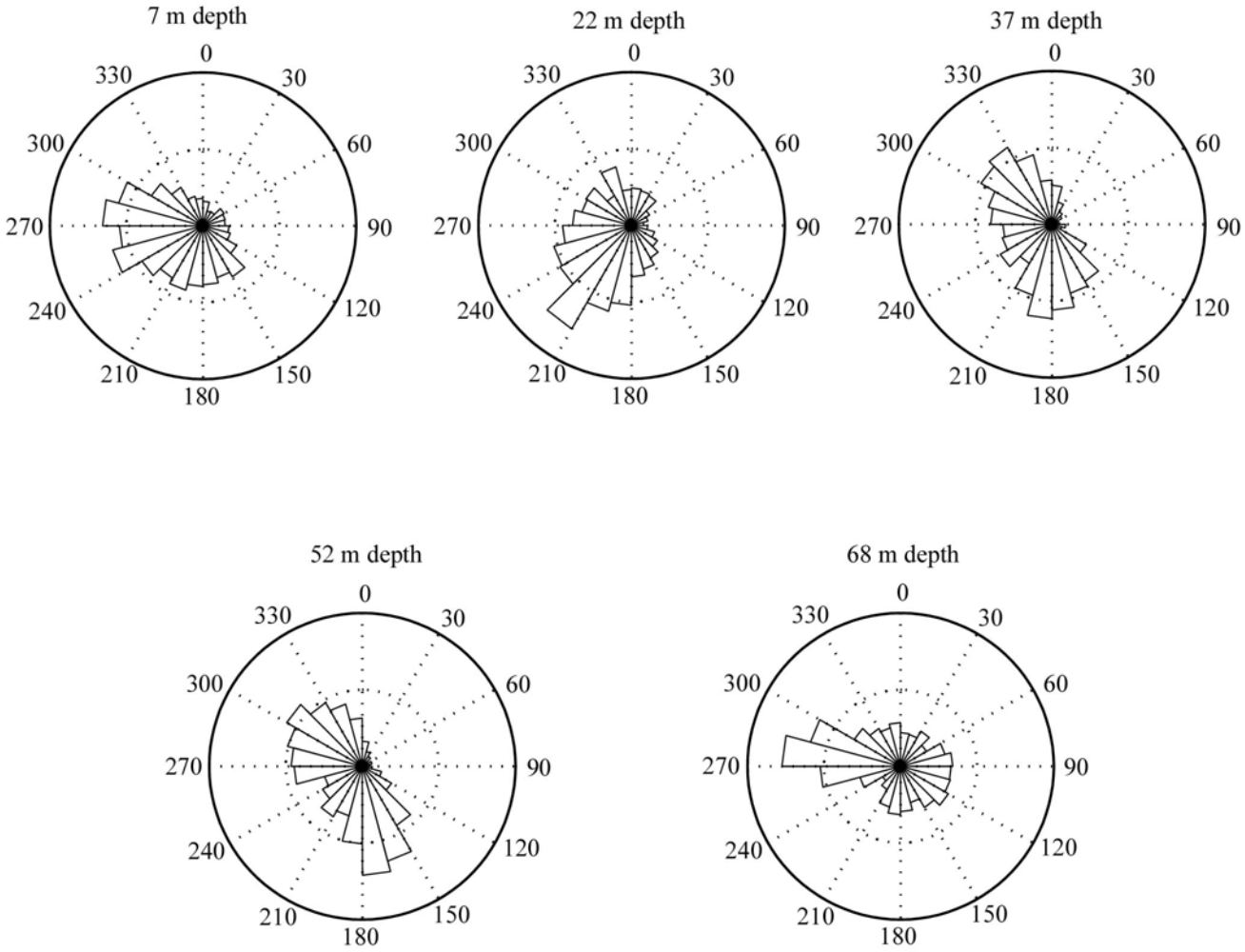

Figure 3-21. Current rose histograms for the five depth horizons of interest within the water column based upon the current profiler record. These diagrams represent statistics based on the number of observations within a degree band, and do not convey any information on current magnitude.

Low-frequency currents such as those associated with the counterclockwise gyre tend to dictate the net displacement (direction and distance) of a suspended particle that resides in the water column over an extended period of time. By filtering the current data with a 40-hour low-pass filter, the residual sub-tidal current is obtained by suppressing all current fluctuations having a duration of one day or less (tides, wind forcing, etc.; Figure 3-22). The results for the five depth horizons of interest indicated the sub-tidal flow was the basis for the southwesterly trends observed in the high frequency data. With the exception of the time periods around 24 March and 14 April, low-frequency currents at the near-surface to mid–depth were predominantly southwestward. However, the near-bottom currents did not reflect this same trend as local bathymetric features likely dictated the direction and magnitude of current flow.

The high frequency data indicate that water column currents are influenced by tidal flow at any one point in time. Given that tidal currents are the most likely mechanism to transport sediments entrained in the water column for relatively short periods of time, a typical flood and typical ebb current profile was isolated from the ADCP data to further evaluate the sediment plume transport in the PDS region. A twelve-hour segment in the current record with quiescent wind conditions (and subsequently lower subtidal currents) and between the periods of spring and neap tides was selected to extract a representative flood and ebb cycle. Two six-hour intervals from the March-April data set were chosen to represent the ebb and flood tide over PDS. The east and north components (U and V) from each interval were averaged by water depth into five depth bins, then a mean velocity was calculated for the entire six-hour time period (Tables 3-8a and 3-8b). A vector speed and direction were calculated from the average east and north components. The depth levels shown in the tables represent the center of the depth-averaged current bin. In this particular instance, there was no substantial difference between flood and ebb current magnitude.

When modeling the transport of particles entrained in the water column for an extended period (spanning tidal cycles), the use of average current speed and direction would be more appropriate for modeling. To facilitate this type of model run, current data representing mean current speed and direction, as well as vector averaged current velocities for the five depth intervals of interest were calculated from the month-long data set (Tables 3-9a and 3-9b). The use of vector-averaged current velocities was expected to better emulate normal oceanographic conditions when used in the modeling routines. In this method, the mean component velocities (U and V) were used to compute the magnitude of the current vector (Table 3-9a). The use of current vectors links the rate at which water and particulate matter flow with the direction to which the water mass is moving.

However, the STFATE modeling runs presented in this document were based on mean speed and direction values that were calculated from the March-April 1999 current data. The mean speed values were determined by developing an average based on all the speed observations (regardless of direction) within the entire record depicted in Figures 3-18

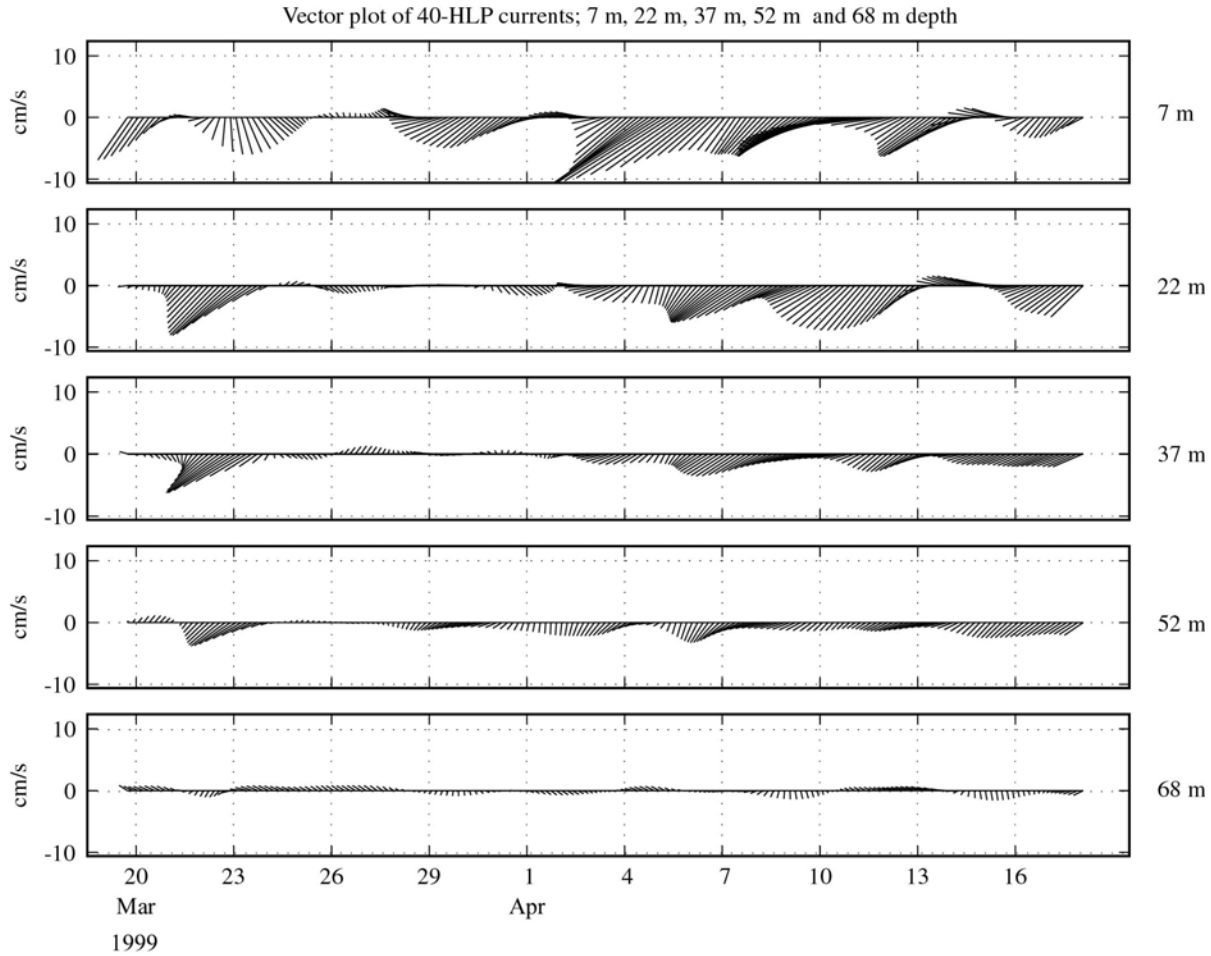

Figure 3-22. Time series plot displaying the residual sub-tidal current vectors for the five depth horizons of interest after the application of 40-hour low-pass filter to suppress all high-frequency current oscillations

Table 3-8a. Water Column Current Velocities over the Portland Disposal Site associated with an Average Flood Tide

Depth m	Mean Speed cm/s	Mean Direction ° True
12.0	8.1	313.7
24.5	6.2	309.4
37.5	7.6	312.0
50.5	6.0	299.1
62.0	5.7	297.5

Table 3-8b. Water Column Current Velocities over the Portland Disposal Site associated with an Average Ebb Tide

Depth m	Mean Speed cm/s	Mean Direction ° True
12.0	11.7	146.4
24.5	6.3	138.7
37.5	7.7	137.6
50.5	7.4	135.3
62.0	5.1	133.2

Table 3-9a. Vector-Averaged Water Column Current Velocities over the Portland Disposal Site

Mean Velocity Vector				
Depth m	**Mean U-component** cm/s	**Mean V-component** cm/s	**Magnitude** cm/s	**Direction** ° True
7	-5.92	-3.89	7.08	236.7
22	-3.31	-2.35	4.06	234.7
37	-2.47	-1.35	2.81	241.3
52	-1.65	-1.41	2.17	229.5
67	-0.6	-0.16	0.62	255.1

Table 3-9b. Mean Speed and Direction of Water Column Current Flow over the Portland Disposal Site

Mean Current Speeds		
Depth m	**Mean Speed** cm/s	**Mean Direction** ° True
7	13.99	240.11
22	10.1	233.57
37	9.11	241.18
52	6.8	232
67	5.16	255.07

and 3-19. The direction values were then developed independently of the speed calculations, based on the mean current vectors (U and V) for each level, then simply assigned to mean speed values. The use of this method yielded current values that were higher relative to vector-averaged results at each depth horizon of interest (Table 3-9b). The primary reason for utilizing mean speed and direction in the STFATE runs was to define the maximum potential transport of the plume sediments as a worst-case scenario.

3.7 Sediment-Profile Imaging

One objective of the REMOTS® sediment-profile imaging survey completed in September 2000 (18 months post disposal) was to delineate the distribution of dredged material around the PDA 98 buoy. Dredged material was evident at the sediment surface at the majority of the 28 REMOTS® stations occupied around the PDA 98 buoy, which also extended into the area around the USCG buoy (Table 3-10 and Figure 3-23). The thickness of the dredged material layer extended from the sediment surface to below the penetration (i.e., imaging) depth of the sediment-profile camera at 27 of the 28 stations sampled (indicated with a "greater than" sign in Table 3-10 and Figure 3-23). The dredged material comprising the sediment surface at the disposal site consisted mainly of fine-grained, cohesive silt-clay (grain size major mode of >4 phi), with an apparent minor fraction of sand (Table 3-10 and Figure 3-24). Apparent ambient sediment was observed in one of the three replicate images obtained at Station 200SW and in the single replicate image obtained at Station 400S (Table 3-10).

The seafloor topography within the confines of PDS and the surrounding areas is characterized as rough and irregular, with pockets of soft sediment accumulation in the basins among bedrock outcrops. Hard bottom at Station 400S prevented sufficient camera penetration, and indicates little to no dredged material or soft sediment accumulation at that location. Patches of extremely soft sediment caused the sediment-profile camera to over-penetrate at other stations, obscuring the sediment-water interface and likewise precluding analysis of the several REMOTS® parameters. Mean camera penetration depths for the disposal site stations ranged from a relatively high value of 21 cm at Station 300NW to an extremely low value of 1.5 cm at Station 400S (overall average of 14 cm; Table 3-10).

The overall average boundary roughness value for the PDA 98 stations was 2 cm, suggesting a moderate amount of small-scale surface relief. Replicate-averaged boundary values ranged from 6 cm at Station 300NE to 0.9 cm at Station 400SE (Table 3-10). There was no obvious spatial pattern to the boundary roughness values. The surface roughness was attributed to physical disturbance at the stations within the disposal site, likely related to the presence of cohesive clay clasts or cohesive dredged material from recent previous disposal (Figure 3-25). Both oxidized and reduced mud clasts, indicative of recent physical disturbance, were observed at the sediment surface at 23 of the 28 stations.

Table 3-10. Summary of Physical Sediment Parameters as Detected by REMOTS® Sediment-Profile Imaging

Station	Camera Penetration Mean (cm)	Dredged Material Thickness Mean (cm)	Number of Reps w/ Dredged Material	Grain Size Major Mode (phi)	Boundary Roughness Mean (cm)
100E	10.11	>10.11	3	>4	2.33
100N	11.08	>11.08	3	>4	1.17
100NE	10.54	>10.54	3	>4	1.18
100NW	15.57	>15.57	3	>4	2.16
100S	13.43	>13.43	3	>4	1.34
100SE	17.99	>17.99	3	>4	2.14
100SW	11.89	>11.89	3	>4	2.66
100W	13.58	>13.58	2	>4	1.13
200E	19.24	>19.24	3	>4	1.30
200N	13.22	>13.22	3	>4	2.12
200NE	14.74	>14.74	3	>4	1.87
200NW	12.28	>12.28	3	>4	2.06
200S	9.59	>9.59	3	>4	1.25
200SE	15.98	>15.98	3	>4	3.61
200SW	16.61	>11.35	2	>4	1.30
200W	20.08	>20.08	3	>4	1.45
300E	9.59	>9.59	3	>4	2.12
300N	16.61	>16.61	3	>4	2.00
300NE	11.76	>11.76	3	>4	5.99
300NW	21.00	>21.00	3	>4	INDET
300S	11.31	>11.31	3	>4	1.54
300SE	15.96	>15.96	3	>4	2.51
400E	15.90	>15.90	3	>4	2.20
400N	14.41	>14.41	3	>4	2.11
400NE	15.93	>15.93	3	>4	1.01
400S	1.54	0	0	>4	1.85
400SE	20.47	>20.47	3	>4	0.90
CTR	10.22	>10.22	3	>4	2.94
AVG	13.95	>13.71	3		2.01
MAX	21.00	>21.00	3		5.99
MIN	1.54	0	0		0.90

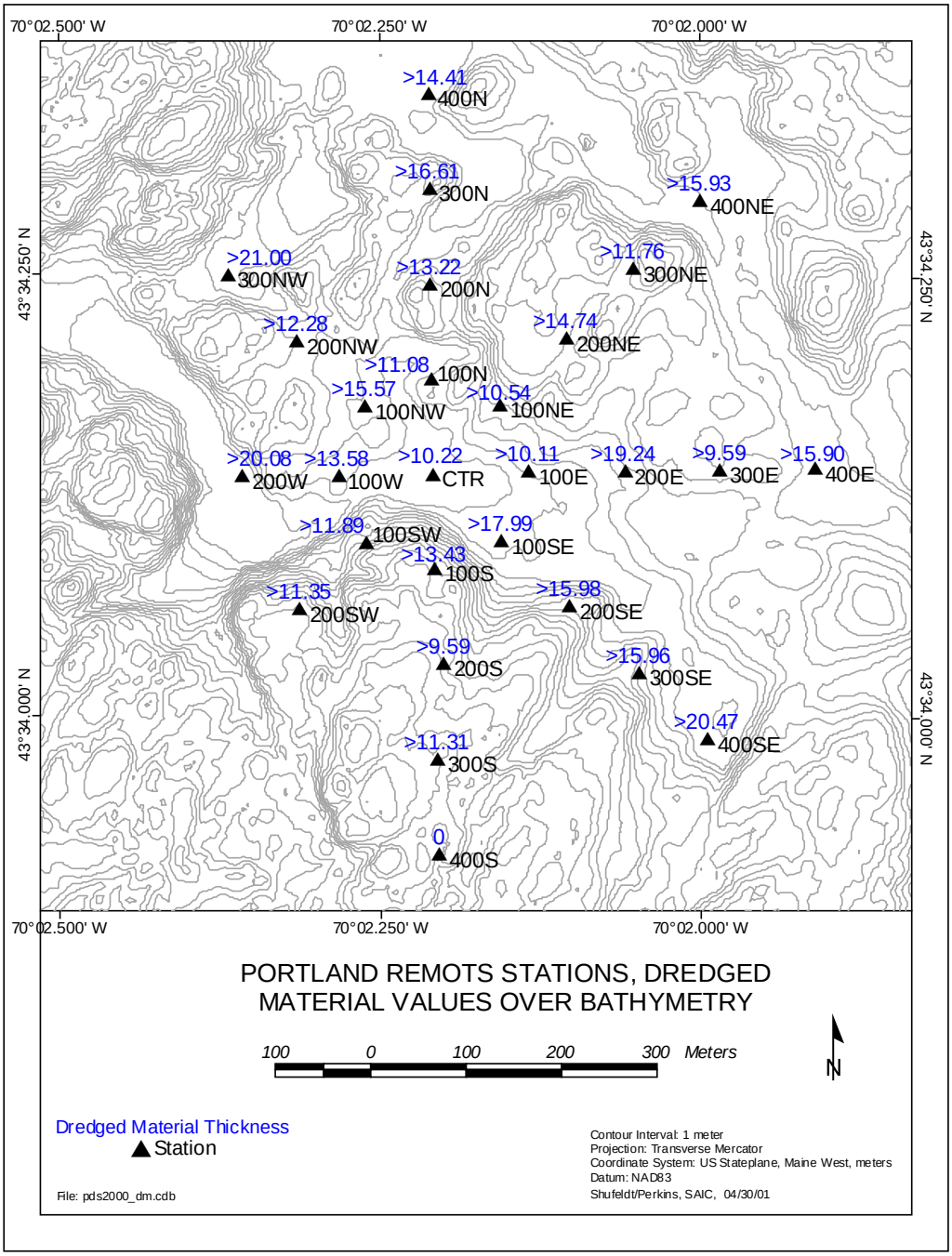

Figure 3-23. Map showing the average thickness of surface layers of dredged material in centimeters observed in REMOTS® sediment-profile images collected at 28 stations across the PDS in September 2000. The "greater than" sign indicates that the average thickness of the dredged material layer exceeded the penetration depth of the sediment-profile camera.

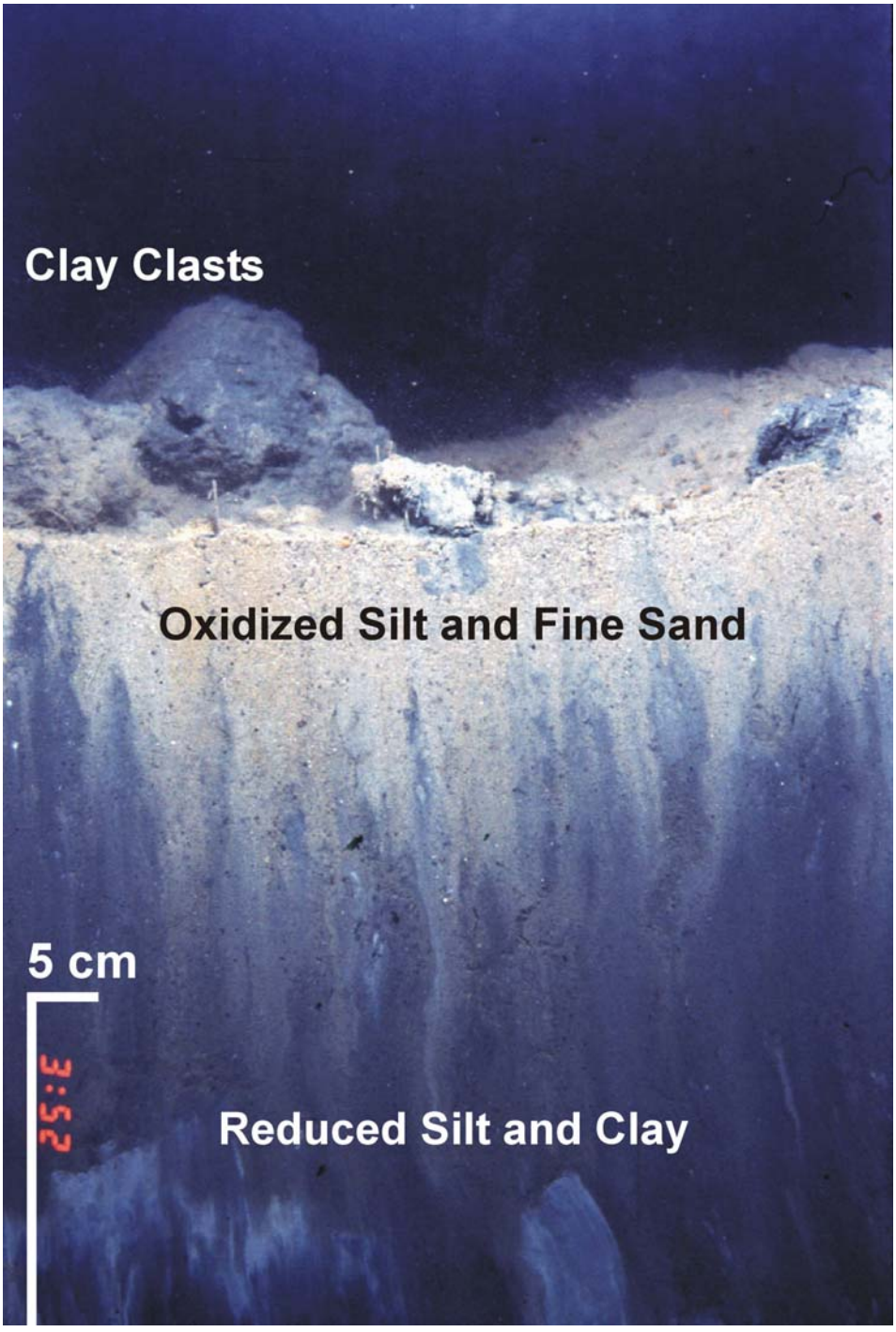

Figure 3-24. REMOTS® image from Station 400E showing predominantly fine-grained dredged material mixed with a small amount of sand extending from the sediment surface to below the imaging depth of the sediment-profile camera. Several large, cohesive clay clasts are visible at the sediment surface.

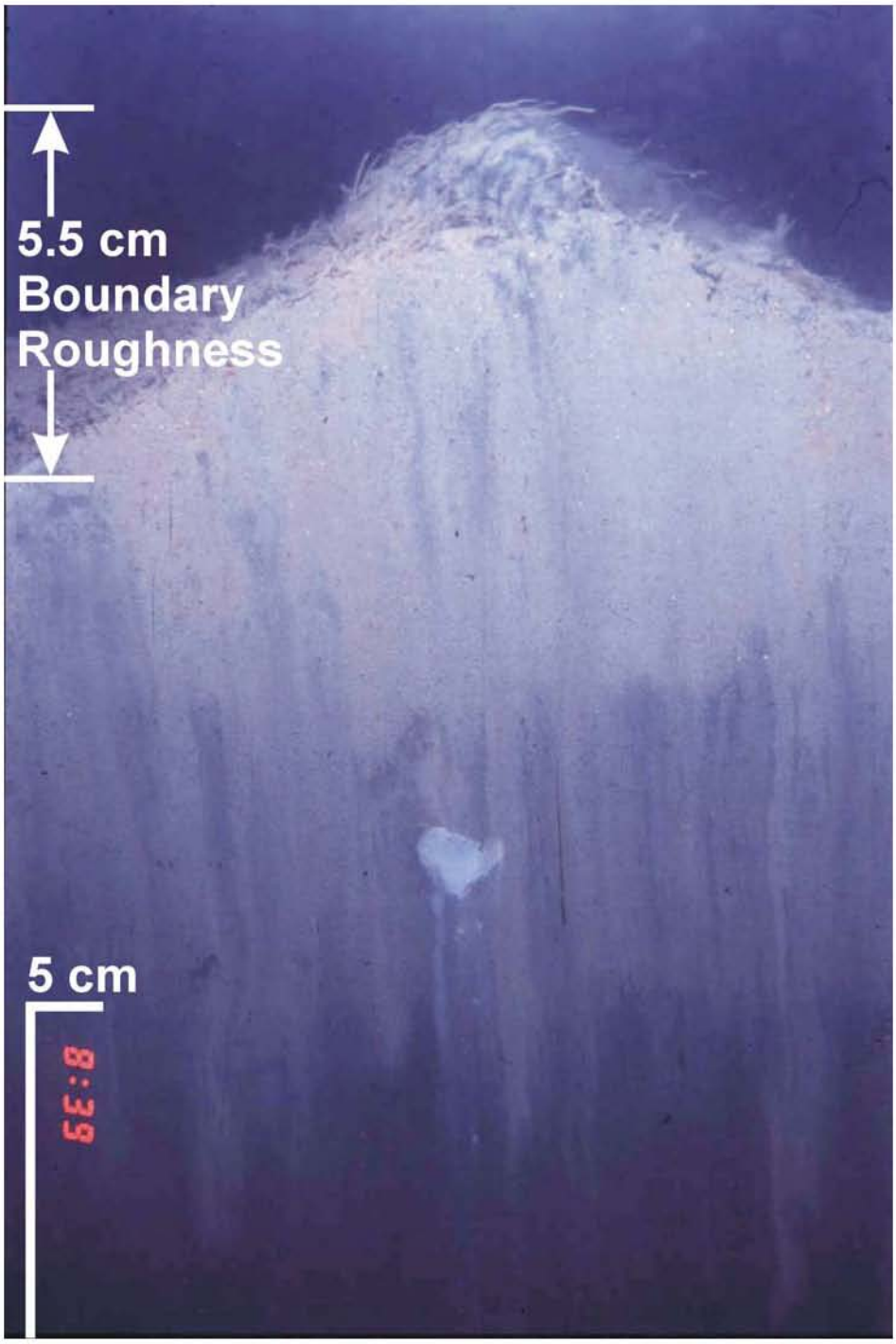

Figure 3-25. REMOTS® image from Station 300SE showing irregular topography (high small-scale boundary roughness) attributed to the presence of cohesive mud at the sediment surface

3.8 Dredged Material Modeling

3.8.1 STFATE Modeling

As previously described, several model runs were completed as part of this study to determine the development and dissipation of a sediment plume formed at the PDS. The input data for each subsequent model run was refined based on the best information available for sediment characteristics, water column currents, and disposal barge attributes.

The sediments removed from Portland Harbor were expected to consist of varying percentages of sand, silt, and clay sized particles. In addition, a clumping factor was applied based on the geotechnical characteristics of the project sediment and the likelihood of forming sizeable chunks, or clumps. The sand fraction, cohesive clumps of material, and the majority of the non-cohesive silt and clay were expected to reach the seafloor shortly after disposal to form a deposit on the bottom. The impact of this material would cause a resuspension event to occur and turbidity to increase significantly over background levels. In addition, a percentage of the fine-grained material (silt and clay sized particles) was expected to become entrained in the water column and slowly settle out of suspension, as well as dissipate through dilution.

The magnitude of the initial sediment plume is directly related to the geotechnical characteristics of the project sediments and configuration of the disposal barge, while the morphology, direction of travel, and dissipation over time is based upon the water column currents and local bathymetry. All of the model runs completed as part of this study demonstrated strong similarities in the transport for silt and clay-sized particles. For simplicity, only the detailed results generated for the transport of clay-sized (<0.004 mm) particles in the sediment plume are presented.

3.8.1.1 First-order STFATE Modeling

The first-order STFATE model was run assuming the use of a 5,350 m^3 (7,000 yd^3) disposal barge, with the material released at the water's surface at the PDA 98 buoy position (43° 34.147´ N, 70° 02.209´ W). The STFATE model results showed that a majority of the material would quickly reach the bottom, creating a conical dredged material mound with a diameter of 600 m and a height of 6.5 cm above the PDS seafloor. The extent and movement of the predicted sediment plume created by this single placement event was evaluated on an hourly basis at several depths within the water column, to determine plume morphology, as well as rates of transport and dissipation. Because the modeled plume effects were consistent and relatively minor in the upper water column, results are presented only for the 30 and 50 m depth intervals.

The direction of transport at both depth intervals was predominantly southeast in response to the USGS current data used to drive the STFATE model run. These current speed and direction data were obtained in the Gulf of Maine at a location well south of PDS. Similar to the results of the current data collected in close proximity to PDS (see Section 3.6), the southeasterly trend in the USGS averaged data is the product of the cyclonic (counter clockwise) flow that drives circulation in the Gulf of Maine, as well as the shape of basin in the area from which the data were collected.

At the 30 m depth interval, the sediment plume is transported approximately 460 m per hour (12.8 $cm \cdot s^{-1}$ or 0.248 knots), with the leading edge of the plume ("clay particle cloud") extending 1,800 m from the central disposal point within four hours (Figure 3-26). The accelerated current, relative to the input value of 0.217 knots (11.2 $cm \cdot s^{-1}$), is due to the functionality of the model. The STFATE model moves the entire water mass over the study area during the model run and decays the current to zero at the sediment-water interface. In areas with significant seafloor relief, this results in accelerated mid-water current flow in response to large-scale obstacles on the seafloor. As a result, small-scale upwelling of bottom water and entrained or resuspended sediment is anticipated in the model output. After four hours (yellow) post-disposal, the plume encompasses 274,500 m^2 and extends nearly 1,800 m from the disposal buoy and approximately 800 m beyond the southern PDS boundary.

The results from the 50 m depth interval show the dependence of the STFATE model on the bathymetry of the disposal site and the capability of the containment cell to restrict the transport of a sediment plume. Relative to horizons higher in the water column, the forecasted morphology of the sediment plume near the seafloor is significantly different in both shape and concentration. It appears the sheer vertical wall south of the PDA disposal buoy serves to restrict the size of the plume and distance the sediment is transported along the bottom (Figure 3-27). The disposal point was established over an area of seafloor approximately 60 m deep with a bedrock containment wall providing 15 m of relief present to the south. At this horizon, the majority of the sediment plume remains within the PDS boundary, only traveling 850 m southeast of the disposal buoy four hours after the disposal event. There is a secondary plume visible at the two, three, and four-hour time intervals that follows the transport patterns of the sediment entrained in the upper water column. This secondary plume is likely attributed to particles settling out from the upper water column over time. At four hours (yellow) post-disposal, the secondary plume is 1,700 m from the buoy and outside of the southern boundary of the disposal site. The sediment concentrations remain just above the background level of 1.5 $mg \cdot l^{-1}$, with a maximum of 8.2 $mg \cdot l^{-1}$ in this area.

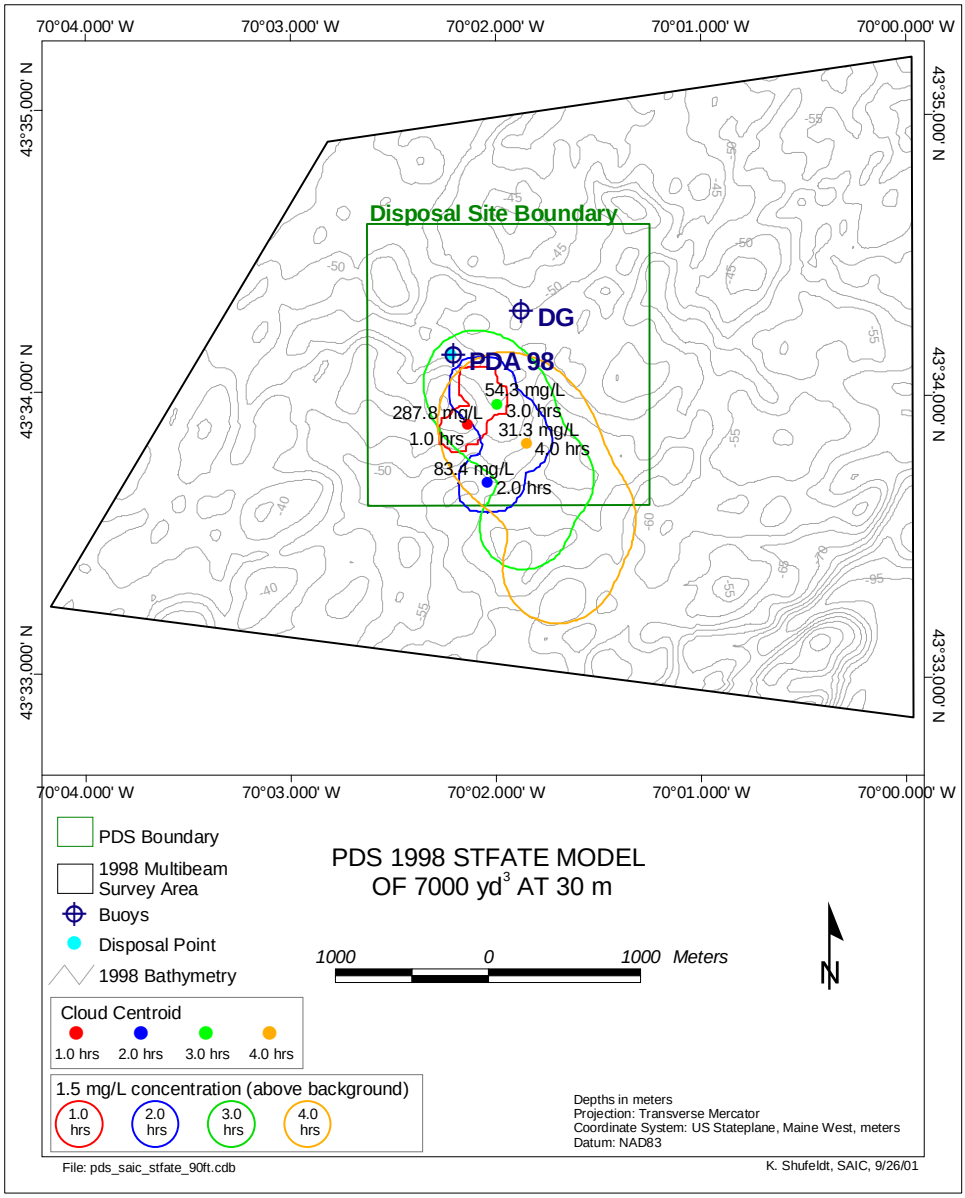

Figure 3-26. Map of first-order STFATE model results showing the horizontal extent of the clay particle cloud at a depth of 30 m following release of 5,350 m^3 (7,000 yd^3) of Portland Harbor dredged material. Each colored dot represents the cloud centroid at an hourly interval and is labeled to show the clay particle concentration in $mg \cdot l^{-1}$ at that point/time. The corresponding ring around each colored dot represents the perimeter of the plume, where the clay particle concentration becomes equal to the background suspended sediment concentration of 1.5 $mg \cdot l^{-1}$

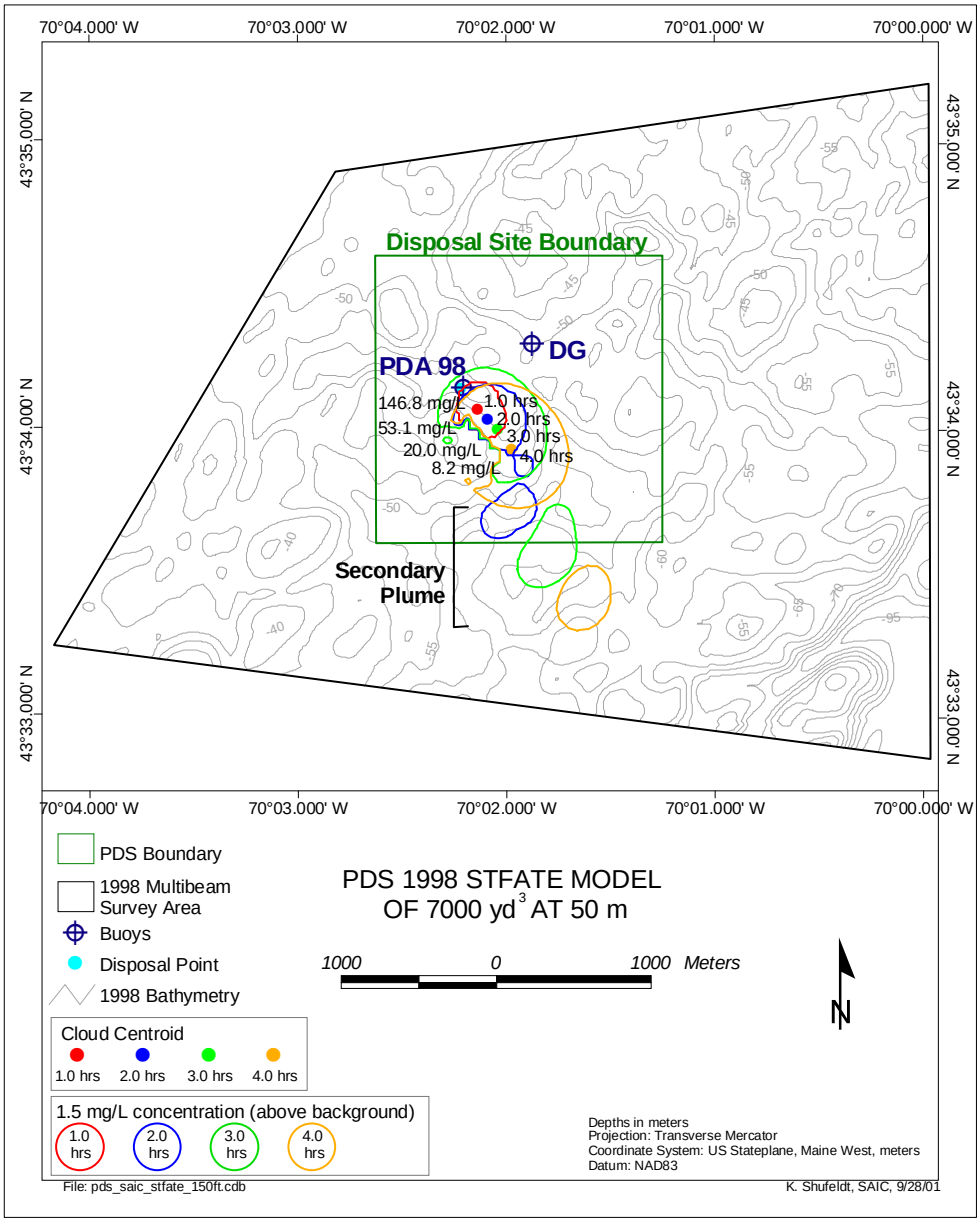

Figure 3-27. Map of first-order STFATE model results showing the horizontal extent of the clay particle cloud at a depth of 50 m following release of 5,350 m^3 (7,000 yd^3) of Portland Harbor dredged material. Each colored dot represents the cloud centroid at an hourly interval and is labeled to show the clay particle concentration in $mg \cdot l^{-1}$ at that point/time. The corresponding ring around each colored dot represents the perimeter of the plume, where the clay particle concentration becomes equal to the background suspended sediment concentration of 1.5 $mg \cdot l^{-1}$

3.8.1.2 Second-order STFATE Model

After the completion of the Portland Harbor dredging project, site-specific information pertaining to the water column currents and the geotechnical properties of the dredged sediment were developed based on the extensive field data acquired before and during the dredging project. The STFATE model was run again using these data to hindcast the behavior of the plume created by placement of the Portland Harbor dredged material. The approach for the second round of modeling was modified slightly based on the results derived from the first-order analysis.

Based on the Portland Harbor coring data analysis, the dredged material was still classified as silt-clay, though the composition was modified (e.g., 7.4% sand, 34.4% silt, and 58.2% clay). Based on the geotechnical analysis, a solids fraction of 27% was calculated for the total volume of sediment dredged. A clumping factor of 60% was used to forecast the percentage of the solid dredged material volume that would exist as clumps in the disposal barge. The clumps were assigned a median size of 35 cm and would be resistant to stripping while in convective descent. In addition, the data obtained from the ADCP current meter deployed near the PDS during the dredging project were used to drive the second-order model runs.

Because the first-order model runs showed limited plume effects near the water surface, the second-order analysis focused on depth intervals ranging from the mid-water column to the seafloor. The second-order STFATE model output consisted of particle concentrations in the water column relative to a background turbidity of 2 $mg \cdot l^{-1}$. The plume morphology and sediment load was estimated every 1.5 hours over a six-hour period. The STFATE model predicted that all clumps would deposit within 15 minutes and the larger non-cohesive particles (sand and coarse silt) within 45 minutes of release. Since clay particle settlement would occur over an extended time scale and the majority of the Portland Harbor sediments were comprised of clay, the model output is presented for clay particle concentrations only. The data display shows maximum extent of the sediment plume, as well as its centroid for each 1.5 hour interval. The simplified results from each model run were presented in both planview and profile format to display the general morphology of the cloud and interaction with the seafloor.

Figure 3-28 displays the STFATE modeling results that simulate a disposal event from a 3,050 m^3 (4,000 yd^3) barge occurring at the beginning stages of a flood tide. The black contour line indicates the estimated dredged material footprint on the seafloor (minimum thickness of 1 mm), while the colored contours represent the lateral extent of the entrained clay particles at concentrations above background. Over a six-hour period, the center of the sediment plume was transported by the flood tide approximately 2.1 km to the northwest at an average velocity of 350 m per hour (9.7 $cm \cdot s^{-1}$). Similar to the first-order

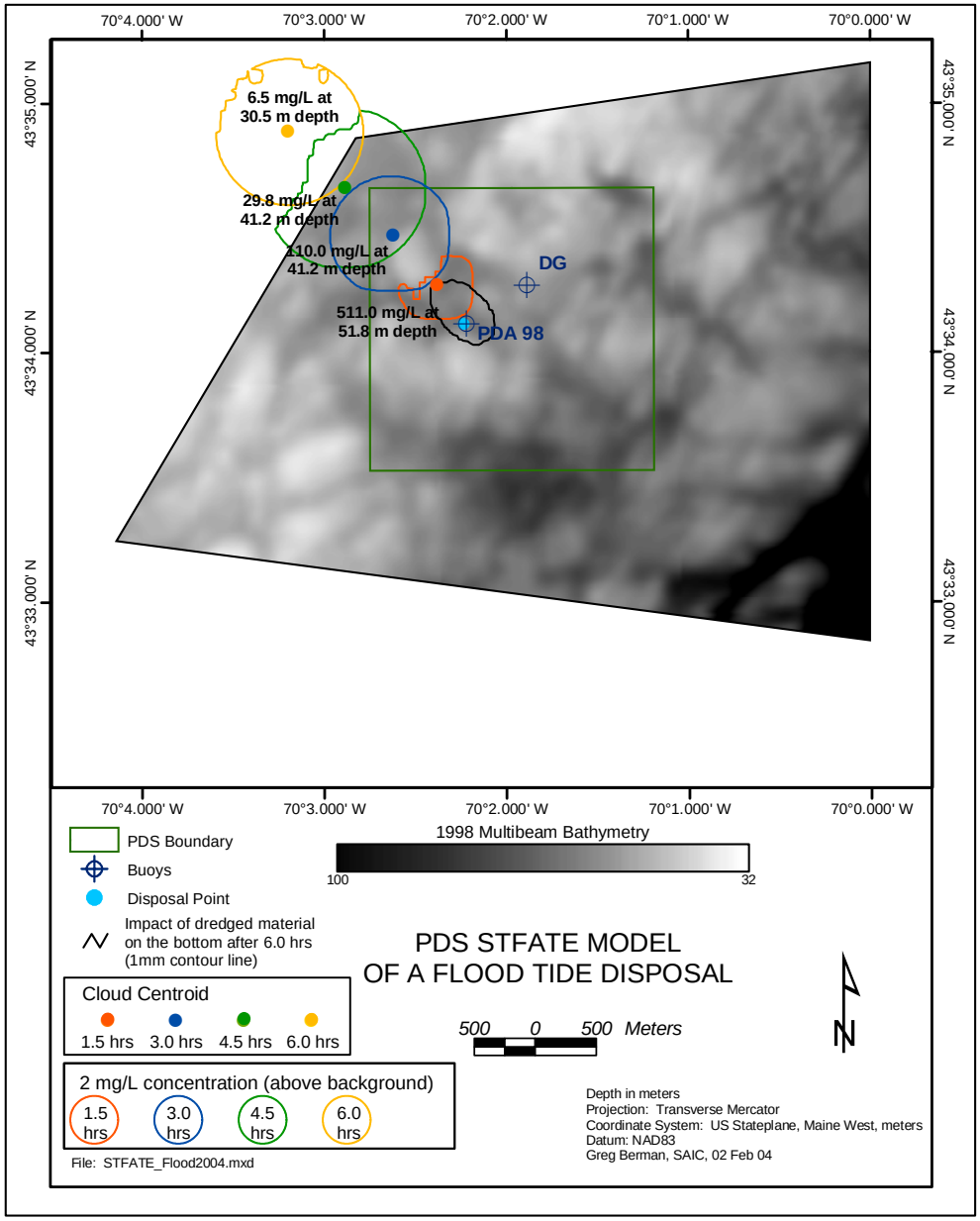

Figure 3-28. Map of second-order STFATE model results showing the horizontal extent of the clay particle cloud from a 3,050 m^3 (4,000 yd^3) disposal event over PDS during an average flood tide. Each colored dot represents the cloud centroid at 1.5 hour intervals and is labeled to show the clay particle concentration in $mg \cdot l^{-1}$ at that point/time. The corresponding ring around each colored dot represents the perimeter of the plume, where the clay particle concentration becomes equal to the background suspended sediment concentration of 2 $mg \cdot l^{-1}$.

modeling results, the higher concentrations of entrained sediment occurred in the lower water column with the overall morphology of a sediment plume dictated by bottom topography.

At 1.5 hours post-disposal, the centroid of the plume was within 300 m of the disposal point displaying a concentration of 511 $mg \cdot l^{-1}$ at a water depth of 51.8 m (Figure 3-29). The lower portions of the plume mimicked the shape of a nearby natural containment ridge, a strong bedrock outcrop to the northwest of the disposal point (see Figure 3-9). The ridge appeared to block the continued transport of dredged material in much of the lower portion of the plume. The STFATE results for subsequent time frames indicated the centroid would exist at shallower water depths and display substantially lower turbidity values (70 to 80% reductions) at each time interval (Figure 3-28).

As time progressed, the margins of the sediment plume widened, facilitating rapid dilution of the entrained sediment cloud with Gulf of Maine water. Three hours into the simulation, both particle settlement and dilution fostered a nearly 80% reduction in turbidity values (110 versus 511 $mg \cdot l^{-1}$) prior to leaving the PDS boundary. At the 4.5 hour time interval, maximum turbidity values were estimated at nearly 30 $mg \cdot l^{-1}$, with the centroid located at a water depth of 41.2 m. The leading edge of the plume appeared to interact with another physical barrier outside the 1998 bathymetric survey area (East Cod Ledge) prompting further reductions in turbidity, as well as the areal extents of the turbidity plume. At six hours post-disposal, the centroid of the plume was located 2.1 km northwest of the original disposal point, at a water depth of 30.5 m. The maximum turbidity value of 6.5 $mg \cdot l^{-1}$ at the 6.0 hour interval was quite close to the background value (2 $mg \cdot l^{-1}$) used in this simulation and would likely be undetectable without comprehensive sampling and laboratory analysis of total suspended solids distribution. At six-hours post disposal, the model predicted the concentration of entrained sediment would exist at approximately 1.1% of suspended load estimated by STFATE at the 1.5 hour time interval.

Figure 3-30 displays the STFATE modeling results that simulate a disposal event from a 3,050 m^3 (4,000 yd^3) barge occurring at the beginning stages of an ebb tide. Once again, the black contour line indicates the estimated dredged material footprint on the seafloor (minimum thickness of 1 mm), while the colored contours represent the lateral extent of the entrained clay particles at concentrations above background. Over a six-hour period, the center of the sediment plume was transported nearly 3 km to the southeast by the ebb tidal flow over PDS. At an average velocity of 500 m per hour (13.9 $cm \cdot s^{-1}$), the dilution process occurred more rapidly in comparison to the flood tide model runs, while the morphology of the plume remained relatively consistent. The disposal plume was transported from a disposal point located in 60 m of water, across a natural bedrock containment ridge displaying water depths of approximately 50 m, then into areas of deeper water (see Figure 3-9).

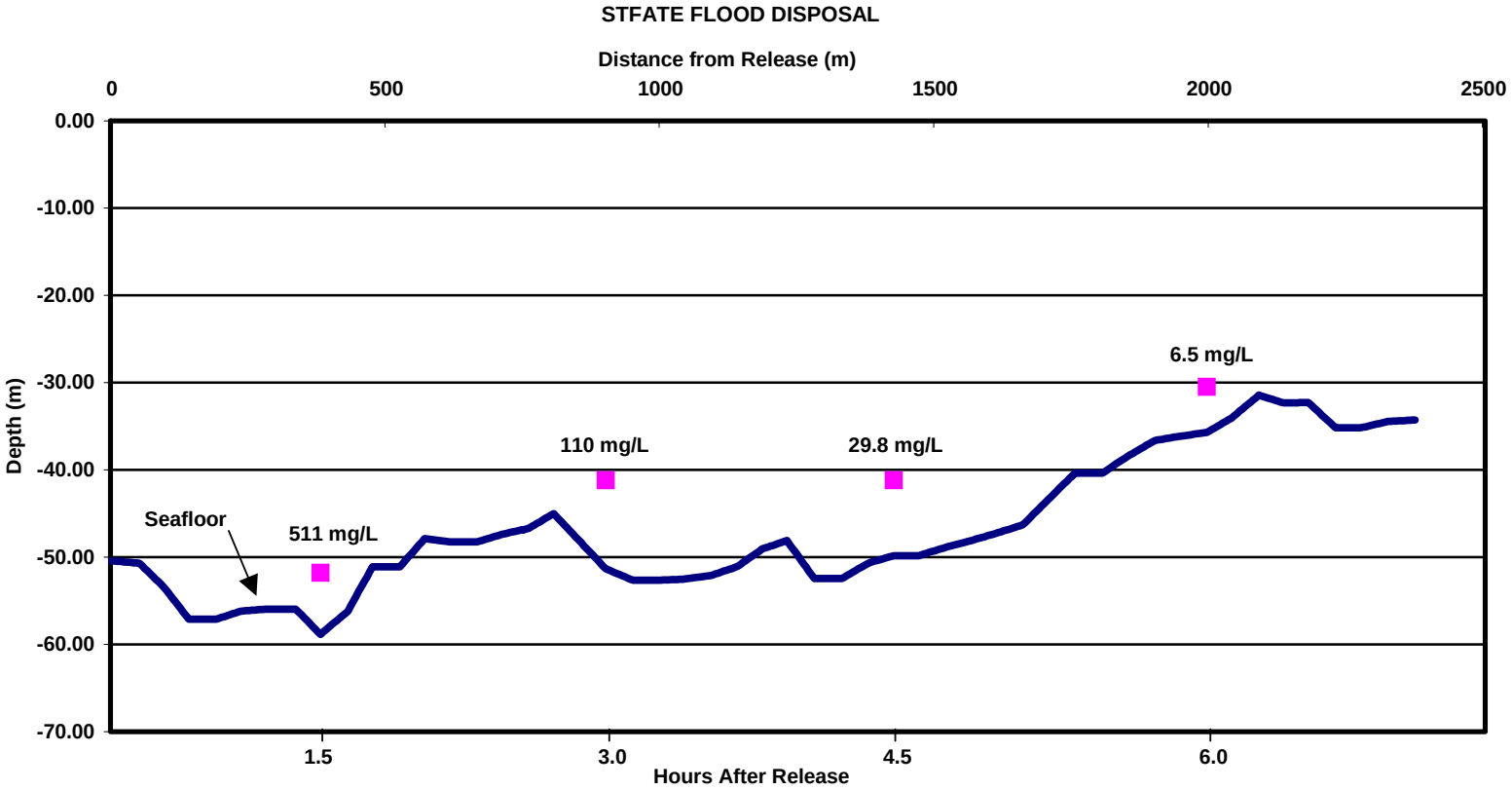

Figure 3-29. Cross-section view showing the maximum STFATE-predicted clay particle concentration at the centroid of the sediment plume over the underlying seafloor topography, with time and distance from the point of release of a 3,050 m^3 (4,000 yd^3) disposal event at PDS during an average flood tide.

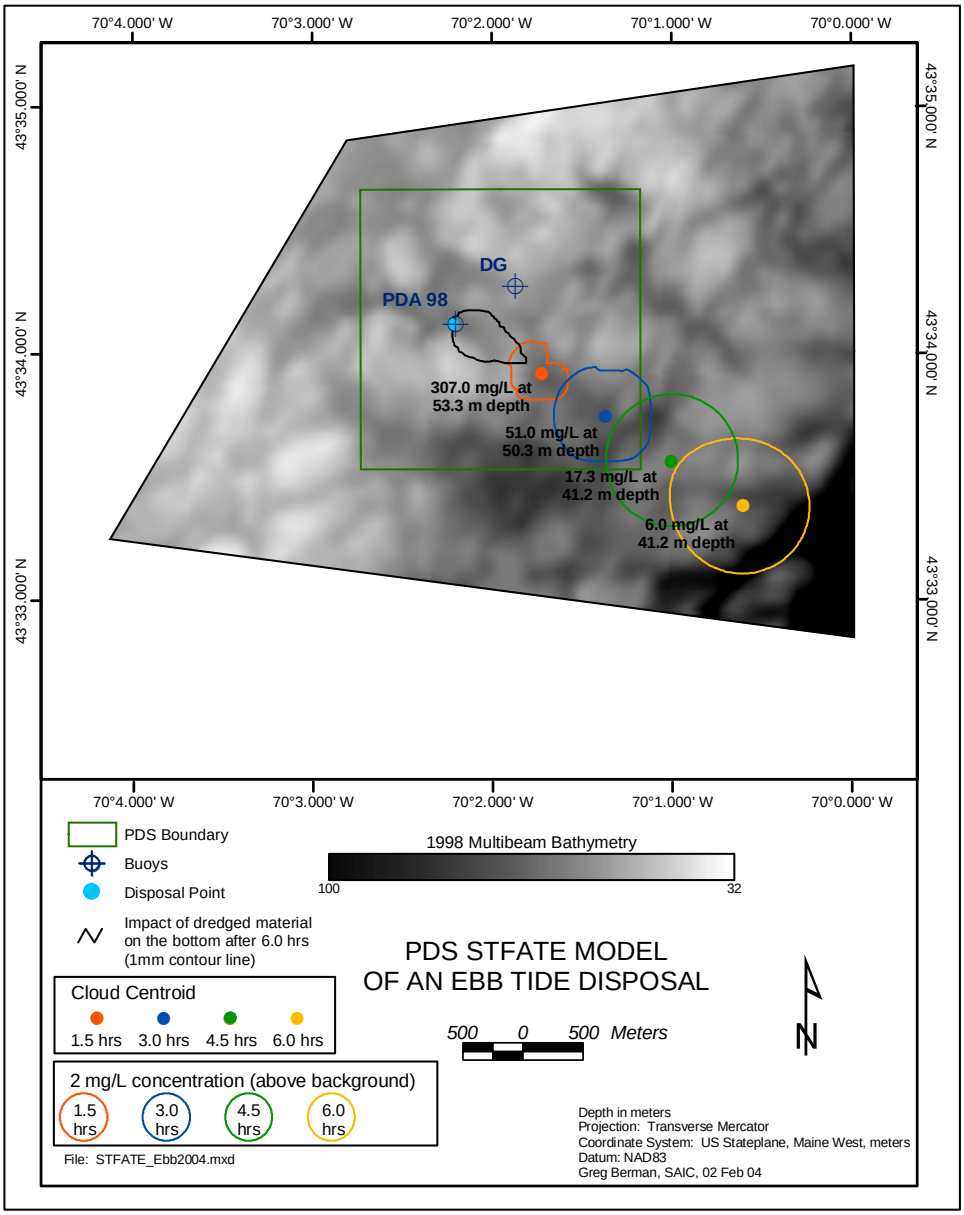

Figure 3-30. Map of second-order STFATE model results showing the horizontal extent of the clay particle cloud from a 3,050 m³ (4,000 yd³) disposal event over PDS during an average ebb tide. Each colored dot represents the cloud centroid at 1.5 hour intervals and is labeled to show the clay particle concentration in $mg \cdot l^{-1}$ at that point/time. The corresponding ring around each colored dot represents the perimeter of the plume, where the clay particle concentration becomes equal to the background suspended sediment concentration of 2 $mg \cdot l^{-1}$.

One and one-half hours after the dredged material disposal event, the centroid of the sediment plume had traveled on the ebbing tide approximately 800 m from the original point of deposition. The STFATE model estimated the centroid to be located at a water depth of 53 m with a maximum turbidity value of 307 $mg \cdot l^{-1}$. The morphology of the plume was significantly affected by the seafloor topography surrounding the disposal point, as the ridge located southeast of the disposal point likely contained most of the sediments entrained in the water column at depths below 50 to 55 m (Figure 3-31).

The subsequent time intervals displayed a near circular (planview) or cylindrical (three-dimensional) sediment plume with concentrations decreasing rapidly with increasing distance from the disposal point. A maximum turbidity value of 51 $mg \cdot l^{-1}$ was estimated by the model at three hours post-disposal, representing an 83% reduction in clay particle concentration relative to the 1.5 hour interval. The processes of dilution and settlement continued through the 4.5 and 6.0 hour intervals as the areal extents of the plume increased slightly, while turbidity values decreased substantially over time. Seafloor topography appeared to influence the morphology of the sediment plume between the 3.0 and 4.5 hour intervals as the plume interacted with another ridge located just outside the eastern boundary of PDS. This interaction caused a shift in the depth of the centroid from 51 to 41 m depth (Figure 3-31). Similar to the results of the flood tide modeling results, the centroid of the plume at the 6.0 hour interval was characterized as an area displaying a maximum turbidity of 6 $mg \cdot l^{-1}$. This low value is approximately 2% of the maximum turbidity value generated by STFATE for the 1.5 hour interval, and would be difficult to distinguish from background levels in a typical field measurement program.

Because the transport of most individual sediment plumes are impacted by gross elements of both flood and ebb tide, additional model runs were performed to examine net transport direction and dilution. To simulate a dredged material plume transport over a time period that spans a mid-flood to mid-ebb tidal cycle, average current speed and direction data obtained from the March-April 1999 deployment (described in Section 3.6 above) were used. The model simulated dredged material releases with volumes of 3,050 m^3 (4,000 yd^3), 4,600 m^3 (6,000 yd^3), and 5,500 m^3 (7,200 yd^3) at the PDA 98 buoy using the sediment characteristics derived from the material sampled in the Portland Harbor cores. The process of utilizing mean speed and direction in the STFATE runs was selected to display the maximum potential transport of the plume sediments as a worst-case scenario.

Figures 3-32 through 3-34 show the horizontal extent of the clay particle cloud from each disposal event, respectively. In general, the results for the different disposal barge sizes were comparable. After release from the barge, the centroid of the sediment plume traveled to the south-southwest 3.4 km at a rate of 567 meters per hour (15.7 $cm \cdot s^{-1}$) in response to the forcing of the average currents. The sediment plume increased in size as time progressed, while the peak clay particle concentrations also diminished as a result of dilution and particle settlement.

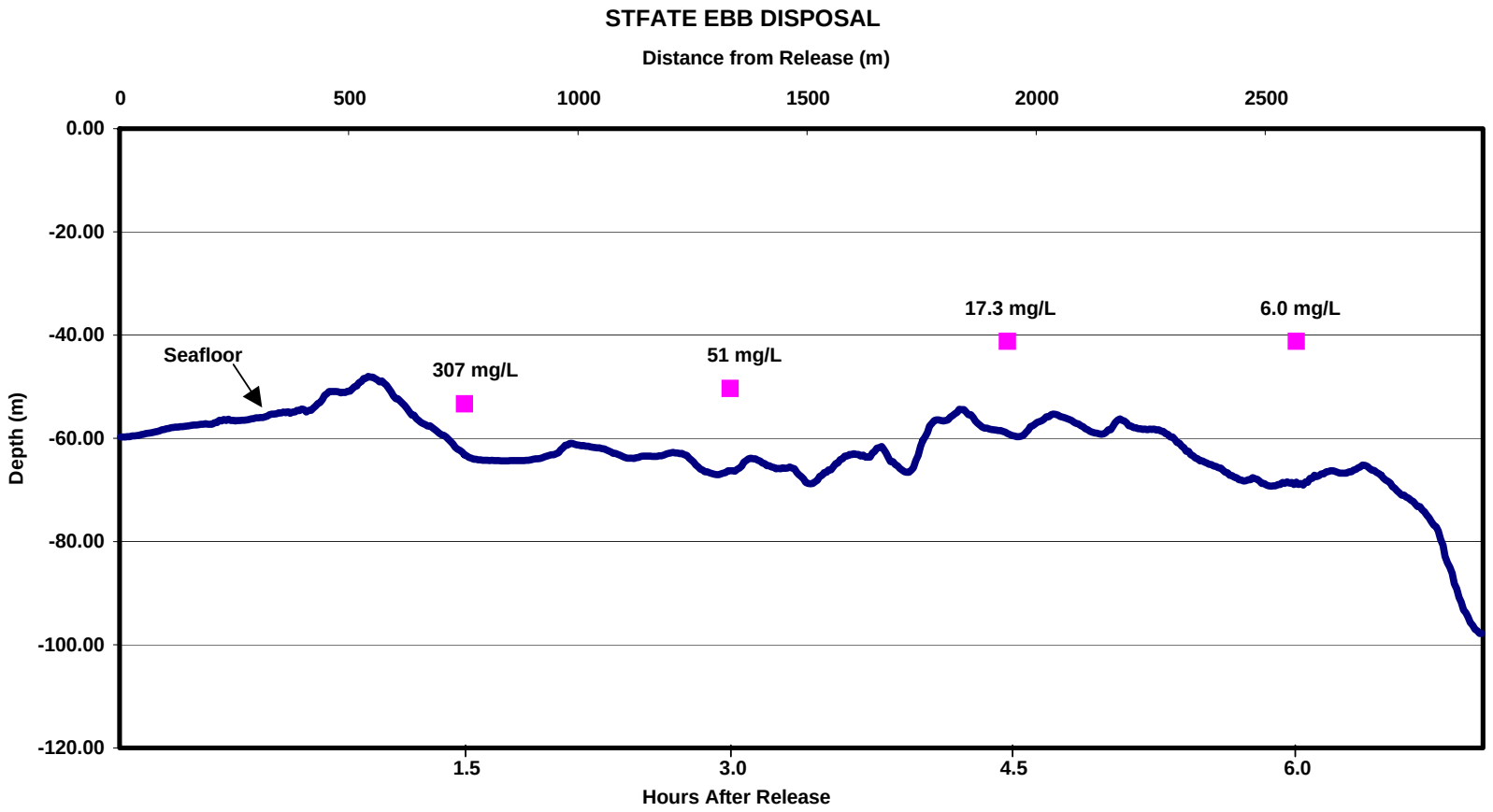

Figure 3-31. Cross-section view showing the maximum STFATE-predicted clay particle concentration at the centroid of the sediment plume over the underlying seafloor topography, with time and distance from the point of release of a 3,050 m^3 (4,000 yd^3) disposal event at PDS during an average ebb tide.

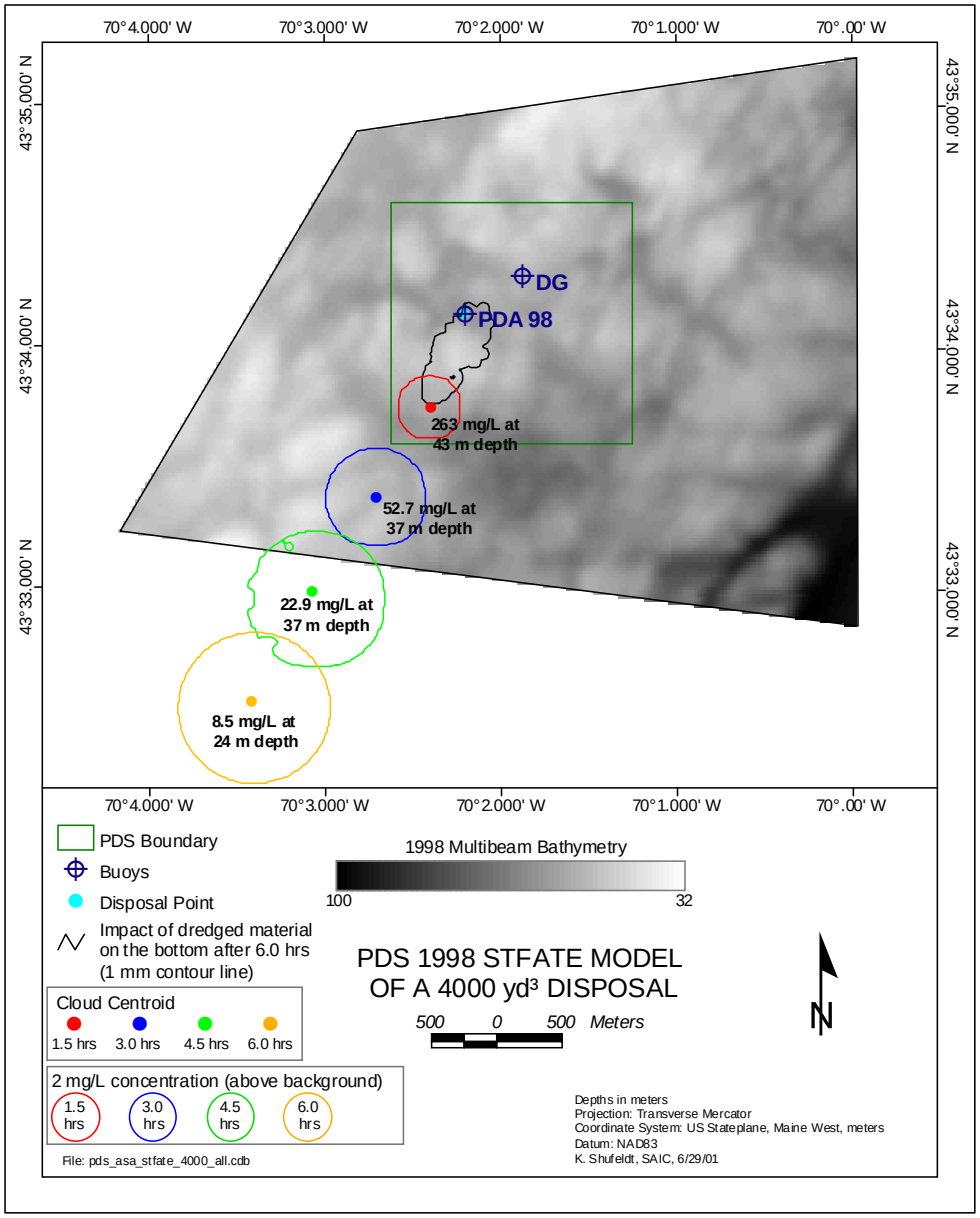

Figure 3-32. Map of second-order STFATE model results showing the vertical and horizontal extent of the clay particle cloud from a 3,050 m³ (4,000 yd³) disposal event utilizing average currents over PDS. Each colored dot represents the cloud centroid at 1.5 hour intervals and is labeled to show the clay particle concentration in $mg \cdot l^{-1}$ at that point/time. The corresponding ring around each colored dot represents the perimeter of the plume, where the clay particle concentration becomes equal to the background suspended sediment concentration of 2 $mg \cdot l^{-1}$.

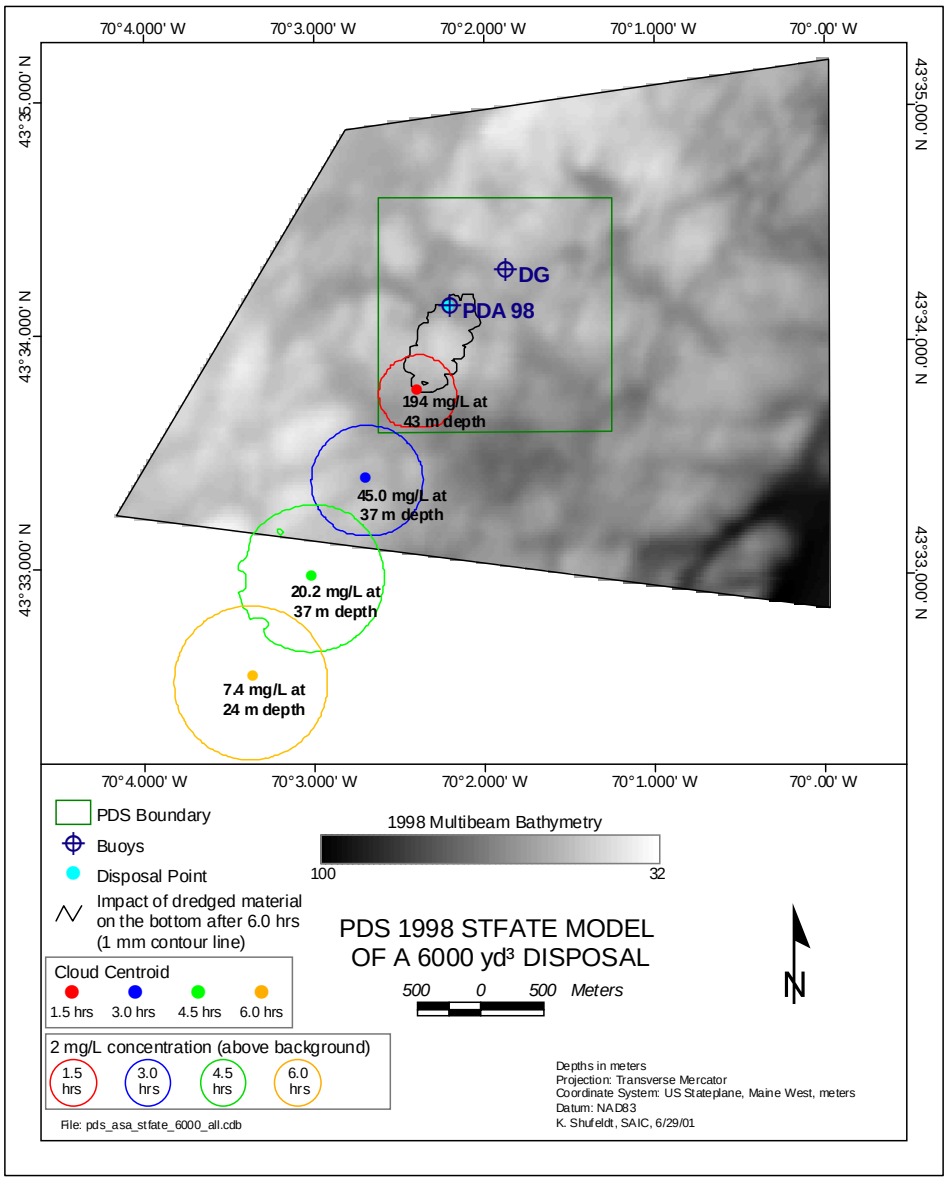

Figure 3-33. Map of second-order STFATE model results showing the horizontal extent of the clay particle cloud from a 4,600 m³ (6,000 yd³) disposal events utilizing average currents over PDS. Each colored dot represents the cloud centroid at 1.5 hour intervals and is labeled to show the clay particle concentration in $mg \cdot l^{-1}$ at that point/time. The corresponding ring around each colored dot represents the perimeter of the plume, where the clay particle concentration becomes equal to the background suspended sediment concentration of 2 $mg \cdot l^{-1}$

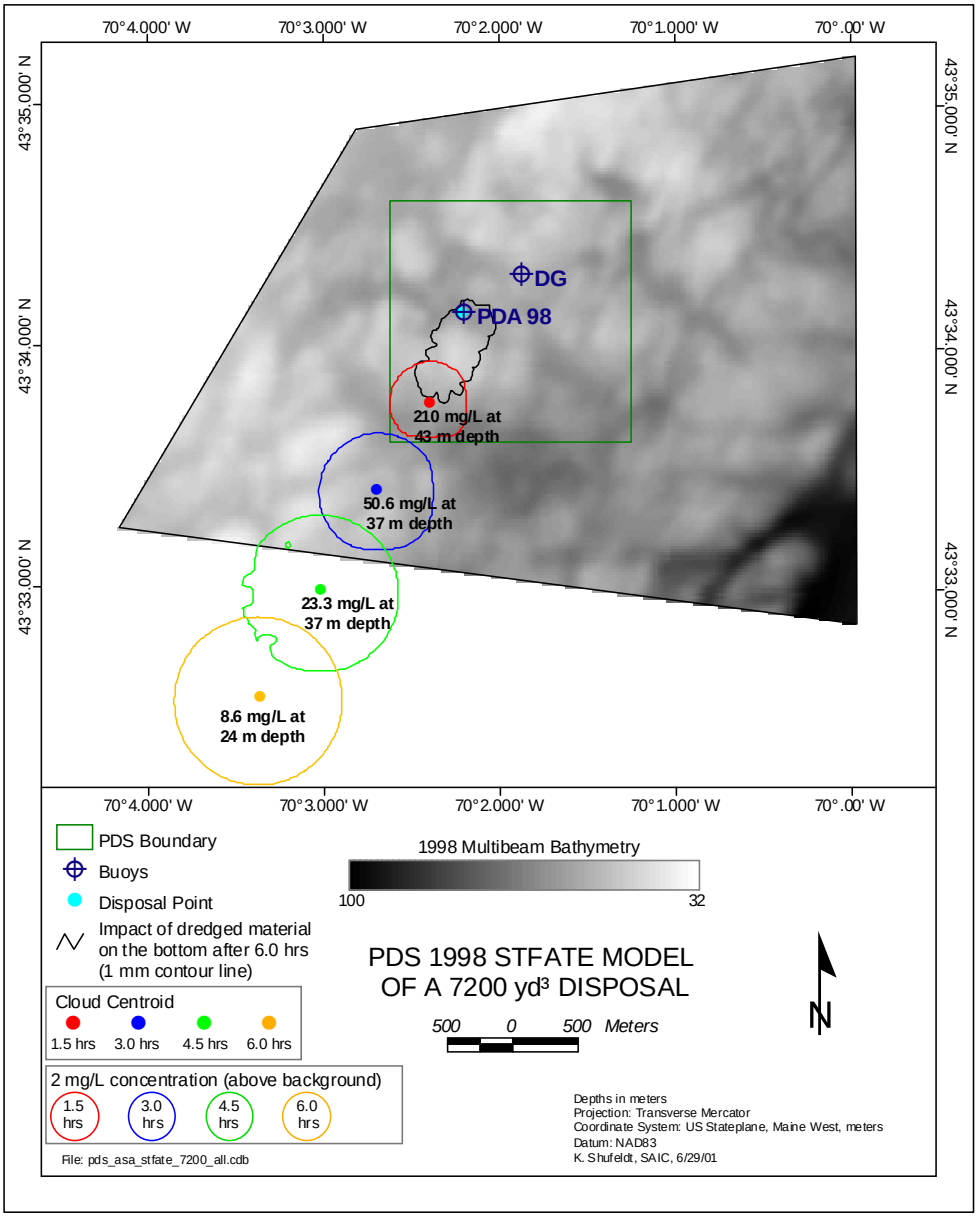

Figure 3-34. Map of second-order STFATE model results showing the horizontal extent of the clay particle cloud from a 5,500 m³ (7,200 yd³) disposal event utilizing average currents over PDS. Each colored dot represents the cloud centroid at 1.5 hour intervals and is labeled to show the clay particle concentration in $mg \cdot l^{-1}$ at that point/time. The corresponding ring around each colored dot represents the perimeter of the plume, where the clay particle concentration becomes equal to the background suspended sediment concentration of 2 $mg \cdot l^{-1}$

Figures 3-35 through 3-37 show in cross-section view the maximum clay concentration at the centroid of the sediment plume over the underlying seafloor topography. At 1.5 hours post-disposal, maximum turbidity values (from 191 to 263 $mg \cdot l^{-1}$) were detected approximately 750 m southwest of the initial disposal point and 10 m above the seafloor. The maximum concentration of sediment remained approximately 10 to 15 m above the bottom as the cloud traveled over rough bottom topography and away from the initial release point. Once again, bottom topography likely affected the sediment plume by impeding the progress of the lower portions of the plume and subsequently containing sediments.

Despite the differences in volume disposed, all three model runs indicated the centroid of the sediment cloud traveled approximately 3.4 km from the release point and expanded to cover an increasingly larger area over the course of the six hours (Figures 3-32 through 3-34). The results of all three model runs indicated the centroid of the plume was consistently located at water depths of 45 m and shallower, with substantially lower turbidity values relative to model runs presented above. These results suggest the shear ridge to the south of the PDA 98 disposal buoy served to contain the lower portions of the sediment plume. The containment measure appeared to have essentially sheared off the bottom 15 m of the plume, which would be expected to contain the highest concentration of entrained sediments.

As time progressed in the model runs, the suspended load concentrations gradually diminished through settlement and dilution. At six hours post-disposal, sediment concentrations were rapidly approaching background concentrations, as a maximum value of 8.6 $mg \cdot l^{-1}$ above background [5,500 m^3 (7,200 yd^3) run] was detected near the center of the cloud and at a water depth of 24 m (Figure 3-34). Independent of the volume of material disposed, turbidity at the centroid of the plume was approximately 3 to 4% of suspended load estimated by STFATE at the 1.5 hour time interval. At such low levels, the cloud of entrained sediments would be difficult to distinguish from background levels in a typical field measurement program.

3.8.2 MDFATE Model

Two different MDFATE model runs were conducted: one to hindcast the seafloor effects from the 166 individual disposal events associated with the 1998-1999 Portland Harbor dredging project and the other to hindcast the seafloor effects from the 197 individual disposal events associated with all of the PDS placement activity between the 1998 and 2000 multibeam surveys. Because the MDFATE results were ultimately compared to the depth difference results, this section will focus only on the model output that reflected all 197 disposal events that occurred between the two multibeam surveys.

Figure 3-38 displays the reported location of all of the individual disposal events from 1998 through 2000, as well as the model-predicted thickness and footprint of the dredged

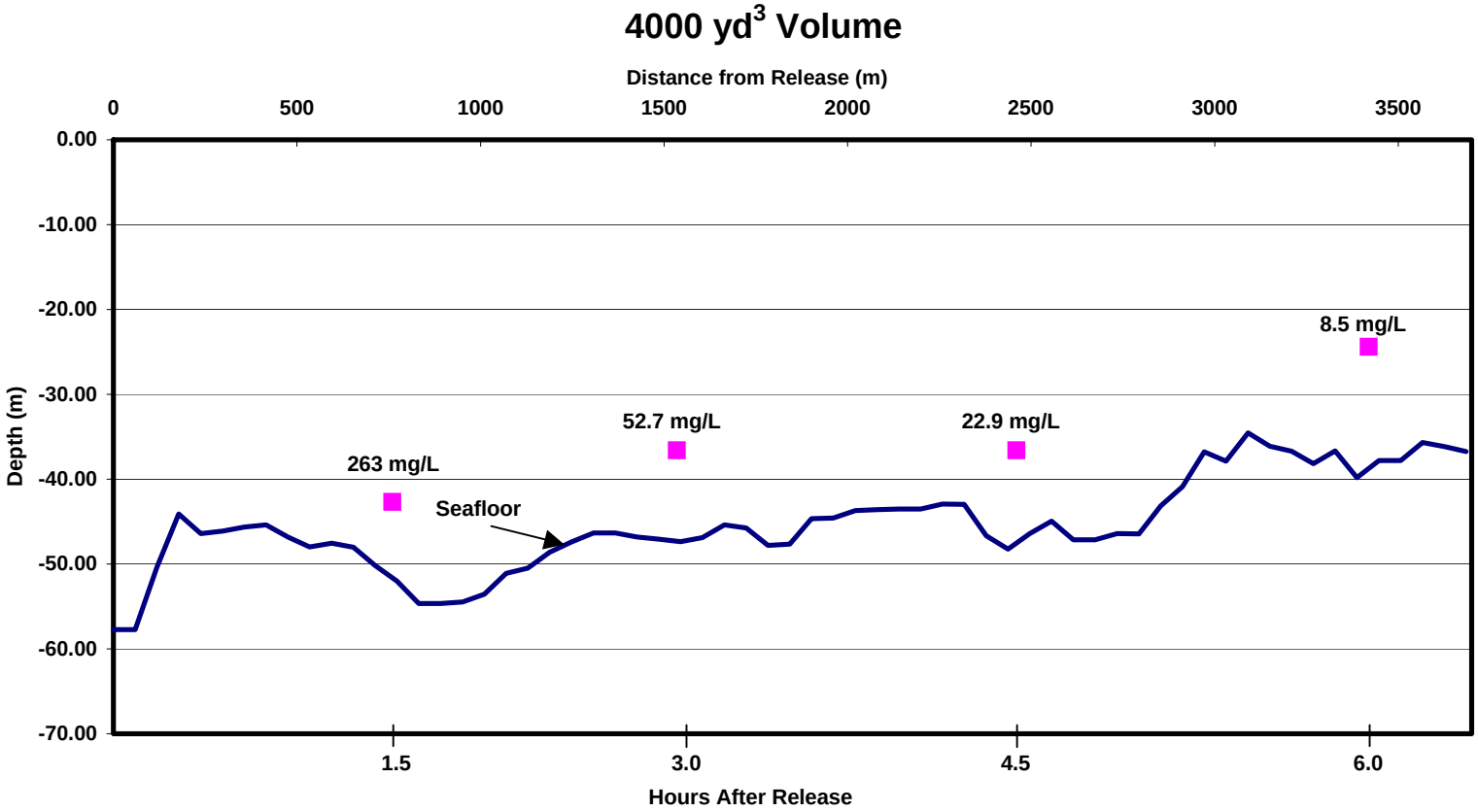

Figure 3-35. Cross-section view showing the maximum STFATE-predicted clay particle concentration at the centroid of the sediment plume over the underlying seafloor topography, with time and distance from the point of release of a 3,050 m^3 (4,000 yd^3) disposal event.

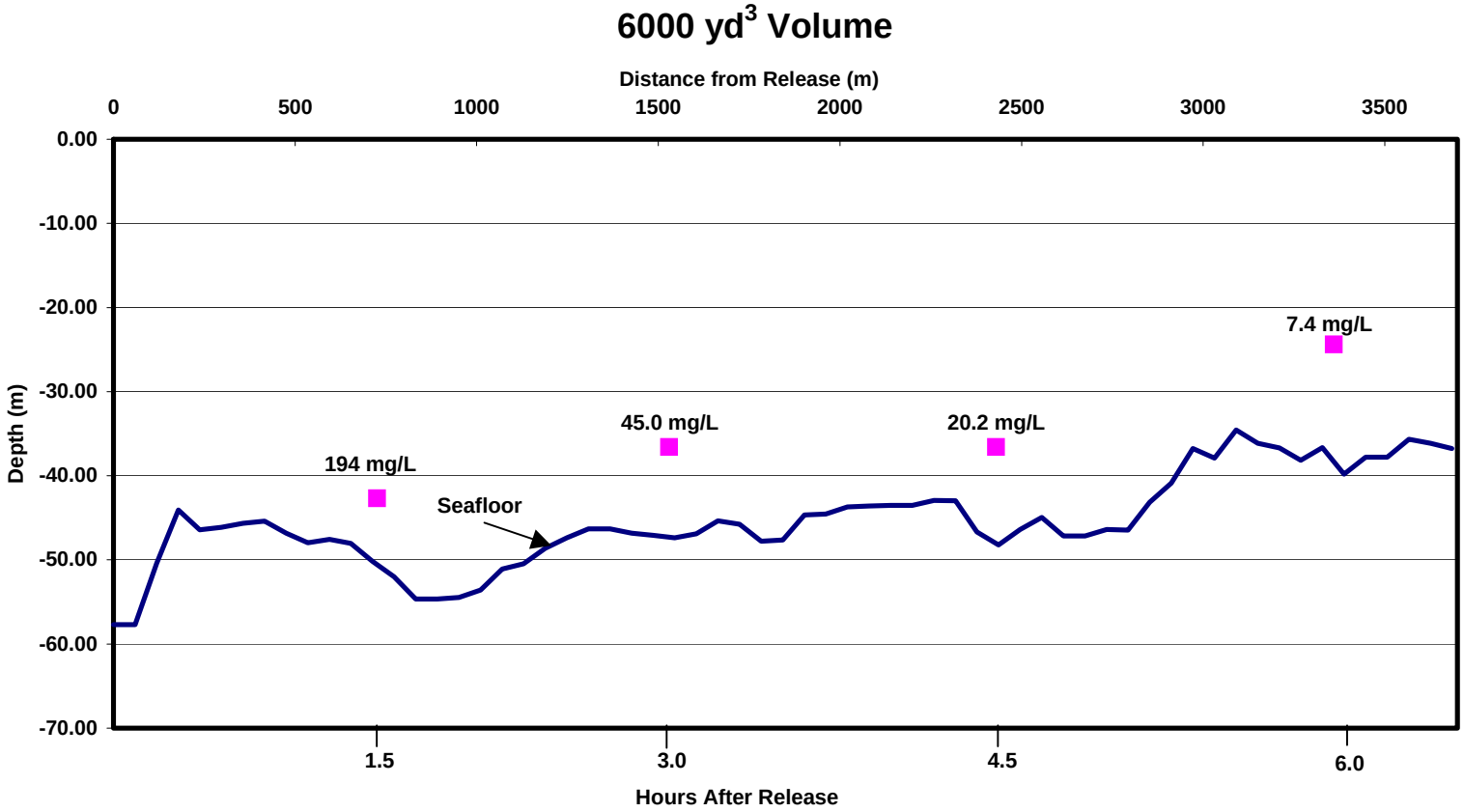

Figure 3-36. Cross-section view showing the maximum STFATE-predicted clay particle concentration at the centroid of the sediment plume over the underlying seafloor topography, with time and distance from the point of release of a 4,600 m³ (6,000 yd³) disposal event.

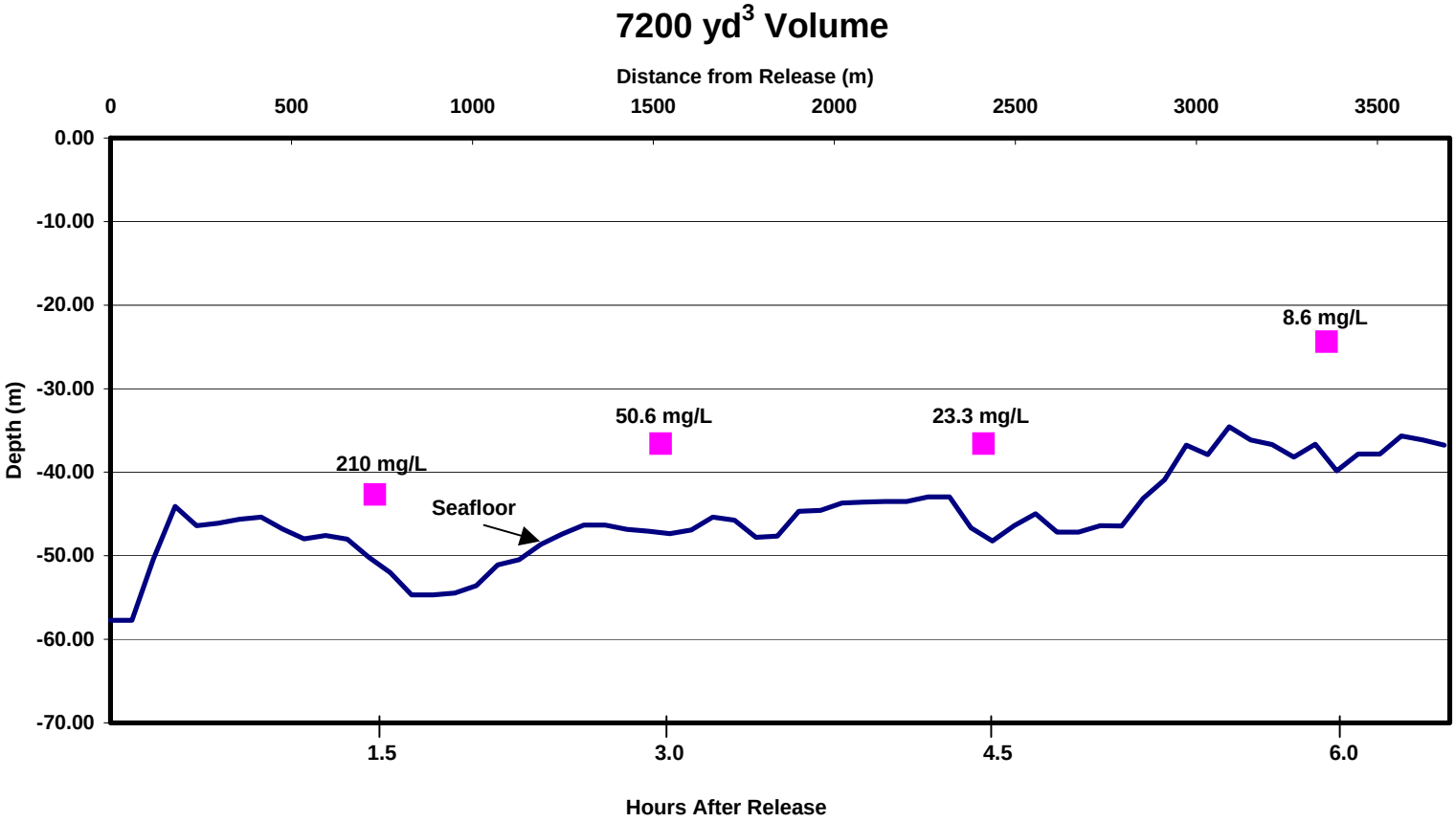

Figure 3-37. Cross-section view showing the maximum STFATE-predicted clay particle concentration at the centroid of the sediment plume over the underlying seafloor topography, with time and distance from the point of release of a 5,500 m^3 (7,200 yd^3) disposal event.

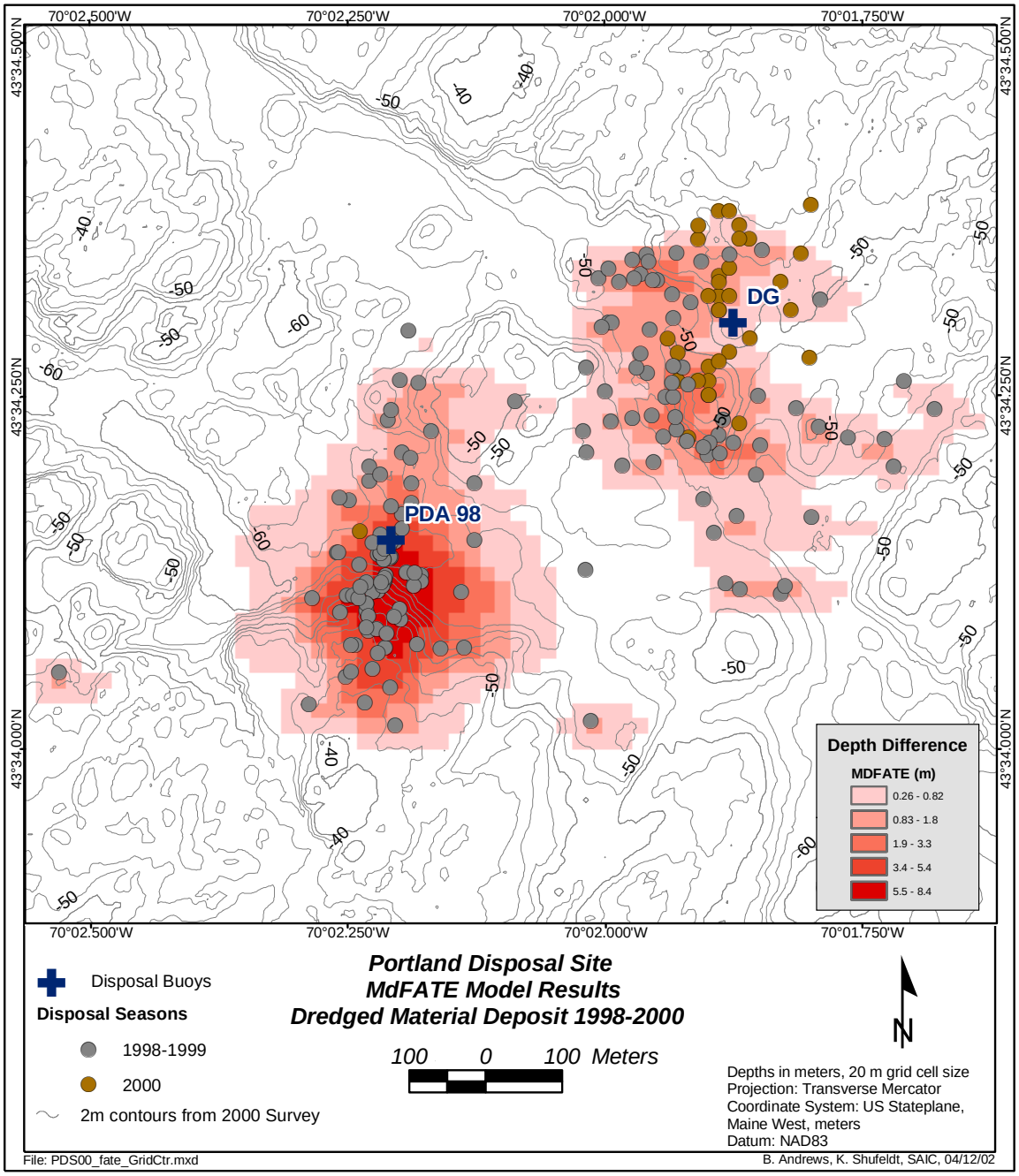

Figure 3-38. Map showing the location of the individual disposal events from 1998 through 2000, in relation to the MDFATE-predicted thickness and footprint of the dredged material deposit at the PDS. The model-predicted thickness was developed by taking the depth difference between pre- and post-disposal bathymetry generated by the MDFATE model.

material deposit at the PDS. This model-predicted thickness was developed by taking the difference between pre- and post-disposal bathymetry generated by the MDFATE model. As shown in this figure, the disposal mound morphology depicted by the MDFATE model appeared very closely correlated with the positions of the disposal events. The MDFATE results showed the largest accumulation of material just to the south of the PDA 98 buoy, where the highest numbers of large scow releases were recorded. The MDFATE model indicated that mound heights in this area of greatest accumulation would approach a maximum of more than 8 m.

The estimated cumulative barge volume of the material associated with all of these events was 482,370 m^3 (630,923 yd^3). The volume of the seafloor deposit calculated by the MDFATE model was 448,000 m^3 (585,971 yd^3), a 7% decrease relative to the total estimated volume of placed material. This volume decrease has two possible causes: 1) the loss of entrained water from the deposited dredged material calculated during the consolidation phase of the model simulation, and 2) the void ratio of the deposited material used for the simulations was underestimated resulting in a smaller total deposit volume.

4.0 DISCUSSION

The primary focus of the following discussion will be to address how well the modeling results agreed with the observed results during and after the 1998-1999 Portland Harbor dredging project. Specifically, the STFATE results showing the trajectory of the sediment plume following disposal will be compared to the sediment trap data used to gain insights into the settlement of plume sediments out of the water column during Phase 3 of the dredging project. In addition, the MDFATE results predicting the configuration of the dredged material deposit on the seafloor will be compared to both the REMOTS® sediment-profile imaging and bathymetric depth difference results. Prior to the modeling results discussion, some of the major findings and issues that arose during the comparative analyses of the different field monitoring data sets will be addressed.

4.1 Evaluation of Field Monitoring Data

4.1.1 Multibeam Bathymetry, Side-scan Imagery, and Sediment-Profile Imaging

In the earlier Portland Disposal Site Capping Demonstration Project, completed between 1995 and 1997, it had proved difficult to develop accurate depth difference comparisons based on single-beam bathymetry (Morris et al. 1998). The irregular bottom topography and the relatively small volume of dredged material placed within the study area introduced survey artifacts (false indications of change in depth) that hindered detection of dredged material thickness and disposal mound morphology. The data provided by supplemental monitoring techniques (e.g., REMOTS® sediment-profile imaging and sediment coring) were utilized in conjunction with the bathymetric data to delineate the size and shape of the capped Royal River disposal mound. Based on the results of that project, a recommendation was made to employ multibeam bathymetric surveying as a monitoring technique for any future projects at PDS (Morris et al. 1998).

Prior to the 1998-99 Portland Harbor dredging project, a high-resolution multibeam bathymetric survey and a full bottom-coverage side-scan sonar survey were completed over a large area surrounding PDS. More than one year after the completion of the 1998-99 dredging project, a second high-resolution multibeam survey and a REMOTS® sediment-profile imaging survey were conducted over PDS. These surveys produced much higher resolution data than had been previously recorded for the area and allowed far better insight into the complexity of the seafloor within the region (Figure 4-1). The multibeam bathymetry and side-scan imagery highlighted the numerous steep, bedrock ridges and a northwest-southeast trending trough within this complex topography. A historic sediment deposit corresponding to the previous position of the DG buoy was visible in the center of the NW-SE trending trough. In addition, several naturally occurring basin features were

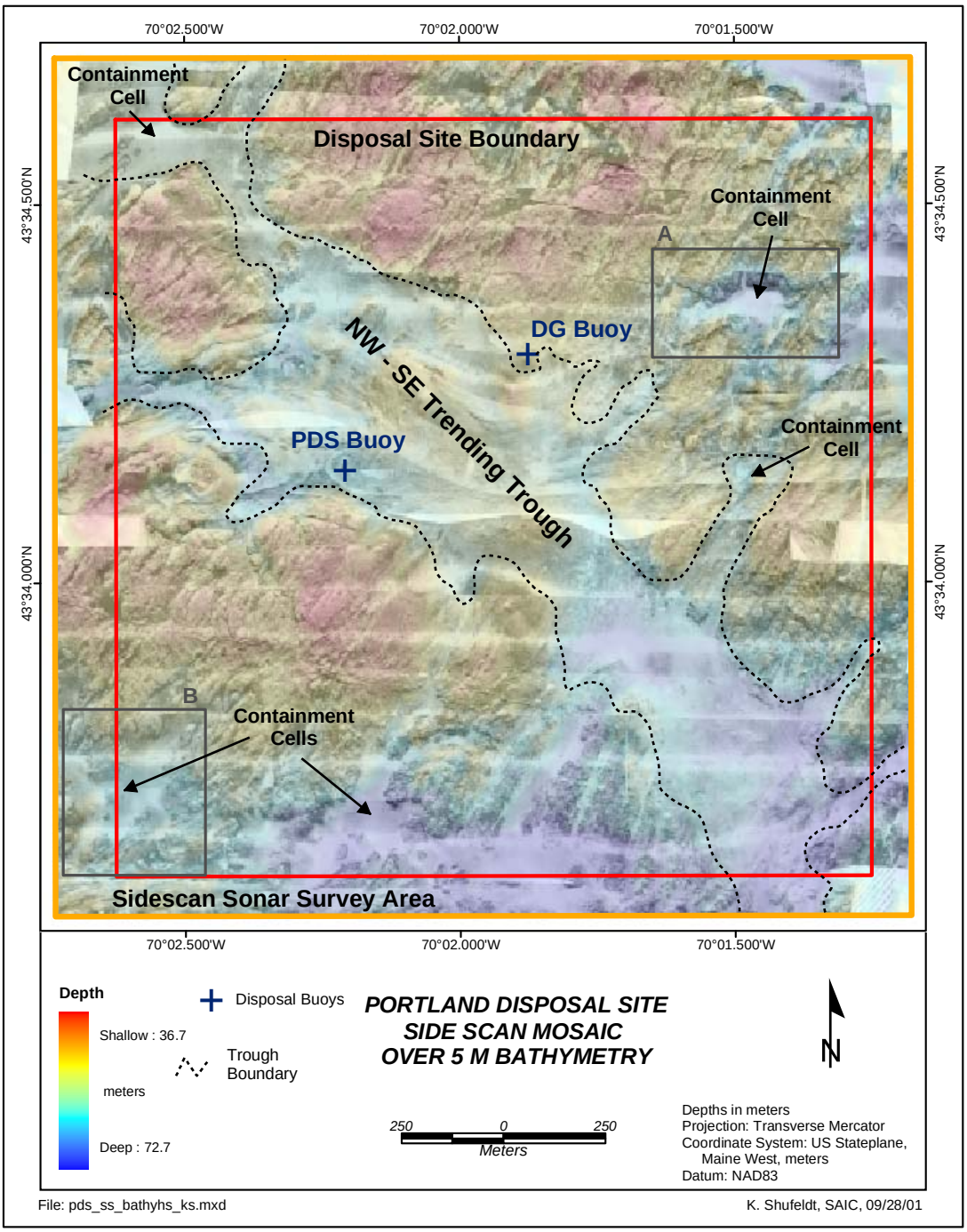

Figure 4-1. Hill-shaded multibeam bathymetry acquired in July 2000 draped over side-scan sonar imagery from September 1998 illustrating many features over the complex Portland Disposal Site seafloor

identified within the bedrock areas that showed potential for use as natural containment cells (Figure 4-1). These features are of various size, configuration, and capacity, and could be utilized as part of future capping projects. The two examples provided in Figure 4-2 each offer dredged material capacities of over 550,000 m^3 if filled to the height of the surrounding seafloor. These cells could be utilized for future small to moderate sized subaqueous capping projects. The PDA 98 Mound was actually developed in a similar natural containment cell that offered a dredged material capacity of nearly 1 million cubic meters.

As discussed in Section 3.3.3, the multibeam depth difference results indicated that most of the dredged material placed near the PDA 98 and DG buoys accumulated in the deeper areas among the rock outcrops, with little acoustically detectable accumulation on the surfaces of the exposed bedrock. However, similar to the limitations of standard single-beam bathymetry, multibeam was unable to reliably detect thin layers (<20 cm) of sediment and required supplemental data (sediment-profile imaging) to comprehensively map the footprint of the Portland Harbor dredged material. REMOTS® sediment-profile imaging results showed that surface layers of dredged material were present at all but the most southerly sampling station (Station 400S; Figure 4-3). Based on the combined results of the REMOTS® survey and bathymetric depth difference, it appears most of the deposited dredged material had settled in the deeper depositional area, but a relatively thin surface layer of this material did exist over the surrounding bedrock areas. Furthermore, the bedrock outcrops offer numerous faults and crevices that are subject to infilling through dredged material placement operations. As a result, a significant volume of soft sediment has likely accumulated within these bedrock features and is now obscured from detection by acoustic sensors.

In contrast to the depth difference results from previous single beam bathymetric surveys, the multibeam depth difference calculations for PDS provided a tool for examining the gross morphology of the PDA 98 Mound as part of a complex seafloor. Two dredged material deposits were clearly identified in close proximity to the PDA and DG disposal buoy positions despite the continued appearance of both positive and negative survey artifacts. Artifacts were fairly widespread within the survey area, but were less substantial than those of historic, single-beam bathymetry surveys conducted at PDS due to the density of the bathymetric data set and the 1 m^2 grid cell size.

The gridding process averages depth soundings collected within a given area to develop a bathymetric model of the seafloor. Swath bathymetry ensonifies the entire seafloor to permit the development of grid cells as small as 1 m^2, while single-beam bathymetry commonly uses depth values obtained along a series of individual lines to represent the seafloor via 312.5 m^2 (25 × 12.5 m) grid cells. Due to the interpolation that

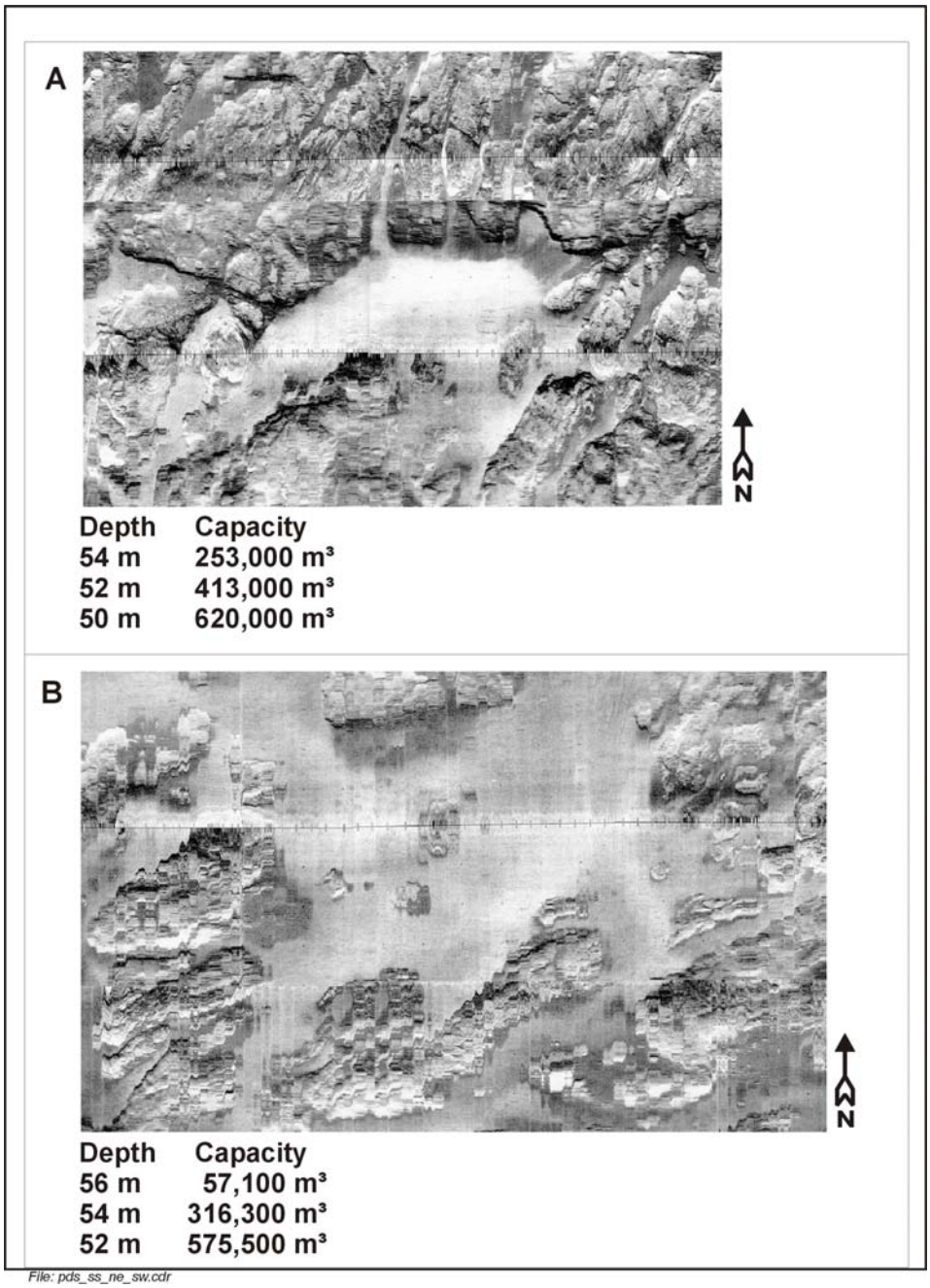

Figure 4-2. Zoomed in view of the side-scan sonar images of the two potential Portland Disposal Site natural containment basins. Included with each graphic are the approximate dredged material capacities of each cell if filled to various water depths

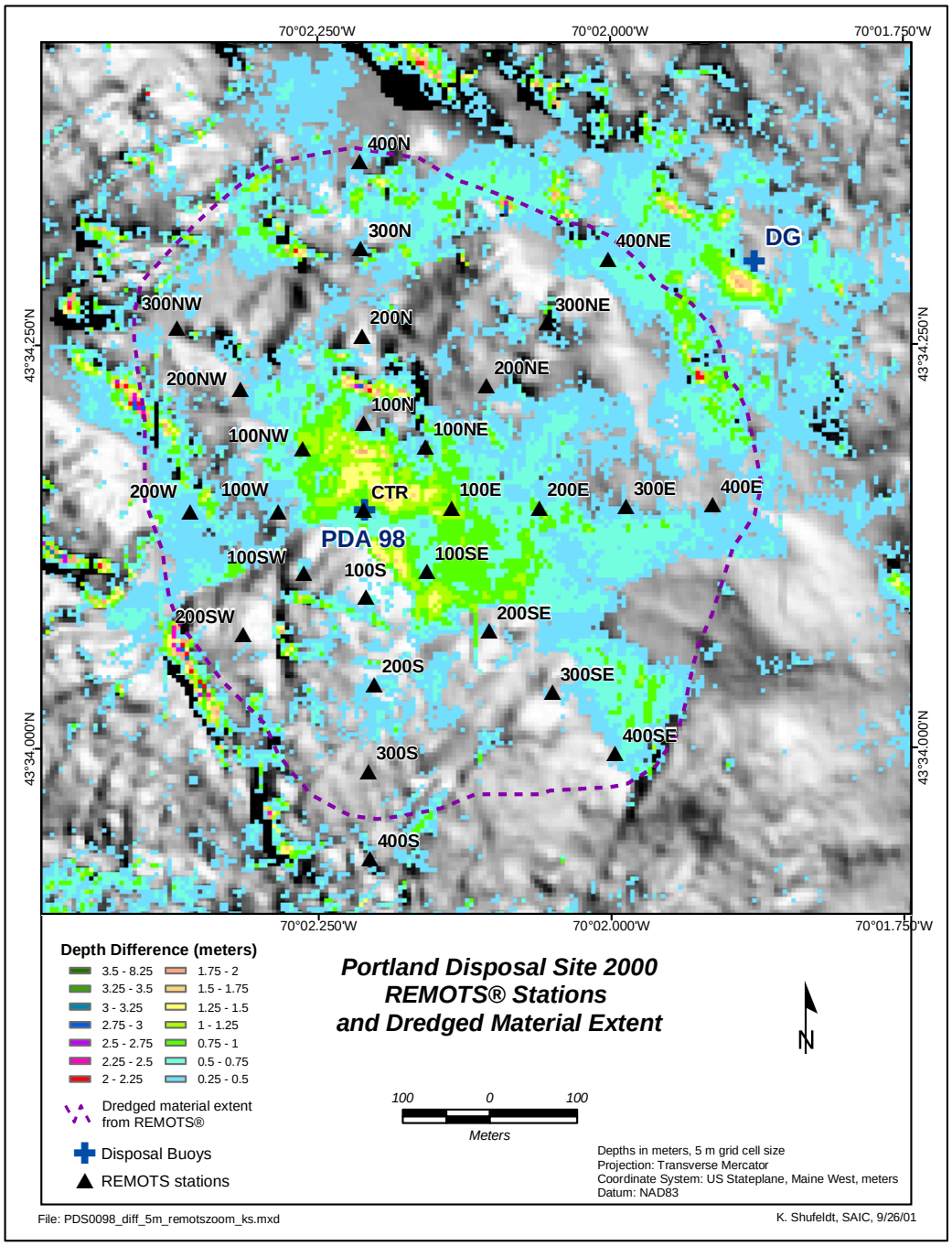

Figure 4-3. Limits of the seafloor dredged material extents as defined with REMOTS® sediment-profile imaging as well as the multibeam depth difference results

occurs between survey lines during the development of a bathymetric model, comparisons between sequential single-beam bathymetric surveys are more susceptible to the formation of survey artifacts in areas of rough, irregular bottom topography relative to an area of low to moderate relief. In general, the ability to grid data into much smaller cells dramatically reduces the amount of averaging and interpolation between cells. As a result, variability in seafloor topography is characterized more accurately by multibeam survey systems and the average values tend to be more consistent between surveys.

The artifacts that appeared within the multibeam depth difference were commonly associated with areas of strong bottom slope (faults and narrow troughs within the bedrock; Figure 3-14). Despite the correctors applied to the data to compensate for vessel position and tide stage, slight variations in positional information (1 to 3 m) from the differential GPS data yielded minor differences in the geographic position assigned to the soundings acquired within these small (1 m^2) depth cells. When two sequential bathymetric surveys are directly compared, the impacts of these positional offsets become magnified to produce survey artifacts in areas of strong seafloor relief. Although the use of multibeam bathymetric surveys did reduce the appearance and significance of artifacts within the depth difference comparison, continued refinement of this technique is required to further diminish the appearance and impacts of these artifacts, as well as enhance its ability to track thin layers of sediment placed over a highly irregular seafloor.

4.1.2 Sediment Sampling

One objective of the sediment coring and grab sampling surveys, as well as the subsequent geotechnical analyses, was to characterize the sediments to be dredged from Portland Harbor for input to the STFATE and MDFATE models. A second objective was to examine the feasibility of using sediment tracers to differentiate between the Portland Harbor sediments and those that already existed within PDS. Assuming such tracers could be found, they would be of potential use in evaluating the likely source of any material retained in the sediment traps deployed at various locations surrounding PDS.

The coring and grab sampling results showed that the Fore River and Portland Harbor sediments were consistently dominated by clay (58% average), with varying amounts of silt (34% average) and sand (7% average). The silt and sand component was largely dependent upon the location of the core in relation to intertidal and subtidal zones.

The grab samples collected from the area in close proximity to the PDA 98 buoy prior to the disposal event displayed a relatively high percentage (71%) of coarse-grained sediment (gravel and sand), while silt and clay comprised only 29% of the sample (Table 3-1). However, given the position of the PDA 98 buoy relative to the DG Buoy, it was theorized that the surficial sediments collected in the grab sample could have been influenced by historic dredged material deposition. As a result, supplemental information regarding

sediment composition and grain size was used to characterize ambient sediments in the PDS region.

Although no detailed grain-size analyses were conducted, the composition of the ambient sediments obtained from the deployment location of Sediment Trap 3 (along the southern boundary of PDS) was described as coarse to medium-grained silty sand (Tables 3-4 and 3-6). These results were also in agreement with the sediment descriptions and grain-size analysis from the July 1992 survey conducted at the PDS reference areas (Wiley 1996). Grab samples obtained from the two PDS reference areas closest to the disposal site boundary (EREF and SREF) displayed very similar grain size distributions, with sand and gravel comprising 83% of each sample and 17% composed of fine-grained material (primarily silt). These findings indicated a distinct difference in composition of the sediments located in the PDS region from those found in the cores and grabs collected from Fore River and Portland Harbor.

The primary intent of the sediment trap analyses was to determine if the material had most likely originated from recently placed Portland Harbor dredged material, resuspended ambient material, or some other source. As discussed in Section 3.2, only three of the ten deployed sediment traps were recovered with any analyzable data. Although the material within Sediment Traps 3, 8, and 10 was visually described as the same material, only Sediment Trap 3 had a sufficient volume of material to allow a complete sediment grain size analysis. The grain size composition of the Sediment Trap 3 material was 80% clay, 19% silt and 1% sand.

The relatively high sand content within the ambient sediments surrounding PDS is presumably a function of the oceanographic conditions within the region. Based on previous studies, significant resuspension of fine-grained sediment over areas of PDS can be correlated to bottom stress triggered by weather events generating surface waves of 3 m or greater (McDowell and Pace 1998). As a result, fine-grained sediments that have settled to the bottom during quiescent periods are subject to resuspension by the bottom stress associated with the passage of storm waves. The silt and clay particles would be most likely to be suspended from the seabed during such events and subject to advection by currents. Therefore, a prevalence of finer-grained material in the sediment traps would be expected if the primary source of the material were resusupension from the substrate in the vicinity. The occurrence of the March 21-23 storm event during the trap deployment period could have contributed to deposition of fine-grained material in the traps.

Based on the fact that the PDS sediments (including likely historic dredged material and ambient sediments at the reference areas) have a component of fine-grained sediments, which would be subject to resuspension and local advection that could have resulted in deposition in the sediment traps, grain size data alone do not provide sufficient information on which to base conclusions about the origins of the material collected in the traps. As

discussed below, the use of sediment tracers provided some additional information that helped to further identify the likely sources for the material collected in the sediment traps at PDS.

4.1.3 Sediment Tracer Technique

The sediment trap, grab sample, and coring sediments were all analyzed for the presence of unique sediment tracers in an attempt to further pinpoint the probable origin of the material retained within the sediment traps. The initial analysis indicated a lack of unique mineralogical tracers having settling properties likely to mirror those of the very fine-grained sediment fraction typically comprising a disposal plume. Diatoms provided a potentially useful tracer based on distinct occurrences, as benthic diatoms occurred only in the Portland Harbor samples, and planktonic diatoms occurred only in the disposal site and sediment trap samples (Table 3-6). However, benthic diatoms were observed only rarely in the harbor samples, and the fact that no benthic diatoms were observed in the sediment trap samples does not provide conclusive evidence that the trap material did not originate from the Portland Harbor dredged material disposal operations.

Further analysis showed that microfossil composition was a potentially useful tracer, with higher numbers of salt marsh and mudflat foraminifera and the presence of freshwater thecamoebians generally serving to differentiate the estuarine sediments of the Fore River and Portland Harbor from the surface sediments on the seafloor at PDS. However, these data must be qualified based on the lack of definitive trends (Table 3-7); the presence of shelf taxa in the Portland Harbor samples suggests a mechanism of exchange exists between the shelf waters and the harbor. Additionally, the pre-disposal sediment grabs collected at the PDA buoy location within PDS indicated the presence of estuarine taxa (three salt marsh taxa and two mudflat taxa at PDS-Buoy2; Table 3-7), likely due to past dredged material disposal activities. The disposal site sample PDS-3G exhibited the most distinctive shelf characteristics when compared to the Portland Harbor samples, with evidence of only one individual of one salt marsh taxon, and no mudflat taxa represented (Table 3-7).

The pre-disposal sediment sample from the Sediment Trap 3 deployment location (PDS-3G) was dominated by shelf agglutinated foraminifera with a minor presence (1 individual) of a single salt marsh species (Figure 3-6; Table 3-7). Although the sediment trap data were generally sparse, the sediment tracer analyses were able to show a similarity between the harbor sediments and a portion of the material retained within Sediment Traps 3 and 8 located in close proximity to the PDS boundary. Samples PDS-ST3 and PDS-ST8 were both dominated by the shelf species that were present in abundance on the ambient seafloor, but also displayed the presence of estuarine species of foraminifera (Figure 3-6). The data from Sediment Trap 3 indicated the majority of the inland species (mudflat calcareous and salt marsh agglutinated foraminifera, as well as freshwater thecamoebians) were detected in the top half of the sediment sample (representing the most recent deposit)

while the continental shelf species dominated the bottom half of the captured sediment sample. These findings suggest that some of the material in these traps may likely have originated from transport of sediment plumes associated with the Portland Harbor dredging project, while the remainder may be the product of local resuspension and settlement.

It is possible that ambient sediment resuspension and settlement in the bottom portion of the trap deposit was partially due to the March 1999 storm event (Figures 3-18 and 3-19). The top interval in the trap (2.5 cm in thickness) contained a number of inland species (salt marsh and freshwater), which are indicative of an estuarine origin and likely the result of settlement of material from the dredged material disposal plume (Figure 3-6). In addition, a substantial number of calcareous foraminifera associated with mudflats were noted throughout the material collected at PDS-ST3 (Figure 3-6). Given the abundance of mudflat calcareous species in the Portland Harbor sediment samples and general lack of these species in pre-disposal sediment samples (PDS-3G), their occurrence within the sediment trap samples suggests the likely presence of estuarine sediments (dredged material) which would have been transported via the sediment plume during disposal operations.

Based on the microfossil content, the sediments analyzed from sample PDS-ST8 also appeared to be a mix of ambient material and plume sediments. However, the overall lack of material retained within Sediment Trap 8 prevented the examination of individual strata to find temporal trends in the data. Shelf species (calcareous and agglutinated) dominated the sediment sample, but the minor presence of salt marsh and mudflat foraminifera served as indication of estuarine sediments, or dredged material within the sample.

The limited information obtained by the sediment traps suggests that some portion of the PDS-ST3 and PDS-ST8 samples may have originated from the sediment plume associated with dredged material disposal operations at PDS. If so, it is likely that material is interspersed with material resulting from resuspension and settlement of surface sediments in the vicinity. Because the sediment traps were carefully lowered to the seafloor during deployment, resuspension caused by the initial placement of these devices was considered unlikely.

Conversely, Sediment Trap 10, located at SEREF, was deployed in an area of seafloor displaying relatively low relief and water depths approximately 30 m deeper than those at the deployment locations for Sediment Traps 3 and 8 (95 m; Figure 2-7). The sediments at the SEREF deployment site prior to the disposal of dredged material at PDS were described as silty clay, suggestive of a consistently depositional environment (Table 3-4). Approximately 2 cm of fine-grained material was detected in sediment trap 10 after a 32-day deployment. Based on the small amount of sediment captured, the predominance of benthic shelf species in the sample, the location of Sediment Trap 10 (approximately 3.8 km southeast of the disposal site), and water depth, it seemed more likely that the material within this trap originated from resuspension of nearby ambient sediments as opposed to settlement of plume

material. The individual mudflat calcareous foraminifera detected in sample PDS-ST10 was identified as *A. becarii*, a species that was not detected in any of the Portland Harbor sediment samples analyzed for microfossil content and likely originating from another estuary in the Casco Bay region.

It should be emphasized that these trends represent relatively weak determinants in terms of confirmation of the source of the material in the sediment traps. The trap material yielded comparable numbers of microfossils (e.g., between 1 and 3 individuals observed from two salt marsh taxa, and between 1 and 16 individuals observed from three mudflat taxa, Table 3-7) to the pre-disposal grab samples from the disposal site. However, trap material yielded fewer salt marsh taxa (two taxa), but more mudflat taxa (three taxa) than the Portland Harbor samples (seven and two taxa represented, respectively). The trap material also included greater numbers of individuals, and greater numbers of taxa, for shelf species, than the pre-disposal grab samples (Table 3-7). This suggests that the data used to make comparisons between sources/sites are too limited to provide conclusive results, and/or possibly that the transport of shelf species to the traps may have occurred from over a fairly broad area (i.e., including more species than were sampled in the direct vicinity of the traps). The variability in the data (e.g., fairly wide range of numbers of individuals from one site or trap to another), likely reflects natural variability in the occurrence of the microfossils from one station to another. Such variability would require a more rigorous approach to sampling (e.g., more sampling stations and/or replicates) to determine if more conclusive findings were feasible.

Additionally, recovery of valid samples from the sediment traps was limited, given that deployment of ten traps yielded only three traps deemed suitable for inclusion in the analysis of results. This limitation would preclude more meaningful comparisons even with more comprehensive characterizations of the possible source material (i.e., dredged material samples and PDS samples). Loss of traps and interference with proper functioning of the traps due to fishing activities and other possible trap disturbances would have to be considered in developing a sampling strategy.

4.2 STFATE Results vs. Sediment Trap Results

The first-order STFATE model was run in the fall of 1998 and the results used to generate the proposed locations for the sediment traps deployed during the third phase of the 1998-1999 dredging project. The second-order STFATE model was run after the completion of the dredging project and was based on the updated input parameters developed from the extensive measurement data acquired in the area before and during the 1998-1999 dredging project. Although some of the model parameters during this second run were still based on general information, many of the critical parameters were developed based on the detailed project sediment data acquired in Portland Harbor and the water column data acquired in and around the PDS.

The two most significant input parameters modified during the second-order model run were the sediment composition data and the ambient current data. Based on the detailed analyses of the Portland Harbor sediment cores, the description of sediment characteristics for the project dredged material was changed from a first-order composition of 4% sand, 48% silt, and 48% clay to a second-order composition of 7.4% sand, 34.4% silt, and 58.2% clay. In addition, based on the ADCP current meter data acquired during the third phase of the dredging project, the average currents used for the model were changed from the first-order values to examine the formation and transport of sediment plumes under a variety of scenarios. In addition, the ambient or background suspended sediment level was changed from a threshold of 1.5 $mg \cdot l^{-1}$ for the first-order run to 2.0 $mg \cdot l^{-1}$ for the second-order run. Because of these modifications to the input parameters, the model results for the first and second-order STFATE runs were somewhat different and difficult to directly compare. However, the main effect was an alteration in the primary plume migration direction based mostly upon the differences in the current data provided by USGS (first-order) versus the data obtained for ADCP measurements in close proximity to PDS (second-order).

As discussed above, based on the analysis of the limited data available, it did appear that some of the material found in Sediment Traps 3 and 8 originated from the recently placed Portland Harbor dredged material. Sediment Trap 3 had the largest accumulation of material, and was located directly south of the PDA 98 buoy along the southern edge of the PDS boundary. Although the STFATE model runs utilizing average flood and ebb currents indicated the sediment plumes were not transported over the positions of either sediment trap, the modeling results employing average current and wave direction data showed the sediment plume migrating in a southwesterly direction away from the PDA buoy (Figure 4-4). This modeled migration path would bring the sediment plume in close proximity to Sediment Trap 3, reinforcing the conclusion that some of the material in that trap originated from recently deposited Portland Harbor dredged material.

Additional evidence may be derived from the total thickness of the sediment deposit captured by Sediment Trap 3, which was approximately three times that of Sediment Trap 8 [5.8 cm (PDS-ST3) versus 1.9 cm (PDS-ST8)]. These data suggest that Sediment Trap 3 appears to have been subjected to a higher degree of sedimentation that may include a greater influence from the dredged material plume relative to Sediment Trap 8. If it is assumed that the natural resuspension and settling of particles is comparable at the trap sites, the effect of sediment plumes from dredged material disposal could lead to increased sediment accumulation in traps closer to the disposal operations. While not conclusive, the sparse sediment trap data supported the STFATE results of expected plume migration patterns associated with the placement of single barge-loads of dredged material at the PDA 98 buoy locations when subjected to “average” hydrodynamic forces.

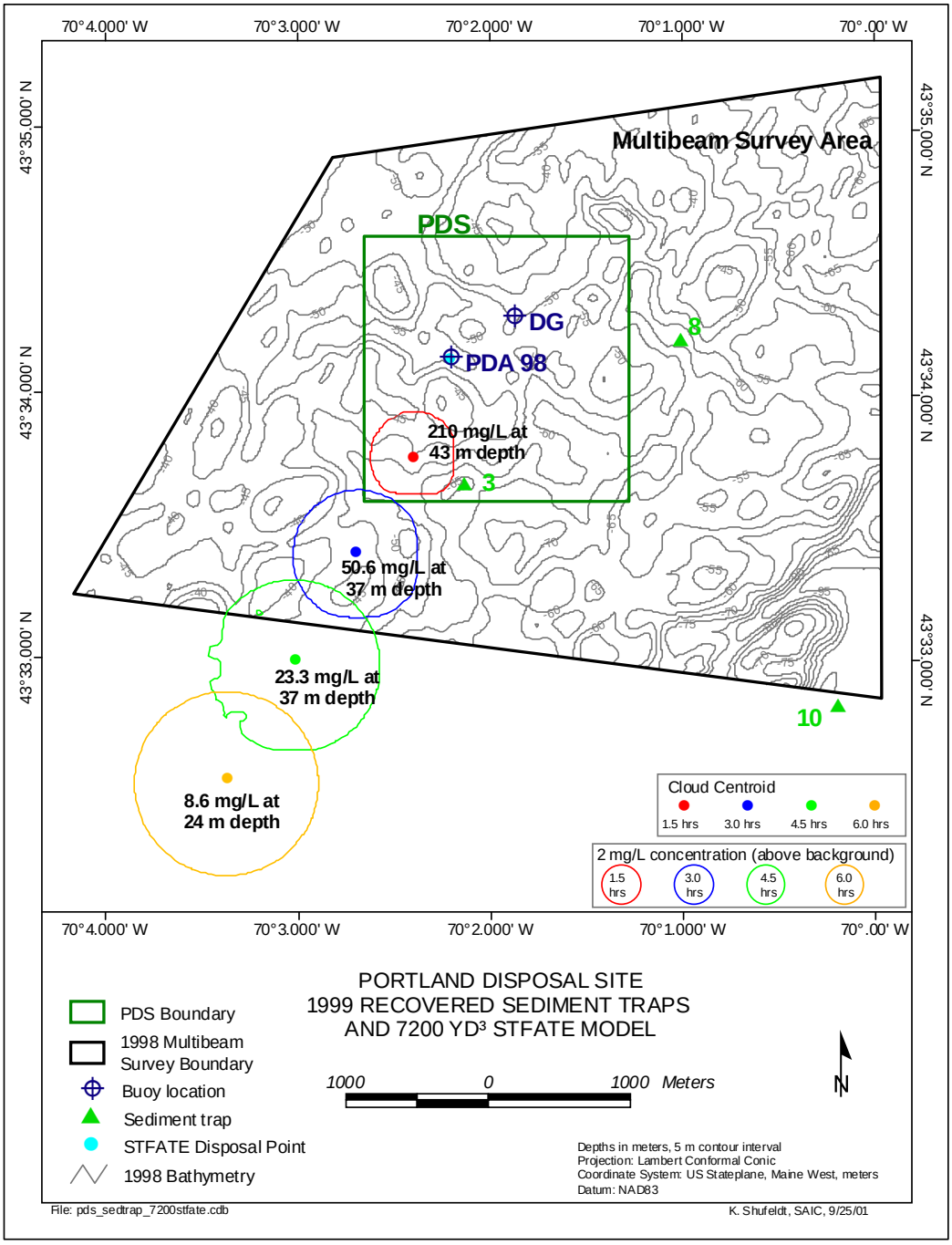

Figure 4-4. Recovery locations of the Portland Disposal Site sediment traps that were found with material present, as well as the representative results from the STFATE model run

The hydrodynamic forces are the most influential parameters in determining the model plume migration pattern using STFATE, and using averaged values can be misleading when evaluating the projected plume path for a single disposal event. Because the model assumes that the plume will be influenced by these average hydrodynamic forces throughout the disposal event, it shows the plume migrating in a consistent manner and direction throughout the event. Obviously, the reality can be quite different, and the plume associated with each disposal event will tend to migrate in response to the variable hydrodynamic forces that occur through the period of that event (i.e., changes in tidal flow).

As discussed in Section 4.1.2 above, although Sediment Trap 3 was the only trap that had sufficient material for full geotechnical analysis, Sediment Trap 8 was recovered with smaller amounts of similar material (both in terms of grain size and microfossil content). As shown in Figure 4-4, Sediment Trap 8 was located well to the east of the PDS eastern boundary, at a considerable distance from the projected plume pattern suggested by the STFATE results. The possible presence of small amounts of Portland Harbor dredged material in this trap would suggest that the actual plume pattern varied throughout the disposal operations, which would have occurred largely in response to the local hydrodynamic forces. For instance, a disposal event occurring on an ebb tide would move a sediment plume in a southeasterly direction from the PDA 98 buoy. Depending on the timing of the disposal event relative to the transition from ebb to flood tide, a rotation to the north and northwest would have the potential to redirect the plume such that its outer margins could drift over the Sediment Trap 8 location. Settlement of plume material, albeit on a relatively small scale, could then have occurred within Sediment Trap 8.

4.3 MDFATE Results vs. Multibeam Depth-Difference Results

Over the two year period between the 1998 and 2000 multibeam surveys, approximately 314,600 m^3 of material was deposited around the PDA 98 buoy, and 174,100 m^3 of material was deposited near the DG buoy. Figure 4-5 presents a view of both the multibeam depth difference results and the MDFATE model results along with the actual recorded disposal locations. The depth difference results between the two multibeam surveys clearly showed the accumulation of anywhere from 0.25 to 2 m of dredged material in close proximity to the PDA 98 buoy and the DG buoy, as well as many of the surrounding areas. The disposal mound morphology depicted by the MDFATE model in the vicinity of both the PDA 98 and DG buoys appears very closely correlated with the positions of the disposal events. In general, the MDFATE results show the largest accumulations of material in close alignment with the highest concentration of disposal events.

The MDFATE model results predicted significantly higher mound heights than actually detected in the depth difference calculations. Specifically, the model results indicate mound heights approaching 8 m in some areas, while the depth difference results showed mound heights of generally less than 2 m, even in the highest spots. The primary reason for

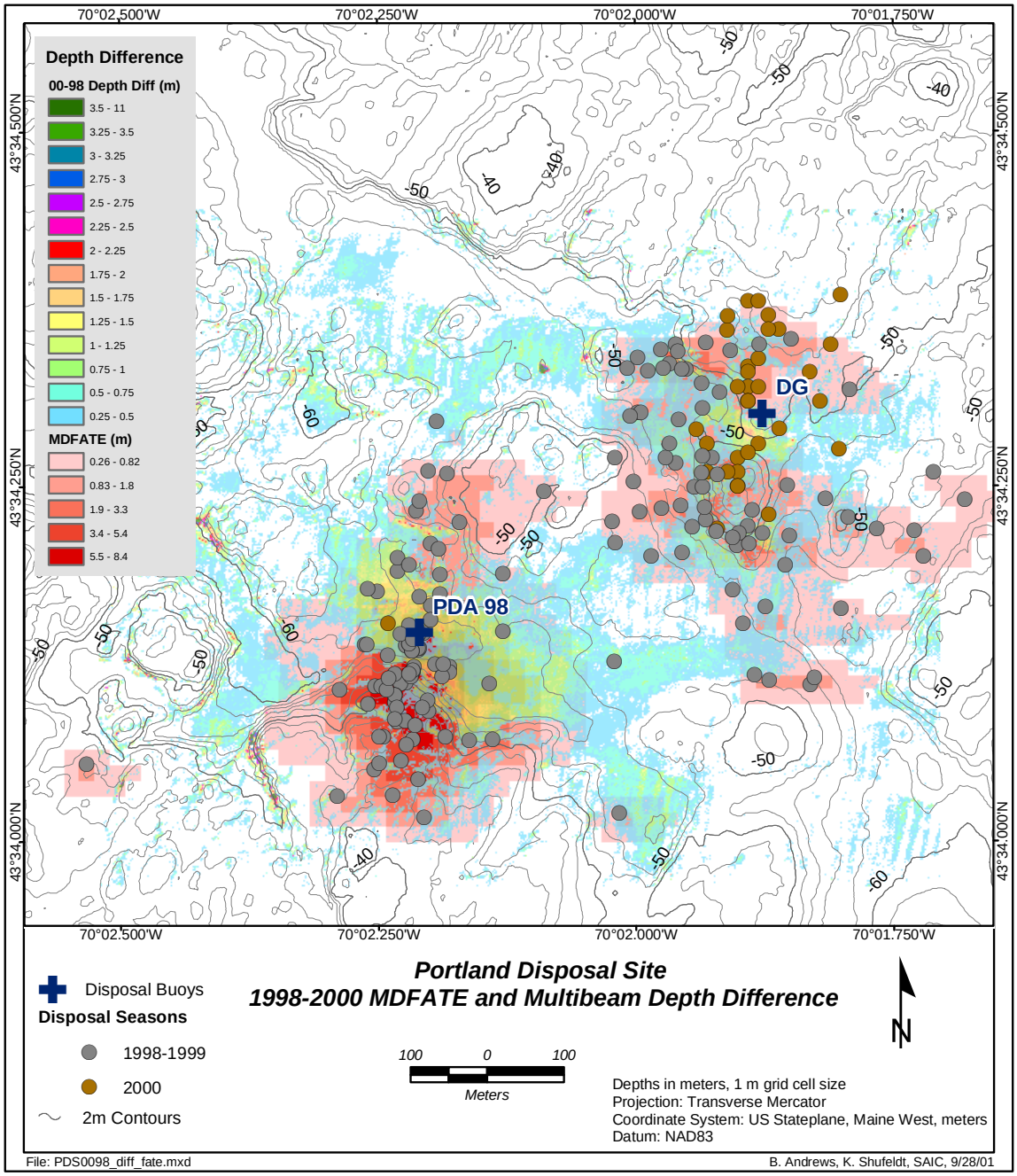

Figure 4-5. Multibeam depth difference results depicting the observed dredged material deposit compared with the MDFATE model results depicting the predicted dredged material deposit. Reported disposal points for the time period are also shown

this difference is that the sediment properties used for the modeling were also used for computing the mound heights immediately after the disposal events. There is a considerable amount of settling and consolidation that occurs shortly after placement that is not accounted for in the model results. In addition, because the final multibeam survey was conducted more than a year after most of the placement events, considerably more consolidation had occurred over the actual placement mounds than MDFATE originally predicted. Furthermore, it is theorized that MDFATE results would predict a higher mound based on the assumption of a solid seafloor. However, this practice would tend to ignore the hidden capacity of the many crevices features in the bedrock outcrops adjacent to the disposal location. In reality, the deposited material would tend to fill these crevice features first and remain at levels below the seafloor as it was detected in the 1998 baseline multibeam survey and therefore undetectable in the depth difference comparisons. As a result, the model adds the volume of sediment trapped in these crevices to the cumulative mound height, creating a positive bias in the relief of the disposal mound.

Other than the large differences in mound height, the most significant difference indicated between the multibeam depth difference results and the MDFATE model results occurred over the shallower, exposed bedrock areas of the seafloor just to the south of both the PDA 98 and DG buoys. In these areas (particularly to the south of the PDA 98 buoy), there was a large concentration of placement events (Figure 4-5), and the MDFATE model results showed these areas as having the largest accumulations of material. However, the depth difference results indicated very little accumulation of material in these same areas. Because the final multibeam survey was conducted more than a year after most of the material had been placed at the site, the depth difference results tended to reflect some longer-term trends in the depositional patterns.

In general, most of the dredged material appeared to have settled within the deeper, depositional pockets, while the higher and more exposed bedrock surfaces showed little accumulation, even though numerous placement events had occurred directly over these areas (e.g., south of the PDA 98 buoy and north and southeast of the DG buoy; Figure 3-15). The bedrock outcrops surrounding the disposal point offer a multitude of small voids and crevices per square meter that permit soft sediments to accumulate through either direct deposition or advection. These pockets of material could contain substantial volumes of deposited sediment that were essentially hidden from acoustic sensors due to resolution of the bathymetric data set and averaging that occurs in the gridding process.

As discussed in Section 4.1.1 above, the REMOTS® data indicated the presence of thin layers of dredged material over most of the exposed bedrock. However, in the time between the completion of disposal operations and the final multibeam survey it is likely, based on hydrodynamic conditions at PDS, that a large percentage of the material that had settled over these exposed bedrock areas would be advected into nearby depositional areas. This would be consistent with past physical oceanographic studies performed over PDS that

suggested that fine-grained material is focused or advected from the surface of the rock outcrop areas into nearby protected, depositional areas by the passage of large surface waves (McDowell and Pace 1998). Significant wave heights of 2 to 3 m or more are usually associated with well-organized ocean storms producing strong wind and/or waves from the easterly or southerly direction. Meteorological and oceanographic records indicated these types of weather events occur relatively frequently, at an average of nine to ten times per year, in the PDS region (McDowell and Pace 1998).

5.0 CONCLUSIONS

The survey data acquisition and analysis conducted at the Portland Disposal Site (PDS) before, during, and after the 1998-1999 Portland Harbor dredging project provided an opportunity to monitor the effects of this project on the PDS seafloor. In addition, several of these PDS data sets were used to generate input parameters needed to run both the STFATE and MDFATE dredged material models, and other PDS data sets were used to evaluate the results of these model runs.

High-resolution, full-bottom coverage multibeam and side-scan sonar surveys conducted before the 1998-1999 Portland Harbor dredging project provided better insight than previous single-beam surveys into the complexity of the PDS seafloor, which is characterized by numerous steep, bedrock ridges and a prominent northwest-southeast trending trough. These data also highlighted numerous natural basin features that could potentially serve as containment cells for future dredging projects. The multibeam data were used to provide the background bathymetry for both the MDFATE and STFATE model runs.

More than a year after the completion of the 1998-1999 dredging project, a second high-resolution multibeam survey and a REMOTS® sediment-profile imaging survey were conducted over the PDS. Based on the combined REMOTS® and multibeam depth difference results, it appeared that most of the deposited dredged material had settled in the deeper depositional areas, though a relatively thin (< 0.25 m) surface layer of recent dredged material existed over the surrounding bedrock areas. The multitude of crevices, voids, and faults per square meter along the surface of the bedrock outcrops likely facilitated the accumulation of a substantial volume of dredged material that was not detectable via acoustic sensors and depth difference comparisons. Material could have filled such voids and crevices through direct deposition or advection following settlement on the more exposed bedrock outcrops.

Prior to the Portland Harbor dredging project, sediment sampling and subsequent analysis were conducted on both Portland Harbor and the PDS sediments. This analysis produced the Portland Harbor sediment characterization data needed for input to the STFATE and MDFATE models, and also provided sediment tracer data it was hoped would aid in differentiating between the Portland Harbor sediments and those that existed within the PDS prior to the disposal operations. These results showed that the Portland Harbor sediments were comprised of mostly clay and silt (92%) and primarily salt marsh and shallow water foraminifera, while the PDS sediments were comprised of mostly fine sand (71%) with a mix of shallow water (presumably from previous disposal operations) and shelf foraminifera.

During Phase 3 of the Portland Harbor dredging project, sediment traps were deployed around the perimeter of the PDS, in an attempt to capture sediment settling through

the water column as part of disposal plumes. Only three of the ten traps were recovered with any analyzable material present, with their proper functioning and retrieval apparently hindered by fishing activity in the area. This type of interference dramatically impacted the sediment trap results (i.e., not many usable trap samples retrieved) and should be considered in future study designs. Limited conclusions could be drawn from the three usable trap samples retrieved. Based on the qualitative evaluation of the volume of material in the traps, their location with respect to disposal operations and hydrodynamics, and the presence of marsh and shallow water foraminifera in traps, it is considered likely that at least some of the material in the two traps nearest to PDS originated from transport of sediment plumes associated with the Portland Harbor dredged material disposal. Additionally, the presence of shelf foraminifera, and the occurrence of a storm event shortly after trap deployment provided an indication that some of the material in the traps likely originated from resuspension of PDS-substrate sediments (i.e., present on the substrate in the vicinity due to historic disposal).

The sediment trap placed to the south of PDS captured substantially more material (predominantly clay) than those placed to the east and southeast of the disposal point, which tended to support the modeling results. The trap material was analyzed for microfossils in two layers (0 – 2.5 cm and 2.5 – 5 cm) which provided some evidence for a stronger influence from local sediments in the lower portion of the material, and stronger evidence for Portland Harbor dredged material in the upper portion of the material. The lower material could be representative of fairly substantial resuspension occurring during the March 1999 storm event. The more recent sediment deposit within the sediment trap sample contained shallow water foraminifera and freshwater thecamoebians, indicative of an estuarine/inland source, which likely indicated contributions to the trap from the Portland Harbor disposal activities.

In general, the sparse data, variability among samples from similar locations, and occurrence of both estuarine and shelf taxa in all study locations prior to any dredging and disposal activities, render the sediment tracer data useful only as supporting evidence for determining the source material in the sediment traps. The tracer data provide evidence in support of the presence of likely disposal plume material in traps in close proximity to the disposal site; the likelihood of such plume settlement occurring in those traps was supported by the regional hydrodynamics regime, as summarized below.

During Phase 3 of the Portland Harbor dredging project, an ADCP was deployed within the PDS to acquire the data necessary to compute input for both the STFATE and MDFATE models. Water column currents displayed a strong northwest-southeast trend related to tidal oscillations within Casco Bay. A distinct south and west bias in flow was discernable in the high frequency current data, which was likely the result of the cyclonic (counter clockwise) gyre that drives circulation patterns within the Gulf of Maine.

Given that tidal currents are the most likely mechanism to transport sediments entrained in the water column for relatively short periods of time, a series of STFATE runs were performed using typical flood and ebb tides to drive the model. The results indicated a sediment plume created by a disposal event during a flood tide would migrate northwest with the water mass. However, seafloor topography would impede the progress of the lower portions of the plume resulting in increased deposition and rapid reductions in turbidity prior to leaving the PDS boundary. The sediment plume formed during an ebb tide would be transported to the southeast with interaction with various bottom features limiting the size of the plume and sediment concentrations near the substrate. At six hours post-disposal, the results from both runs indicated turbidity within the plume would approach background levels (2 $mg \cdot l^{-1}$) with maximum concentrations of 6 to 6.5 $mg \cdot l^{-1}$, or 1.2% of the estimated turbidity for the original disposal plume.

Average currents were also utilized as part of the STFATE modeling exercise to evaluate the transport and dissipation of a sediment plume that would span a transition between flood and ebb tide. Average speed and direction data were used to drive the model for a six-hour duration to represent a worst-case scenario with regards to velocity and distance transported outside the PDS boundaries. The modeled release of various disposal volumes showed similar results with the sediment plume migrating in a southwest direction away from the PDA 98 buoy. The centroid of the plume was confined to the upper portion of the water column for each model run, presumably due to the effects of a ridge evident in the bathymetric data immediately south of the disposal point that would serve to contain the plume and limit transport of material. The areal extent of the plume for each model run increased as time progressed with a corresponding decrease in the maximum turbidity at the centroid attributable to settlement and dilution. At six hours post-disposal, the results from each run indicated turbidity within the plume would approach background levels (2 $mg \cdot l^{-1}$) with maximum concentrations ranging from 7.4 to 8.6 $mg \cdot l^{-1}$, or 3 to 4% of the estimated turbidity for the original disposal plume.

The modeled plume migration path was consistent with the sediment trap results that indicated the presence of recent Portland Harbor dredged material along the southern PDS boundary. The results depicted the expected plume migration pattern associated with the placement of a barge-load of “average” Portland Harbor dredged material subjected to “average” PDS hydrodynamic forces. However, the actual transport and dissipation of a sediment plume is both variable and dependent upon a multitude of oceanographic and meteorological factors that influence hydrodynamic forcing.

The relatively sparse sediment trap results show the cumulative effects from all of the disposal events that occurred within the PDS while the traps were deployed, while the STFATE results show the expected plume associated with a single, representative disposal event at the PDA 98 buoy position. To more effectively evaluate water column effects associated with the placement of material in the PDS, a more comprehensive water quality

monitoring or plume tracking effort, involving water column sampling and turbidity monitoring, would have to be conducted in the immediate vicinity of the placement operations.

The MDFATE modeling results provided a prediction of disposal mound morphology based upon the position and volume information obtained for each of the 197 individual disposal events associated with all of the PDS placement activity between the 1998 and 2000 multibeam surveys. The disposal mound morphology depicted by the MDFATE model was very closely correlated with the positions of the disposal events. The MDFATE results showed the largest accumulations of material over the shallower bedrock outcrop south of the PDA 98 buoy, where the highest numbers of large scow releases were recorded. In contrast, the depth difference results showed little or no accumulation over these exposed bedrock areas. In the time between the completion of disposal operations and the final multibeam survey it is likely that a large percentage of the material that had settled over these exposed bedrock areas had accumulated in the fault and crevice features and therefore was hidden from detection by acoustic sensors, or advected into deeper, depositional areas adjacent to the placement site.

6.0 REFERENCES

Belknap, D.F., R.C. Shipp, R. Stuckenrat, J.T. Kelley, and H.W. Borns, Jr. 1989. Holocene sea-level change in coastal Maine. IN: Walter A. Anderson and Harold W. Borns, Jr. (Eds.), Neotectonics of Maine, Studies in Seismicity, Crustal Warping, and Sea-Level Change. Maine Geological Survey, Dept. of Conservation, Augusta, ME.

Bigelow, H.B. 1927. Physical Oceanography of the Gulf of Maine. U.S. Dept. of Comm. Bur. Fish. 40:511-1027

Caldwell, D.W. 1998, Roadside Geology of Maine. Mountain Press Publishing Company. Missoula, Montana.

Clausner, J., J. Gailani, S. Bratos, B. Johnson, P. Schroeder, and A. Teeter. 2001. Status of Corps Dredged Material Fate Models. Proceedings of the Western Dredging Association Twenty-first Technical Conference, June 24-27, 2001, Houston, TX, pp. 55-70.

EPA. 1996. Management plan for the Portland Dredged Material Disposal Site. US Environmental Protection Agency, Region I, Boston, MA.

Morris, J.T. 1996. DAMOS Site Management Plans. SAIC Report No. 365. Final report submitted to the U.S. Army Corps of Engineers, New England Division, Waltham, MA.

Morris, J.T.; Saffert, H.S.; Murray P.M. 1998. The Portland Disposal Site capping demonstration project 1995-1997. DAMOS Contribution No. 123. U.S. Army Corps of Engineers, New England District, Concord, MA.

Murray, J.W. 1991. Ecology and Paleoecology of Benthic Foraminifera: Longman Scientific and Technical Publishers, 451 p. Harlow, Essex, UK

McDowell, S.C.; Pace S.D. 1998. Oceanographic measurements at the Portland Disposal Site during the spring of 1996. DAMOS Contribution No. 121. U.S. Army Corps of Engineers, New England Division, Concord, MA.

Rhoads, D. C.; Germano, J. D. 1982. Characterization of organism-sediment relation using sediment-profile imaging: An effective method of Remote Ecological Monitoring of the Seafloor (REMOTS® System). Mar. Ecol. Prog. Ser. 8:115-128.

Rhoads, D. C.; Germano, J. D. 1986. Interpreting long-term changes in benthic community structure: A new protocol. Hydrobiologia 142:291-308.

Wentworth, C.K. 1922. A scale of grade and class terms for clastic sediments. Journal of Geology 30: 377-92.

Wiley, M.B. 1996. Monitoring cruise at the Portland Disposal Site, July 1992. DAMOS Contribution Number 108. U.S. Army Corps of Engineers, New England Division, Waltham, MA.

Appendix A
Disposal Logs

Appendix A1, Disposal Logs

1998 **PDS**
Project: PORTLAND HARBOR MAINE
Permit Number: 1998C0018 **Permittee:** COE-PORTLAND HARBOR

Buoy	Departure	Disposal	Return	Latitude	Longitude	Buoy's Vector	Volume (CY)
PDA98	11/17/1998	11/17/1998	11/17/1998	43.5687	-70.03645	100' SW	6133
PDA98	11/17/1998	11/17/1998	11/17/1998	43.570983333	-70.03636666	100' W	6000
PDA98	11/18/1998	11/18/1998	11/18/1998	43.569116666	-70.03675	100' E	6000
PDA98	11/18/1998	11/18/1998	11/18/1998	43.5696	-70.0375	100' E	6000
PDA98	11/19/1998	11/19/1998	11/19/1998	43.570416666	-70.03616666	65' W	5600
PDA98	11/19/1998	11/19/1998	11/19/1998	43.568283333	-70.03765	100' W	6500
PDA98	11/19/1998	11/19/1998	11/19/1998	43.568533333	-70.03703333	80' W	6000
PDA98	11/19/1998	11/19/1998	11/19/1998	43.568066666	-70.03718333	100' E	6000
PDA98	11/20/1998	11/20/1998	11/20/1998	43.568716666	-70.03633333	100' W	6500
PDA98	11/20/1998	11/20/1998	11/20/1998	43.567583333	-70.0422	50' W	6000
PDA98	11/21/1998	11/21/1998	11/21/1998	43.58125	-70.03686666	75' W	5800
PDA98	11/21/1998	11/21/1998	11/21/1998	43.569566666	-70.03648333	60' E	6000
PDA98	11/22/1998	11/22/1998	11/22/1998	43.567516666	-70.03755	80' E	5800
PDA98	11/22/1998	11/22/1998	11/22/1998	43.569433333	-70.03663333	40' E	6100
PDA98	11/22/1998	11/22/1998	11/22/1998	43.57055	-70.03686666	60' W	5800
PDA98	11/23/1998	11/23/1998	11/23/1998	43.581266666	-70.03685	85' W	5600
PDA98	11/23/1998	11/23/1998	11/23/1998	43.56885	-70.03733333	85' W	6100
PDA98	11/25/1998	11/25/1998	11/25/1998	43.5679	-70.0374	90' W	6000
PDA98	11/25/1998	11/25/1998	11/25/1998	43.568516666	-70.03711666	90' W	5600
PDA98	11/25/1998	11/25/1998	11/25/1998	43.56875	-70.03656666	90' W	6000
PDA98	11/26/1998	11/26/1998	11/26/1998	43.568983333	-70.0377	100' W	5900
PDA98	11/27/1998	11/27/1998	11/27/1998	43.568983333	-70.03766666	90' W	6100
PDA98	11/28/1998	11/28/1998	11/28/1998	43.56695	-70.03675	90' W	6100
PDA98	11/28/1998	11/28/1998	11/28/1998	43.568483333	-70.03753333	50' W	6000
PDA98	11/29/1998	11/29/1998	11/29/1998	43.568383333	-70.03721666	60' W	6000
PDA98	11/29/1998	11/29/1998	11/29/1998	43.5683	-70.03721666	60' W	6200
PDA98	11/30/1998	11/30/1998	11/30/1998	43.568083333	-70.03705	60' W	6100
PDA98	11/30/1998	11/30/1998	11/30/1998	43.568383333	-70.03721666	70' W	6500
DG	12/2/1998	12/2/1998	12/2/1998	43.567866666	-70.03563333	100' W	6000
PDA98	12/2/1998	12/2/1998	12/2/1998	43.568916666	-70.03683333	50' W	6300
DG	12/3/1998	12/3/1998	12/3/1998	43.568516666	-70.03568333	100' W	6000
PDA98	12/3/1998	12/3/1998	12/3/1998	43.568233333	-70.03718333	90' W	6000
PDA98	12/3/1998	12/3/1998		43.569116666	-70.03691666		6000
PDA98	12/4/1998	12/4/1998	12/4/1998	43.567616666	-70.03711666	80' W	6000
PDA98	12/4/1998	12/4/1998	12/4/1998	43.5679	-70.03746666	80' W	6000
PDA98	12/5/1998	12/5/1998	12/5/1998	43.56785	-70.03601666	80' W	6000
PDA98	12/5/1998	12/5/1998	12/6/1998	43.568483333	-70.03743333	70' W	6000
PDA98	12/6/1998	12/6/1998	12/6/1998	43.568966666	-70.03703333	80' W	6000
PDA98	12/6/1998	12/6/1998	12/6/1998	43.56865	-70.03633333	60' W	6000
PDA98	12/6/1998	12/6/1998	12/6/1998	43.569066666	-70.03685	60' W	6000
PDA98	12/7/1998	12/7/1998	12/7/1998	43.56845	-70.0381	60' W	5500
PDA98	12/7/1998	12/7/1998	12/7/1998	43.569266666	-70.03663333	50' W	5500

Project: PORTLAND HARBOR MAINE

Permit Number: 1998C0018 **Permittee:** COE-PORTLAND HARBOR

Buoy	Departure	Disposal	Return	Latitude	Longitude	Buoy's Vector	Volume (CY)
DG	12/7/1998	12/7/1998	12/7/1998	43.567	-70.03358333	80' W	6000
PDA98	12/8/1998	12/8/1998	12/8/1998	43.5682	-70.03666666	100' W	6000
PDA98	12/8/1998	12/8/1998	12/8/1998	43.5679	-70.0364	90' W	5500
PDA98	12/8/1998	12/8/1998	12/8/1998	43.567866666	-70.03691666	100' W	5500
PDA98	12/9/1998	12/9/1998	12/9/1998	43.568316666	-70.03668333	75' W	5800
DG	12/9/1998	12/9/1998	12/9/1998	43.568783333	-70.03366666	100' W	5800
PDA98	12/9/1998	12/9/1998	12/10/1998	43.5672	-70.03815	60' W	5500
PDA98	12/10/1998	12/10/1998	12/10/1998	43.5678	-70.03703333	100' W	5900
PDA98	12/10/1998	12/10/1998	12/10/1998	43.568233333	-70.03676666	100' W	6250
PDA98	12/11/1998	12/11/1998	12/11/1998	43.568033333	-70.03688333	80' W	5800
PDA98	12/11/1998	12/11/1998	12/11/1998	43.56845	-70.03735	80' W	6300
PDA98	12/12/1998	12/12/1998	12/12/1998	43.56865	-70.03691666	80' W	6000
PDA98	12/12/1998	12/12/1998	12/12/1998	43.567216666	-70.03725	100' W	6200
PDA98	12/13/1998	12/13/1998	12/13/1998	43.568716666	-70.0369	100' W	5500
PDA98	12/13/1998	12/13/1998	12/13/1998	43.568666666	-70.03691666	40' W	6100
PDA98	12/14/1998	12/14/1998	12/14/1998	43.5686	-70.03695	60' W	5600
PDA98	12/14/1998	12/14/1998	12/14/1998	43.569633333	-70.03765	80' W	6100
PDA98	12/15/1998	12/15/1998	12/15/1998	43.568683333	-70.03691666	80' W	6000
PDA98	12/15/1998	12/15/1998	12/15/1998	43.5674	-70.03683333	100' W	6100
PDA98	12/15/1998	12/15/1998	12/15/1998	43.567583333	-70.03746666	100' W	5800
PDA98	12/16/1998	12/16/1998	12/16/1998	43.5681	-70.03721666	100' W	6200
PDA98	12/16/1998	12/16/1998	12/16/1998	43.568633333	-70.03721666	80' W	5600
					Project Total Volume:	**291,529 CM**	**381,283 CY**
					Report Total Volume:	**291,529 CM**	**381,283 CY**

Appendix A2, Disposal Logs

1999 **PDS**

Project: LONG WHARF, FORE RIVER
Permit Number: 199402879 **Permittee:** SOUTHPORT MARINE

Buoy	Departure	Disposal	Return	Latitude	Longitude	Buoy's	Vector	Volume (CY)
DG	2/19/1999	2/19/1999	2/19/1999	43.570166666	-70.03365	60'	W	125
					Project Total Volume:	**96**	**CM**	**125 CY**

Project: LONG WHARF, FORE RIVER
Permit Number: 199702334 **Permittee:** STEVEN DIMILLO

Buoy	Departure	Disposal	Return	Latitude	Longitude	Buoy's	Vector	Volume (CY)
PDA98	1/20/1999	1/20/1999	1/20/1999	43.569116666	-70.03681666	60'	W	725
DG	1/25/1999	1/25/1999	1/25/1999	43.572216666	-70.03345	60'	E	700
PDA98	2/2/1999	2/2/1999	2/2/1999	43.5716	-70.03653333	60'	W	750
DG	2/19/1999	2/19/1999	2/19/1999	43.571166666	-70.03365	60'	W	375
					Project Total Volume:	**1,950**	**CM**	**2,550 CY**

Project: FORE RIVER
Permit Number: 199800133 **Permittee:** SPRAGUE ENERGY

Buoy	Departure	Disposal	Return	Latitude	Longitude	Buoy's	Vector	Volume (CY)
PDA98	3/2/1999	3/2/1999	3/2/1999	43.568983333	-70.03698333	75'	N	1100
PDA98	3/3/1999	3/3/1999	3/3/1999	43.5692	-70.03698333	100'	W	1305
PDA98	3/5/1999	3/5/1999	3/5/1999	43.568933333	-70.03681666	50'	NE	1566
PDA98	3/12/1999	3/12/1999	3/12/1999	43.568933333	-70.03683333	100'	E	1355
PDA98	3/17/1999	3/17/1999	3/17/1999	43.570666666	-70.03681666	100'	SE	1355
PDA98	3/19/1999	3/19/1999	3/19/1999	43.5686	-70.03645	100'	S	1316
PDA98	3/20/1999	3/20/1999	3/20/1999	43.56875	-70.03643333	10'	N	1166
PDA98	4/13/1999	4/13/1999	4/13/1999	43.568583333	-70.03731666	100'	SW	1566
					Project Total Volume:	**8,203**	**CM**	**10,729 CY**

Project: FORE RIVER
Permit Number: 199803142 **Permittee:** MOBIL OIL COMPANY

Buoy	Departure	Disposal	Return	Latitude	Longitude	Buoy's	Vector	Volume (CY)
PDA98	2/24/1999	2/24/1999	2/24/1999	43.5689	-70.03693333	100'	S	1305
PDA98	2/24/1999	2/24/1999	2/25/1999	43.570166666	-70.03663333	50'	N	1050
PDA98	2/27/1999	2/27/1999	2/27/1999	43.5689	-70.03693333	100'	S	1305
PDA98	3/2/1999	3/2/1999	3/2/1999	43.568983333	-70.03698333	75'	N	500
PDA98	3/8/1999	3/8/1999	3/8/1999	43.569833333	-70.03716666	50'	SE	1504
PDA98	3/9/1999	3/9/1999	3/9/1999	43.57	-70.03716666	50'	S	1566
PDA98	3/10/1999	3/10/1999	3/10/1999	43.5691	-70.03711666	50'	W	1566
DG	3/14/1999	3/14/1999	3/14/1999	43.569133333	-70.03546666	100'	E	1566
DG	3/17/1999	3/17/1999	3/17/1999	43.5698	-70.03546666	50'	E	1516
PDA98	3/24/1999	3/24/1999	3/24/1999	43.569533333	-70.03681666	50'	W	1266
PDA98	3/24/1999	3/24/1999	3/24/1999	43.5698	-70.03648333	50'	N	1366
PDA98	3/25/1999	3/25/1999	3/25/1999	43.568633333	-70.03698333	75'	SW	1500
PDA98	3/31/1999	3/31/1999	3/31/1999	43.569033333	-70.03691666	100'	SW	1044
					Project Total Volume:	**13,039**	**CM**	**17,054 CY**

Project: PORTLAND HARBOR MAINE

Permit Number: 1998C0018 **Permittee:** COE-PORTLAND HARBOR

Buoy	Departure	Disposal	Return	Latitude	Longitude	Buoy's Vector		Volume (CY)
DG	3/6/1999	3/6/1999	3/6/1999	43.570533333	-70.03325	60'	W	3200
PDA98	3/6/1999	3/7/1999	3/7/1999	43.5701	-70.0365	80'	E	3600
DG	3/8/1999	3/8/1999	3/8/1999	43.570333333	-70.02941666	100'	W	2800
DG	3/9/1999	3/9/1999	3/9/1999	43.568483333	-70.02431666	100'	E	2500
DG	3/9/1999	3/9/1999	3/10/1999	43.5685	-70.0305	80'	E	1622
DG	3/10/1999	3/10/1999	3/10/1999	43.570666666	-70.028	70	SE	3050
DG	3/10/1999	3/10/1999	3/10/1999	43.57055	-70.03143333	80'	E	1200
DG	3/10/1999	3/10/1999	3/10/1999	43.570816666	-70.03236666	80'	E	1933
DG	3/10/1999	3/10/1999	3/11/1999	43.570466666	-70.02988333	100'	SE	3050
DG	3/11/1999	3/11/1999	3/11/1999	43.570366666	-70.0315	80'	SE	2900
DG	3/11/1999	3/11/1999	3/11/1999	43.5694	-70.03	90'	W	2360
DG	3/12/1999	3/12/1999	3/12/1999	43.57005	-70.03256666	40'	SE	2720
DG	3/12/1999	3/12/1999	3/12/1999	43.570316666	-70.02881666	90'	E	2600
DG	3/12/1999	3/12/1999	3/13/1999	43.570833333	-70.03086666	50'	E	3000
DG	3/13/1999	3/13/1999	3/13/1999	43.571	-70.0285	75'	S	2300
DG	3/13/1999	3/13/1999	3/13/1999	43.568583333	-70.03043333	100'	SE	2700
DG	3/13/1999	3/13/1999	3/13/1999	43.572266666	-70.02626666	75'	E	2250
DG	3/13/1999	3/13/1999	3/13/1999	43.570283333	-70.03126666	90'	SE	2894
DG	3/14/1999	3/14/1999	3/14/1999	43.570133333	-70.03168333	80'	S	2570
DG	3/14/1999	3/14/1999	3/14/1999	43.568616666	-70.0314	100'	SE	2300
DG	3/14/1999	3/14/1999	3/14/1999	43.572433333	-70.0329	80'	SW	2650
DG	3/14/1999	3/14/1999	3/15/1999	43.570566666	-70.0329	80'	SE	2720
DG	3/14/1999	3/15/1999	3/15/1999	43.570683333	-70.03025	70'	SE	2300
DG	3/15/1999	3/15/1999	3/15/1999	43.571466666	-70.01975	90'	W	2450
DG	3/15/1999	3/15/1999	3/15/1999	43.569416666	-70.03121666	100'	SE	2900
DG	3/17/1999	3/17/1999	3/17/1999	43.57025	-70.03083333	100'	S	2670
DG	3/17/1999	3/17/1999	3/17/1999	43.571166666	-70.03208333	50'	E	3400
DG	3/18/1999	3/18/1999	3/18/1999	43.571183333	-70.03223333	100'	SE	3300
DG	3/18/1999	3/18/1999	3/18/1999	43.570816666	-70.03223333	60'	S	2300
DG	3/18/1999	3/18/1999	3/18/1999	43.56855	-70.03116666	75'	SE	3300
DG	3/19/1999	3/19/1999	3/19/1999	43.569616666	-70.03175	100'	S	3000
DG	3/19/1999	3/19/1999	3/19/1999	43.57	-70.02866666	25'	E	2360
DG	3/19/1999	3/19/1999	3/20/1999	43.5702	-70.02491666	75'	SE	3300
DG	3/19/1999	3/20/1999	3/20/1999	43.5711	-70.03266666	70'	SE	2400
DG	3/20/1999	3/20/1999	3/20/1999	43.57035	-70.0324	60'	SE	2360
DG	3/20/1999	3/20/1999	3/20/1999	43.571966666	-70.02985	80'	NE	3200
DG	3/20/1999	3/20/1999	3/20/1999	43.57015	-70.03148333	100'	S	2360
PDA98	3/21/1999	3/21/1999	3/21/1999	43.571016666	-70.03666666	50'	SE	3200
DG	3/21/1999	3/21/1999	3/21/1999	43.5706	-70.03258333	90'	S	2730
DG	3/21/1999	3/21/1999	3/21/1999	43.571516666	-70.0177	50'	SW	3200
DG	3/22/1999	3/23/1999	3/23/1999	43.571933333	-70.03195	50'	NE	2730
PDA98	3/24/1999	3/24/1999	3/24/1999	43.569916666	-70.03698333	75'	NW	2600
PDA98	3/24/1999	3/24/1999	3/24/1999	43.564016666	-70.13106666			2000
DG	3/25/1999	3/25/1999	3/25/1999	43.570766666	-70.0348	100'	SE	3000
DG	3/25/1999	3/25/1999	3/25/1999	43.570433333	-70.03218333	100'	SE	2800

Project: PORTLAND HARBOR MAINE

Permit Number: 1998C0018 **Permittee:** COE-PORTLAND HARBOR

Buoy	Departure	Disposal	Return	Latitude	Longitude	Buoy's Vector	Volume (CY)
DG	3/26/1999	3/26/1999	3/26/1999	43.571166666	-70.03283333	70' SE	2800
DG	3/26/1999	3/26/1999	3/26/1999	43.572416666	-70.03178333	80' NNE	3300
DG	3/27/1999	3/27/1999	3/27/1999	43.57255	-70.0308	80' NE	3200
DG	3/27/1999	3/27/1999	3/28/1999	43.572183333	-70.03311666	80' N	2800
DG	3/28/1999	3/28/1999	3/28/1999	43.570283333	-70.03165	90' E	3800
DG	3/28/1999	3/28/1999	3/28/1999	43.572333333	-70.03328333	85' NW	3500
DG	3/29/1999	3/29/1999	3/29/1999	43.570583333	-70.0322	100' SW	2670
DG	3/29/1999	3/29/1999	3/30/1999	43.5722	-70.0325	75' N	3800
DG	3/30/1999	3/30/1999	3/30/1999	43.5699	-70.0309	90' SSE	2720
DG	3/30/1999	3/30/1999	3/30/1999	43.569216666	-70.03158333	50' E	2800
DG	3/31/1999	3/31/1999	3/31/1999	43.5717	-70.03328333	50' S	2720
DG	3/31/1999	3/31/1999	3/31/1999	43.57175	-70.03223333	25' SE	3000
DG	3/31/1999	3/31/1999	3/31/1999	43.571616666	-70.03261666	40' NW	2250
DG	3/31/1999	3/31/1999	4/1/1999	43.5717	-70.03323333	50' S	3000
DG	4/1/1999	4/1/1999	4/1/1999	43.5725	-70.03131666	100' N	2250
DG	4/1/1999	4/1/1999	4/1/1999	43.5703	-70.03201666	80' S	2500
DG	4/1/1999	4/1/1999	4/1/1999	43.572266666	-70.03276666	80' SE	2250
DG	4/1/1999	4/1/1999	4/1/1999	43.570883333	-70.03335	80' SSW	2500
DG	4/2/1999	4/2/1999	4/2/1999	43.5722	-70.03256666	80' N	2400
DG	4/2/1999	4/2/1999	4/2/1999	43.5725	-70.03266666	100' NE	2600
DG	4/2/1999	4/2/1999	4/3/1999	43.57165	-70.0334	40' S	2632
DG	4/3/1999	4/3/1999	4/3/1999	43.572216666	-70.03286666	50' SW	2600
DG	4/3/1999	4/3/1999	4/3/1999	43.572416666	-70.03263333	50' NW	1800
DG	4/4/1999	4/4/1999	4/4/1999	43.571333333	-70.03276666	40' NE	2250
DG	4/4/1999	4/4/1999	4/4/1999	43.570966666	-70.032	80' E	2500
DG	4/4/1999	4/5/1999	4/5/1999	43.572516666	-70.03218333	100' NE	2500
DG	4/5/1999	4/5/1999	4/5/1999	43.570416666	-70.0337	100' S	2250
DG	4/5/1999	4/5/1999	4/5/1999	43.570233333	-70.03175	100' SE	2800
DG	4/6/1999	4/6/1999	4/6/1999	43.570983333	-70.03225	50' SE	2350
DG	4/6/1999	4/6/1999	4/6/1999	43.572033333	-70.03225	60' N	1800
DG	4/7/1999	4/7/1999	4/7/1999	43.570016666	-70.03306666	80' SW	2700
					Project Total Volume:	**155,842 CM**	**203,821 CY**
					Report Total Volume:	**179,130 CM**	**234,279 CY**

Appendix A3, Disposal Logs

2000 **PDS**

Project: Casco Bay - Portland, ME

Permit Number: 198902221 **Permittee:** YACHT HAVEN INC.

Buoy	Departure	Disposal	Return	Latitude	Longitude	Buoy's Vector	Volume (CY)
DG	2/8/2000	2/8/2000	2/8/2000	43.571266666	-70.03003333	90' SW	750
DG	2/10/2000	2/10/2000	2/10/2000	43.571166666	-70.03166666	80' W	750
DG	2/11/2000	2/11/2000	2/11/2000	43.572666666	-70.031	100' E	750
DG	2/15/2000	2/15/2000	2/15/2000	43.571	-70.03166666	90' W	750
DG	2/17/2000	2/17/2000	2/17/2000	43.571333333	-70.03133333	80' WS	750
DG	2/17/2000	2/17/2000	2/18/2000	43.570833333	-70.03166666	90' E	750
DG	2/22/2000	2/22/2000	2/22/2000	43.572	-70.0315	100' E	630
DG	2/23/2000	2/23/2000	2/23/2000	43.5725	-70.03016666	80' E	750
DG	2/24/2000	2/24/2000	2/24/2000	43.572833333	-70.03116666	80' E	750
DG	2/25/2000	2/25/2000	2/25/2000	43.571	-70.03183333	90' E	750
DG	2/28/2000	2/28/2000	2/28/2000	43.572666666	-70.03183333	100' E	750
DG	3/1/2000	3/1/2000	3/1/2000	43.573	-70.0315	100' E	750
DG	3/2/2000	3/2/2000	3/2/2000	43.571	-70.03216666	100' W	750
DG	3/3/2000	3/3/2000	3/3/2000	43.570833333	-70.03166666	100' W	750
DG	3/6/2000	3/6/2000	3/6/2000	43.570333333	-70.032	100' W	750
DG	3/8/2000	3/8/2000	3/8/2000	43.571833333	-70.0315	100' W	700
DG	3/8/2000	3/8/2000	3/8/2000	43.572166666	-70.0305	100' E	700
DG	3/9/2000	3/9/2000	3/9/2000	43.571833333	-70.0315	90' E	800
DG	3/13/2000	3/13/2000	3/13/2000	43.571333333	-70.03216666	90' W	750
DG	3/16/2000	3/16/2000	3/16/2000	43.57267	-70.03117	80 ft E	750
DG	3/20/2000	3/20/2000	3/21/2000	43.57123	-70.0315	80 ft E	750
DG	3/21/2000	3/21/2000	3/21/2000	43.5715	-70.03233	60 ft E	750
DG	3/22/2000	3/22/2000	3/22/2000	43.57183	-70.03033	60 ft E	750
DG	3/23/2000	3/23/2000	3/23/2000	43.572	-70.03167	80 ft E	750
DG	3/24/2000	3/24/2000	3/24/2000	43.5722333	-70.0315	80 ft E	750
DG	3/27/2000	3/27/2000	3/27/2000	43.57233	-70.03133	80 ft E	750
DG	3/29/2000	3/29/2000	3/29/2000	43.57283	-70.03183	80 ft E	750
DG	3/30/2000	3/30/2000	3/30/2000	43.5705	-70.03117	100 ft E	750
DG	3/31/2000	3/31/2000	3/31/2000	43.572	-70.03133	80 E	500
DG	4/5/2000	4/5/2000	4/6/2000	43.57217	-70.0315	80 ft E	750
DG	4/6/2000	4/6/2000	4/6/2000	43.57307	-70.03	80 ft E	700
					Project Total Volume:	**17,418 CM**	**22,780 CY**

Project: FORE RIVER

Permit Number: 199803142 **Permittee:** MOBIL OIL COMPANY

Buoy	Departure	Disposal	Return	Latitude	Longitude	Buoy's Vector	Volume (CY)
PDA98	3/1/2000	3/1/2000	3/1/2000	43.569233333	-70.03731666		379
DG	3/8/2000	3/8/2000	3/8/2000	43.5715	-70.031	50' S	376
DG	3/19/2000	3/19/2000	3/19/2000	43.573	-70.03133	100 N	376
					Project Total Volume:	**865 CM**	**1,131 CY**
					Report Total Volume:	**18,282 CM**	**23,911 CY**

Appendix B
Sediment Core Photographs and Descriptions

Portland Harbor Cores
Core 3

Dark greenish-gray, wet to moist, soft, silty clay

Greenish-gray, moist, soft, silty clay

Greenish-black to dark greenish-gray, moist, soft, silty clay

Greenish-black, moist to dry, firm clay

Greenish-gray, moist to dry, firm clay

Portland Harbor Cores
Core 4

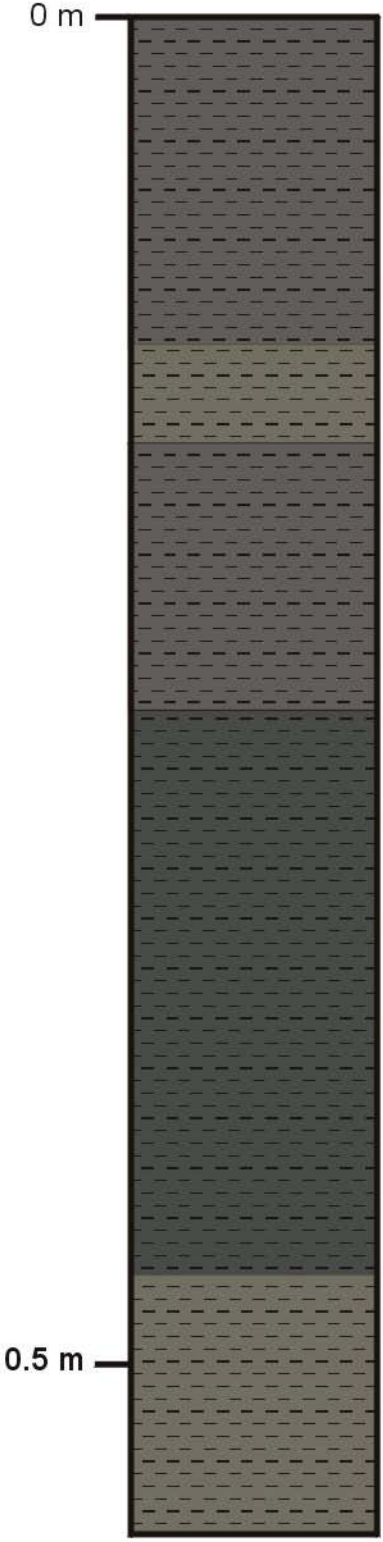

Black and very dark gray, firm silty clay with hydrocarbon odor

Dark greenish-gray firm, sandy, silty clay with hydrocarbon odor

Black and very dark gray, firm, silty clay with hydrocarbon odor

Black and very dark gray to greenish gray, firm, silty clay

Dark greenish gray sandy, silty clay

Portland Harbor Cores
Core 5

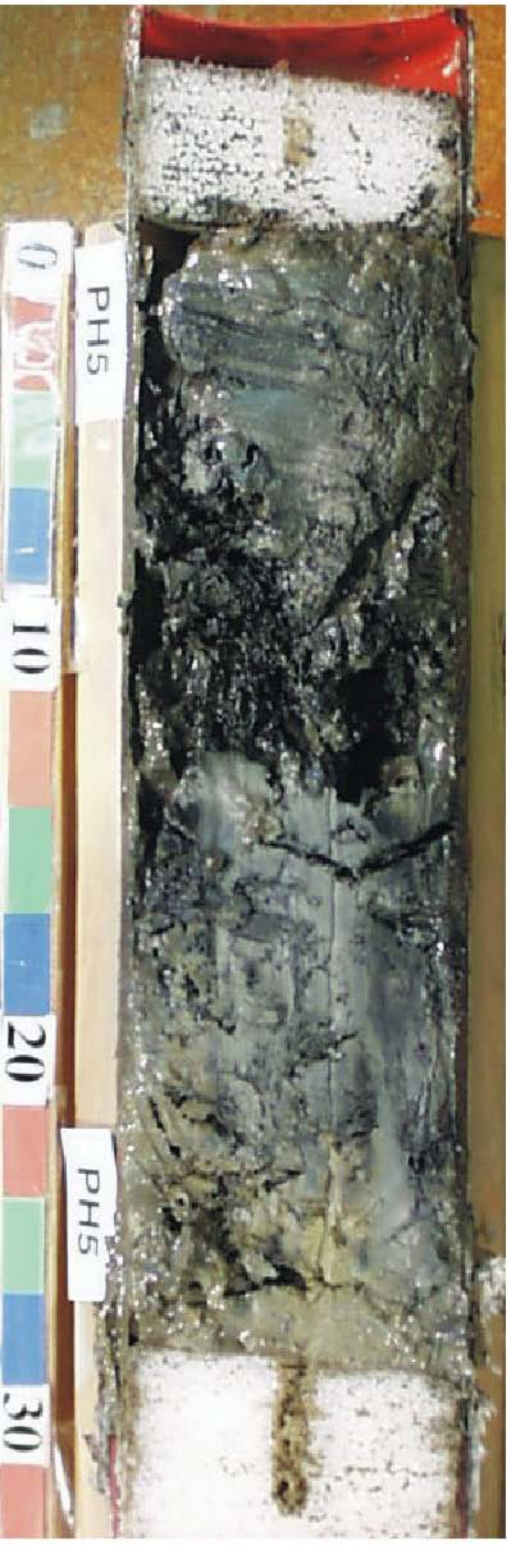

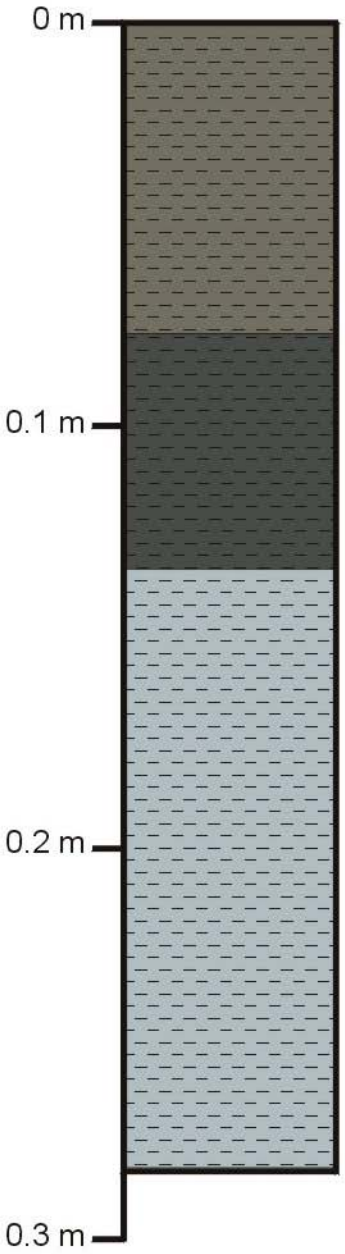

Dark greenish-gray to greenish-gray, moist, soft, silty clay, homogenous

Greenish-black, moist, soft to firm, clay, blocky

Blue-gray, dry, firm, clay

Portland Harbor Cores
Core 6

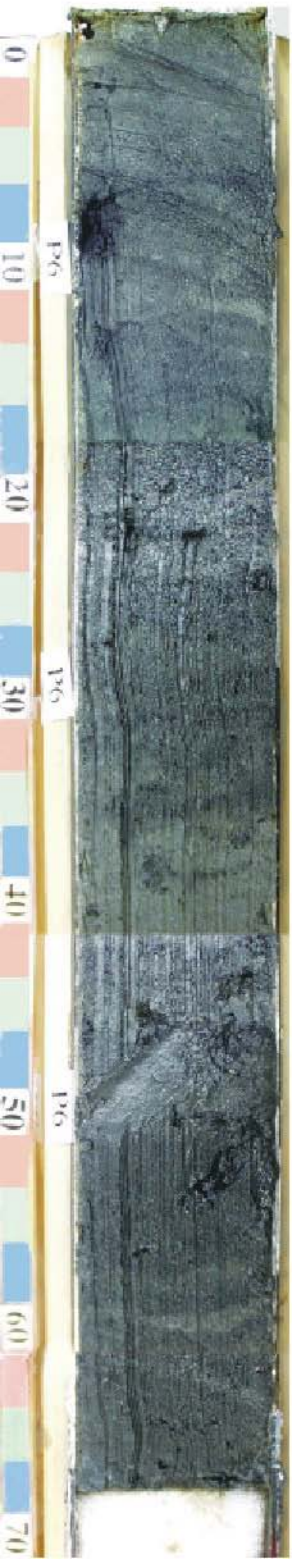

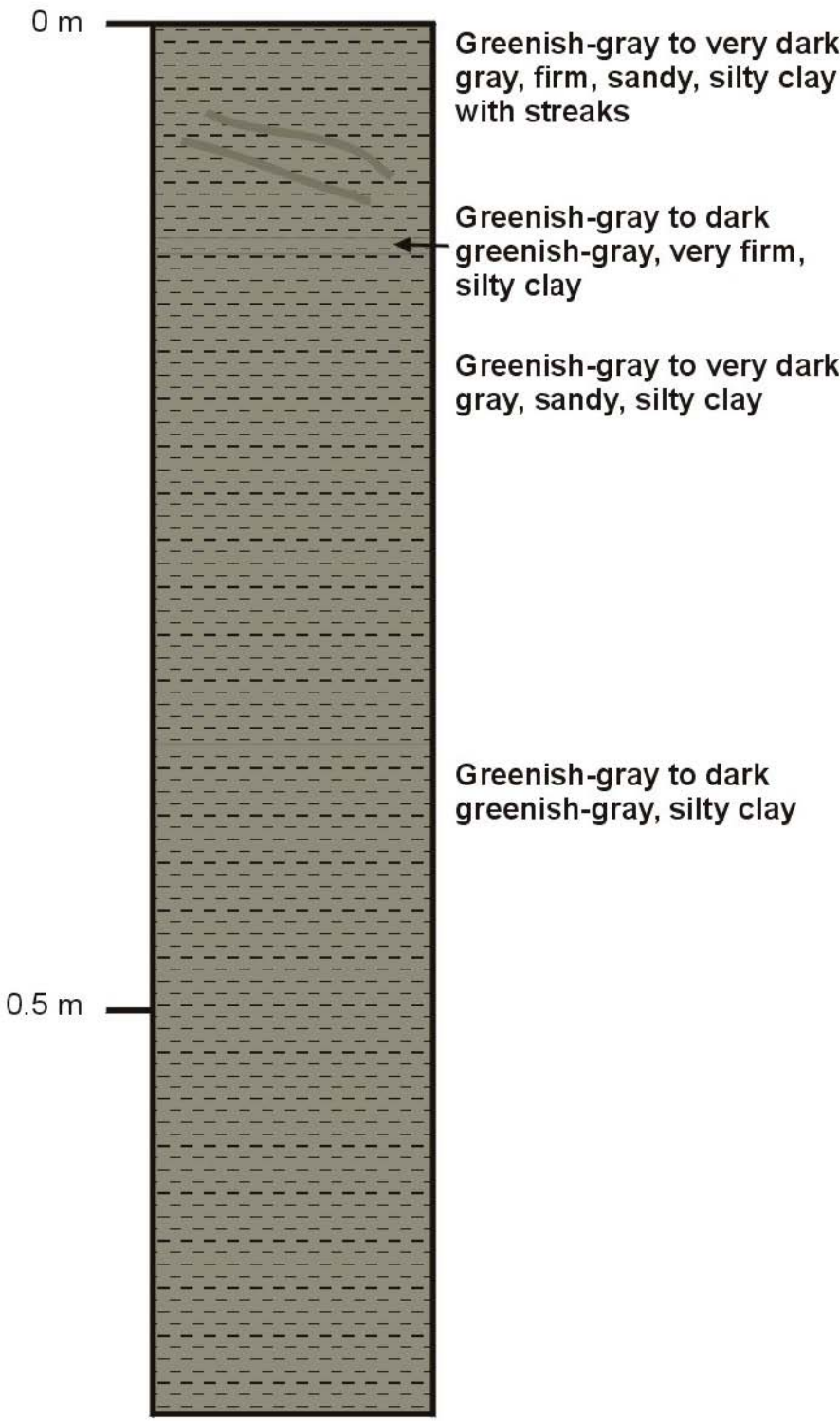

Portland Harbor Cores
Core 7

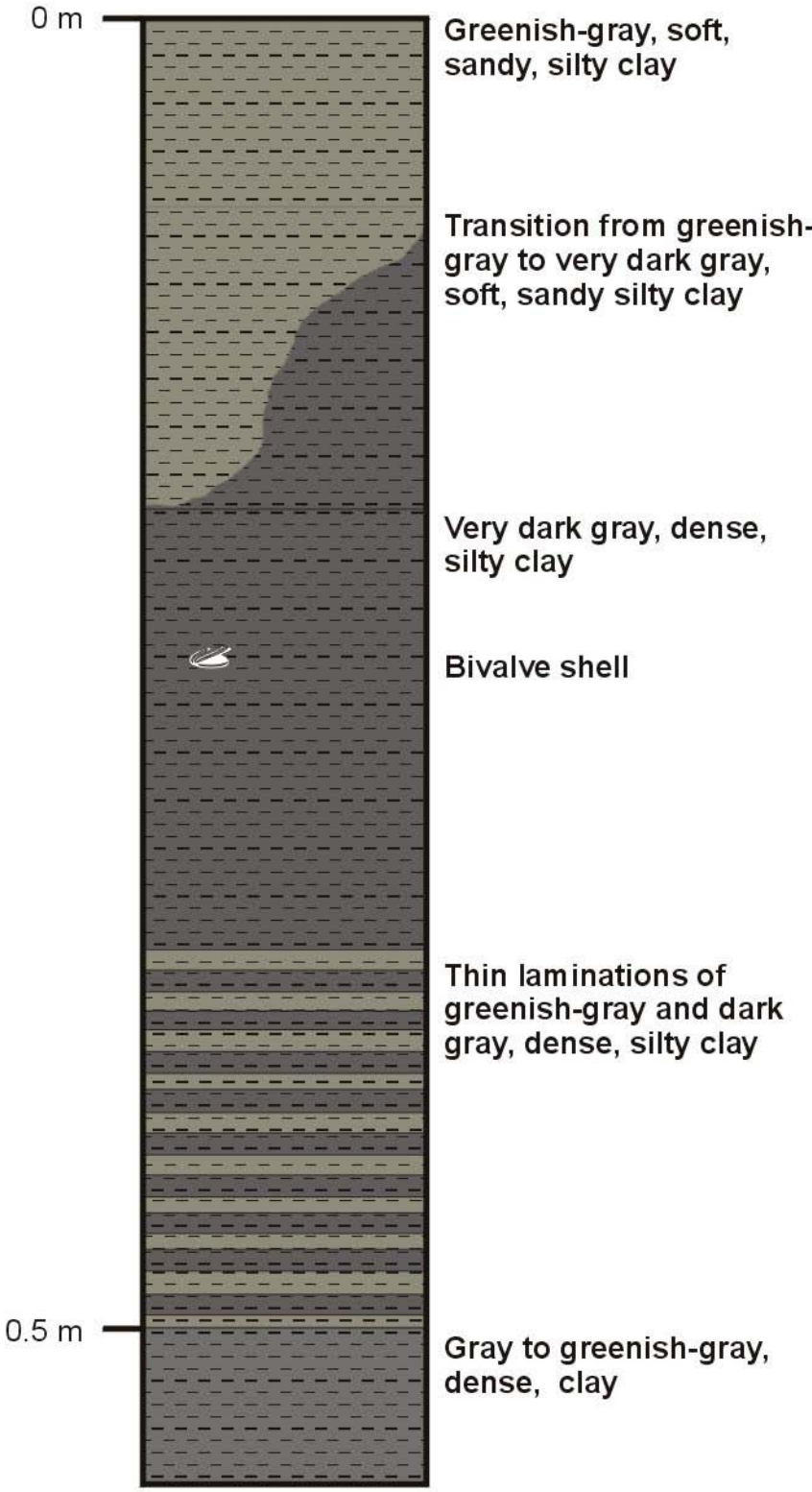

Portland Harbor Cores
Core 8

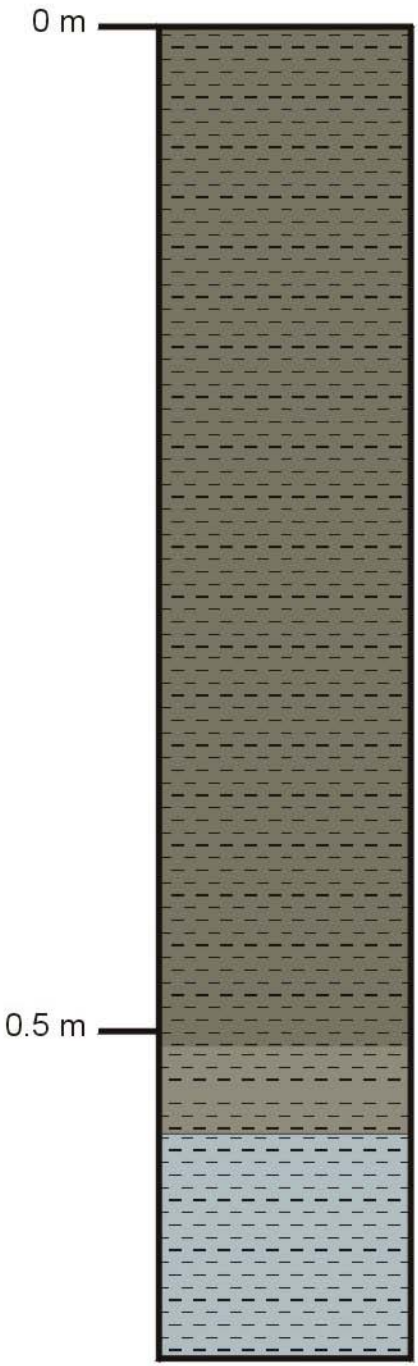

Dark greenish-gray to greenish-gray, moist, soft, silty clay

Greenish-gray, moist to dry, firm, silty clay

Blue-gray, dry, firm, clay

Portland Harbor Cores
Core 9

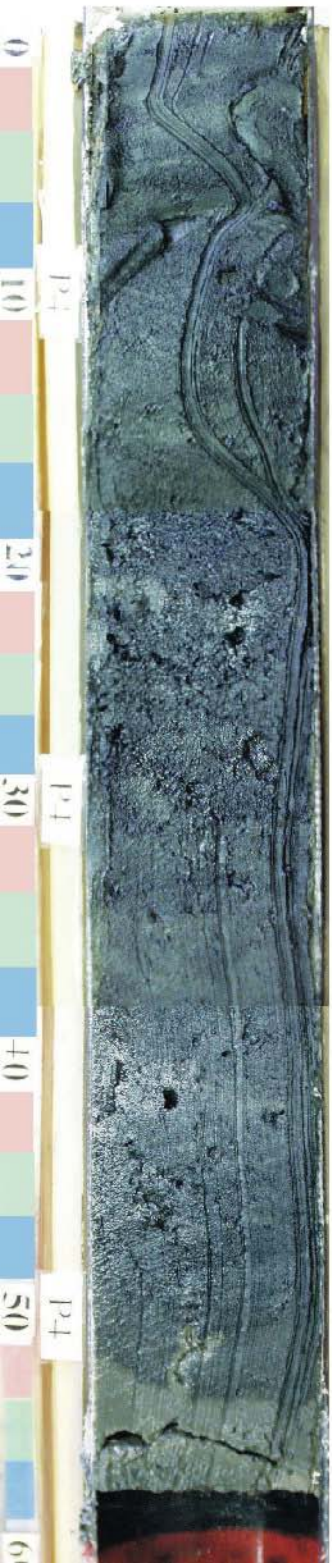

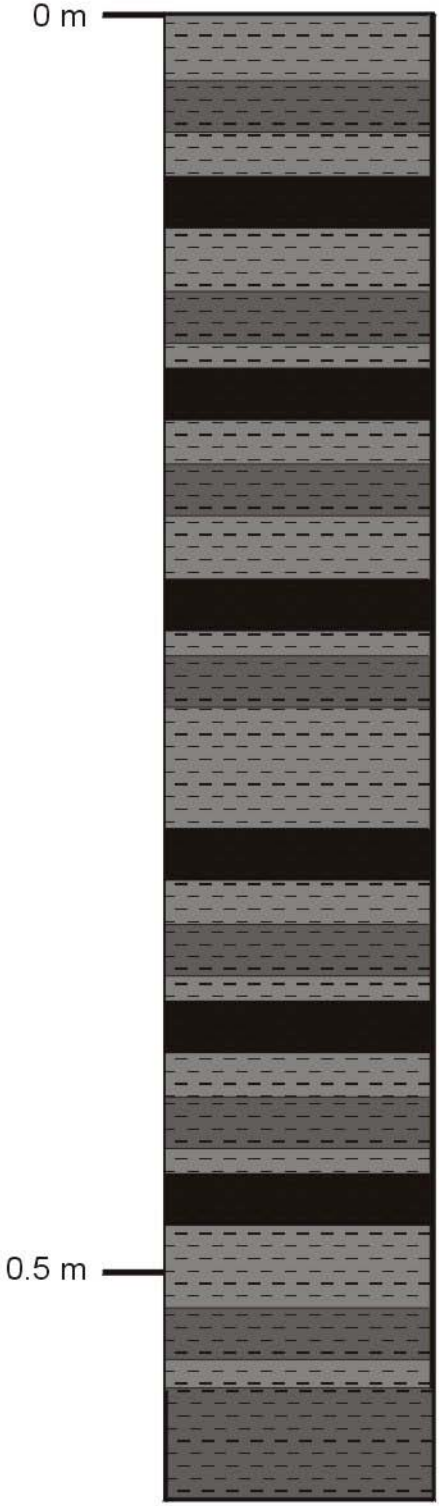

Laminations of gray, dark gray, very dark gray, and black silty clay with consistent texture

Dark gray to gray, sandy, silty clay

Portland Harbor Cores
Core 10

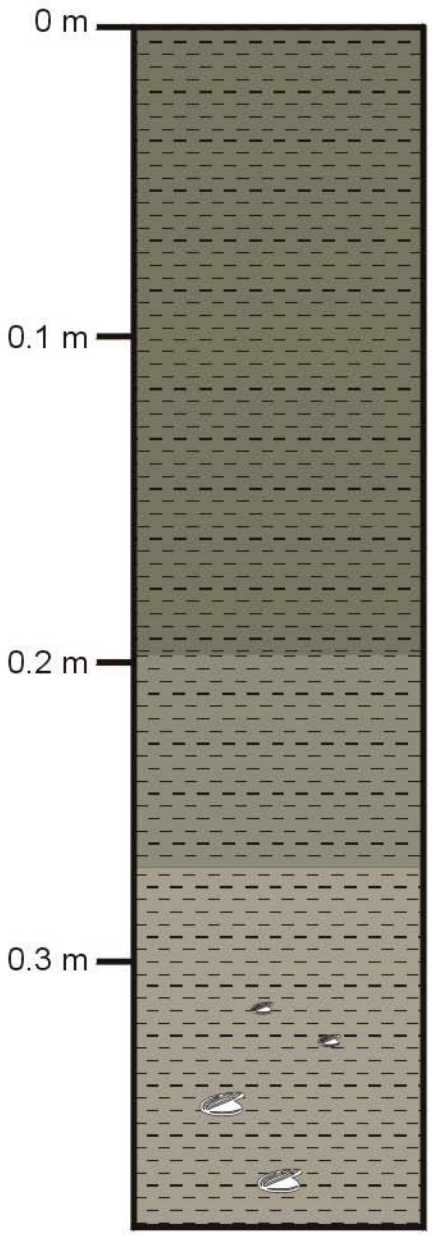

Dark greenish-gray to greenish-gray, moist, soft, silty clay, homogenous

Greenish-gray, moist, soft, silt, sediments coarsen downward

Light olive-brown, moist, soft, fine sandy silt

Shell hash

Portland Harbor Cores
Core 11

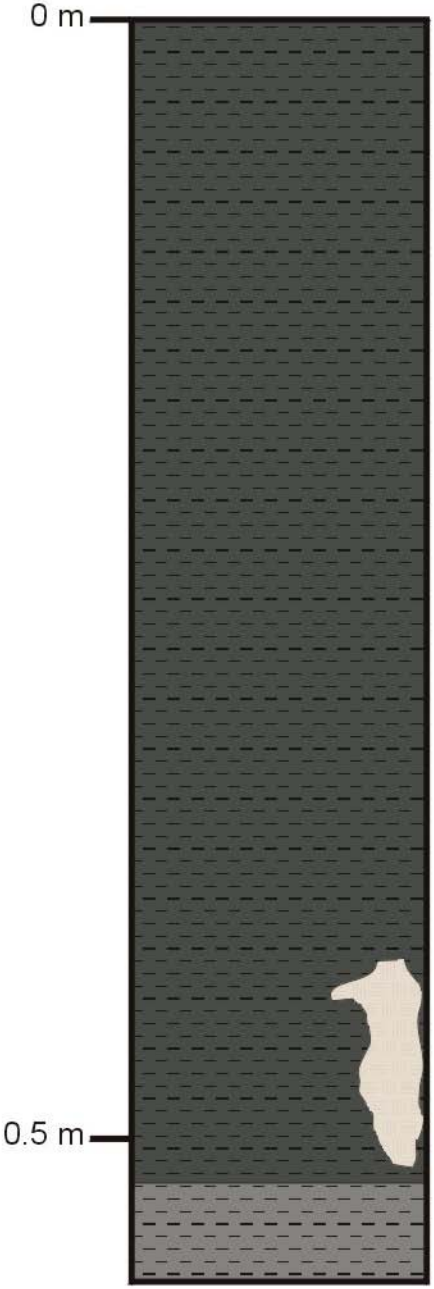

Dark greenish-black to black, wet, soft, silty clay

Thin plastic sheet

Gray, moist to dry, soft to firm, clay

Portland Harbor Cores
Core 13

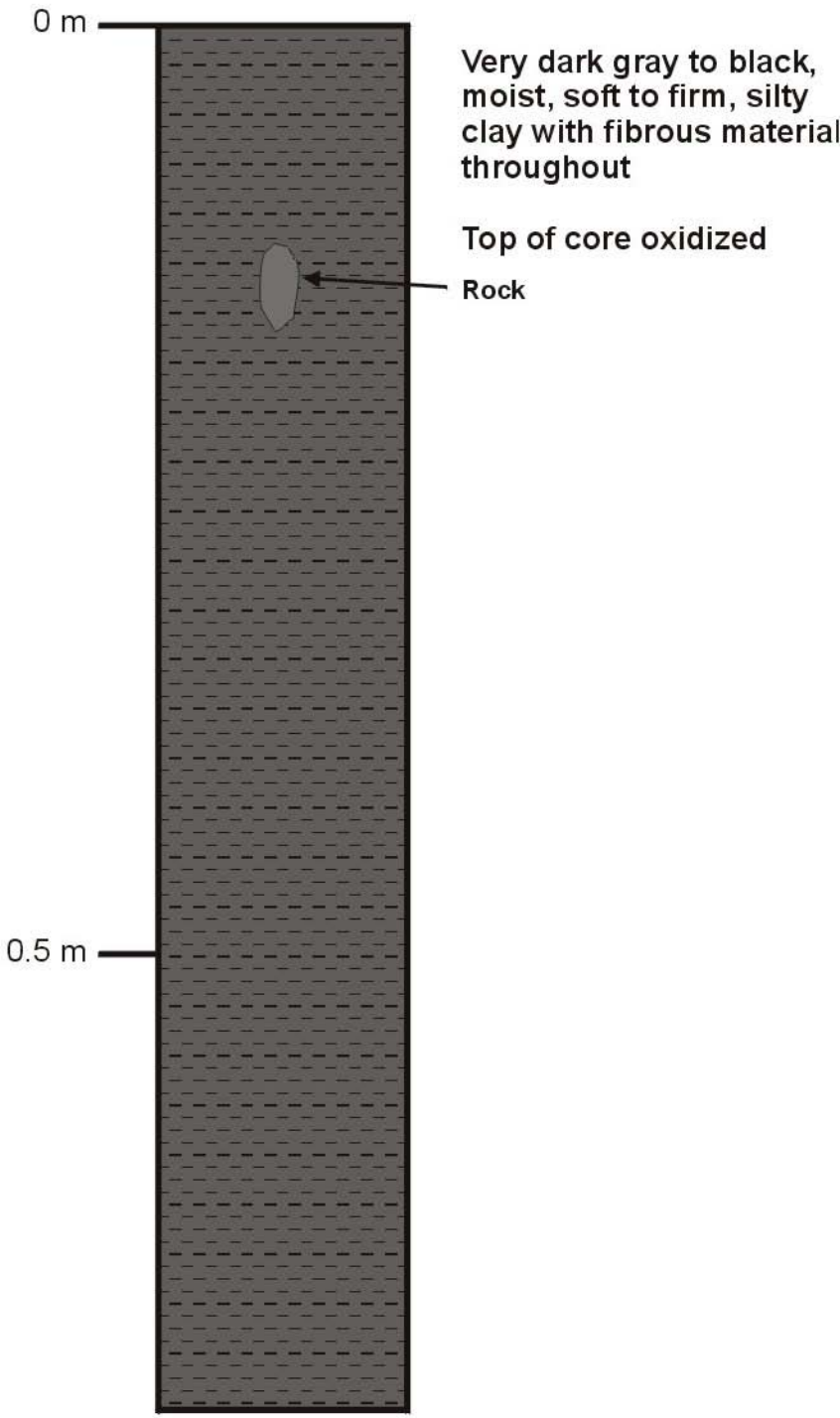

Portland Harbor Cores
Core 14

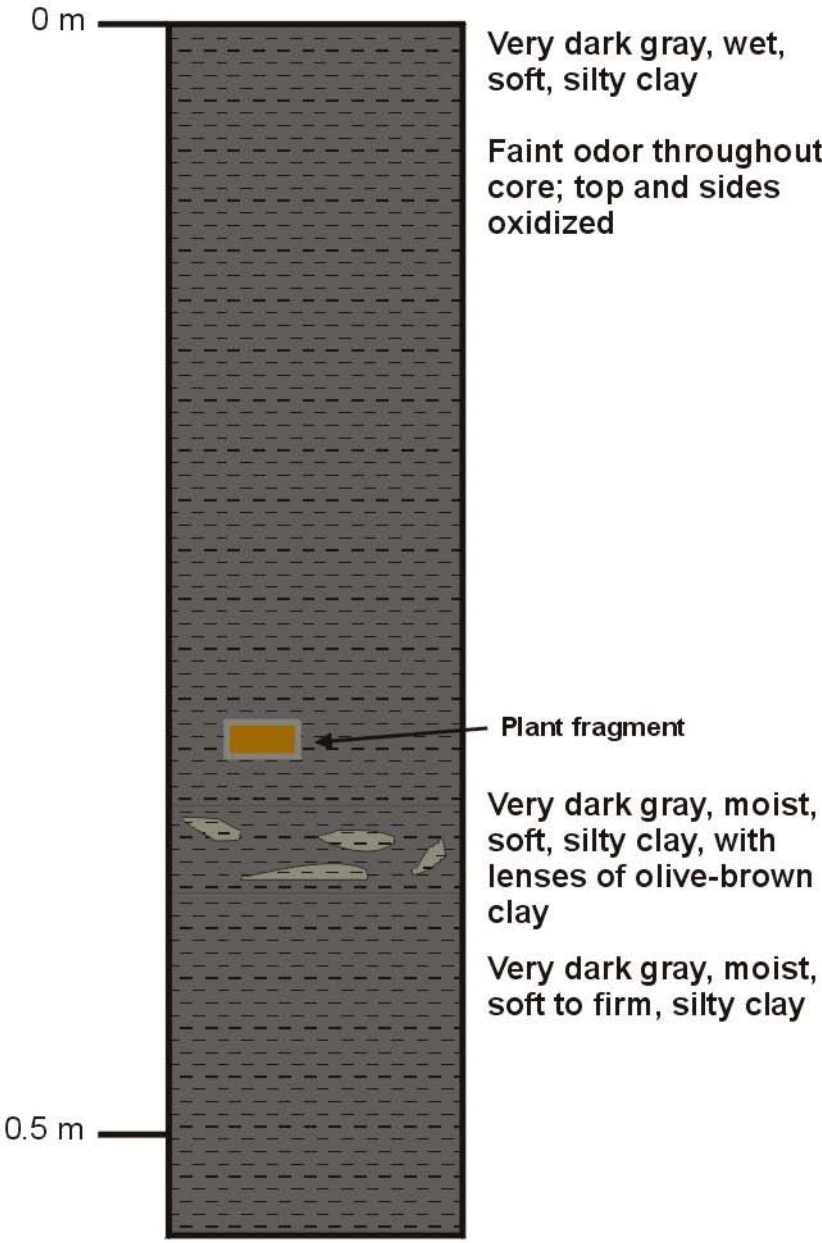

Portland Harbor Cores
Core 15

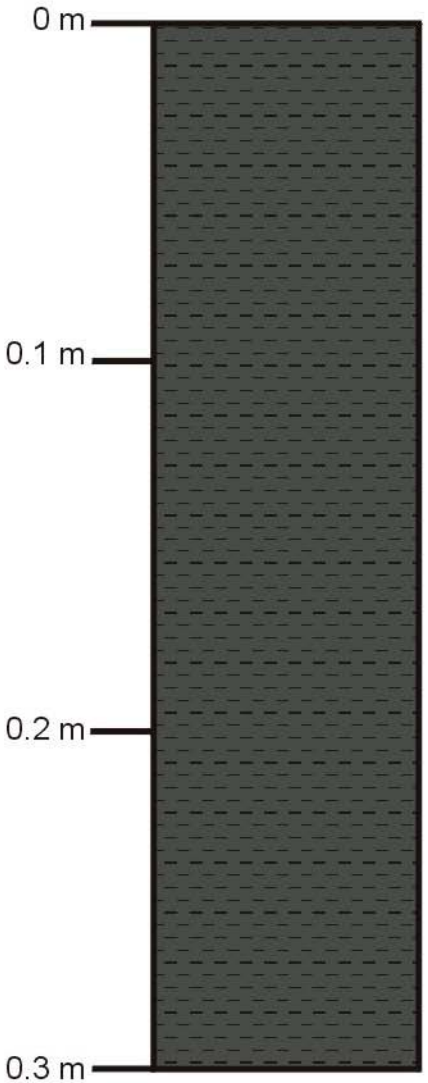

Greenish-black, moist, soft, silty clay, homogenous

Portland Harbor Cores
Core 16

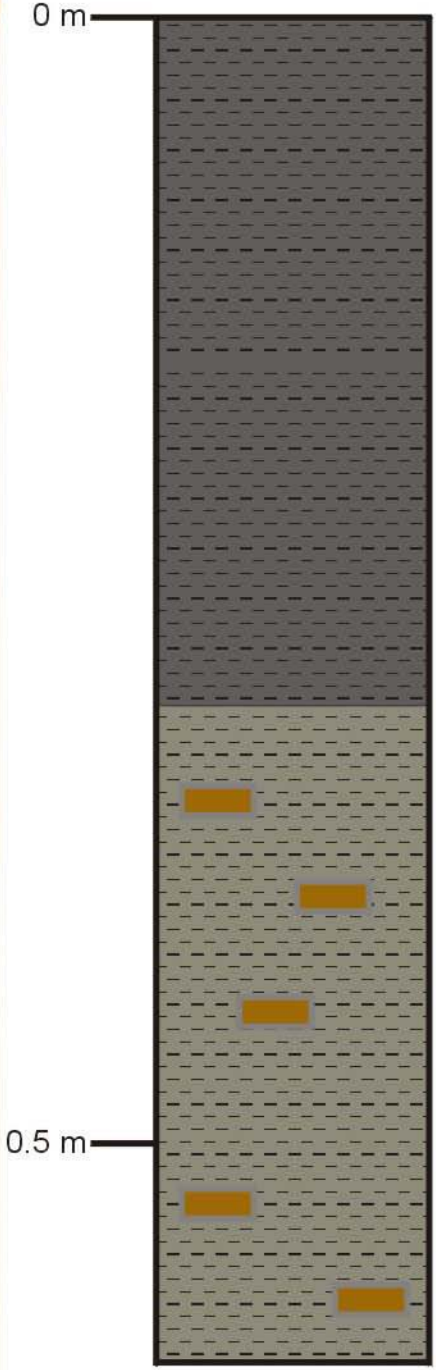

Very dark gray, wet to moist, soft, clay

Core oxidized at top

Olive-brown, dry, firm, silty clay with wood fragments

Portland Harbor Cores
Core 17

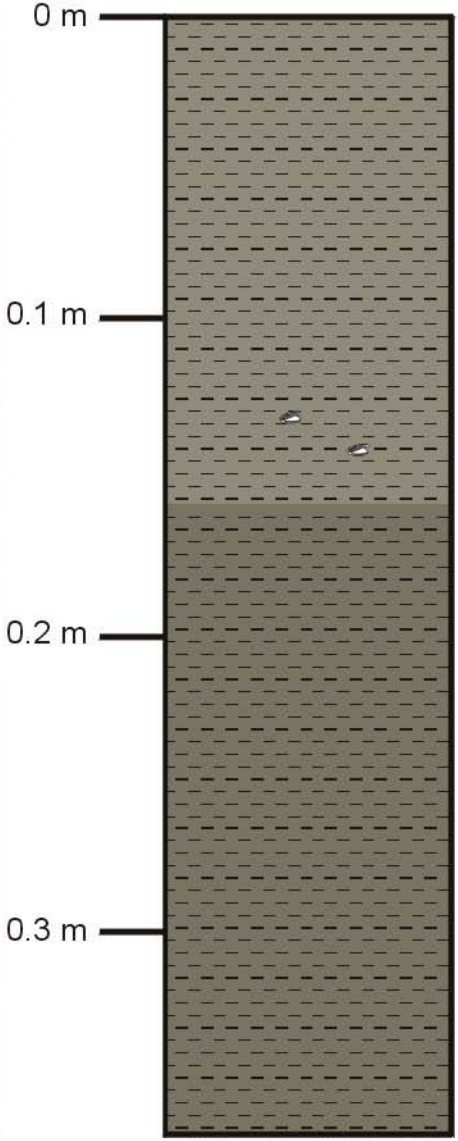

Greenish-gray, moist, soft to firm, silty clay

Minor shell fragments

Dark greenish-gray, moist to dry, firm, silty clay

Portland Harbor Cores
Core 18

Dark greenish-gray, moist, soft, silty clay

Two 2-cm stratified bands of greenish-gray to dark greenish-gray, moist, soft, silty clay

Greenish-gray to dark greenish-gray, moist, soft, silty clay, fines downward

Greenish-gray, moist, soft, clay

Portland Harbor Cores
Core 20

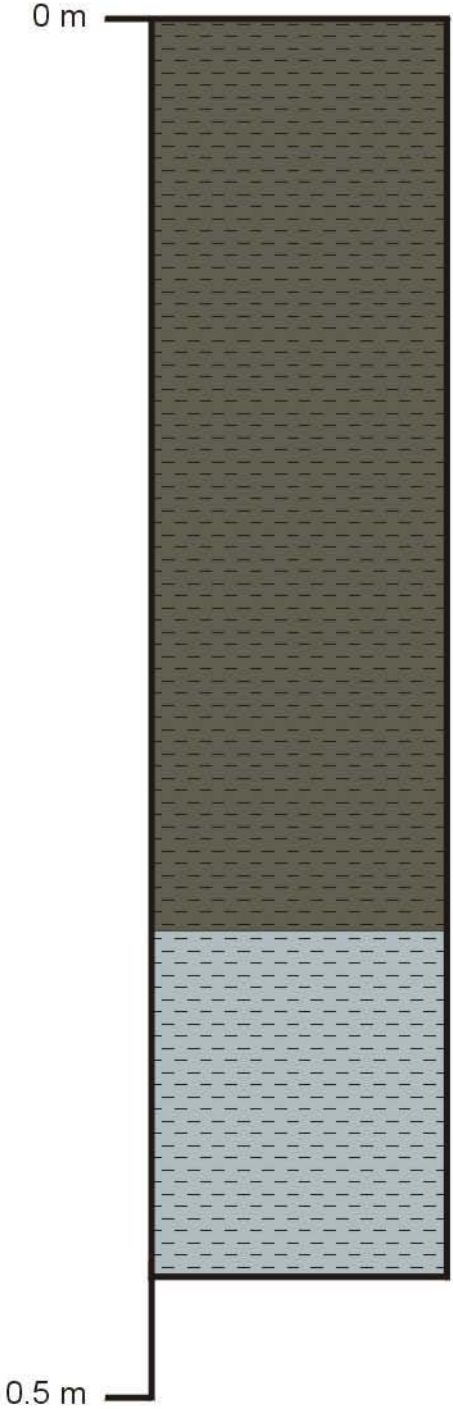

Appendix C
Multibeam Survey Methods

1.0 MULTIBEAM SURVEY METHODS

Two high-resolution multibeam bathymetric surveys were completed over PDS in support of the dredged material fate study. The baseline survey for this study was performed in September 1998 and covered a large area of seafloor surrounding PDS. This was the first master bathymetric survey completed with the use of DGPS in the horizontal control datum of NAD 83. It provided the high-resolution bathymetry of the PDS seafloor that was an important component for the subsequent dredged material disposal modeling efforts. The second survey was performed in July 2000 and covered a much smaller area over PDS. This data set was used in conjunction with the baseline survey to determine the actual morphology of the dredged material deposit at PDS resulting from the disposal operations associated with dredging projects conducted between the two surveys.

1.1 September 1998 Survey

1.1.1 Field Data Acquisition

The M/V *Beavertail* was mobilized at its homeport in Jamestown, RI where it was equipped with the hydrographic surveying system housed within a modified 20-ft cargo container configured as a portable laboratory. This container was securely mounted to the aft center deck of the survey vessel and served as the data collection and analysis center during the survey. A DGPS antenna and a pole mounted multibeam transducer were installed on the vessel in a manner that would ensure accurate geodetic positioning of each sounding.

Swath bathymetry data was collected using the Reson Model 8101 SeaBat Multibeam Echo Sounder System interfaced to a Reson SeaBat 6042 Multibeam Data Collection System (Table C-1). The RESON 8101 utilizes 101 individual narrow beam (1.5°) transducers capable of yielding a total swath coverage of 150° (75° per side). The actual width of coverage is adjustable through range scale settings with a maximum equivalent to 7.4 times the water to a maximum 300 m slant range. The SeaBat 6042 Multibeam Data Collection System combines both hardware and software into a stand-alone system that provides real-time corrected displays of multibeam bathymetry data.

The primary positioning control equipment consisted of a Trimble 7400 DSi GPS receiver for obtaining satellite-based positioning information. Differential correctors emanating from USCG differential beacon broadcasting from Brunswick, ME (316 kHz) were used to improve geodetic positions to a tolerance of ±3 m. A Leica 41R Differential Beacon Receiver was used to capture and decode the correctors, then transmit them to the Trimble 7400 GPS receiver (Table C-1). The GPS receiver was configured to navigate using a minimum of four satellites at an elevation angle no lower than 8°. Horizontal dilution of precision (HDOP) and age of the differential correctors were monitored automatically by the survey system so that the resulting hydrographic positioning control met predetermined specifications.

Table C-1. September 1998 Multibeam Survey Vessel Configuration

M/V Beavertail 1998

Subsystem	Components
Positioning	TSS-POS/MV Model 320 Position and Orientation System (Dual GPS receivers and IMU)
Vessel Position Quality Monitoring	Leica 41R Differential Beacon Receiver Trimble 7400 DSi GPS Receiver (Quality Monitoring)
Integrated Navigation System	HB-2000 Survey System
Multibeam Sonar	Reson Model 8101 240 kHz SeaBat Multibeam Echo Sounder System Reson 6042 topside control unit
Motion Sensor	TSS-POS/MV Model 335B motion sensor
Data Acquisition and Display	SAIC HydroBat 2000 Survey System
Sound Velocity Profiler	Model SBE 1901 Sea-Cat CTD (Conductivity, Temperature, and Depth) logger Sea-Bird Systems

Hydrographic surveying operations during the 1998 field activity were conducted using the SAIC HydroBat 2000 ™ (HB-2000) Survey System (Table C-1). The HB-2000 is a powerful data acquisition and processing system that is used for in-shore, near-shore, and off-shore hydrography and seabed mapping. The system is a complete multibeam survey system with integrated sensors, software, computers and peripherals. The functional capabilities of the HB-2000 include real-time data acquisition and navigation, survey planning support, real-time helmsman and autopilot steering guidance, and post-processing of hydrographic data collected during operations. The HB-2000 consists of several major subsystems including: Integrated Navigation Subsystem (INS); System control display console; Multibeam display; Multibeam sonar subsystem; and Helmsman display console.

The system control console is the primary module of the HB-2000 system and is used to control all functions including survey planning, survey control, and survey data analysis as well as other utility functions such as file handling, printing, and plotting. Data are transferred between the major subsystems using a high-speed local area network (LAN). The Integrated Navigation Subsystem was used to collect all external data including DGPS position, gyrocompass heading information, and the ship's attitude data. These data are time tagged and broadcast over the LAN to the other subsystems of the HB-2000.

The multibeam display subsystem was used to display near-real-time multibeam sonar data. Data can be displayed in several formats including swath cross-section, waterfall display, or textual data. This allows the operator to perform quality control checks on the incoming data and to quickly take corrective action should a malfunction occur.

The helmsman display console was located in the ship's pilothouse and consisted of a terminal node and a graphics monitor. The helmsman display provided the pilothouse with data on the ship's position as well as position relative to the survey lane and cross-track error. The helmsman display is controlled using a standard computer keyboard and pointing device giving the helmsman the ability to change many display parameters such as display scale and center as well as display orientation. The helmsman display cannot be used to alter any HB-2000 functions other than the appearance of the pilothouse display.

1.1.2 Real-time Corrections to Soundings - 1998

A multibeam fathometer swath extends a great distance perpendicular to the precise aspect of the transducer at the time of the transmit pulse. As a result, the quality and accuracy of the multibeam data (particularly in the outer beams) is highly dependent upon the precise measurement of the position, motion, and attitude of the survey vessel (e.g., heading, heave, pitch, and roll). As a result, the RESON 8101/6042 multibeam fathometer system was supplemented with various other sensors to verify correct referencing of each sonar ping on the seafloor.

1.1.2.1 Attitude and Heading Compensation

Real-time attitude compensation was accomplished in the SeaBat 6042 system using ship's attitude data collected using a TSS Model 335B motion sensor (Table C-1). This instrument uses heading sensors and accelerometers to calculate roll, pitch, and relative heave. Heading data for both the motion sensor and HB-2000 INS was provided by a Sperry MK-32 gyrocompass. The accuracy of the TSS 335B sensor is 5 percent of 10 or 5 cm for heave, ±0.10° dynamic accuracy for roll and pitch, and ±0.05° static accuracy for roll and pitch. Attitude data was continually uploaded into the RESON 6042 and applied to the multibeam echo sounder data. Because the ship's center of gravity, the motion sensor location, and the location of the echo sounder differ, lever arm compensation was applied to the motion sensor data within the motion sensor units.

1.1.2.2 Sound Velocity

Any acoustic echosounder (single or multibeam) computes a depth by precisely measuring the travel time of a sound pulse that originates from the transducer, reflects off of the seafloor, and returns back to the transducer. The acoustic travel time is multiplied by the speed of sound within the water column, and then divided in half to obtain a depth value. As a result, the accurate determination of the speed of sound within the water column is required for the correct calculation of depth during the survey operation.

Sound velocity in seawater is a function of density, a variable characteristic controlled by water temperature and salinity. A variety of tools exist for the determination of an average water column speed of sound that satisfies the requirements of a single beam system, where the acoustic signal is transmitted straight down through the water column. However, because multibeam systems generate numerous acoustic beams angled off of the vertical, strong water column density gradients, or pycnoclines, can have a greater impact on multibeam data (particularly in the outer beams). When the non-vertical multibeam pings encounter pycnoclines, they tend to be refracted by the change in speed, causing them to strike the seafloor at a different location relative to those traveling through a well-mixed water column. The effects of pycnoclines on multibeam data are corrected in the RESON 6042 in real-time during multibeam surveys by generating refraction models that are based on periodic density profiles for the entire water column.

The Portland Disposal Site is located in the mouth of Casco Bay, where the water column generally reflects open ocean conditions (well–mixed water column). However, stratification is possible in mid to late summer as temperature differences can establish pycnoclines at depth. In addition, the semi-diurnal tidal cycle promotes changes in seawater properties within a survey day as less saline and warmer water flows out of Casco Bay into the Gulf of Maine.

Sound velocity profiles were calculated during the 1998 survey from conductivity, temperature, and depth data that were collected using a Model SBE 19-01 Sea-Cat CTD logger manufactured by Sea-Bird Systems (Table C-1). This instrument was allowed to freefall to the seafloor and collected CTD data at a rate of 2 Hz. Data from the CTD was uploaded into a stand-alone computer where profiles were computed using the SBE Term19 software package version 4.0. Computed profiles were copied to the HB-2000 for comparison on the screen. A selected profile was applied to the system, recorded, and transferred to the SeaBat 6042 Multibeam Data Collection System where a refraction lookup table was computed for application of distance and range correctors to the multibeam sounding data. CTD profiles were collected prior to commencing surveying on each survey day. Standard procedure called for repeat CTD casts whenever the sound velocity profile changed appreciably during the course of the survey. Sound velocity profile changes are indicated by a readily observable upward bending of the outermost beams of the swath, and can been readily seen on the 8101 display. Due to the relatively small areas covered by these surveys and the restriction of surveying to daylight hours, no ray bending was observed and repeat CTD casts were not required.

1.1.2.3 Static Draft

Raw soundings collected by the Reson 8101 multibeam system reference depth values to the transducer mounted on the side of the survey vessel. In order to adjust the depth values to the water's surface, a draft corrector was applied to the raw soundings in the

RESON 6042 topside control unit. Depth of the transducer below still water level was determined from measurements made by reading the markings on the transducer pole. Daily draft measurements were taken to check for changes in vessel draft due to fuel and water consumption. If the static draft value changed from the previously noted value, the new value was entered into the SeaBat 6042 system. The static draft value was passed to the HB-2000 as part of the header packet from the RESON 6042 where it was recorded in the bathymetric data.

1.1.2.4 Alignment

HB-2000 Alignment Procedures were developed for the determination of system biases for Roll, Pitch, and Heading. These procedures were automated to reduce the chance of operator errors and the time required to obtain valid measurements for statistical comparisons. Alignment data layers are gridded from lines of multibeam data collected for Roll, Pitch and Heading bias calculations, and then compared via statistical analysis to calculate a bias for each pair of lines. Multiple comparisons are made for each type of bias to assure the most accurate results. Data are also collected from the same lines after the biases have been entered in order to verify their accuracy. Details regarding the individual alignment procedures and the data from these calibrations are presented in Appendix D1.

1.1.2.5 Tidal Corrections

Tide level corrections for PDS were applied during survey operations in real-time based on predicted tidal heights at Portland Harbor. During post-processing, historical water level observations were downloaded from the NOAA Ocean and Lakes Level Division. The observed data were compared to the predicted data during post-processing and no appreciable differences were noted. Consequently, no additional tidal corrections were applied during post-processing of the 1998 multibeam data set.

1.1.3 Multibeam Bathymetric Data Processing - 1998

Multibeam data were collected by the HB-2000 system and stored in the Generic Sensor Format (GSF), which allows ping and beam flags to be set to indicate the validity of each ping or beam of the bathymetric data. These flags can be set either in real time or later during post-processing of the data. The GSF combined with history records inserted into the files in real time and during post-processing provides complete traceability of all correctors and processing steps as applied to the data. Thus, the original GSF file is continually updated without creating multiple redundant multibeam files; no data are deleted, they are only flagged.

The first step in post-processing was to analyze the navigation data. The differential corrections broadcast from the Brunswick, ME station encountered occasional interference during real-time operations, thus making it necessary to reject fixes acquired during several periods of the survey. After these fixes were rejected, navigation reconstruction using a

forward-backward Kalman filter was done. This updated navigation information was then combined with the multibeam data files. Following this, multibeam data files were then examined to determine times when survey line data were acceptable. All files were re-examined to mark final "off-line" and "on-line" periods. Data determined to be "off-line" were not used to create final data products.

For this project, only dynamic pitch, roll, heave, and heading values and corrections for draft and tide were applied in real time; these correctors were checked during post-processing and accepted as valid. Because of the uncommonly benign weather conditions experienced during this survey, the resultant data was of extremely high quality and very little data was discarded during post-processing. Continual visual monitoring of the real-time data as it was collected, combined with ping-by-ping examination of each data point during post-processing revealed no detectable evidence of any real-time roll or pitch biases.

Tide corrections were made in real-time to multibeam data collected at both survey sites based upon predicted tides at the nearest NOAA tide recording station. As stated above, subsequent comparison of the predicted tides with those recorded at Portland, ME confirmed the tidal predictions.

There are two Reson-generated quality estimates provided with the real-time sensor data; one is for brightness (amplitude) and one for colinearity (slope). These sensor-specific quality factors are logged in the GSF data file so that the processor can flag each beam based upon acceptance or rejection of either quality factor. For this project, data were rejected if either or both of the two flags were set. Data were also filtered based upon user-defined minimum and maximum depths within survey area. Manual swath editing was performed on each multibeam file using the SAIC Geoswath program. The individual processing data reviews each ping and beam by scrolling through the data and viewing all beam and ping flags set by the automatic filters or during data acquisition. Soundings falling outside the user-defined range were flagged and not included in the generation of products.

Valid multibeam data were gridded into a data layer that allows further quality control of the data. The processor can examine any contour "bulls eyes" (i.e., areas with abrupt changes in depth) to pinpoint possible outliers that have escaped automated filters and/or manual examination. Swath data were again reviewed using Geoswath to flag any remaining outliers. After this final cleaning, bathymetric data were gridded (averaged) into depth files of various cell size (resolution), from which track files and contour files were developed. These bathymetric grid, track, and contour files were then used to create the final project plots.

1.2 July 2000 Survey

1.2.1 Field Data Acquisition

The R/V *Ocean Explorer* was used as the survey platform for the July 2000 multibeam bathymetry survey operations conducted at PDS (Table C-2). This specialized

survey vessel is specifically designed and outfitted for high speed (~11 knots) swath bathymetric data collection. The main cabin of the vessel serves as the data collection and first-order-processing center. Upon completion of the survey, all data were delivered to the Data Processing Center for post-processing.

Table C-2. July 2000 Multibeam Survey Vessel Configuration

R/V Ocean Explorer 2000

Subsystem	**Components**
Positioning	TSS-POS/MV Model 320 Position and Orientation System (Dual GPS receivers and IMU)
Vessel Position Quality Monitoring	Trimble 7400 RSi GPS Receiver (Quality Monitoring) Trimble DGPS Beacon Receiver
Integrated Navigation System	SAIC ISS2000
Survey Autopilot	Robertson AP9 Mk II
Multibeam Sonar	RESON 8101 240 kHz Multibeam Depth Sounder
Motion Sensor	TSS-POS/MV Model 320 Position and Orientation System.
Data Acquisition and Display	Windows NT Computer running ISS2000 Integrated Survey System
Sound Velocity Profiler	Brooke Ocean Technology MVP 30, Moving Vessel Profiler (SVP System)

During the July 2000 survey, precision navigation, helmsman display, and data integration from the multitude of sensors aboard the survey vessel were accomplished with the use of SAIC's Integrated Survey System 2000 (ISS-2000; Table C-2). ISS-2000 has the same functionality as the HB-2000 employed during the September 1998 survey, providing real-time navigation, data time tagging, and data logging within a Windows NT 4.0 environment.

Similar to the 1998 survey operation, a Reson 8101 shallow water, multibeam system was employed for the acquisition of sounding data over the PDS survey area (Table C-2). However, the RESON 8101 was mounted on the keel of this survey vessel to facilitate rapid data collection and increased stability. The RESON 8101 transducer can transmit up to 12 high frequency (240 kHz) sound pulses, or pings, per second, though that number may be reduced in deeper water where sound travel times are greater. This rapid ping rate provides dense along-track data coverage and allows the survey boat to be operated at higher speeds. During the 2000 survey over PDS, vessel speed was controlled to yield average along-track coverage of 2.0 pings per square meter of seafloor. Due to the complex bottom topography at PDS, the RESON 8101 horizontal range scale was set for auto tracking to optimize the

efficiency of the survey. Acoustic returns from the seafloor were detected by the transducer array and raw depth values were transmitted to the RESON 6042 topside control unit. The RESON 6042 then applied a series of real-time corrections (i.e., sound velocity, attitude, predicted tides, draft, squat, etc.) to the raw soundings before transmitting them to the ISS-2000 for position stamps and data storage. An Odom DF 3200 single-beam Echotrac echosounder was also operated to provide a real-time quality check of the RESON 8101 data.

Positioning information was recorded from multiple, independent GPS receiver networks in NAD 83. Two, linked GPS receivers embedded within a TSS POS/MV 320, 3-axis Inertial Motion compensation Unit (IMU) were used as the primary source for vessel position and attitude correctors applied to the multibeam data. The POS/MV IMU was interfaced with a Trimble Probeacon differential beacon receiver to improve the positioning data to an accuracy of ±3 m. Correctors to the satellite information broadcast from the USCG differential station at Brunswick, ME (316 kHz) were applied to the satellite data (Table C-2). The ISS-2000 monitored horizontal dilution of precision (HDOP; quality of the signal); number of satellites, elevation of satellites, and age of correctors to ensure the resulting bathymetric positioning errors did not exceed five meters at the 95% confidence level.

The second GPS system served as a source of position confidence checks and a real-time monitor to verify the navigation information provided by the POS/MV IMU. The secondary system consisted of a Trimble 7400 RSi GPS receiver interfaced with a Leica MX41R Differential Beacon Receiver. Differential correctors broadcasted from the US Coast Guard station in Penobscot, ME (290 kHz) were applied to the satellite data. The real-time monitor within ISS-2000 raised an alarm when the two DGPS positions differed by more than 10 meters horizontally. All positioning confidence checks were well within the allowable inverse distance of five meters.

1.2.2 Real-time Corrections to Soundings - 2000

1.2.2.1 Attitude and Heading Compensation

Real-time heading and attitude compensation were accomplished in the multibeam system based on the data output by the POS/MV GPS-aided inertial navigation system (Table C-2). The primary positioning unit (POS/MV IMU) was mounted on the vessel centerline just forward and above the RESON 8101 transducer to minimize positional offsets. The POS/MV heading, heave, pitch, and roll data were transferred to the RESON 6042, which applied corrections to the raw soundings before they were transmitted to the ISS-2000 and stored for post processing.

With the vessel underway, the azimuth accuracy of the POS/MV system is ±0.05°, one order of magnitude better than the gyrocompass employed in 1998. The accuracy of the system for heave was 5% of one meter or five centimeters, and ±0.10° dynamic accuracy for

roll and pitch, and ±0.05° static accuracy for roll and pitch. Heading, roll, and pitch biases were determined in a series of patch tests performed in Narragansett Bay during the Sea Acceptance Test. These biases are required to account for any minor misalignment between the mounting of the 8101 transducer and the POS/MV IMU. A complete description of the POS/MV calibration procedure and resulting bias calculations are presented in Appendix D2.

1.2.2.2 Sound Velocity

A Brooke Ocean Technology Ltd., Moving Vessel Profiler-30 (MVP) sound velocity profiling system was used to determine water column speed of sound (Table C-2). After examining the records, the data are sent to the RESON 6042 topside control unit. Within the RESON 6042, a beam refraction model was computed from the speed of sound data, and beam angle correctors were applied to the raw multibeam sounding data received from the RESON 8101 transducer.

1.2.2.3 Static Draft

Raw soundings collected by the RESON 8101 multibeam system reference depth values to the transducer mounted on the underside of the survey vessel. In order to adjust the depth values to the water surface, a draft corrector was applied to the raw soundings in the RESON 6042 topside control unit. Depth of the transducer below the vessel's main deck (3.07 m) was determined from measurements made during a dry dock period in May 2000 (Figure C-1). This measurement remains constant as both the deck and the keel are fixed structures on the survey vessel. However, daily draft measurements were made between the main deck and the still water level to compensate for changes in vessel draft due to fuel and water consumption.

At the beginning and end of each survey day, static draft measurements were made on the port and starboard sides of the survey vessel. The height of the vessel's main deck above the still water level was subtracted from 3.07 m to yield actual draft of the transducer array (Figure C-1). The draft measured for the PDS 2000 survey was 1.41 m, which in turn was added to the raw soundings.

1.2.2.4 Settlement and Squat

The configuration of the R/V *Ocean Explorer* allows the collection of high-quality swath bathymetry data at speeds approaching 11 knots. The displacement of water by the survey vessel's hull allows the boat to settle into the water slightly. The faster the hull moves through the water, the greater the volume of water displaced, promoting further settlement. In addition, higher speeds and the resulting increased shaft revolutions per minute (RPMs) also cause the bow of the survey vessel to rise higher in the water and the stern to dip further into the water. This apparent change in vessel's vertical position, relative to the water line, is capable of impacting the hydrographic data set unless settlement and squat correctors are applied.

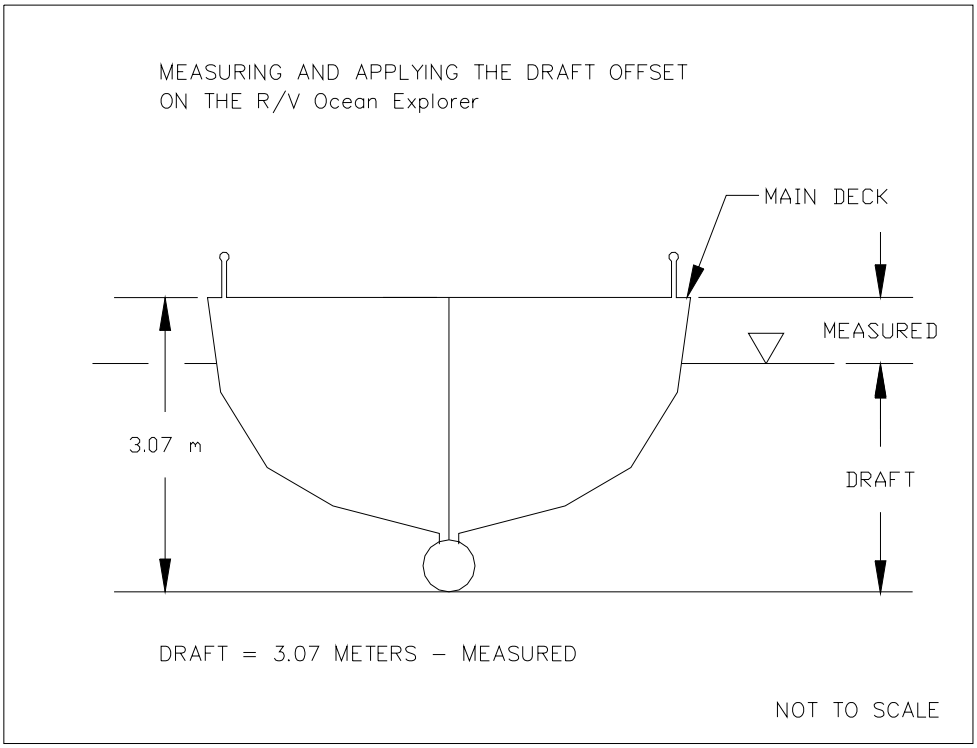

Figure C-1. R/V *Ocean Explorer* and draft determination

Measurements of settlement and squat for the R/V *Ocean Explorer* were conducted on 13 May 2000 (Julian day 134), in Narragansett Bay, RI over an area of seafloor 18 meters below the water's surface. As expected, the correction values increase proportionally with the vessel's speed over ground. A complete description of the measurement procedure is presented in Appendix D3.

1.2.2.5 Tidal Corrections

Tidal height corrections for the PDS survey were obtained via the National Oceanographic and Atmospheric Administration (NOAA). Both predicted and observed tide information was based on the NOAA tide station at Portland Harbor, ME (8418150) corrected to the appropriate local tide zone. The local tide zone correctors applied to the Portland tide data were -6 minutes for time difference and 95% for height.

Predicted tides were applied in the RESON 6042 topside control unit in real-time during the survey operations. Verified, observed tidal data downloaded from the NOAA CO-OPS web page were applied during the post-processing effort. Tide-corrector files for each tide zone were created from actual tide data using the ISS-2000 "TID2HMPS" routine. These corrector files were then applied to the multibeam data using the "APPCORS" program within the ISS-2000 Survey Analysis software.

1.2.3 Multibeam Data Processing - 2000

Similar to the 1998 survey, the multibeam depth data were collected by the RESON 8101/6042 system in the Generic Sensor Format (GSF) that allows flags to be set as an indication of the validity of each ping or beam within the bathymetric data. A real-time coverage monitor was used during data collection to ensure adequate coverage of multibeam data that met or exceeded International Hydrographic Organization (IHO) standards. Multibeam backscatter imagery data, similar to side-scan sonar, were collected in eXtended Triton Format (XTF). These data were collected by the RESON 6042 and stored to the hard drive. The imagery data are useful for bottom-type classification and can be mosaiced into a 1×1 m grid using the Triton Elics ISIS processing software.

All data processing was conducted using the SAIC ISS-2000 system. Initial navigation quality control was done on the vessel shortly after the data was collected. Where time allowed, multibeam data were edited onboard the vessel using the Geoswath editor, which provides both plan and profile views of each beam in its true geographic position and depth. At the end of each day, both the raw and processed data were backed up onto 4 mm tape and shipped to the Data Processing Center in Newport, RI.

In the processing center, manual data editing was completed and reviewed by an ACSM-certified Hydrographer. Verified tide data from the Portland, ME (8418150) station were applied to the multibeam data during this phase of the post-processing. The data

collected along the three cross lanes were compared to soundings obtained from the same locations along the mainscheme survey lanes as a quality control tool. Any questionable data were noted and later evaluated by the lead Hydrographer.

Once the data were fully processed and reviewed, the depth data were gridded into 1 × 1 m, 5 × 5 m, and 20 × 20 m cells. Each cell contained a single depth value derived from averaging all of soundings that fell within that cell. When large differences were detected between soundings within the same cell, the edited multibeam files were re-examined and re-edited as needed. The resulting gridded data sets were used to evaluate coverage and quality, and to facilitate comparison with other bathymetric data sets.

Appendix D1
1998 Heave, Pitch, Roll Biases

A TSS Model 335B motion sensor (Table 2-5) was used to calculate real-time roll, pitch, and relative heave corrections. Heading data for both the motion sensor and HB-2000 INS was provided by a Sperry MK-32 gyrocompass. The accuracy of the TSS 335B sensor is 5 percent of 10 m or 5 cm for heave, ± 0.10° dynamic accuracy for roll and pitch, and ±0.05° static accuracy for roll and pitch.

The Heading Alignment Test compares the depths from two lines of Multibeam data collected in opposite directions over a smooth, sloping bottom. The optimum comparison uses the largest distance between tracks without looking at the outer beams at the edge of the swath where the noise may prevent valid calculation of biases. The test measures the horizontal displacement of depth contours and the distance between tracklines.

Because of the shallow depth of the water in the calibration area it was not deemed useful to perform heading bias calibration because of the difficulty of detecting heading biases under those conditions. Significant heading bias would have been readily apparent during the actual surveys in deeper water, however none were noted during the PDS survey.

The Roll alignment test compares center beam and outer beam depths from two survey lines of multibeam data collected at the same heading on a relatively flat, smooth bottom and seperated by a distance up to half the swath width. The optimum comparison uses the largest distance between tracks without looking at the outer beams at the edge of the swath where the noise may prevent valid calculation of biases.

The Pitch alignment test compares the depths from two lines of multibeam data collected on the same line in opposite directions over a smooth, sloping bottom. The test measures the horizontal displacement of depth contours and the distance between tracklines.

The Roll bias calibration was performed in a test conducted in Narragansett Bay immediately following the system checkout. Prior to conducting the test, a CTD cast was taken to determine the sound velocity profile and entered in the SeaBat system. The Roll bias test was run in an area with a relatively flat bottom and consisted of three lines spaced 40 m apart. Roll bias in the SeaBat system was initially set to 0.0 and the range scale set to 100 m. Each line was run in both directions and the data from parallel in the same direction were used for Roll Bias Calculations. The measured Roll bias was recorded and entered into the SeaBat system and one of the lines was re-run to verify the calibration.

The Pitch calibration was perfomed along a previously defined course in Jamestown Harbor channel. The seafloor in this area slopes gently towards the center of the bay and three lines were defined which ran down the channel along the slope of the bottom. Each line was occupied once in each direction ant the center beam data from each line was compared with that of the same line run in the opposite direction.

Data from these calibrations are presented in Table 1.

Roll Calibration					
		Count	Bias	Std. Dev.	
	d02_d06	168	1.46	0.4	
	d02_d04	172	2.01	0.03	
	d08_d06	68	1.53	0.74	
	d07_d05	81	1.94	0.24	
	d07_d09	167	1.96	0.12	
	d07_d03	178	1.99	0.2	
Roll Bias		834	1533.72		
Initial Setting	-0.88	+	1.84	=	0.96

Pitch Calibration					
		Count	Bias	Std. Dev.	
	d32_d27	115	-1.77	1.29	
	d27_d28	116	-2.12	1.33	
	d28_d29	101	-1.44	1.17	
	d27_d30	74	-2.26	0.9	
	d29_d30	95	-1.5	1.08	
	d30_d31	102	-2.4	1.39	
	d31_d28	96	-2.88	1.32	
	d32_d29	103	-1.9	1.08	
	d31_d32	97	-2.31	1.25	
Pitch Bias		899	-1650		
Initial Setting	0	+	-1.84	=	-1.84

Appendix D2
2000 Heave, Pitch, Roll Biases

The POS/MV IMU was used for heave, roll, pitch, and heading. The accuracy of the sensor was 5 cm for heave, ± 0.10° dynamic accuracy (±0.05° static) for roll and pitch. The dynamic heading accuracy of the unit is ±0.05°.

Heading, roll, and pitch biases were determined in a series of tests performed in Narragansett Bay during the Sea Acceptance Test. Prior to conducting any of the tests, an SVP was collected by the MVP-30 and entered into the RESON system. Initially, the roll, pitch, and heading biases were set to 0° in the RESON system.

SAIC used a combination of the geoswath editor and a spreadsheet to compute the roll bias between the POS/MV IMU and the transducer. This technique was developed and used on the Gulf of Mexico project for roll bias determination over flat bottom. Because the bottom is seldom truly flat, the test is accomplished by running the same line in opposite directions over a smooth bottom. An area is selected for the measurements, and an equal number of port and starboard depth pairs is measured from each direction. The apparent port to starboard slope of the bottom is computed for each pair of measurements. Averaging the equal number of slopes from each direction removes the bottom slope and leaves the roll bias. If a roll bias was in the system at the time of the test, it is added algebraically to the apparent slope to compute the values to be averaged. On 11 May 2000 (Julian day 132), three separate determinations of roll bias were made and then averaged for a bias value of 0.18. Roll bias results are shown in Table D2-1.

After the roll bias was calculated and entered into the RESON system, timing latency test and then pitch bias tests were conducted. Timing latency testing was conducted by running the same line in the same direction, at slow speeds then at fast speed, over distinct rocks on the bottom. The geoswath editor was used to measure the positions of the rocks from data taken at the two speeds. Differences in positions of the rocks were less than one meter and were both positive and negative in sign as well as across track. This indicated no timing latency, only the scatter associated with DGPS positioning.

Pitch bias testing was conducted by running the same line as for timing latency, but in the opposite direction at the same speed. Positioning of the rocks was similar to the timing results, indicating no pitch bias. Since there was no discernable timing latency or pitch bias as a result of these tests, a bias of 0.0° was kept in the system for the survey.

Following the roll and pitch bias tests, a heading bias test was conducted by running parallel lines in opposing directions so that the outer beams of adjacent swaths ensonified the same rocks used for timing and pitch. Positioning of the rocks was similar to the results of the timing and pitch tests, indicating no heading bias. Therefore, a heading bias of 0.0° was kept in the system for this survey. Table D2-1 contains the results of the Accuracy test conducted on 13 May 2000 (Julian day 134). Roll, pitch, and heading biases applied in the CLIS survey are shown in Table D2-2.

Table D2-1. Roll Bias Results for R/V *Ocean Explorer*

	Roll Bias Determination		Julian Day:	132	date:	11 May 2000
	File numbers:	132.d06 & 132.d08				
	from geoswath		from geoswath	apparent	bias already	bias to enter
#	depth port m.	depth stbd m.	swath width m.	slope	in ISS2000	in ISS2000
1	40.33	37.36	105.30	0.81	0.00	0.81
2	40.38	37.45	105.30	0.80	0.00	0.80
3	40.25	37.41	105.30	0.77	0.00	0.77
4	40.16	37.74	105.30	0.66	0.00	0.66
5	40.20	38.11	105.30	0.57	0.00	0.57
6	40.74	38.29	105.30	0.67	0.00	0.67
7	40.34	38.16	105.30	0.59	0.00	0.59
8	40.25	38.09	105.30	0.59	0.00	0.59
9	40.36	37.97	105.30	0.65	0.00	0.65
10	40.36	38.02	105.30	0.64	0.00	0.64
11	39.27	40.20	105.30	-0.25	0.00	-0.25
12	39.36	40.27	105.30	-0.25	0.00	-0.25
13	39.41	40.40	105.30	-0.27	0.00	-0.27
14	39.47	40.81	105.30	-0.36	0.00	-0.36
15	39.34	40.29	105.30	-0.26	0.00	-0.26
16	39.13	40.13	105.30	-0.27	0.00	-0.27
17	38.98	39.86	105.30	-0.24	0.00	-0.24
18	38.84	39.77	105.30	-0.25	0.00	-0.25
19	38.63	39.83	105.30	-0.33	0.00	-0.33
20	38.56	39.77	105.30	-0.33	0.00	-0.33
			mean bias to enter in ISS2000			0.20
			standard deviation first direction			0.09
			standard deviation second direction			0.04

	Roll Bias Determination		Julian Day:	132	date:	11 May 2000
	File numbers:		132.d05 & 132.d10			
	from geoswath		from geoswath	apparent	bias already	bias to enter
#	depth port m.	depth stbd m.	swath width m.	slope	in ISS2000	in ISS2000
1	37.11	37.81	105.30	-0.19	0.00	-0.19
2	37.09	37.88	105.30	-0.21	0.00	-0.21
3	37.20	37.98	105.30	-0.21	0.00	-0.21
4	37.20	38.36	105.30	-0.32	0.00	-0.32
5	37.43	38.65	105.30	-0.33	0.00	-0.33
6	37.84	38.82	105.30	-0.27	0.00	-0.27
7	38.11	38.84	105.30	-0.20	0.00	-0.20
8	38.16	38.91	105.30	-0.20	0.00	-0.20
9	37.11	37.79	105.30	-0.18	0.00	-0.18
10	37.08	37.77	105.30	-0.19	0.00	-0.19
11	39.98	37.59	105.30	0.65	0.00	0.65
12	39.83	37.54	105.30	0.62	0.00	0.62
13	39.75	37.50	105.30	0.61	0.00	0.61
14	39.70	37.52	105.30	0.59	0.00	0.59
15	39.59	37.50	105.30	0.57	0.00	0.57
16	39.54	37.50	105.30	0.55	0.00	0.55
17	39.45	37.41	105.30	0.55	0.00	0.55
18	39.56	37.30	105.30	0.61	0.00	0.61
19	39.27	36.84	105.30	0.66	0.00	0.66
20	39.31	36.75	105.30	0.70	0.00	0.70
			mean bias to enter in ISS2000			0.19
			standard deviation first direction			0.05
			standard deviation second direction			0.05

	Roll Bias Determination		Day:	132	date:	11-May-00
	File numbers:		132.d04 & .d09			
	from geoswath		from geoswath	apparent	bias already	bias to enter
#	depth port m.	depth stbd m.	swath width m.	slope	in ISS2000	in ISS2000
1	37.68	36.04	105.30	0.45	0.00	0.45
2	37.68	36.13	105.30	0.42	0.00	0.42
3	37.70	36.16	105.30	0.42	0.00	0.42
4	37.70	36.18	105.30	0.41	0.00	0.41
5	37.77	36.11	105.30	0.45	0.00	0.45
6	37.75	36.11	105.30	0.45	0.00	0.45
7	37.79	36.13	105.30	0.45	0.00	0.45
8	37.81	36.09	105.30	0.47	0.00	0.47
9	37.84	36.09	105.30	0.48	0.00	0.48
10	37.91	36.11	105.30	0.49	0.00	0.49
11	36.84	37.24	105.30	-0.11	0.00	-0.11
12	36.83	37.29	105.30	-0.13	0.00	-0.13
13	36.88	37.31	105.30	-0.12	0.00	-0.12
14	36.86	37.34	105.30	-0.13	0.00	-0.13
15	36.83	37.31	105.30	-0.13	0.00	-0.13
16	36.86	37.27	105.30	-0.11	0.00	-0.11
17	36.86	37.36	105.30	-0.14	0.00	-0.14
18	36.83	37.43	105.30	-0.16	0.00	-0.16
19	36.84	37.34	105.30	-0.14	0.00	-0.14
20	36.86	37.27	105.30	-0.11	0.00	-0.11
			Mean bias to enter in ISS2000			0.16
			Standard deviation first direction			0.03
			Standard deviation second direction			0.02
Average of three tests			***Mean bias to enter in ISS2000***			***0.18***

Table D2-2. Roll, Pitch, and Heading Bias for the R/V *Ocean Explorer*

Bias	Value
Roll	0.18
Pitch	0.00°
Heading	0.00°

Appendix D3
Settlement and Squat Calculations for the R/V *Ocean Explorer*

Measurements of settlement and squat were conducted near 41° 31’ 56”N, 071° 19’ 30”W on 13 May 2000 (Julian day 134), in 18 meters of water off the end of the Coddington Cove breakwater, Narragansett Bay, RI. The following procedures were used to determine the settlement correctors:

Measurement by Surveyor’s Level and Rod, the preferred method when the attitude sensor (IMU) and the transducer are not co-located.

1. Used a surveyor’s level and a level rod with target, or a stadia board to measure the elevation of a spot above the attitude sensor (IMU) on the survey boat as the boat was operated at different shaft RPMs.
2. Selected a location to set up a surveyor’s level (“level”) overlooking adequate water for the survey vessel to run a survey line at various speeds, including full speed. Established communication between “level” and the boat.
3. Selected the “static” point for initial measurements, which was the point at which the vessel was to hold station.
4. Planned the “settlement and squat” survey line through “static.” The vessel ran this line at various shaft RPM settings to make settlement and squat measurements. The line ran more nearly toward the “level” than across in front of it. This made it more likely that the observer was able to focus on and read, or direct the reading, of the level rod on the boat. For this reason, a breakwater end was chosen.
5. Marked a spot on the vessel above the attitude sensor (IMU) so that the level rod was always held at the same point on the boat.
6. Stopped the vessel at “static” with the starboard side toward “level.”
   A. Held the rod on mark with face toward “level.”
   B. Adjusted the rod target according to signals from “level.”
   C. On signal from “level,” recorded time and rod reading from target.
   D. Repeated the reading at least three times.
   E. The NOAA water level gauge at Newport was used to record water levels.
7. On a signal from the surveyor at “level,” made way on “settlement and squat” survey lines at predetermined shaft RPM.
   A. On survey track, held rod on mark with face toward “level.”
   B. Adjusted rod target according to signals from “level.”
   C. On signal from “level,” recorded time and rod reading from target. Readings were taken as nearly as possible at “static” to reduce errors from level instrument adjustment and earth curvature.
   D. Repeated the reading at least three times.
   E. The NOAA water level gauge at Newport was used to record water levels.
8. Increased speed to the predetermined shaft RPM settings up to and including full speed, and reran “settlement and squat” tests as described in Step 7.
9. Computed the settlement and squat correctors:

A. Computed the water level correctors from the time of the "static" reading to the time of each of the shaft RPM observations. (Water level during shaft RPM pass minus water level "static").
B. Applied the water level corrector to each of the shaft RPM rod observations.
C. Subtracted the corrected rod reading at each shaft RPM from the rod reading at "static." These differences are the settlement and squat correctors to be applied when operating at the corresponding shaft RPM.
D. Constructed a lookup table of shaft RPM and settlement and squat correctors so that the computer may interpolate a corrector based upon the shaft RPM entered into the system during the survey.
E. Entered these values in the ISS2000 *.cfg file.

All results are reported in Table D3-1.

Table D3-1. Settlement Results for the R/V *Ocean Explorer*

Engine RPM	Speed Knots*	Settlement Meters
0	0	0.00
600	5	0.01
800	7	0.02
1100	10	0.03
1300	11	0.04
1500	12	0.08
1900	15	0.22

* NOTE: The speed in knots listed in Table D3-1 were not used in the Settlement and Squat Lookup Table, but are given here as approximate average values.

Appendix E
Detailed Evaluation of Currents and Meteorological Conditions at the Portland Disposal Site

1.0 Introduction

In March 1999, SAIC deployed two bottom-mounted Acoustic Doppler Current Profilers (ADCPs) in close proximity to the Portland Disposal Site (PDS) to characterize the water column current flow over the seafloor at this location. Upon recovery in mid-April 1999, it was determined that only one instrument (ADCP 1) had recovered valid data during the 31-day deployment period. The valid record profiled the entire water column from a depth of 71 m to the surface.

SAIC utilized the bottom-mounted ADCP data set to address the overall objective of characterizing near bottom, surface, and mid-water currents over the PDS relative to sea state and atmospheric weather conditions. In particular, the ADCP data record was processed to obtain a mean current speed and direction for five horizons within the PDS water column, for use in STFATE modeling routines. Additionally, the ADCP record was compared to meteorological and oceanographic observations obtained from the National Oceanic and Atmospheric Administration (NOAA) National Data Buoy Center's (NDBC) buoy 44007 located in the Gulf of Maine about 10 km southwest of the PDS (Figure 1-1). The goal of this comparison was to evaluate water column dynamics at the disposal site during normal and storm conditions. The results of this effort are presented and discussed below.

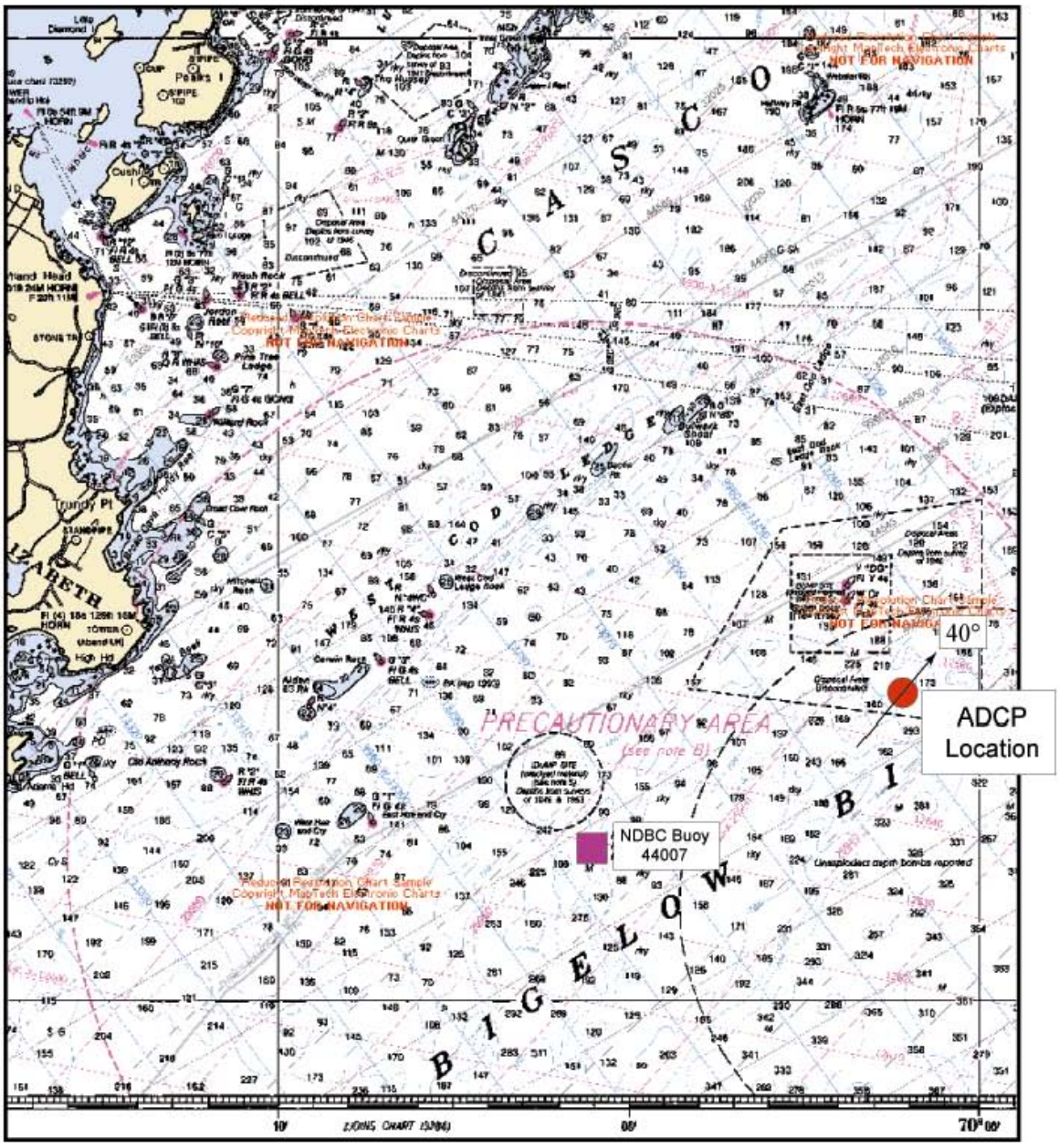

Figure 1-1. Map showing the general bathymetry in the vicinity of the ADCP measurements as well as the location of NDBC Buoy 44007.

2.0 Results

ADCP 1 unit that collected current measurements over a 31-day period in March and April 1999 was located in an area southeast of the PDS in approximately 71 m of water (Figure 1-1). The local isobath orientation in this area was estimated to be approximately 40° (east of north or on the line oriented 40°-220°), which establishes a general framework for considering along-isobath and cross-isobath current patterns (Figure 1-1).

2.1 Meteorology and Waves

2.1.1 Long Term Average conditions – ten year record

With the goal of providing an historical perspective within which to interpret the current data obtained during March/April 1999, a ten-year interval of wind speeds and direction and wave conditions were evaluated from NOAA Buoy 44007 at the nearby location shown in Figure 1-1. The bivariate data (wind speed and wind direction FROM) are shown in Table 2-1; these data are presented graphically in the wind rose shown in Figure 2-1. During the months of March and April, winds over the ten year period occurred in all thirty degree directional segments, however, the 60° interval from 150°-210° contained 24% of the observations (Table 2-1). An examination of the maximum wind speeds by direction class indicates that the strongest wind speed recorded, approximately 24 m/s, was from the NNE (30-60°). This quadrant encompasses the general orientation of the isobaths at the measurement site. Other maximum wind speeds ranged from 15.8 m/s from the NNW (300-330°) to 20.1 m/s from the ENE (60-90°). The March-April mean speeds for all direction classes for the 1990-99 interval were fairly comparable, varying from 5.4 m/s to 6.8 m/s (Table 2-1).

To provide a more complete linking of meteorological forcing to local conditions, the wave measurements taken near the site over the interval from 1990-99 were analyzed. These are shown graphically as histograms in Figure 2-2. Note that in the relative frequency description of wave period, the discontinuous peaks result from the discrete, constant wave frequency values in the measured wave spectrum. The incremental frequency in the spectrum produces an increasingly large gap between adjacent peak wave periods. The significant wave height (assumed equal to H_{mo}) had an average value of approximately 1 m, with a local, and fairly unique, maximum of 7.3 m. The most frequent wave periods were in the 8-11 second interval.

Initial computations of growth of wave fields indicate that an 18 m/s wind with unlimited fetch and duration creates a significant wave height of approximately 6 m and a prevailing period of 11.5 seconds. It should be noted that the computed spectral estimates of significant wave height can have a 10-15% error, and the instrumentation used can also contribute errors for such extreme conditions. An examination of the details of Figure 2-2 indicates that a significant wave height of over 6 m occurred with a cumulative frequency

Table 2-1

Bivariate Analysis of Wind Speed and Direction for March and April over a Ten Year Period at Buoy 44007

FREQUENCY DISTRIBUTION

1.00 Hrly Wind Data **Station:** 44007 **Spanning** 3/ 1 TO 4/30 for Years: 1990 - 1999 13,269 DATA POINTS - 90.7 % of Tot.

DIRECTION FROM DEGREES													Percent In Class	Mean Speed	Min. Speed	Max. Speed	Std. Dev.
0- 30	0.8	1.5	2.0	2.2	1.5	0.6	0.5	0.3	0.2	0.0	0.0	0.0	9.6	6.74	0.10	18.50	3.87
30- 60	0.7	1.4	1.6	1.3	0.8	0.6	0.3	0.2	0.1	0.1	0.0	0.0	7.0	6.60	0.10	24.00	4.23
60- 90	0.5	1.3	1.2	0.9	0.8	0.5	0.2	0.1	0.0	0.0	0.0	0.0	5.6	6.06	0.10	20.10	3.60
90-120	0.8	1.3	1.2	0.7	0.3	0.2	0.2	0.0	0.0	0.0	0.0	0.0	4.6	5.06	0.20	18.70	3.40
120-150	0.6	1.6	1.2	0.6	0.3	0.2	0.1	0.1	0.0	0.0	0.0	0.0	4.7	4.86	0.10	17.40	3.20
150-180	0.8	2.2	2.7	2.0	1.2	0.6	0.3	0.0	0.0	0.0	0.0	0.0	9.8	5.75	0.10	16.70	3.04
180-210	0.8	2.5	3.6	3.5	2.3	1.0	0.3	0.2	0.0	0.0	0.0	0.0	14.2	6.23	0.10	16.80	3.03
210-240	0.5	2.2	2.3	1.8	0.6	0.4	0.1	0.1	0.0	0.0	0.0	0.0	8.1	5.40	0.10	17.60	2.93
240-270	0.6	1.5	1.9	1.6	0.8	0.3	0.1	0.1	0.0	0.0	0.0	0.0	7.0	5.60	0.20	16.10	3.04
270-300	0.6	1.3	1.9	1.5	1.1	0.7	0.4	0.1	0.0	0.0	0.0	0.0	7.6	6.40	0.10	16.00	3.51
300-330	0.6	1.5	1.7	2.4	1.8	1.1	0.5	0.2	0.0	0.0	0.0	0.0	9.8	6.85	0.20	15.80	3.45
330-360	0.8	2.0	2.3	3.0	1.9	1.0	0.4	0.2	0.1	0.0	0.0	0.0	11.8	6.57	0.10	17.10	3.41
CALM	0.1												0.1				

Speed (m/s)	0 ! 2	2 ! 4	4 ! 6	6 ! 8	8 ! 10	10 ! 12	12 ! 14	14 ! 16	16 ! 18	18 ! 20	20 ! 22	22 ! 24	
PERCENT	8.4	20.2	23.5	21.6	13.5	7.2	3.5	1.5	0.5	0.1	0.0	0.0	100.00
CUM PRCT	100.0	91.6	71.4	47.9	26.3	12.9	5.7	2.2	0.6	0.2	0.1	0.0	
MEAN DIR	178	186	190	203	204	205	190	168	103	57	52	55	
STD DEV	106	100	100	107	110	111	119	124	123	19	16	0	

SUMMARY STATISTICS

MEAN SPEED = 6.12 Maximum Spd. = 24.00 Minimum Spd. = 0.00 Speed Range = 24.00
STANDARD DEVIATION = 3.29

IN A COORDINATE SYSTEM WHOSE Y AXIS IS POSITIONED 0.00 DEGREES CLOCKWISE FROM TRUE NORTH
MEAN X COMPONENT = 0.68 STANDARD DEVIATION = 4.30
MEAN Y COMPONENT = -0.36 STANDARD DEVIATION = 5.41

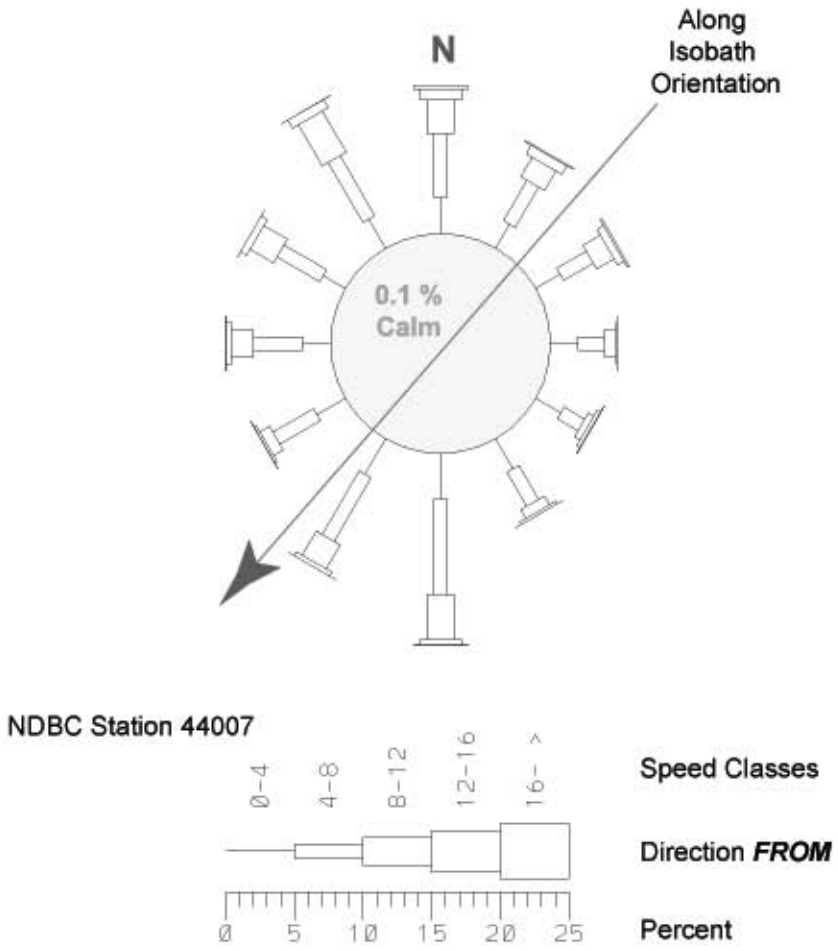

Wind speed in 30¡ direction classes. Data taken from March and April for the years 1990 through 1999. This should provide a larger scale perspective on the range of wind speeds and directions that might be expected during these months.

Figure 2-1. Graphic presentation of bivariate (speed and direction) information presented in Table 4-1. Data were taken during March and April for the ten-year interval from 1990-99.

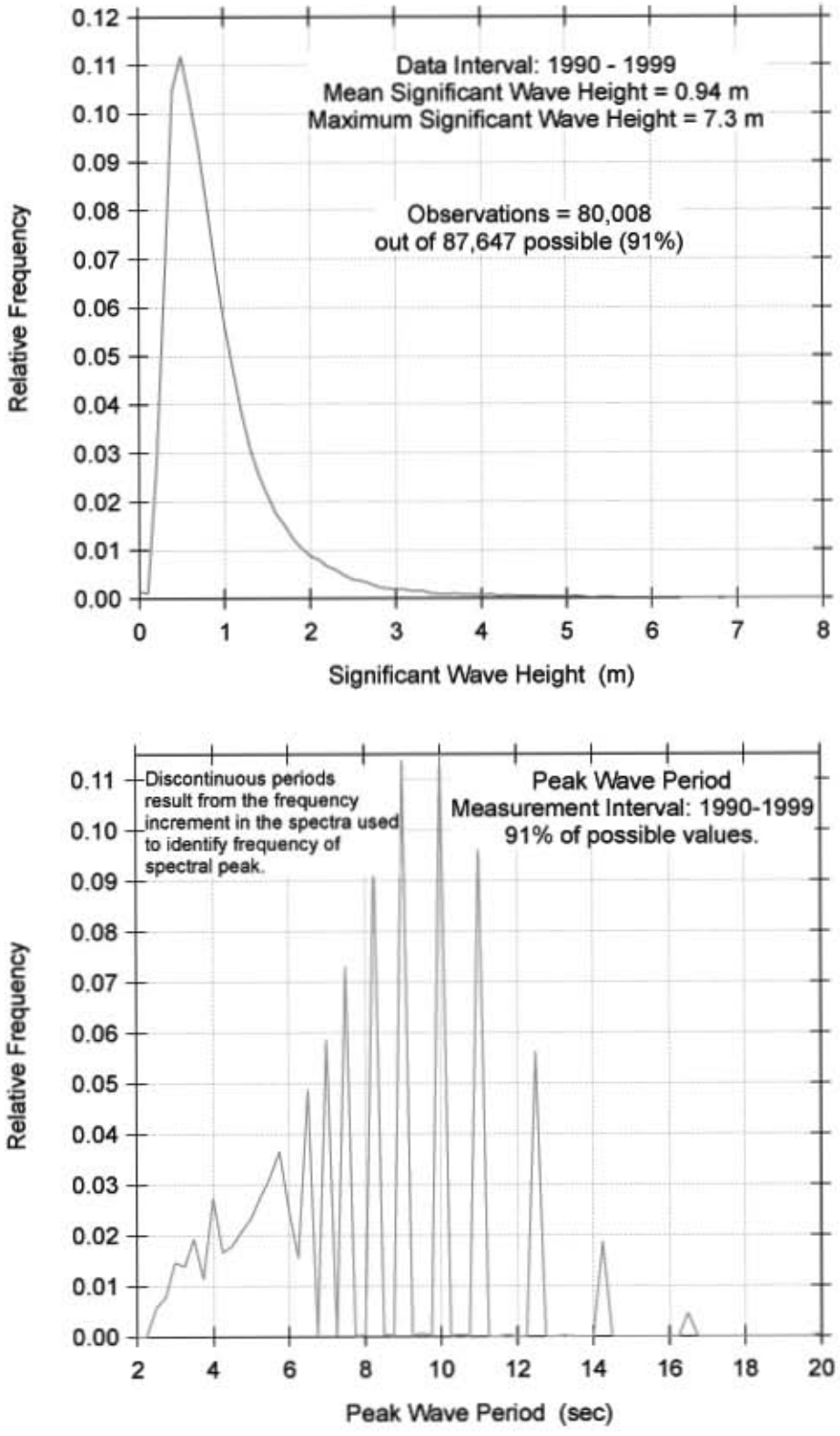

Figure 2-2. Relative frequency (histograms) of significant wave height and peak or dominant wave period based on ten years of measurements at Buoy 44007.

of 3.48×10^{-4}, or about once every two years during these months. Thus, on average, one expects waves in excess of 6 m only about 5 times over a ten year period in the months of March and April. The relative infrequency of these conditions point to general agreement between observations and computational estimates. The wave period estimates are for wind conditions directly affecting the study site. Thus, longer period swell generated by remote storms would not be estimated in these computations.

2.1.2 Wind and Wave Conditions during the Field Measurements

The wind and wave conditions measured at Buoy 44007 during the 31-day deployment interval of the ADCP in March-April 1999 indicate a general agreement between the most significant wind event that occurred between approximately March 21 – 24, 1999 and the concurrent wave field (Figure 2-3). With maximum wind speeds of approximately 18 m/s, significant wave height grew to approximately 5.75 m. During this wind event, wind direction sequentially changed such that winds initially were from the east followed by rotation to generally being from the south and south-southwest (Figure 2-3). These latter directions allow for greater fetch and hence greater potential growth of wave heights and periods. Other somewhat less vigorous wind events (e.g. April 4-5, 1999) created much less significant wave heights and periods. This is in part due to the wind direction, which was from the north and northwest (i.e., from the land) and thus generating fetch-limited wave fields.

2.2 Currents

2.2.1 Vertical Profiles

Using the single 300 kHz Acoustic Doppler Current Profiler (ADCP), horizontal current vectors were estimated every thirty minutes in one meter vertical bins. The resulting profile extended from nominally 7 m below the water surface to 68 m below the water surface at a site where the water depth was approximately 71 m. Data were recorded in N/W and E/W component velocity time series (Figure 2-4a and b). To help relate these component velocities to potential meteorological forcing events, the strong wind event in late March 1999 is indicated by the shaded rectangle in Figures 2-4a and b.

Conditions between the near surface and near bottom differ, as is evident from a visual examination of the component time series. Several time series between the top and bottom have been selected to provide a representation of conditions over the vertical water column. The depths selected are at 15-m intervals, from 7 m downward (7, 22, 37, 52 and 67 m depths).

Vector mean currents at these selected depths are shown in Figure 2-5. Shear in the mean profile is evident by the decreasing magnitude of the vector mean, however, the direction remains relatively constant with increasing depth. The orientation of the mean vector is in reasonable agreement with the estimated regional isobath trends for the measurement site. At all depths, the net volume flux over the measurement interval was to

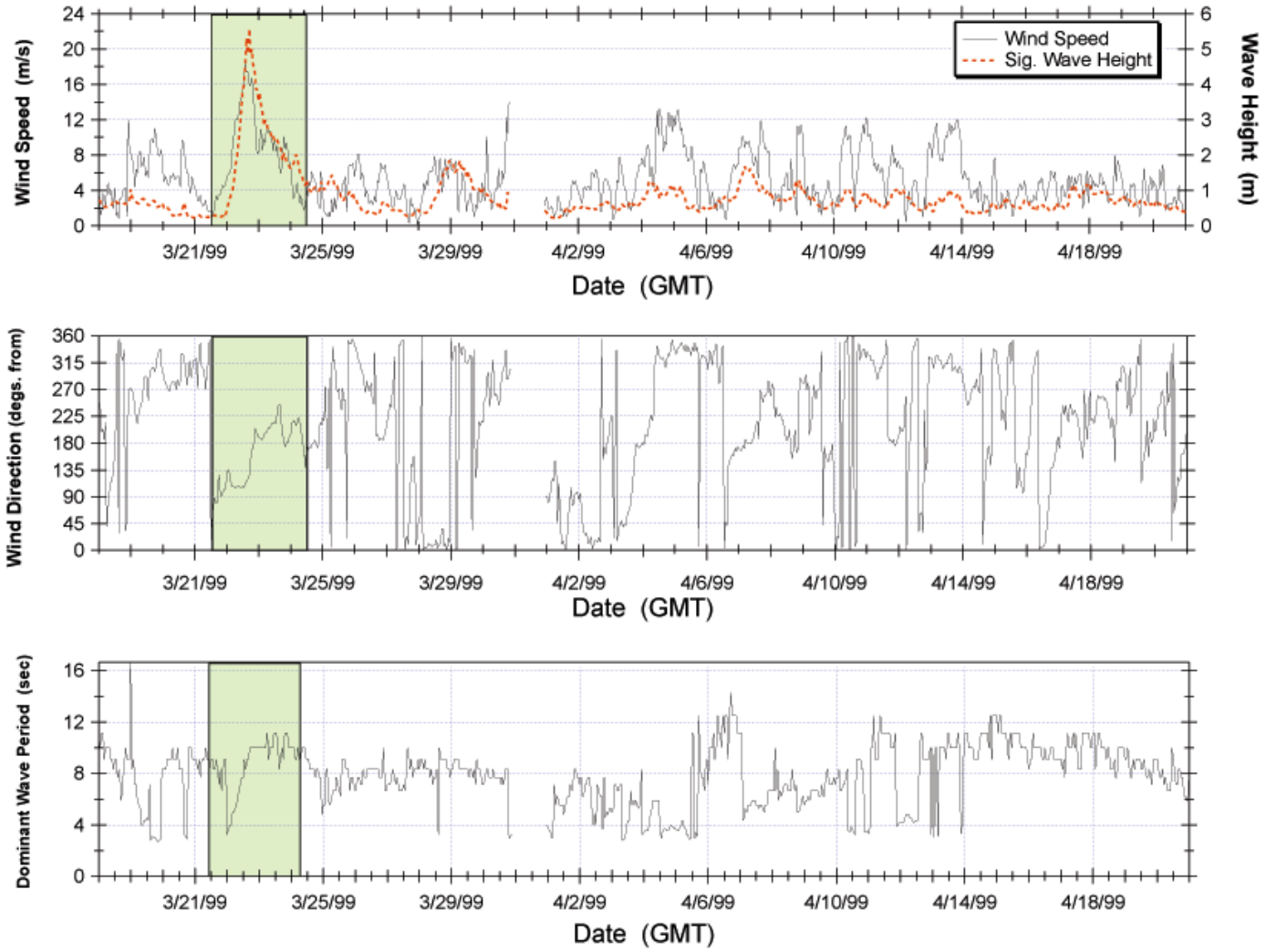

Figure 2-3. The upper panel shows time series plots of wind speed and significant wave height as measured at Buoy 44007. The middle panel shows wind direction and the lower panel shows the dominant wave period as a function of time.

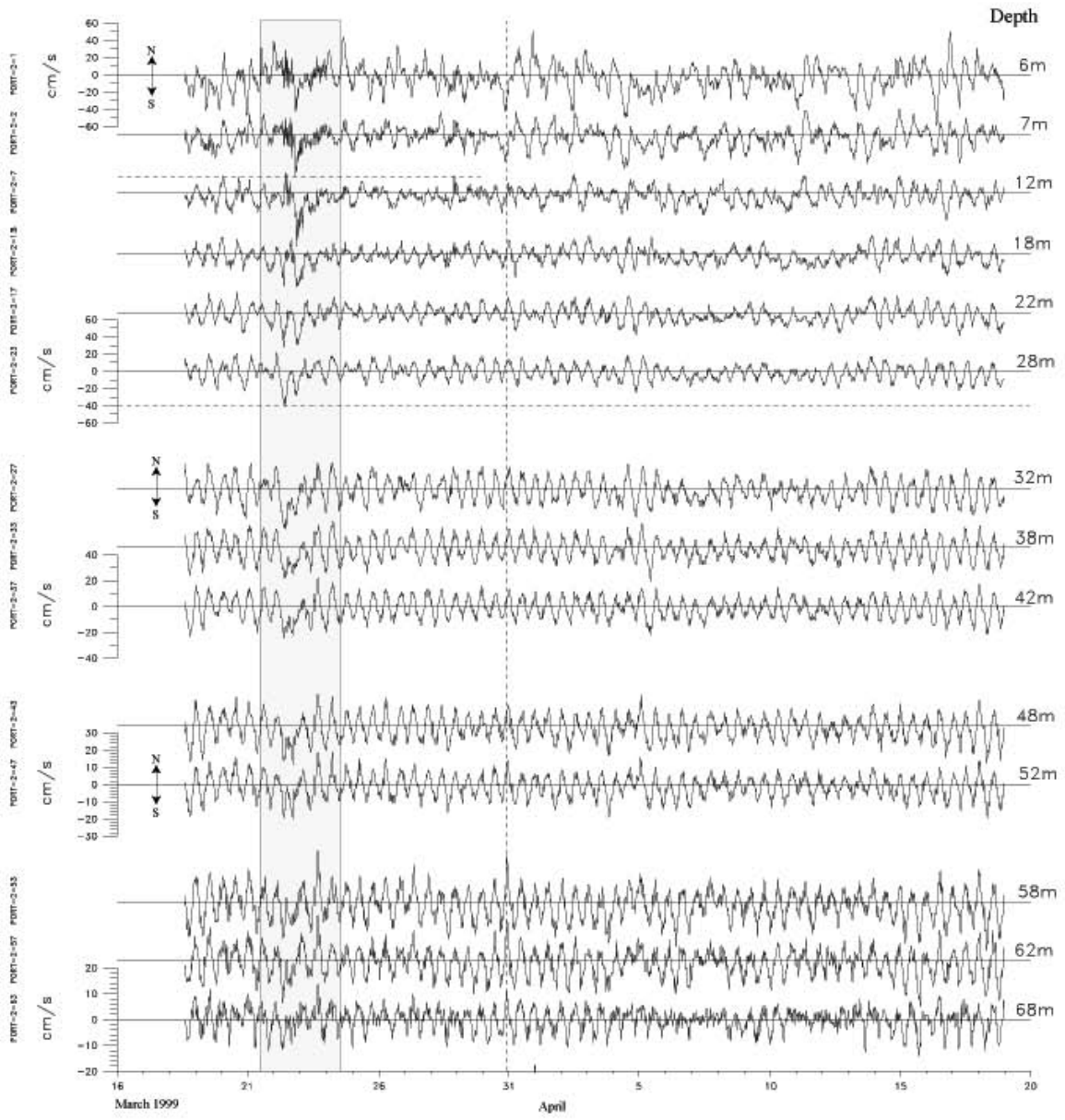

Figure 2-4a. Time series plots of the v-component of velocity (N/S component) at approximately four meter intervals from the near surface to near bottom. The shaded rectangle is to help relate time on these graphs as well as to wind events.

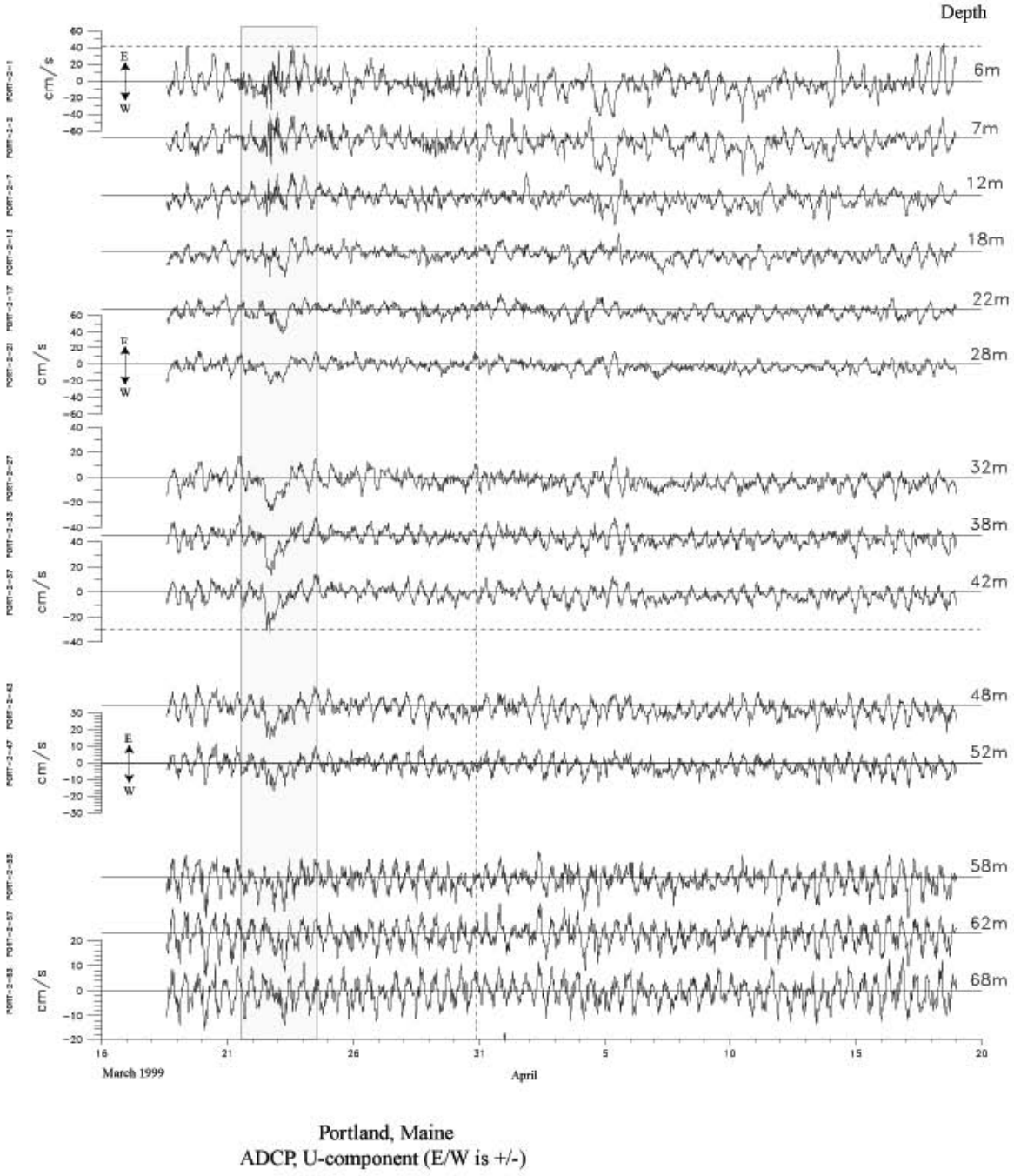

Portland, Maine
ADCP, U-component (E/W is +/-)

Figure 2-4b. Time series plots of the u-component of velocity (E/W component) at approximately four-meter intervals from the near surface to near bottom. The shaded rectangle is to help relate time on these graphs as well as to wind events.

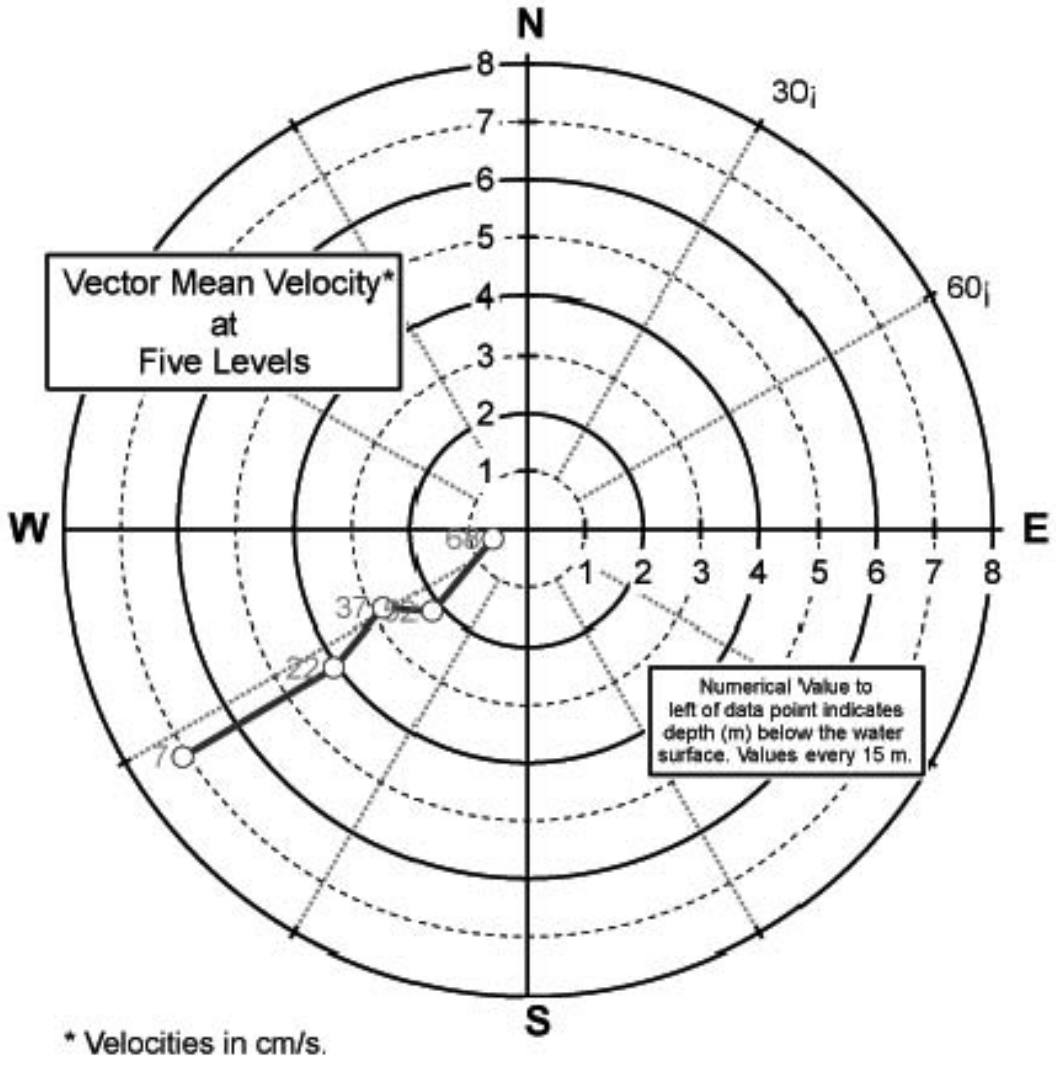

Figure 2-5. Presentation of vector mean currents at the five representative depths. Current values are in cm/s.

the SW (i.e., downcoast). Principal axis orientation was computed, and the component variances were found to be comparable in the upper portion of the water column. This allows for small changes to produce relatively large changes in the principal axis orientation. Generally, from approximately 7 to 11 m depths, the principal axis rotated clockwise by approximately 60°. For the interval from 18-51 m, the principal axes were relatively constant, in the 45-65° range. Between 52 m and 68 m, the principal axis rotated counterclockwise approximately 80° with increasing depth

2.2.2 Tidal Currents

The measured currents were analyzed to extract characteristics of the various tidal constituents that contribute to the total observed current field. Results of these analyses can be presented as tidal ellipses; a labeled example of this presentation is shown in Figure 2-6. Key elements in this graphic presentation are the magnitude of the major and minor axes (maximum and minimum tidal currents), as well as the direction of rotation of that component current vector. The tidal constituent labels provide information concerning the cause of the fluctuation as well as the approximate period of the tidal constituent. Tides having a subscript of "2" (e.g., M_2) have approximately two cycles per day. Those with a subscript of "1" have approximately one cycle per day.

Tidal ellipses for observed currents are presented in Figure 2-7 for five tidal constituents that provide the largest contributions to the current field. For each of these tidal constituents, tidal ellipses are presented for currents at five selected depths. It is important to note in Figure 2-7, the scale of the axes differs between the semi-diurnal lunar tide (M_2) and all the other constituents. Generally, the M_2 tidal current is on the order of five times that for the other tidal constituents. The M_2 tidal current vector rotates counterclockwise at all levels. The maximum M_2 current near the surface is on the order of 10 cm/s and approximately 5 cm/s near the bottom. For constituents other than the lunar semi-diurnal tide (M_2), the contributions to the measured velocity field have a maximum of 2 cm/s or less.

The complete tidal current analyses can be used to reconstruct/predict the current record resulting from the combined contributions of essentially all tidal constituents. As an example, the estimated/predicted tidal current time series from 7 m depth is shown in Figure 2-8 in both polar and component frames of reference. The expected periodic variations of the tidal currents are clearly discernible in this figure. The relative importance of the M_2 tide to the cumulative tidal currents is readily identifiable in the twice daily periodic variation of the component velocity time series. What is not as easily discernible is the actual speed and direction of the resultant tidal currents. Because the discussion to follow focuses on the timing of current speed events, the presentation of velocity time series in this polar framework is preferred.

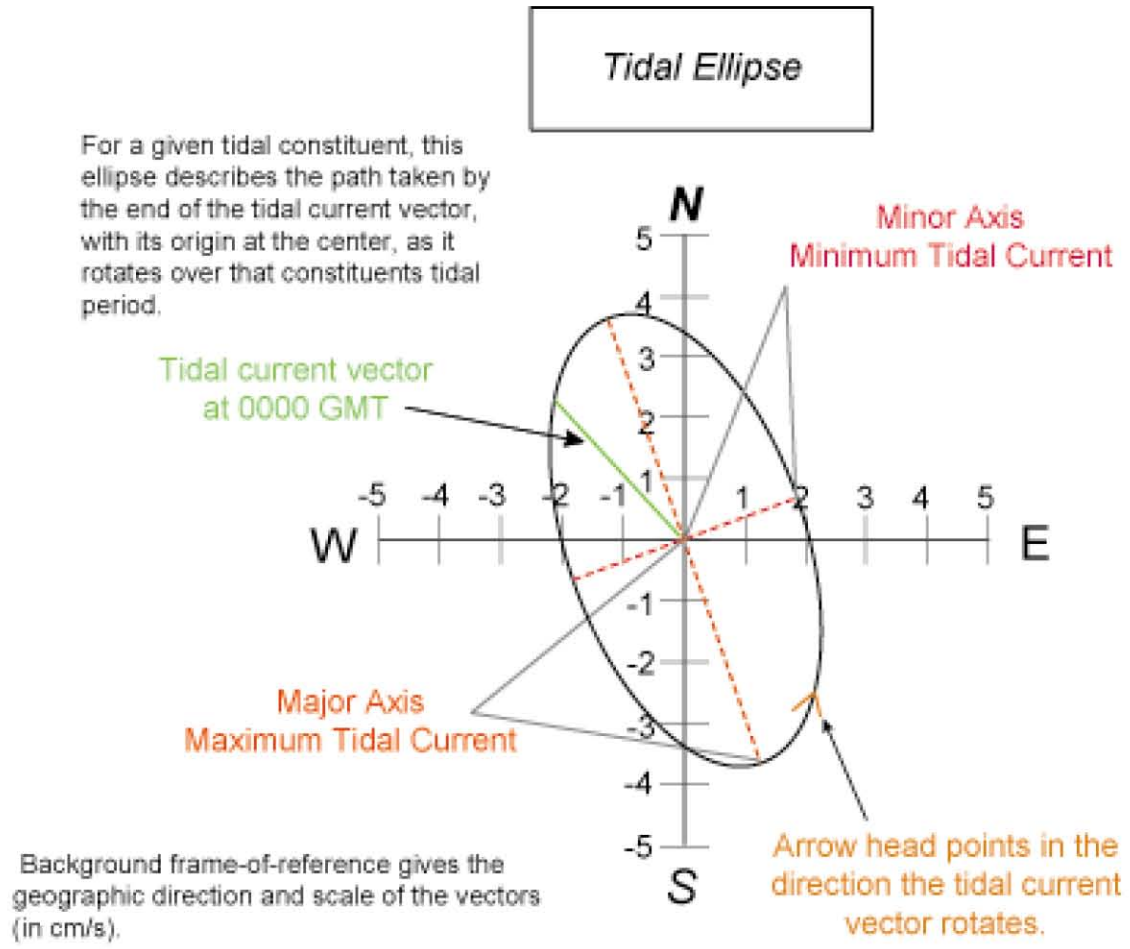

Figure 2-6. An illustration of information as presented by tidal ellipses. This provides the scheme for interpreting tidal ellipses in Figure 2-7.

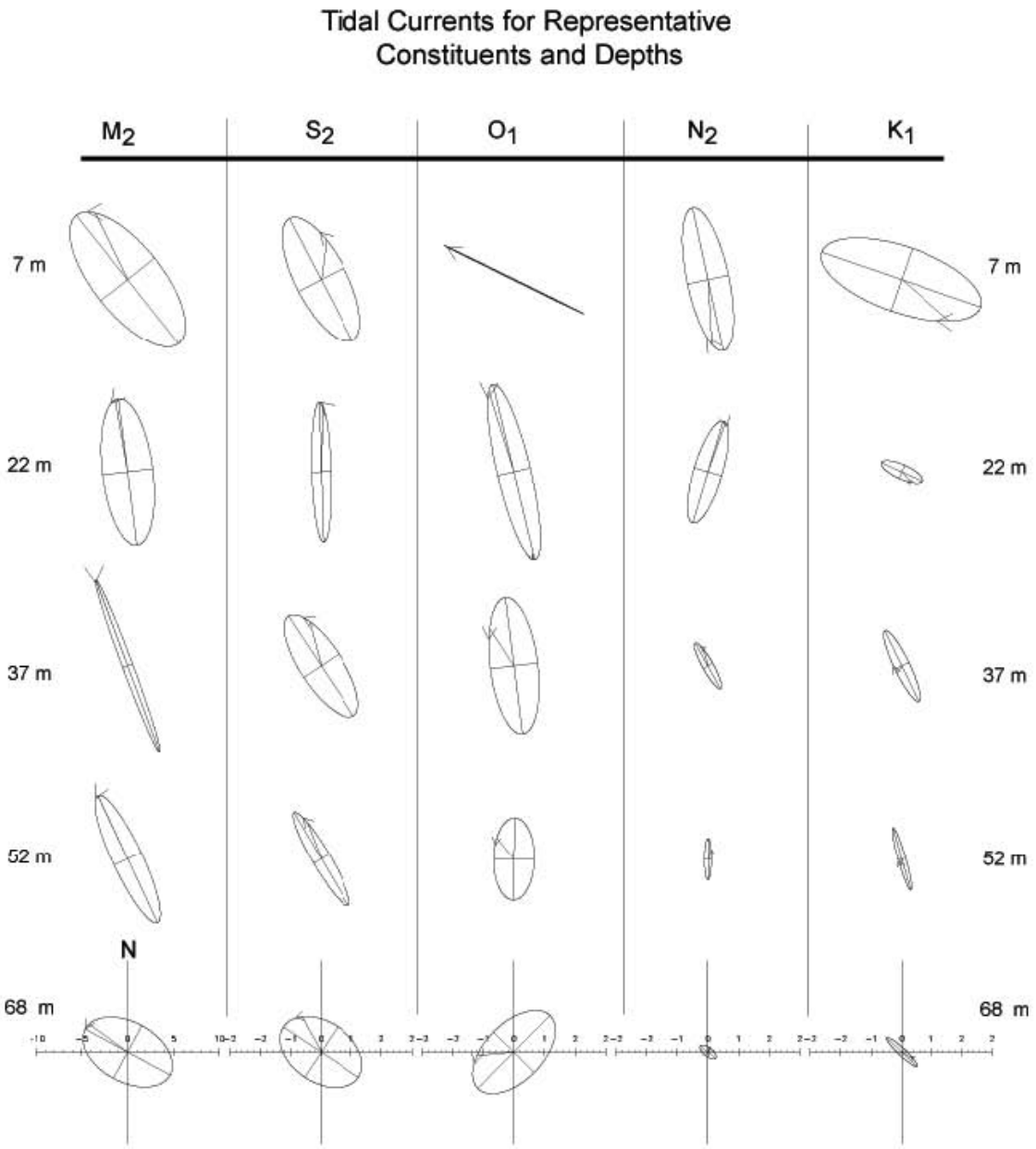

Figure 2-7. Tidal ellipses for the five larger tidal current constituents. The subscript "2" indicates approximately two cycles per day. The subscript "1" indicates approximately one cycle per day. See Figure 2-6 for an explanation of the components of each ellipse. Note that the scale for the M_2 tide is larger than all the others.

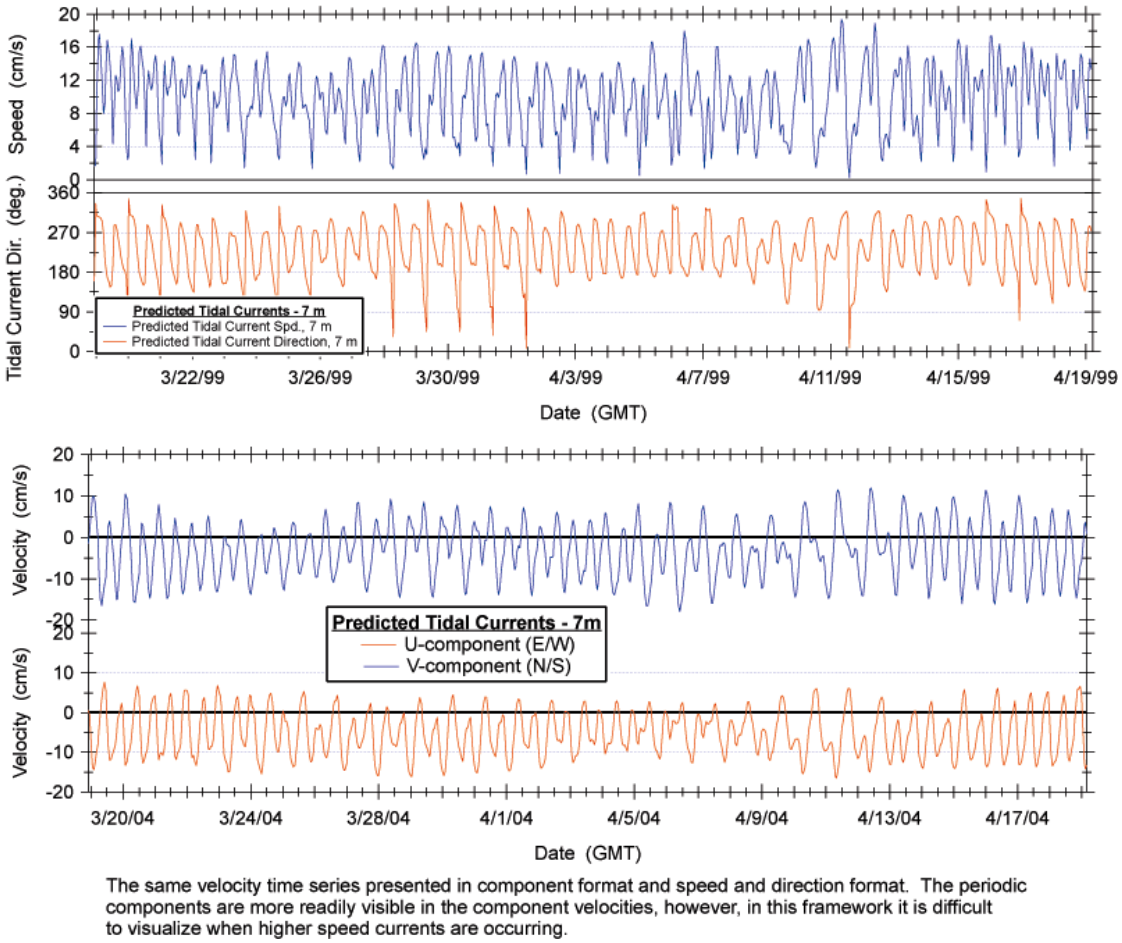

The same velocity time series presented in component format and speed and direction format. The periodic components are more readily visible in the component velocities, however, in this framework it is difficult to visualize when higher speed currents are occurring.

Figure 2-8. Time series plots of velocity measured at 7 m presented in polar coordinates in the upper panel and component coordinates in the lower panel.

Observed Currents

Current speeds for the five selected measurement depths between 7 and 68 m below the water surface help identify the differences in currents that occur with time over the vertical water column (Figure 2-9). The magnitude of the periodic and background currents tend to decrease with depth. Aperiodic current events (e.g., sstorm/wind induced) also seem to diminish with depth (e.g., March 21-23 and April 4-5, 1999). Mean current speeds reflect this general diminution of speed with depth, such that the mean speed for the lowest level (68 m) was approximately 35% of that from the highest level (7 m), as shown in Figure 2-10. Additionally, the maximum speed decreases by a comparable amount. As shown in Figure 2-10, the maximum measured speed at 68 m was on the order of 15 cm/s.

Tidal Currents

Examples of tidal current speeds for the current time series from the upper, middle, and bottom portion of the water column (Figure 2-11) show a general decrease in the amplitude of the speed fluctuations with increasing depth, as would be expected based on the above discussion of tides. The predicted tidal currents include the mean current vector. This explains why, in looking only at the u and v components plotted in Figure 2-8, there is an obvious offset of the current components from being centered around zero. This mean current vector is also incorporated in the predicted tidal currents when presented in polar coordinates.

Residual Currents

For the present discussion, residual currents are computed by a vector subtraction (using component velocities) of the predicted tidal currents from the observed currents. An example of the impact of this vector operation on the associated speed time series is shown in Figure 2-12. Since the predicted tidal currents incorporate the overall recorded mean current vector, the residual currents have had the mean current removed. The residual currents computed at each of the five representative levels are shown in Figure 2-13. These records incorporate all contributions to the observed currents other than tides, including locally forced wind-driven currents. This record is not sufficiently long to compute correlations with wind vectors. Consequently, the approach of removing tides and then visually evaluating correspondence of wind and current events will be used to identify the relation of wind forcing to currents. Note that such an approach does not support identification of any currents that are remotely forced by winds.

Several near surface current events are clearly discernable in these time series. In particular, the interval from April 4-6 had a residual current that was large and of relatively long duration (Figure 2-13). Currents remained above 20 cm/s for most of the interval. Maximum current speed was approximately 40 cm/s. No other event is as clearly defined as this. Three other less well-defined events appear to have occurred:

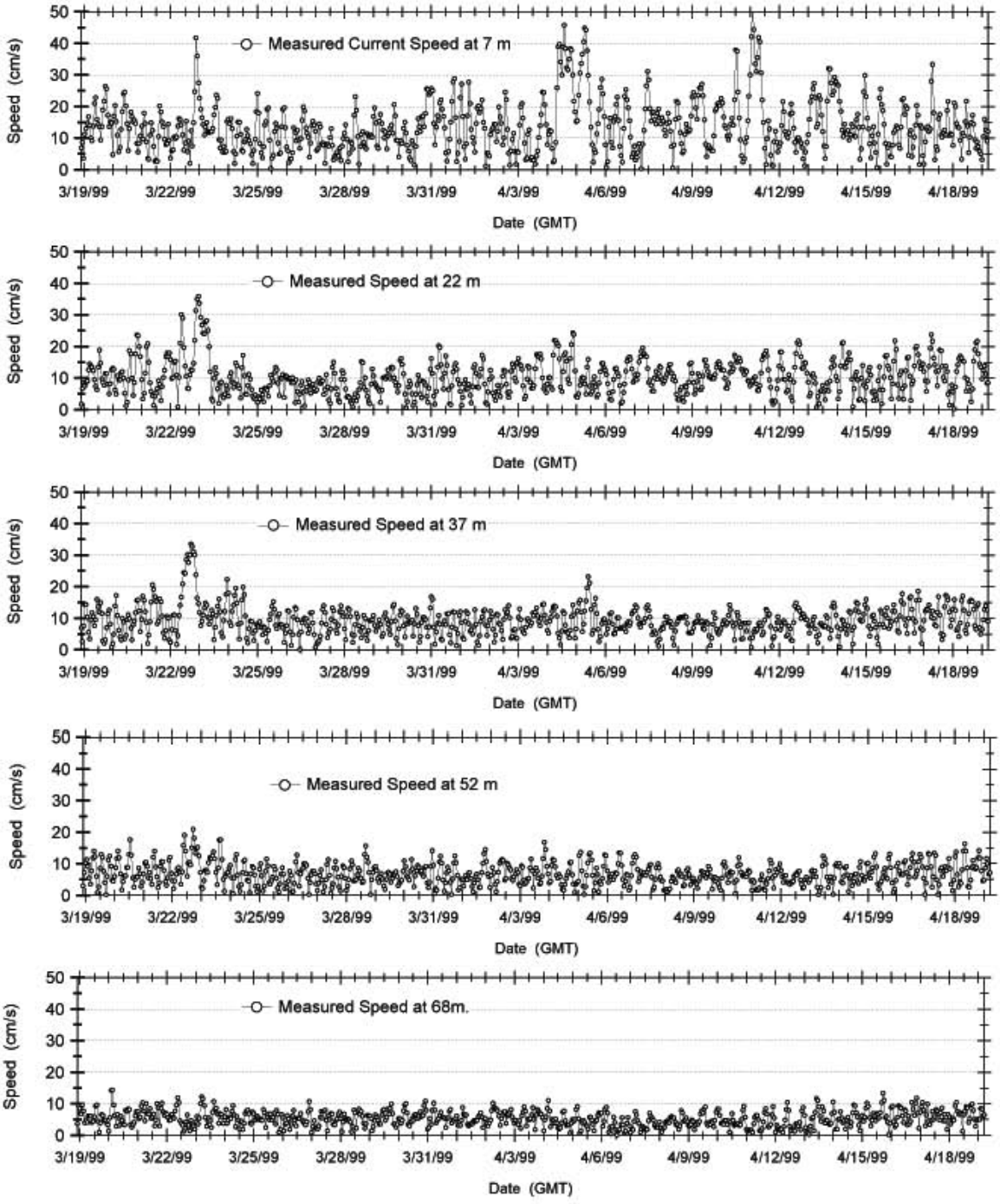

Figure 2-9. Time series of measured current speed at the indicated five representative depths.

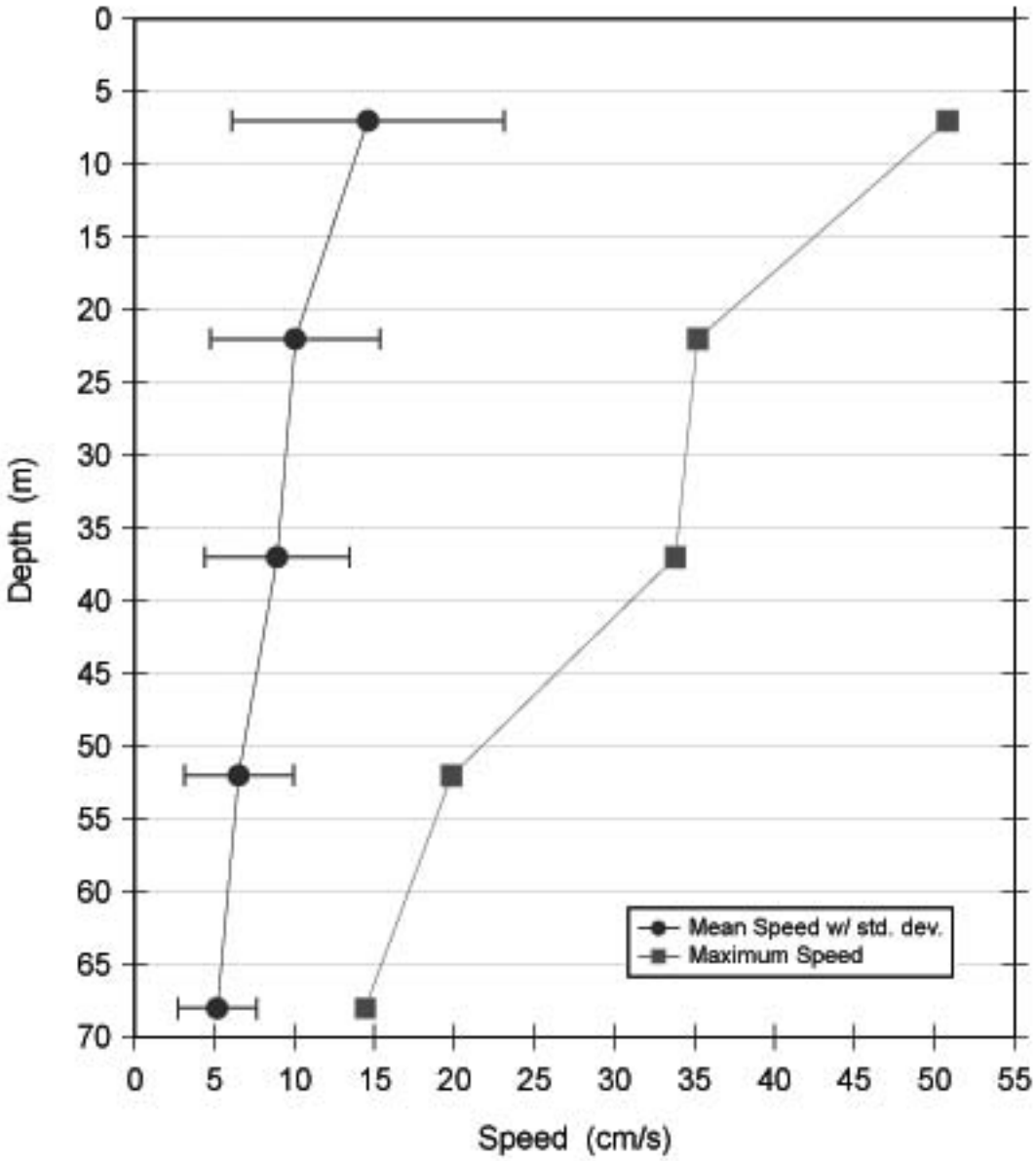

Figure 2-10. Mean and maximum current speed at the five representative depths. The error bars indicate the standard deviation of speed at that depth.

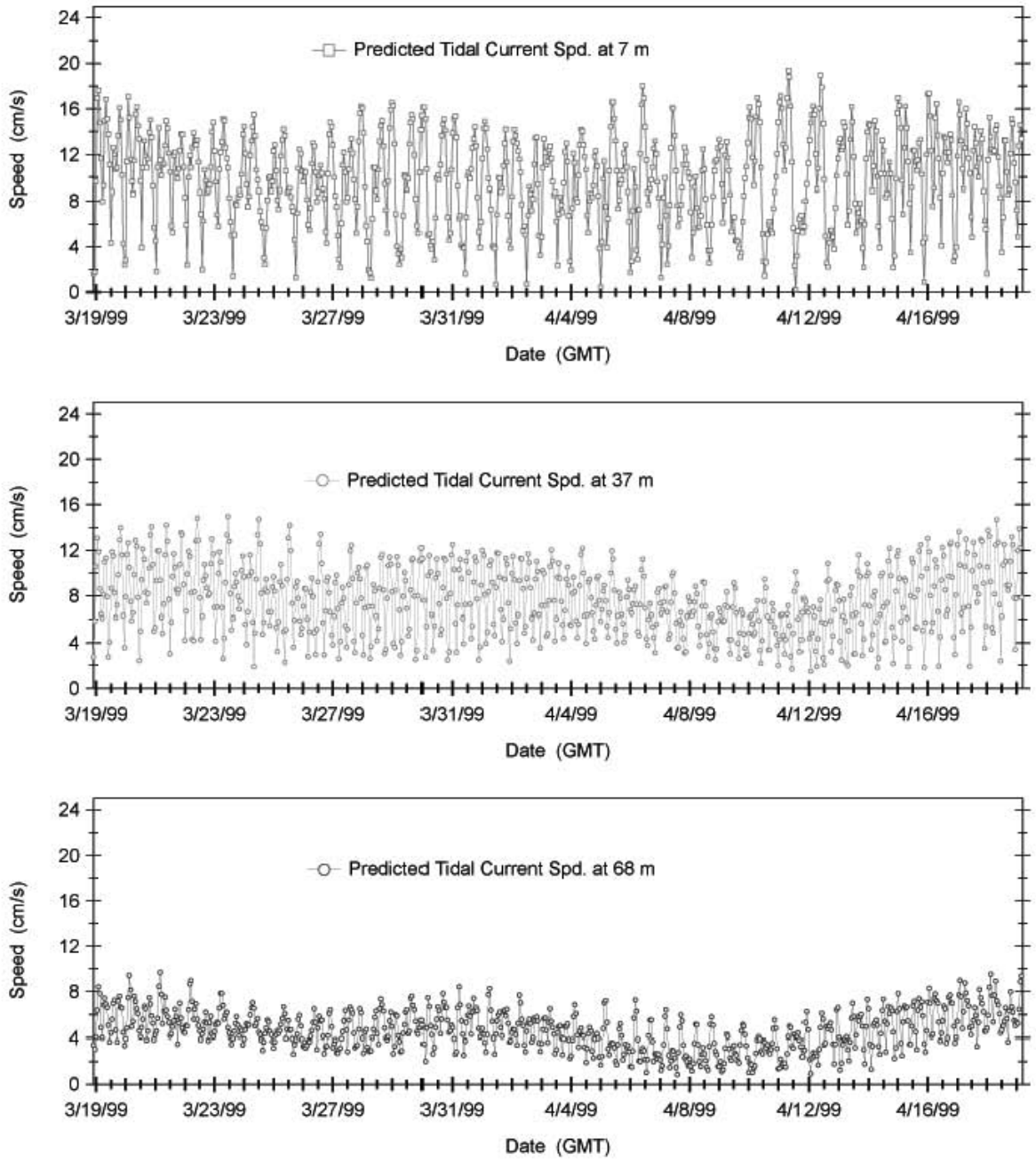

Figure 2-11. Time series plot of the predicted tidal current speed at the indicted three levels. These provide an indication of the sequential changes in the speed values with increasing depth.

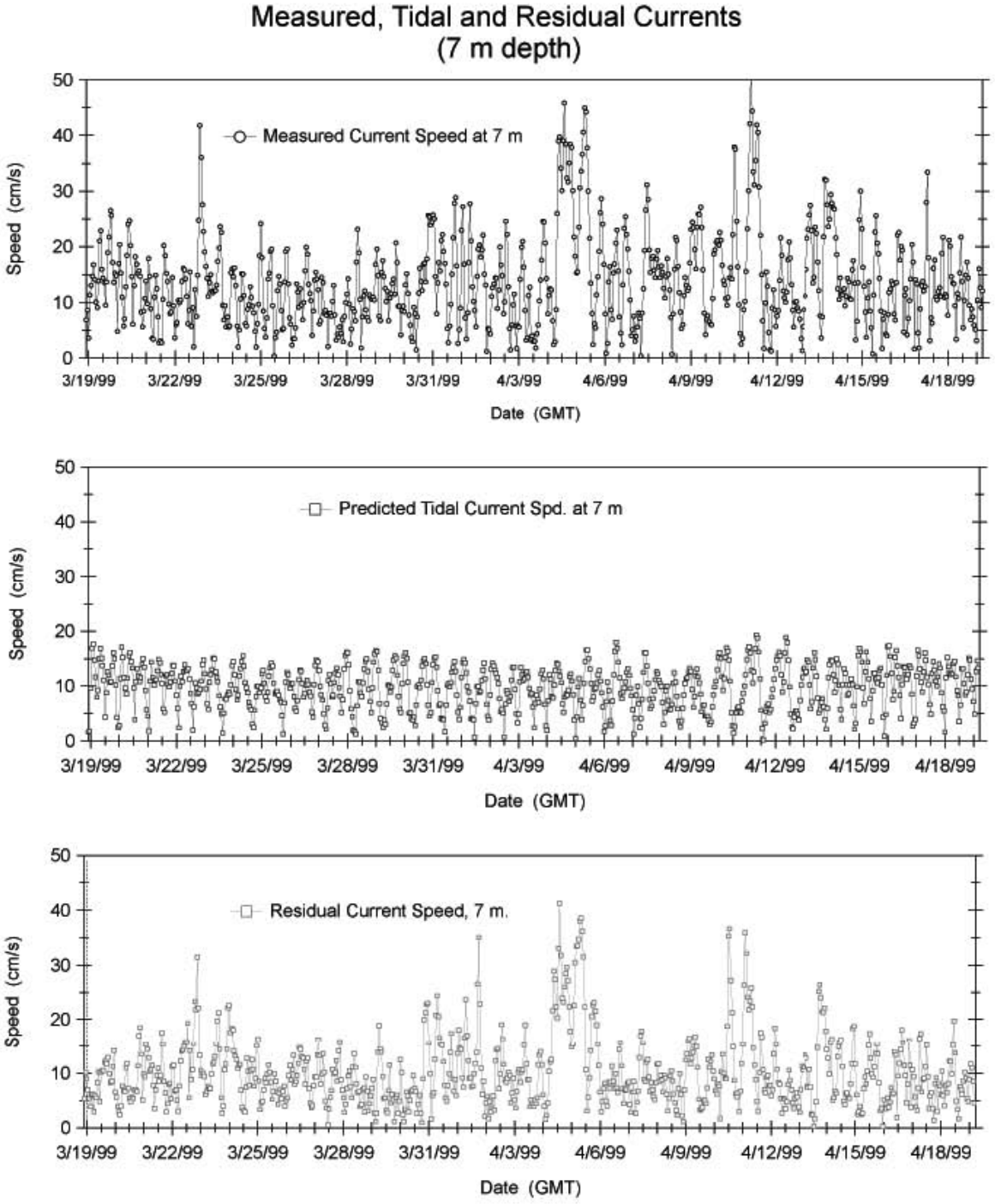

Figure 2-12. Time series plots of measured, tidal and residual current speeds at 7 m depth. This is to illustrate the impact of the vector subtraction of the predicted tidal currents from the measured currents to get the residual currents.

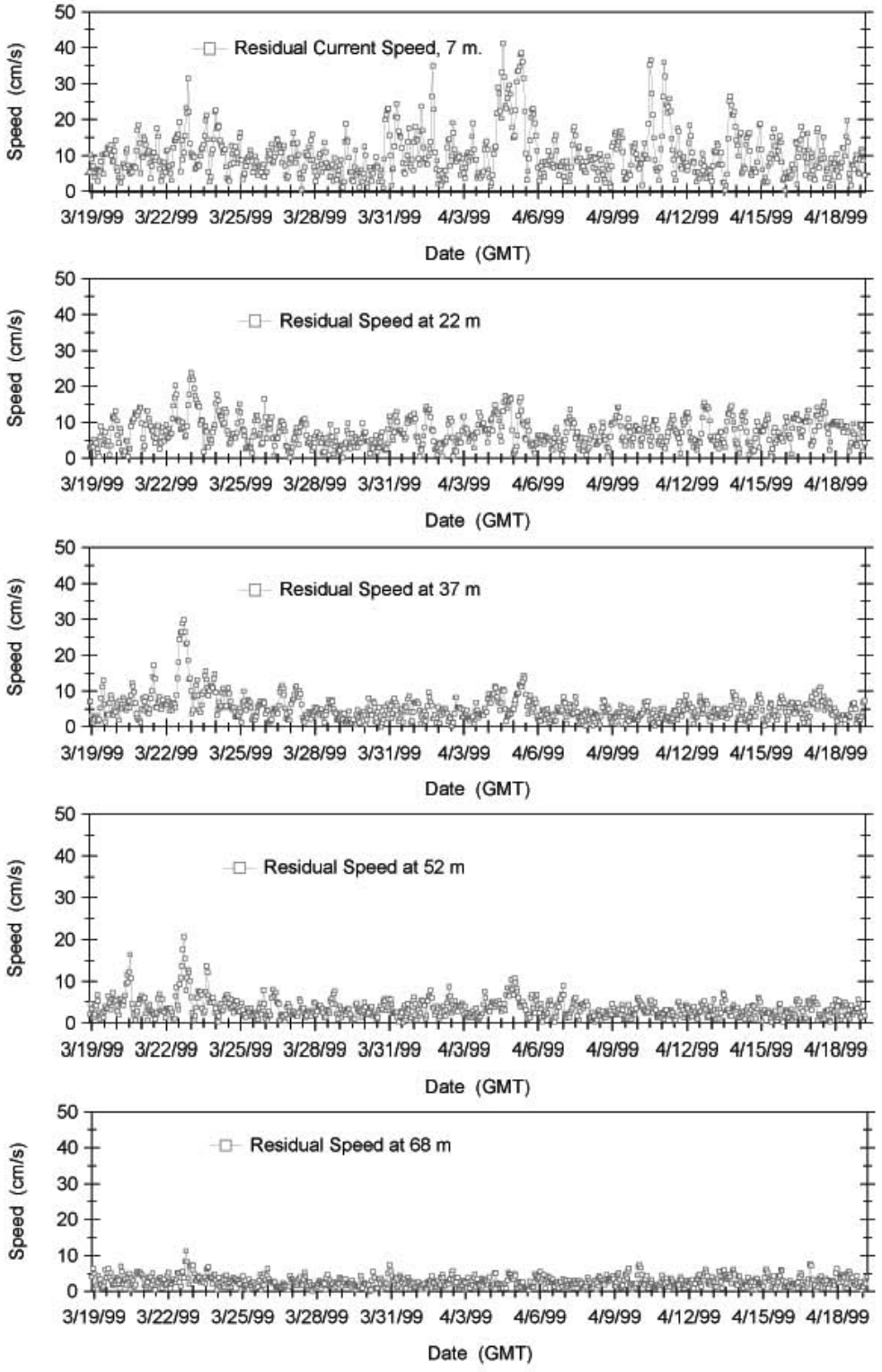

Figure 2-13. Time series plots of the speed (magnitude of the residual velocity vector) at the five representative depths.

March 22-24, March 31-April 2, and April 11 (Figure 2-13). These were weakly defined by minimum speeds tending to stay above zero and maximum speeds being visually identified as stronger than adjacent speeds. Only two of these four events (March 22-24 and April 4-6) remain identifiable in the speed records at depths of 22 m and greater (Figure 2-13). Although the latter of these two episodes (April 4-6) was most vigorous near the surface, the former interval (March 22-24) was associated with the more vigorous response lower in the water column (Figure 2-13).

Another alternative approach to examining residual currents is to apply a low pass filter to each component time series, which suppresses all fluctuations having a period of approximately one day or less. While this will eliminate most tidal currents, it also suppresses the daily and higher frequency fluctuations that are non-tidal. In addition, the filtering processes and associated tapering cause four days of velocity observations to be lost at the beginning and end of the time series. Both the loss of non-tidal higher frequency fluctuations and shortening of the time series would reduce the potential for relating local winds to local current speeds. Currents over the vertical profile that have had the low pass filtered applied to suppress daily and higher frequency fluctuations are shown as vector plots in Figure 2-14.

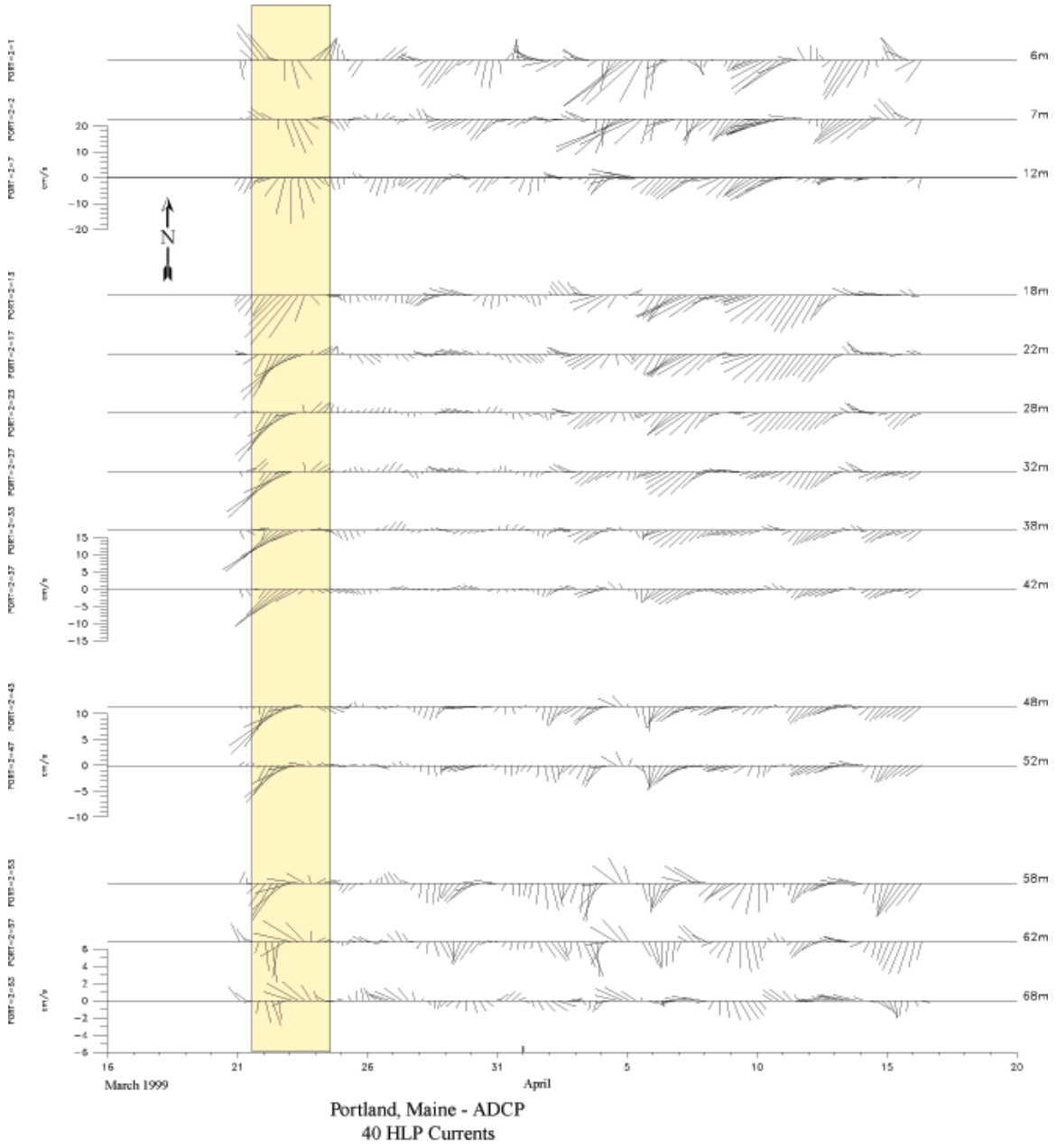

Figure 2-14. Stick plots of 40-HLP filtered velocity time series. Each "stick" represents a velocity vector at six-hour intervals. The stick points in the direction of the vector and has length proportional to the magnitude of the vector.

3.0 Discussion

3.1 Coincidence of Wind and Current Events.

To relate wind and current events, the corresponding time series were jointly evaluated for general coincidence events defined by increased speeds. Since wind is the forcing mechanism of interest, the objective is to identify wind events and then look for a possible corresponding increase in residual currents that occurred throughout the water column.

The apparent increased residual currents identified in the preceding section and their relation to local wind speed are shown in Figure 3-1. Three of the current events can be related to local increased wind speed. In particular, the wind events of March 22-24 (Event 1) and April 3-5, 1999 (Event 2) seem to be well correlated with corresponding increases in residual velocities. The most vigorous winds occurred during Event 1. There was a corresponding increase in nontidal currents which was more readily identifiable in the middle portion of the water column. Although weak, there does appear to have been a slight increase in near bottom current speeds to slightly over 10 cm/s. This was the most vigorous nontidal current speed measured at the 68 m level.

In contrast with the apparent influence of surface winds throughout the water column during Event 1, the most vigorous effect of Event 2 was near the surface, where residual currents at 7 m remained above 20 cm/s for over a day (Figure 3-1). At the mid-water level, current speed increased slightly, and actually was at a minimum when near surface currents were near the maximum. The maximum currents at 37 m during Event 2 were approximately 12 cm/s. There does not appear to be an identifiable response of near-bottom currents (68 m) that can be associated with surface winds or currents higher in the water column (Figure 3-1).

These data suggest that local winds do not have a substantial impact on near bottom currents. Although the combined impacts of wind speed and direction can not easily be considered, the wind speed of greater than 18 m/s that occurred during Event 1, was greater than 99.8% of the wind speeds recorded at Buoy 44007 during the 1990-99 decade. Approximately 94% of the measured wind speeds were less than the 12 m/s measured during Event 2. These two wind events differed in the surface wave field and response of currents in the water column. This could reflect any one or a combination of the following variations: wind magnitude, duration of wind event and wind direction.

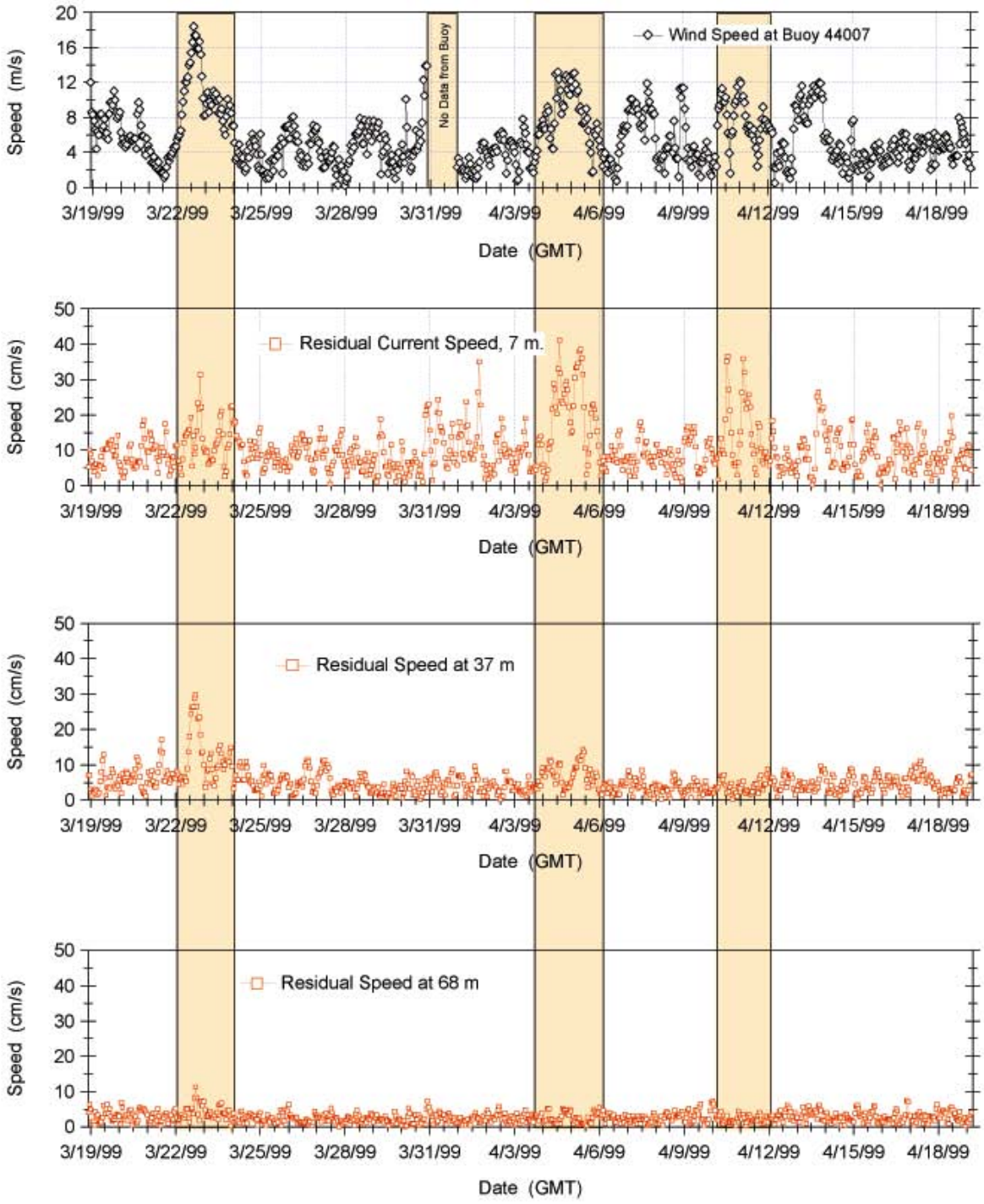

Figure 3-1. Time series of wind speed at Buoy 44007 and residual current speed at the indicated depths. The shaded rectangles are to help relate wind events to concurrent residual current speeds at three depths over the water column.

INDEX